

PB91218230



U.S. Department  
of Transportation

**National Highway  
Traffic Safety  
Administration**

---

DOT-HS-807-672  
DOT-TSC-NHTSA-90-3  
Final Report

February 1991

# **Intermediate Maneuver Induced Rollover Simulation (IMIRS) and Sensitivity Analysis**

Dr. Andrzej G. Nalecz

3602 Augusta Drive  
Columbia, MO 65203

Prepared for  
Research and Development  
Office of Crash Avoidance Research  
Washington, DC 20590

---

This document is available to the public from the National Technical Information Service, Springfield, Virginia 22161.

REPRODUCED BY  
U.S. DEPARTMENT OF COMMERCE  
NATIONAL TECHNICAL  
INFORMATION SERVICE  
SPRINGFIELD, VA 22161

NOTICE

This document is disseminated under the sponsorship of the Department of Transportation in the interest of information exchange. The United States Government assumes no liability for its contents or use thereof. The views expressed herein are those of the author and do not necessarily reflect those of the United States Department of Transportation.

NOTICE

The United States Government does not endorse products or manufacturers. Trade or manufacturer's names appear herein solely because they are considered essential to the object of this report.

1. Report No. DOT-HS-807-672		PB 91-218230		3. Recipient's Catalog No.	
4. Title and Subtitle INTERMEDIATE MANEUVER INDUCED ROLLOVER SIMULATION (IMIRS) AND SENSITIVITY ANALYSIS				5. Report Date February 1991	
7. Author(s) ANDRZEJ G. NALECZ				6. Performing Organization Code DTS-74	
9. Performing Organization Name and Address DR. ANDRZEJ G. NALECZ * 3602 AUGUSTA DRIVE COLUMBIA, MO 65203				8. Performing Organization Report No. DOT-TSC-NHTSA-90-3	
12. Sponsoring Agency Name and Address U.S. DEPARTMENT OF TRANSPORTATION NATIONAL HIGHWAY TRAFFIC SAFETY ADMINISTRATION RESEARCH AND DEVELOPMENT OFFICE OF CRASH AVOIDANCE RESEARCH WASHINGTON, DC 20590				10. Work Unit No. (TRAI5) HS978/S9002	
15. Supplementary Notes *UNDER CONTRACT TO:				11. Contract or Grant No. DTRS57-88-P-82668	
U.S. DEPARTMENT OF TRANSPORTATION RESEARCH AND SPECIAL PROGRAMS ADMINISTRATION VOLPE NATIONAL TRANSPORTATION SYSTEMS CENTER CAMBRIDGE, MA 02142				13. Type of Report and Period Covered FINAL REPORT SEPTEMBER 1988-SEPTEMBER 1989	
16. Abstract <i>DE</i> This report describes the development of the Intermediate Maneuver Induced Rollover Simulation (IMIRS) which can be used to investigate the phenomenon of maneuver induced rollover of light vehicles. The IMIRS represents an enhancement of the existing Lateral Weight Transfer Simulation (LWTS) and is capable of investigating cornering, cornering and braking, and cornering and accelerating limit maneuvers as well as vehicle skidding or spinning conditions. A rollover model added to the IMIRS simulation enables users to investigate the influence of vehicle design and environmental parameters on rollover stability.  The validation of the IMIRS simulation is provided in the report and is based on a comparison with vehicle experimental tests. The Fortran version of the IMIRS model is used to perform a time domain sensitivity analysis in four different vehicle maneuvers which include J-Turn without rollover, J-Turn with rollover, S-Turn without rollover and S-Turn with rollover. A complete description of the sensitivity results of vehicle's Rollover Prevention Energy Reserve (RPER) is presented in the report. The report also contains a user's manual with complete instructions for installation and use of the IMIRS simulation. ←				14. Sponsoring Agency Code NRD-51	
17. Key Words VEHICLE ROLLOVER VEHICLE DYNAMICS SENSITIVITY ANALYSIS			18. Distribution Statement  DOCUMENT IS AVAILABLE TO THE PUBLIC THROUGH THE NATIONAL TECHNICAL INFORMATION SERVICE, SPRINGFIELD, VIRGINIA 22161		
19. Security Classif. (of this report) UNCLASSIFIED		20. Security Classif. (of this page) UNCLASSIFIED		21. No. of Pages 168	22. Price



## PREFACE

The Office of Crash Avoidance Research of the U.S. Department of Transportation (DOT) has tasked Dr. Andrezej G. Nalecz, working under contract to the Research and Special Programs Administration of DOT, to develop a package of programs entitled Intermediate Maneuver Induced Rollover Simulation (IMIRS). These programs can be used to investigate the handling and stability properties of a wide range of passenger vehicles, light trucks, and utility vehicles under maneuver induced forces (non-tripped). A comparison with vehicle experimental tests is provided. A complete description of a vehicle's sensitivity results in different maneuvers is also included.

Preceding page blank

## METRIC / ENGLISH CONVERSION FACTORS

### ENGLISH TO METRIC

#### LENGTH (APPROXIMATE)

1 inch (in) = 2.5 centimeters (cm)  
 1 foot (ft) = 30 centimeters (cm)  
 1 yard (yd) = 0.9 meter (m)  
 1 mile (mi) = 1.6 kilometers (km)

#### AREA (APPROXIMATE)

1 square inch (sq in, in<sup>2</sup>) = 6.5 square centimeters (cm<sup>2</sup>)  
 1 square foot (sq ft, ft<sup>2</sup>) = 0.09 square meter (m<sup>2</sup>)  
 1 square yard (sq yd, yd<sup>2</sup>) = 0.8 square meter (m<sup>2</sup>)  
 1 square mile (sq mi, mi<sup>2</sup>) = 2.6 square kilometers (km<sup>2</sup>)  
 1 acre = 0.4 hectares (he) = 4,000 square meters (m<sup>2</sup>)

#### MASS - WEIGHT (APPROXIMATE)

1 ounce (oz) = 28 grams (gr)  
 1 pound (lb) = .45 kilogram (kg)  
 1 short ton = 2,000 pounds (lb) = 0.9 tonne (t)

#### VOLUME (APPROXIMATE)

1 teaspoon (tsp) = 5 milliliters (ml)  
 1 tablespoon (tbsp) = 15 milliliters (ml)  
 1 fluid ounce (fl oz) = 30 milliliters (ml)  
 1 cup (c) = 0.24 liter (l)  
 1 pint (pt) = 0.47 liter (l)  
 1 quart (qt) = 0.96 liter (l)  
 1 gallon (gal) = 3.8 liters (l)  
 1 cubic foot (cu ft, ft<sup>3</sup>) = 0.03 cubic meter (m<sup>3</sup>)  
 1 cubic yard (cu yd, yd<sup>3</sup>) = 0.76 cubic meter (m<sup>3</sup>)

#### TEMPERATURE (EXACT)

$$[(x - 32)(5/9)]^{\circ}\text{F} = y^{\circ}\text{C}$$

### METRIC TO ENGLISH

#### LENGTH (APPROXIMATE)

1 millimeter (mm) = 0.04 inch (in)  
 1 centimeter (cm) = 0.4 inch (in)  
 1 meter (m) = 3.3 feet (ft)  
 1 meter (m) = 1.1 yards (yd)  
 1 kilometer (km) = 0.6 mile (mi)

#### AREA (APPROXIMATE)

1 square centimeter (cm<sup>2</sup>) = 0.16 square inch (sq in, in<sup>2</sup>)  
 1 square meter (m<sup>2</sup>) = 1.2 square yards (sq yd, yd<sup>2</sup>)  
 1 square kilometer (km<sup>2</sup>) = 0.4 square mile (sq mi, mi<sup>2</sup>)  
 1 hectare (he) = 10,000 square meters (m<sup>2</sup>) = 2.5 acres

#### MASS - WEIGHT (APPROXIMATE)

1 gram (gr) = 0.036 ounce (oz)  
 1 kilogram (kg) = 2.2 pounds (lb)  
 1 tonne (t) = 1,000 kilograms (kg) = 1.1 short tons

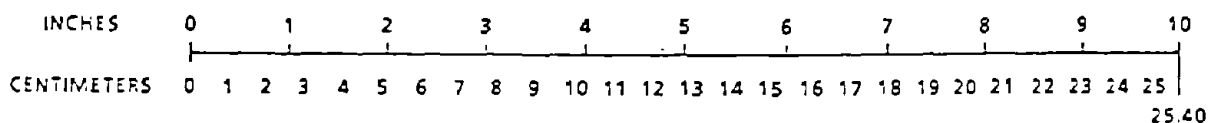
#### VOLUME (APPROXIMATE)

1 milliliter (ml) = 0.03 fluid ounce (fl oz)  
 1 liter (l) = 2.1 pints (pt)  
 1 liter (l) = 1.06 quarts (qt)  
 1 liter (l) = 0.26 gallon (gal)  
 1 cubic meter (m<sup>3</sup>) = 36 cubic feet (cu ft, ft<sup>3</sup>)  
 1 cubic meter (m<sup>3</sup>) = 1.3 cubic yards (cu yd, yd<sup>3</sup>)

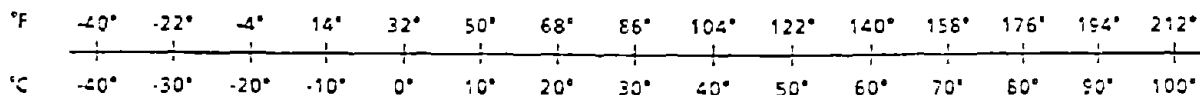
#### TEMPERATURE (EXACT)

$$[(9/5)y + 32]^{\circ}\text{C} = x^{\circ}\text{F}$$

### QUICK INCH-CENTIMETER LENGTH CONVERSION



### QUICK FAHRENHEIT-CELCIUS TEMPERATURE CONVERSION



For more exact and/or other conversion factors, see NBS Miscellaneous Publication 286, Units of Weights and Measures. Price \$2.50. SD Catalog No. C13 10 286.



## CONTENTS

<u>Section</u>	<u>Page</u>
1. USER'S MANUAL . . . . .	1
1.1 General Information . . . . .	1
1.2 Software Requirements And Installation . . . . .	3
1.3 Program Execution . . . . .	7
1.4 Sample Results . . . . .	20
2. DEVELOPMENT OF IMIRS SIMULATION . . . . .	38
2.1 Introduction . . . . .	38
2.2 IMIRS Model Description . . . . .	39
2.2.1 IMIRS Handling Model . . . . .	42
2.2.2 IMIRS Rollover Model . . . . .	56
2.3 Validation of IMIRS Simulation . . . . .	73
3. APPLICATION OF IMIRS SIMULATION . . . . .	80
3.1 Development of Fortran Version of IMIRS Model . . . . .	80
3.2 Dynamic Criteria to Assess Stability of Vehicles in Maneuver Induced Rollover Situations . . . . .	80
3.3 Sensitivity Analysis of IMIRS Model . . . . .	83
3.3.1 Parameter Sensitivity in J-Turn Maneuver Rollover Case . . . . .	83
3.3.2 Parameter Sensitivity in J-Turn Maneuver Non-Rollover Case . . . . .	85
3.3.3 Parameter Sensitivity in S-Turn Maneuver Rollover Case . . . . .	85
3.3.4 Parameter Sensitivity in S-Turn Maneuver Non-Rollover Case . . . . .	86
4. CONCLUSIONS AND RECOMMENDATIONS . . . . .	87
REFERENCES . . . . .	89
APPENDIX A - Illustrations of Suspension Systems . . . . .	A-1
APPENDIX B - Vehicle Data Used in Sensitivity Analysis . . . . .	B-1
APPENDIX C - Nomenclature Used in Sensitivity Plots. . . . .	C-1

LIST OF ILLUSTRATIONS

<u>Figure</u>	<u>Page</u>
1. IMIRS Handling Model . . . . .	39
2. IMIRS Rollover Model . . . . .	40
3. Notation Used in IMIRS Rollover Model . . . . .	42
4. Vehicle Components Which Store Potential Energy . . . . .	61
5. External Forces Applied to Planar Rollover Model. . . . .	68
6. Validation of IMIRS Simulation in J-Turn Handling Maneuver. . . . .	75
7. Steering Input Used in Validation of the IMIRS Simulation in Rollover and Non-Rollover Situations. . . . .	76
8. Comparison of Simulation and Experimental Lateral Accelerations in Rollover and Non-Rollover Situations . . . . .	77
9. Comparison of Simulation and Experimental Roll Angles in Rollover and Non-Rollover Situations . . . . .	78
10. Comparison of Simulation and Experimental Yaw Rates in Rollover and Non-Rollover Situations. . . . .	79
11. Steering Inputs Applied in J-Turn and S-Turn Maneuvers.	91
12. Vehicle Roll Angles in J-Turn Maneuver Rollover Case. . . . .	92
13. Vehicle Roll Angles in J-Turn Maneuver Non-Rollover Case . . . . .	93
14. Vehicle Roll Angles in S-Turn Maneuver Rollover Case. . . . .	94
15. Vehicle Roll Angles in S-Turn Maneuver Non-Rollover Case . . . . .	95
16. RPER in J-Turn Maneuver Rollover and Non-Rollover Cases	96
17. RPER in S-Turn Maneuver Rollover and Non-Rollover Cases	97
18. Percentage Sensitivity of RPER for Geometric Parameter Set #1 in J-Turn Maneuver Rollover. . . . .	98
19. Percentage Sensitivity of RPER for Geometric Parameter Set #2 in J-Turn Maneuver Rollover. . . . .	99
20. Percentage Sensitivity of RPER for Mass Parameter Set in J-Turn Maneuver Rollover . . . . .	100
21. Percentage Sensitivity of RPER for Stiffness Parameter Set in J-Turn Maneuver Rollover . . . . .	101
22. Percentage Sensitivity of RPER for Damping Parameter Set in J-Turn Maneuver Rollover . . . . .	102
23. Percentage Sensitivity of RPER for Aerodynamic Parameter Set in J-Turn Maneuver Rollover . . . . .	103
24. Percentage Sensitivity of RPER for Tire Frictional Parameter Set in J-Turn Maneuver Rollover . . . . .	104
25. Percentage Sensitivity of RPER for Geometric Parameter Set #1 in J-Turn Maneuver Non-Rollover . . . . .	105
26. Percentage Sensitivity of RPER for Geometric Parameter Set #2 in J-Turn Maneuver Non-Rollover . . . . .	106
27. Percentage Sensitivity of RPER for Mass Parameter Set in J-Turn Maneuver Non-Rollover . . . . .	107
28. Percentage Sensitivity of RPER for Stiffness Parameter Set in J-Turn Maneuver Non-Rollover . . . . .	108
29. Percentage Sensitivity of RPER for Damping Parameter Set in J-Turn Maneuver Non-Rollover . . . . .	109
30. Percentage Sensitivity of RPER for Aerodynamic Parameter Set in J-Turn Maneuver Non-Rollover . . . . .	110



LIST OF ILLUSTRATIONS (CONTINUED)

<u>Figure</u>	<u>Page</u>
31. Percentage Sensitivity of RPER for Tire Frictional Parameter Set in J-Turn Maneuver Non-Rollover . . . . .	111
32. Percentage Sensitivity of RPER for Geometric Parameter Set #1 in S-Turn Maneuver Rollover. . . . .	112
33. Percentage Sensitivity of RPER for Geometric Parameter Set #2 in S-Turn Maneuver Rollover. . . . .	113
34. Percentage Sensitivity of RPER for Mass Parameter Set in S-Turn Maneuver Rollover . . . . .	114
35. Percentage Sensitivity of RPER for Stiffness Parameter Set in S-Turn Maneuver Rollover . . . . .	115
36. Percentage Sensitivity of RPER for Damping Parameter Set in S-Turn Maneuver Rollover . . . . .	116
37. Percentage Sensitivity of RPER for Aerodynamic Parameter Set in S-Turn Maneuver Rollover . . . . .	117
38. Percentage Sensitivity of RPER for Tire Frictional Parameter Set in S-Turn Maneuver Rollover . . . . .	118
39. Percentage Sensitivity of RPER for Geometric Parameter Set #1 in S-Turn Maneuver Non-Rollover . . . . .	119
40. Percentage Sensitivity of RPER for Geometric Parameter Set #2 in S-Turn Maneuver Non-Rollover . . . . .	120
41. Percentage Sensitivity of RPER for Mass Parameter Set in S-Turn Maneuver Non-Rollover . . . . .	121
42. Percentage Sensitivity of RPER for Stiffness Parameter Set in S-Turn Maneuver Non-Rollover . . . . .	122
43. Percentage Sensitivity of RPER for Damping Parameter Set in S-Turn Maneuver Non-Rollover . . . . .	123
44. Percentage Sensitivity of RPER for Aerodynamic Parameter Set in S-Turn Maneuver Non-Rollover . . . . .	124
45. Percentage Sensitivity of RPER for Tire Frictional Parameter Set in S-Turn Maneuver Non-Rollover . . . . .	125



# 1. IMIRS USER'S MANUAL

## 1.1 GENERAL INFORMATION

The Intermediate Maneuver Induced Rollover Simulation (IMIRS) represents a package of computer programs which can be used to investigate the handling and stability properties of a wide range of passenger vehicles, light trucks, and utility vehicles. The package is capable of accurately predicting vehicle directional response (the forward, lateral and yawing degrees of freedom), as well as vehicle rolling motion (the roll angles of sprung and unsprung masses as well as the relative translation between sprung and unsprung masses). The tire model utilized in the IMIRS is based on the non-dimensional approach and is capable of operating over a very wide regime of operating conditions (i.e. slip angle, normal load, and slip ratio.) This model uses tire data which is currently available for a wide variety of different tires. Eight different kinematic configurations of front suspension systems can be employed in conjunction with any one of 19 different rear independent and dependent suspension systems. The user may investigate vehicle response using a variety of different steering and braking input signals including (but not limited to) step, ramp and sinusoidal inputs. These inputs may be stored for subsequent simulation runs.

The IMIRS represents an enhanced version of the Lateral Weight Transfer Simulation (LWTS) developed by Dr. A.G. Nalecz [1], [2] in 1986 (NHTSA-U.S. DOT Contract No. DTNH22-86-P-07326). The following additions and improvements have been made in this newer version:

- \* The ability to simulate vehicle skidding motion after the tire limits of adhesion have been reached.
- \* The ability to simulate maneuver induced vehicle rollover.
- \* Separate roll degrees of freedom for sprung and unsprung masses.
- \* A more sophisticated braking model which uses slip ratio to determine braking force.
- \* The use of additional Calspan tire data to determine tire aligning moment, camber thrust, sliding friction, and the slip ratio at peak braking as functions of tire normal and side load.

- \* The additional choice of step, ramp, sinusoidal, or arbitrary steering inputs. These inputs can be stored and recalled for later runs.
- \* The additional choice of step, ramp or arbitrary braking/thrust inputs which can be stored and recalled for later runs.
- \* The addition of simple aerodynamics to compute the affects of airflow on vehicle yaw.
- \* Complete graphics support for CGA, EGA, and VGA graphics cards, partial support for Hercules graphics cards.

The entire software package is menu driven (using menus identical to those employed in the LWTS) and requires a minimum of computer expertise on the part of the user. The user need only be familiar with rudimentary vehicle dynamics terminology in order to effectively use the software.

NOTE

Skid number (SN) used in this report is defined as a ratio of the skid number of the simulated surface to the skid number of the surface on which tire characteristics were measured multiplied by 100.

$$SN = \frac{\text{skid number of simulated surface}}{\text{skid number of tested surface}} \times 100$$

## 1.2 SOFTWARE REQUIREMENTS AND INSTALLATION

### System Requirements

The IMIRS requires the following hardware:

- \* An IBM-PC (or compatible) with 640 Kb of RAM
- \* Graphics Capability (CGA, EGA, VGA, or Hercules)
- \* A Hard Drive, or
  - 1.44M 3 1/2" High Density Drive or
  - 1.2M 5 1/4" High Density Drive.

For best results the following additional hardware is recommended:

- \* A math coprocessor chip
- \* A dot matrix printer

### Installation Procedure

The IMIRS comes on three (3) 5 1/4" DSDD disks. Copies on one (1) 3 1/2" high density (1.44M) microfloppy disk are available if requested.

The IMIRS routines can be installed on a hard drive, a 3 1/2" high density (1.44M) microfloppy disk, or a 1.2M 5 1/4" DSHD disk. To install the IMIRS software on any of the media listed above the user should insert disk 1 into drive B and type:

```
B>INSTALL
```

The installation program will then prompt the user for drive and directory where the software is to be installed. (Please note that the installation program will create this directory and it should not already exist on the selected drive.) Once a valid drive and directory name has been entered then the installation program creates the directory on the selected drive and begins copying files from disk 1 to the selected drive. After these files have been copied the installation program prompts the user to insert disk 2 into drive B and to press 'C' to continue. Once this step has been completed the installation program copies the files from disk 2 onto the selected drive and prompts the user to insert disk 3 into drive B, and to press 'C' to continue. After the installation program has copied the files from disk 3 onto the selected drive it prompts the user to select the type of graphics adapter which is installed on the computer.

The user should type 'A' if its computer is equipped with a CGA, EGA, or VGA graphics adapter, and the user should type 'B' in case its computer is equipped with a Hercules (Monochrome) graphics adapter. Once the user has made his selection the installation process is complete.

(Note for Hercules Users: The IMIRS programs contain some graphics statements which are not supported by Hercules graphics adapters. The programs will run without error in these sections, however, some images which are normally displayed on CGA, EGA, and VGA monitors will not appear on Hercules monitors. In these instances the user must refer to the manual for reference.)

The following list contains files that are supplied on the disk 1:

BEGIN	EXE	- starts simulation, provides the main menu
BRUN45	EXE	- QuickBasic runtime module
DATA	EXE	- allows user to enter data and print format
FRONTA	EXE	- control arms (converging towards car center)
FRONTB	EXE	- control arms (converging away from car center)
FRONTC	EXE	- parallel upper and lower control arms
FRONTD	EXE	- Macpherson strut
FRONTE	EXE	- trailing link
FRONTF	EXE	- twin I-beam
FRONTG	EXE	- sliding pillar
FRONTH	EXE	- live hotchkiss drive
GRPONEA	EXE	- hotchkiss drive
GRPONEB	EXE	- torque tube with Panhard rod
GRPONEC	EXE	- three link with Panhard rod
GRPONED	EXE	- four link with parallel lower links
GRPONEE	EXE	- four link with non-parallel lower links
GRPONEF	EXE	- beam twist axle with Panhard rod FWD
INSTALL	EXE	- software installation routine

Disk 2 contains the following files:

FRONT	EXE	- chains front suspensions
GRPONEG	EXE	- rear wheel drive with sideways location on axle
GRPONEH	EXE	- De Dion axle
GRPONEI	EXE	- beam axle with lateral locating device
GRPTWOA	EXE	- swing axle
GRPTWOB	EXE	- low pivot swing axle
GRPTWOC	EXE	- single transverse a-arms for FWD
GRPTWOD	EXE	- single trailing arm
GRPTWOE	EXE	- semi-trailing
GRPTWOF	EXE	- Chapman strut
GRPTWOG	EXE	- semi-independent for FWD
GRPTWOH	EXE	- Weissach axle
GRPTWOI	EXE	- control arms (converging towards car center)
GRPTWOJ	EXE	- control arms (converging away from car center)
MODEL	EXE	- transient simulation, non-linear tire model

PIC EXE - draws vehicle with roll axis  
 REAR EXE - chains rear suspensions

Disk 3 (the data disk) contains the following files:

FRONTA PIC - picture for fronta, grptwoi, grptwoh  
 FRONTB PIC - picture for frontb, grptwoj  
 FRONTC PIC - picture for frontc  
 FRONTD PIC - picture for frontd  
 FRONTE PIC - picture for fronte  
 FRONTF PIC - picture for frontf  
 FRONTG PIC - picture for frontg  
 FRONTH PIC - picture for fronth, grponea  
 GRPONED PIC - picture for grponea, grponeb, grponec, grponed,  
 grponee, grponeg, grptwoe  
 GRPONEF PIC - picture for grponef  
 GRPONEH PIC - picture for grponeh  
 GRPTWOA PIC - picture for grptwoa  
 GRPTWOB PIC - picture for grptwob  
 GRPTWOC PIC - picture for grptwoc  
 GRPTWOD PIC - picture for grptwod  
 GRPTWOF PIC - picture for grptwof  
 GRPTWOG PIC - picture for grptwog  
 MSHERC COM - utilizes Hercules video graphics card  
 GRAPHICS COM - for graphical output on the printer  
 SAMPLE1 DAT - sample data file in metric units  
 SAMPLE2 DAT - sample data file in English units

The following list contains files that are supplied on the source disk:

BEGIN BAS - source code to begin.exe  
 FRONT BAS - source code to front.exe  
 REAR BAS - source code to rear.exe  
 PIC BAS - source code to pic.exe  
 DATA BAS - source code to data.exe  
 MODEL BAS - source code to model.exe  
 INSTALL BAS - source code to install.exe  
 FRONTA BAS - source code to fronta.exe  
 FRONTB BAS - source code to frontb.exe  
 FRONTC BAS - source code to frontc.exe  
 FRONTD BAS - source code to frontd.exe  
 FRONTE BAS - source code to fronte.exe  
 FRONTF BAS - source code to frontf.exe  
 FRONTG BAS - source code to frontg.exe  
 FRONTH BAS - source code to fronth.exe  
 GRPONEA BAS - source code to grponea.exe  
 GRPONEB BAS - source code to grponeb.exe  
 GRPONEC BAS - source code to grponec.exe  
 GRPONED BAS - source code to grponed.exe  
 GRPONEE BAS - source code to grponee.exe  
 GRPONEF BAS - source code to grponef.exe  
 GRPONEG BAS - source code to grponeg.exe

GRPONEH BAS - source code to grponeh.exe  
GRPONEI BAS - source code to grponei.exe  
GRPTWOA BAS - source code to grptwoa.exe  
GRPTWOB BAS - source code to grptwob.exe  
GRPTWOC BAS - source code to grptwoc.exe  
GRPTWOD BAS - source code to grptwod.exe  
GRPTWOE BAS - source code to grptwoe.exe  
GRPTWOF BAS - source code to grptwof.exe  
GRPTWOG BAS - source code to grptwog.exe  
GRPTWOH BAS - source code to grptwoh.exe  
GRPTWOI BAS - source code to grptwoi.exe  
GRPTWOJ BAS - source code to grptwoj.exe



### 1.3 PROGRAM EXECUTION

To start software type BEGIN followed by return to execute the begin.exe program. (Note for Hercules Users: If your computer is equipped with a Hercules display adapter then resident program MSHERC.COM must run prior to starting program execution). The following choices are presented:

R - REVISE EXISTING DATA FILE  
S - START SIMULATION USING AN EXISTING DATA FILE  
C - CREATE NEW DATA FILE  
E - END PROGRAM

For an example of a simulation run, type the letter S. Note that the program does not require the S to be followed by the return key. The following screen is then displayed:

E - ENHANCED GRAPHICS  
S - STANDARD GRAPHICS

If your computer is equipped with an EGA or VGA display adapter you can press E and take advantage of the higher resolution of these monitors. If your computer is equipped with a CGA or Hercules display adapter then you may only display graphics in the Standard mode. If your computer is using a version of DOS issued prior to version 4.0 (i.e. 2.10, 3.10, 3.20, 3.30, ect.) then it should be noted that the graphics screen dump to the printer (obtained using the print screen key and program GRAPHICS.COM) may not be supported in the enhanced graphics screen mode. If your computer is equipped with an EGA or VGA display adapter and is running under a version of DOS issued prior to version 4.0 you must select the standard graphics mode if you desire hard copy of the graphic output. If your computer is equipped with a CGA or Hercules display adapter and enhanced graphics are chosen no error will occur, however the resolution will be identical to that obtained in the standard mode.

Now program will list all the vehicle data files on the disk and prompt the user to enter the file to run. Type in sample1 as follows:

ENTER FILENAME ( ONLY ) OF THE FILE YOU WISH TO RUN  
[A:<FN>.DAT] sample1

and hit return. Thus the program will run the vehicle data file sample1.dat.

Type in a filename so the program can create a printer output file. For example type the filename sample1,

ENTER FILENAME ( ONLY ) FOR PRINTER FILE  
[A:<FN>.PRN] sample1

and hit return. The program will create a file sample1.prn. This file can later be copied to the printer using a command

COPY SAMPLE1.PRN PRN:

Next, enter the vehicle's initial speed:

INITIAL SPEED FOR TEST [m/s] 25

The following screen then appears:

\*\*\* STEERING SELECTION \*\*\*

- 1) STEP INPUT
- 2) RAMP INPUT
- 3) SINUSOIDAL INPUT
- 4) OTHER
- 5) READ FROM DATA FILE
- 6) OTHER

INPUT THE NUMBER OF YOUR CHOICE (1-6)

Enter 1 for step input, the following questions will then appear, answer them as shown below:

ENTER THE TIME OF STEP STEERING APPLICATION (SEC) 0

ENTER THE MAGNITUDE OF THE FRONT WHEEL STEERING ANGLE (DEG) 6

The following screen will then appear:

\*\*\* BRAKING SELECTION \*\*\*

- 1) STEP INPUT
- 2) RAMP INPUT
- 3) OTHER
- 4) READ FROM FILE
- 5) NONE

INPUT THE NUMBER OF YOUR CHOICE (1-5)

Enter 5 for no braking input.

The following questions will then appear, answer them as shown below:

ENTER THE TIME STEP SIZE FOR INTEGRATION .01

ENTER TIME INCREMENT FOR PRINTING .2

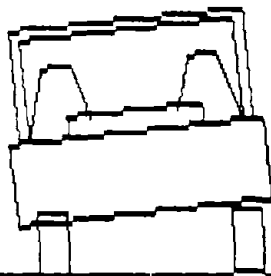
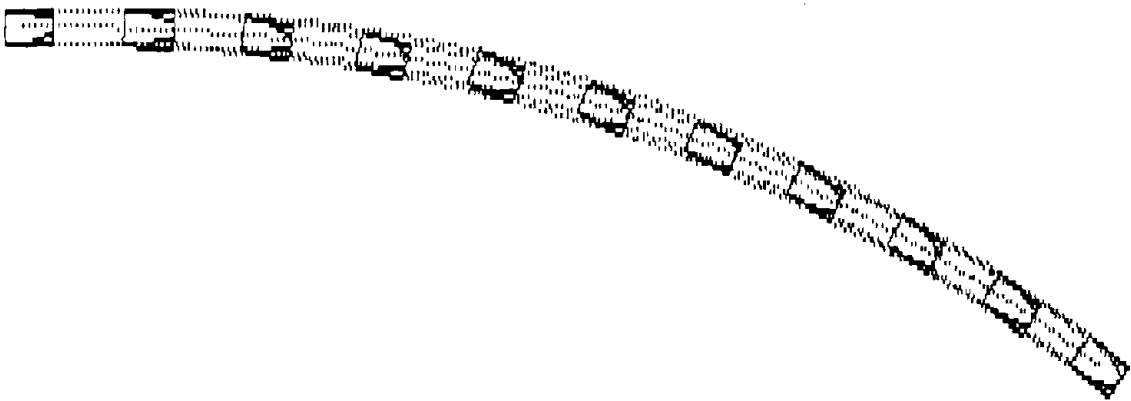
ENTER TOTAL RUN TIME FOR TEST 2

IS DATA CORRECT Y OR N ? Y

The simulation proceeds with the following final result:

Yaw angle = 38.48 deg      X-Path = 45.34 meters      Y-Path = 12.87 meters

Total velocity = 82.00 KPH      Steer angle = 6.00 deg      Time = 2.00 sec  
\*\*\*\*\* TIME \*\*\*\*\*



Scale: 1cm = 2.63 meters, Press Q to quit

Note to print this result it can be screen dumped with the print screen key. The MS-DOS GRAPHICS command must be issued before the screen dump is performed. See your MS-DOS reference manual for more information on the graphics command. After the simulation starts flashing \*\*\*\*\* TIME \*\*\*\*\* push any key and the following prompt will appear at the bottom of the screen:

Do you want another run ?

Hit return, which is equivalent to typing a Y. Note that after each run the program returns to the main menu:

R - REVISE EXISTING DATA FILE  
S - START SIMULATION USING AN EXISTING DATA FILE  
C - CREATE NEW DATA FILE  
E - END PROGRAM

### Revision of Vehicle Data And Output Data Files

This time type R to revise a vehicle data file. Type in also the filename of the data file to revise. For example type sample1,

ENTER FILENAME ( ONLY ) OF FILE TO REVISE  
[A:<FN>.DAT] sample1

and hit return. Now enter any filename up to 8 characters in length. For example, type sample3,

ENTER FILENAME ( ONLY ) FOR REVISED VERSION  
[A:<FN>.DAT] sample3

and hit return. Note that if sample1 was typed above instead of sample3 then any changes would replace the old sample1 version. Typing sample3 simply copies the sample1 version so that any changes would be in the sample3 data file only. Now the screen offers the following choices:

- S - SI UNITS [METERS]
- E - ENGLISH UNITS [INCHES]

Type the letter S to select SI units. Note that sample3 will be a revised version of sample1, where sample1 was already in SI units. The screen offers the following choices:

- F - PICK NEW FRONT SUSPENSION
- R - PICK NEW REAR SUSPENSION
- U - PICK NEW UNITS
- C - CONTINUE PROGRAM
- S - START SIMULATION
- E - END PROGRAM

Since sample3.dat is a copy of sample1.dat it would be possible to run sample3 without any changes. However, let's make some changes to the file. Type the letter F to select a new front suspension. The following choices appear:

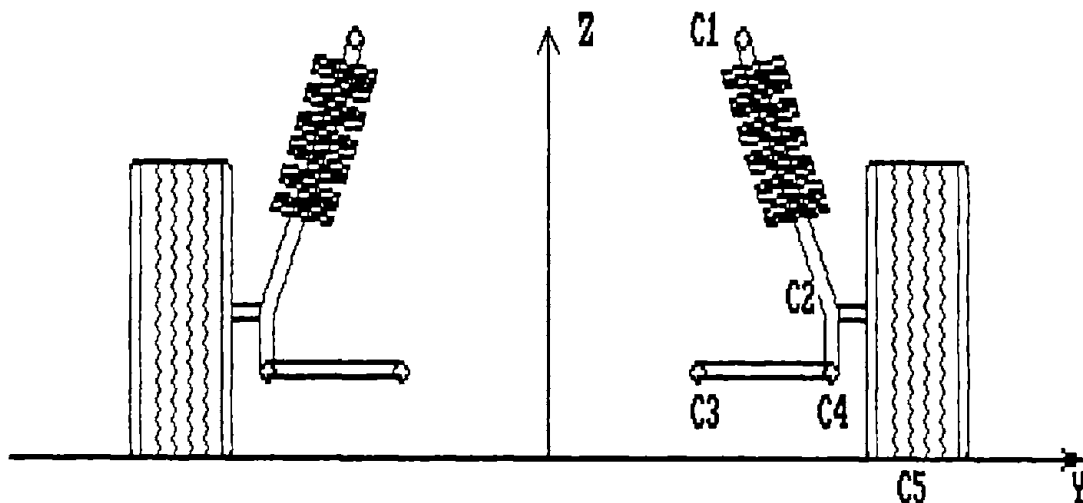
- A - UPPER AND LOWER CONTROL ARMS (CONVERGING TOWARDS CAR CENTER)
- B - UPPER AND LOWER CONTROL ARMS (CONVERGING AWAY FROM CAR CENTER)
- C - PARALLEL UPPER AND LOWER CONTROL ARMS
- D - MACPHERSON STRUT
- E - TRAILING LINK
- F - TWIN I-BEAM
- G - SLIDING PILLAR
- H - LIVE HOTCHKISS DRIVE
- I - NONE
- J - END PROGRAM

Now type the letter D to select the MacPherson Strut. Make sure the files from the data disk are present or an error will result. A picture of the selected suspension will appear on the screen.

(Note for Hercules Users: This image cannot be displayed on computers equipped with Hercules display adapters. Hercules users must consult the illustrations contained in Appendix A of this report.)

### MACPHERSON STRUT

ENTER FOR C1: C1X, C1Y, C1Z 2.6, 0.55, 0.70  
ENTER FOR C2: C2X, C2Y, C2Z 2.6, 0.60, 0.30  
ENTER FOR C3: C3X, C3Y, C3Z 2.6, 0.45, 0.20  
ENTER FOR C4: C4X, C4Y, C4Z 2.6, 0.60, 0.18  
ENTER FOR C5: C5X, C5Y 2.6, 0.70



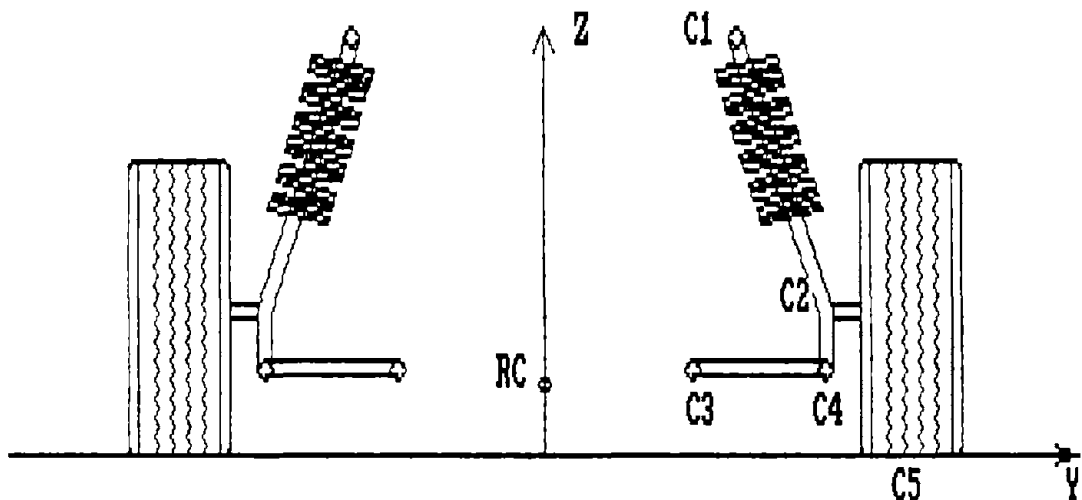
IS DATA CORRECT Y OR N

Type the letter N to the prompt. Note the program returns back to the front suspension menu. This feature allows the user to view any suspension without entering in any data. There is no danger in viewing the different suspensions because no changes will be made to the data file. Now type the letter D again for the MacPherson strut suspension. This time hit return to the prompt. Enter the data as shown below and hit return. If the input data is correct, the position of suspension roll center is determined as shown:

(Note for Hercules Users: This image cannot be displayed on computers equipped with Hercules display adapters. Hercules users must consult the illustrations contained in Appendix A of this manual.)

MACPHERSON STRUT

ENTER FOR C1: C1X,C1Y,C1Z 2.6, 0.55, 0.70  
ENTER FOR C2: C2X,C2Y,C2Z 2.6, 0.60, 0.30  
ENTER FOR C3: C3X,C3Y,C3Z 2.6, 0.45, 0.20  
ENTER FOR C4: C4X,C4Y,C4Z 2.6, 0.60, 0.18  
ENTER FOR C5: C5X,C5Y 2.6, 0.70



ROLL CENTER RC [ 2.6000, 0.0000, 0.1479]

Note that the x values are co-planar and are measured from the rear axle. The value of 2.6 above will be used for the wheel base of the vehicle and  $2 \times 0.7$  will be used for the front track width. Once the roll center is displayed hit any key to clear the screen. Type the letter R to select a rear suspension. Select a non-independent suspension by typing the letter N and the following list will be displayed:

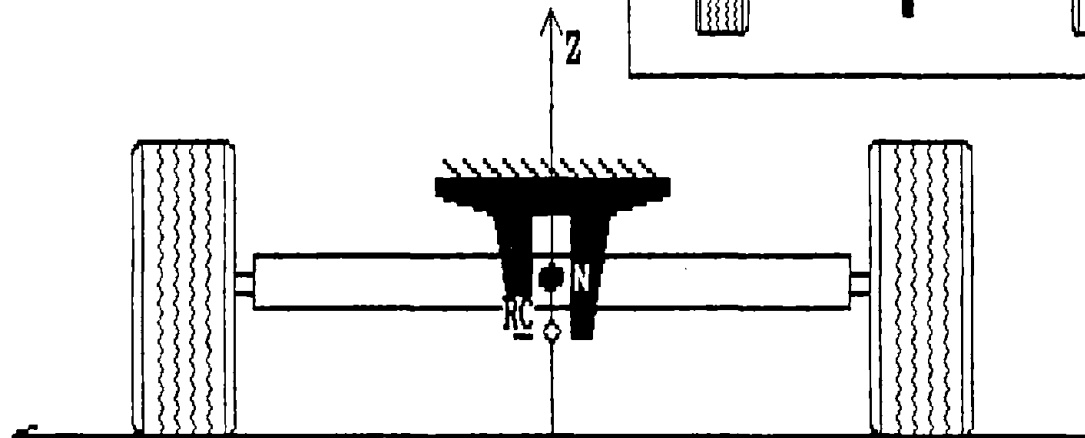
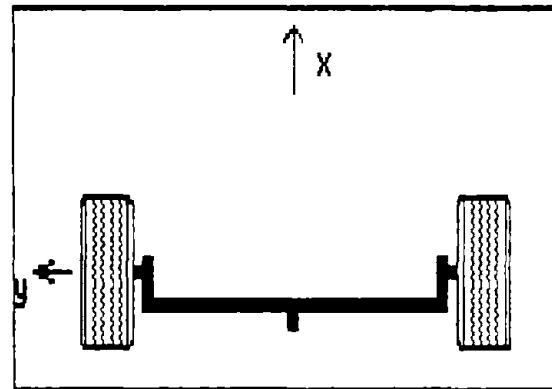


- A - HOTCHKISS DRIVE
- B - TORQUE TUBE WITH PANHARD ROD
- C - THREE LINK WITH PANHARD ROD
- D - FOUR LINK WITH PARALLEL LOWER LINKS
- E - FOUR LINK WITH NON-PARALLEL LOWER LINKS
- F - BEAM TWIST AXLE WITH PANHARD ROD FWD
- G - REAR WHEEL DRIVE WITH SIDEWAYS LOCATION ON THE CENTER OF AXLE
- H - DE DION AXLE
- I - BEAM AXLE WITH LONGITUDINAL LEAF SPRINGS AND LATERAL LOCATING DEVICE
- J - NONE
- K - END PROGRAM

Type the letter H to select the De Dion axle and hit return at the prompt. Enter the data as follows and hit return, if the data is correct, to find the roll center:

### DE DION AXLE

ENTER REAR TRACK WIDTH 1.38  
 ENTER FOR N: NZ 0.22



ROLL CENTER RC [ 0.0000, 0.0000, 0.2200]

Now the Macpherson strut and the De Dion axle have been selected as the front and rear suspensions, respectively. Hit any key to clear the screen. Type the letter C to continue the program and the following will appear:

ENTER FOLLOWING PARAMETERS:

SPRUNG MASS CG HEIGHT 0.6930  
DISTANCE FROM SPRUNG MASS CG TO FRONT AXLE 1.034  
GRAPHICS JEEP [J] OR CAR [C] J

Type the letter N to the prompt and enter the data as follows:

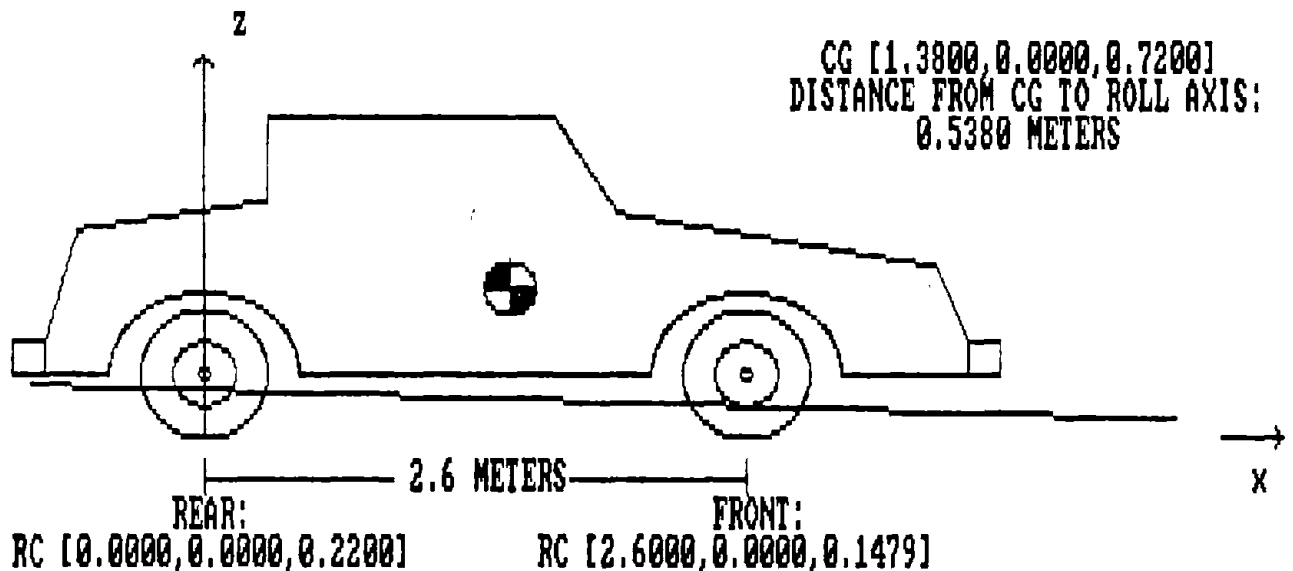
SPRUNG MASS CG HEIGHT 0.720  
DISTANCE FROM SPRUNG MASS CG TO FRONT AXLE 1.22  
GRAPHICS JEEP [J] OR CAR [C] C

Now hit return at the prompt and the following will appear on the screen:

ROLL AXIS USING FOLLOWING SUSPENSIONS:

FRONT SUSPENSION: MACPHERSON STRUT

REAR SUSPENSION: DE DION AXLE



Hit any key to clear the screen and type the letter C to continue the program. The following data menu will appear:

VEHICLE MASS -----	1014.0000 [kg]
VEHICLE SPRUNG MASS -----	778.1000 [kg]
DISTANCE FROM SPRUNG MASS C.G. TO FRONT AXLE -----	1.0340 [m]
DISTANCE FROM SPRUNG MASS C.G. TO ROLL AXIS -----	0.6072 [m]
HEIGHT OF SPRUNG MASS C.G. -----	0.6930 [m]
YAW MOMENT OF INERTIA -----	1175.5000 [kg*m^2]
ROLL MOMENT OF INERTIA OF SPRUNG MASS -----	240.2600 [kg*m^2]
ROLL MOMENT OF INERTIA OF UNSPRUNG MASS -----	71.8300 [kg*m^2]
AUXILIARY ROLL DAMPING OF FRONT AND REAR SUSPENSIONS --	0.0000 [Nm-s/rad]
WHEELBASE -----	2.0320 [m]
FRONT TRACK WIDTH -----	1.3081 [m]
REAR TRACK WIDTH -----	1.3081 [m]
UNSPRUNG MASS OF FRONT SUSPENSION -----	117.4800 [kg]
UNSPRUNG MASS OF REAR SUSPENSION -----	117.4800 [kg]
UNSPRUNG MASS CG HEIGHT OF FRONT SUSPENSION -----	0.3302 [m]
UNSPRUNG MASS CG HEIGHT OF REAR SUSPENSION -----	0.3302 [m]
FRONT SUSPENSION AUXILIARY ROLL STIFFNESS -----	3443.7300 [Nm/rad]
REAR SUSPENSION AUXILIARY ROLL STIFFNESS -----	5277.3301 [Nm/rad]
FRONT PROPORTION OF TOTAL VEHICLE ROLL STIFFNESS -----	0.5600 [-]
VERTICAL STIFFNESS OF TIRES -----	113140.000 [N/m]
VERTICAL DAMPING COEFFICIENT OF TIRE -----	980.000 [N-s/m]

Using the cursor keys allows the user to move through the data and edit any numbers. Push down the cursor key and hold it to see what happens. Next, position cursor to the vehicle sprung mass entry and hit the delete key. Now type the number 764 and then hit down the cursor key. Next, place cursor down and replace the front and rear unsprung masses with 120 and 130 respectively. After typing the 130 number, type the letter P to go to the next page of data, where the following will appear:

RATE OF CHANGE OF FRONT TIRE INCLINATION -----	-0.0400
RATE OF CHANGE OF REAR AXLE STEER -----	0.0000
FRACTION OF BRAKING TORQUE APPLIED TO FRONT WHEELS ----	0.6500
HEAVY BRAKING PROPORTIONALITY FACTOR FOR FRONT WHEELS -	0.2000
1 - FWD 2 - RWD 3 - 4WD -----	3
FRACTION OF DRIVING TORQUE APPLIED TO FRONT (4WD) -----	0.6000

\*\*\*\*\*TIRE DATA\*\*\*\*\*

TIRE SKID NUMBER	85.00		
A0 = -668.4600	A1 = 26.5400	A2 = 2146.6101	
A3 = 1.2740000	A4 = 2225.0701		
B1 = -6.7450E-04	B3 = 1.3070	B4 = 2.9530E-07	
P0 = 1.2073	P1 = -5.8430E-04	P2 = 3.9770E-07	
S0 = 1.17379999	S1 = -8.4580E-04	S2 = 3.9450E-07	
R0 = -0.23771000	R1 = 8.5360E-05		
K1 = -2.0610E-04	K2 = -1.7680E-04	K3 = 0.0740	
CTN = 6.000000	CA1 = 30.000000	CR1 = 0.300000	

Use the cursor and delete keys to change the tire skid number to 90, then type P to view the third and final page of data:

```
*****SUSPENSION PARAMETERS*****
SUSPENSION SPRING TRACK WIDTH ----- 0.9320 [m]
STATIC SUSPENSION SPRING LENGTH ----- 0.1016 [m]
UNDEFORMED BUMP STOP LENGTH ----- 0.0709 [m]
HEIGHT OF LOWER SUSPENSION SPRING MOUNT ABOVE GROUND -- 0.2032 [m]
COMBINED FRONT AND REAR SUSPENSION SPRING STIFFNESSES - 84850.00 [N/m]
COMBINED FRONT AND REAR BUMP STOP STIFFNESSES ----- 464030.0 [N/m]
COMBINED FRONT AND REAR SUSPENSION DAMPING COEFF. ----- 3000.0000 [N-s/m]
```

```
*****AERODYNAMIC PARAMETERS*****
VEHICLE FRONTAL AREA ----- 2.0000 [m^2]
CHARACTERISTIC HEIGHT OF VEHICLE ----- 1.5000 [m]
AERODYNAMIC SIDE FORCE COEFFICIENT ----- 1.0000000 [-]
AERODYNAMIC ALIGNING MOMENT COEFFICIENT ----- 2.5000000 [-]
AERODYNAMIC YAW DAMPING COEFFICIENT ----- 1000.0000 [N-m-s]
```

Move to cursor to vehicle frontal area and change its value to 2.400.

Please note that all of this data was originally copied from the sample1.dat file. If the "CREATE NEW DATA FILE" was selected, all this data would have to be entered in from scratch. Now type the letter C to continue the program where the following menu is offered:

- P - PAGE THROUGH DATA
- F - PICK NEW FRONT SUSPENSION
- R - PICK NEW REAR SUSPENSION
- O - SELECT NEW OUTPUT FORMAT
- S - START SIMULATION
- E - END PROGRAM

Now type the letter O and the following format menu will appear:

This routine allows the user to select the output format. Place a number in front of desired variable. The number that appears signifies the columnwise order that data will be printed. Only eleven (11) variables can be printed at one time.

1	TIME	,time	[s]	0	FZfl	,normal force fr. l.	[N]
3	U	,forward velocity	[m/s]	0	FZrr	,normal force r. rt.	[N]
4	LATV	,lateral velocity	[m/s]	0	FZrl	,normal force r. l.	[N]
5	YAWV	,yaw velocity	[rad/s]	0	SLIPfr	,slip ratio fr. rt.	[-]
7	HEADING	,heading of vehicle	[deg]	0	SLIPfl	,slip ratio fr. l.	[-]
0	Alphaf	,front slip angle	[deg]	0	SLIPrr	,slip ratio r. rt.	[-]
0	Alphar	,rear slip angle	[deg]	0	SLIPrl	,slip ratio r. l.	[-]
0	FYfr	,side force fr. rt.	[N]	8	PHIU	,unsprung roll angle	[deg]
0	FYfl	,side force fr. l.	[N]	9	PHISa	,absolute sprung roll	[deg]
0	FYrr	,side force r. rt.	[N]	10	PHISr	,relative sprung roll	[deg]
0	FYrl	,side force r. l.	[N]	0	TFWT	,weight transfer front	[N]
0	RADIUS	,radius of turn	[m]	0	TRWT	,weight transfer rear	[N]
6	ACC	,lateral acceleration	[g's]	0	FWTRCH	,by R.C. height front	[N]
0	BETABfr	,slip angle var. fr r.	[-]	0	RWTRCH	,by R.C. height rear	[N]
0	BETABfl	,slip angle var. fr l.	[-]	0	FWTBR	,by body roll front	[N]
0	BETABrr	,slip angle var. r. r.	[-]	0	RWTBR	,by body roll rear	[N]
0	BETABrl	,slip angle var. r. l.	[-]	2	STEER	,steer angle	[deg]
0	FZFr	,normal force fr. rt.	[N]	11	AX	,braking acceleration	[g's]

USE CURSOR AND DELETE KEYS TO ENTER NUMBERS. TYPE C TO CONTINUE

This routine allows the user to select the variables that will appear when the printer files (those with a .PRN filetype) are copied to the printer. For example, the format from above would look like the following:

TIME STEER U LATV YAWV ACC HEADING PHIU PHISa PHISr AX

Let's reconfigure the sample3.dat file by deleting the 6 in front of the variable ACC. Next, move the cursor to TFWT and delete the 0. Then press 2. The format of the printer output will now have the following form:

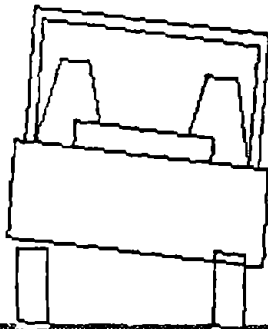
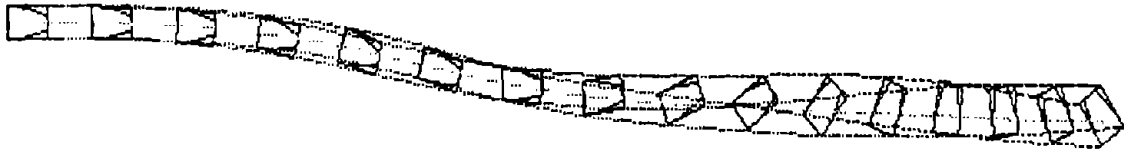
TIME STEER U LATV YAWV TFWT HEADING PHIU PHISa PHISr AX

Type the letter C to continue the program. Note that the program has many places where the choice to end the program is offered. There is no problem to end the program during a revision of a file. All revisions are saved automatically.

## 1.4 SAMPLE RESULTS

### Example 1

Yaw angle = -126.22 deg      X-Path = 57.01 meters      Y-Path = 3.80 meters  
Total velocity = 44.59 KPH      Steer angle = -15.00 deg      Time = 3.00 sec  
\*\*\*\*\* TIME \*\*\*\*\*



Front Rt. Tire Saturated  
Front Lf. Tire Locked & Saturated  
Rear Rt. Tire Locked & Saturated  
Rear Lf. Tire Locked & Saturated

Scale: 1cm = 3.28 meters, Press Q to quit

This run shows the response of a rear weight bias car with brakes biased toward the rear. The wheels are first steered 5 degrees to the right and then 15 degrees to the left. Heavy braking is applied at 1.5 seconds and the vehicle spins out. The vehicle data used in the simulation and numerical output obtained are shown below.

VEHICLE MASS -----	1014.0000	[kg]
VEHICLE SPRUNG MASS -----	778.1000	[kg]
DISTANCE FROM SPRUNG MASS C.G. TO FRONT AXLE -----	1.3000	[m]
DISTANCE FROM SPRUNG MASS C.G. TO ROLL AXIS -----	0.6034	[m]
HEIGHT OF SPRUNG MASS C.G. -----	0.6930	[m]
YAW MOMENT OF INERTIA -----	1175.5000	[kg*m^2]
ROLL MOMENT OF INERTIA OF SPRUNG MASS -----	240.2600	[kg*m^2]
ROLL MOMENT OF INERTIA OF UNSPRUNG MASS -----	71.8300	[kg*m^2]
AUXILARY ROLL DAMPING OF FRONT AND REAR SUSPENSIONS ---	0.0000	[Nm-s/rad]
WHEELBASE -----	2.0320	[m]
FRONT TRACK WIDTH -----	1.3081	[m]
REAR TRACK WIDTH -----	1.3081	[m]
UNSPRUNG MASS OF FRONT SUSPENSION -----	117.4800	[kg]
UNSPRUNG MASS OF REAR SUSPENSION -----	117.4800	[kg]
UNSPRUNG MASS CG HEIGHT OF FRONT SUSPENSION -----	0.3302	[m]
UNSPRUNG MASS CG HEIGHT OF REAR SUSPENSION -----	0.3302	[m]
FRONT SUSPENSION AUXILARY ROLL STIFFNESS -----	3443.7300	[Nm/rad]
REAR SUSPENSION AUXILARY ROLL STIFFNESS -----	5277.3301	[Nm/rad]
FRONT PROPORTION OF TOTAL VEHICLE ROLL STIFFNESS -----	0.5600	[-]
VERTICAL STIFFNESS OF TIRES -----	113140.000	[N/m]
VERTICAL DAMPING COEFFICIENT OF TIRE -----	980.000	[N-s/m]
RATE OF CHANGE OF FRONT TIRE INCLINATION -----	-0.0400	
RATE OF CHANGE OF REAR AXLE STEER -----	0.0000	
FRACTION OF BRAKING TORQUE APPLIED TO FRONT WHEELS ----	0.2000	
HEAVY BRAKING PROPORTIONALITY FACTOR FOR FRONT WHEELS -	0.0500	
1 - FWD 2 - RWD 3 - 4WD -----	3	
FRACTION OF DRIVING TORQUE APPLIED TO FRONT (4WD) -----	0.6000	

\*\*\*\*\*TIRE DATA\*\*\*\*\*

TIRE SKID NUMBER	70.00				
A0 =	-668.4600	A1 =	26.5400	A2 =	2146.6101
A3 =	1.2740000	A4 =	2225.0701		
B1 =	-6.7450E-04	B3 =	1.3070	B4 =	2.9530E-07
P0 =	1.2073	P1 =	-5.8430E-04	P2 =	3.9770E-07
S0 =	1.17379999	S1 =	-8.4580E-04	S2 =	3.9450E-07
R0 =	-0.23771000	R1 =	8.5360E-05		
K1 =	-2.0610E-04	K2 =	-1.7680E-04	K3 =	0.0740
CTN =	6.000000	CA1 =	30.000000	CR1 =	0.300000

\*\*\*\*\*SUSPENSION PARAMETERS\*\*\*\*\*

SUSPENSION SPRING TRACK WIDTH -----	0.9320	[m]
STATIC SUSPENSION SPRING LENGTH -----	0.1016	[m]
UNDEFORMED BUMP STOP LENGTH -----	0.0709	[m]
HEIGHT OF LOWER SUSPENSION SPRING MOUNT ABOVE GROUND --	0.2032	[m]
COMBINED FRONT AND REAR SUSPENSION SPRING STIFFNESSES -	84850.00	[N/m]
COMBINED FRONT AND REAR BUMP STOP STIFFNESSES -----	464030.0	[N/m]
COMBINED FRONT AND REAR SUSPENSION DAMPING COEFF. -----	3000.0000	[N-s/m]

\*\*\*\*\*AERODYNAMIC PARAMETERS\*\*\*\*\*

VEHICLE FRONTAL AREA -----	2.0000	[m^2]
CHARACTERISTIC HEIGHT OF VEHICLE -----	1.5000	[m]
AERODYNAMIC SIDEFORCE COEFFICIENT -----	0.3000000	[-]
AERODYNAMIC ALIGNING MOMENT COEFFICIENT -----	0.2000000	[-]
AERODYNAMIC YAW DAMPING COEFFICIENT -----	100.0000	[N-m-s]

COPYRIGHT (C) 1988 ANDRZEJ G. NALECZ. ALL RIGHTS RESERVED. THIS SOFTWARE  
 WAS FIRST PRODUCED IN PERFORMANCE OF CONTRACT DTRS57-88-P-82688  
 SPONSORED BY TSC/RSPA/U.S.DOT

VARIABLE STEERING INPUT STEP BRAKING INPUT = 0.70 [g's] STEP SIZE = 0.0100 [Sec]

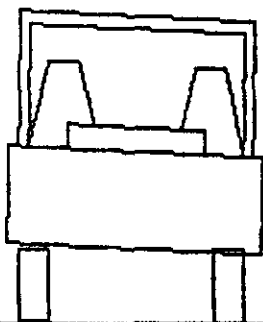
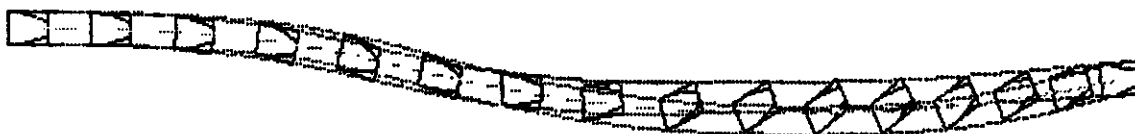
TIME	STEER	U	LATV	YAW	ACC	HEADING	PHIU	PHISa	PHISr	AX
0.2000	3.7997	21.9900	-0.0882	0.2137	0.2855	0.9050	-0.3092	-0.8398	-0.5306	-0.0131
0.4000	4.9996	21.9171	-0.8755	0.4753	0.5221	5.0404	-1.0414	-4.3428	-3.3013	-0.0215
0.6000	1.3999	21.7266	-2.0482	0.5545	0.6086	11.1214	-1.4774	-6.7174	-5.2399	-0.0055
0.8000	-6.5995	21.4955	-2.9995	0.3023	0.4145	16.5067	-0.9967	-4.9007	-3.9039	0.0023
1.0000	-14.9989	21.4694	-2.0777	-0.5892	0.0335	15.3766	-0.2174	-1.3207	-1.1032	-0.0708
1.2000	-14.9989	21.3776	1.3235	-1.0853	-0.6170	4.6737	1.0499	3.7345	2.6845	-0.0702
1.4000	-14.9989	20.6028	4.5448	-1.0560	-0.6787	-7.6722	2.1924	8.5870	6.3944	-0.0696
1.6000	-14.9989	18.7037	7.7728	-1.1687	-0.4044	-19.9493	0.8552	5.0522	4.1969	-0.5544
1.8000	-14.9989	15.3318	11.2641	-1.3218	-0.4133	-34.3310	0.2317	0.1022	-0.1295	-0.4395
2.0000	-14.9989	11.0638	13.9787	-1.4056	-0.4846	-50.0117	0.8583	3.0998	2.2414	-0.2549
2.2000	-14.9989	6.2678	15.4349	-1.4170	-0.5019	-66.3048	1.3364	6.7765	5.4399	-0.2243
2.4000	-14.9989	1.5806	15.4689	-1.3941	-0.5315	-82.3912	0.9746	4.6516	3.6769	-0.1246
2.6000	-14.9989	-2.3888	14.3038	-1.3010	-0.4967	-97.7960	0.8187	3.2208	2.4020	0.1719
2.8000	-14.9989	-5.3168	12.3544	-1.2269	-0.4969	-112.2222	1.0588	4.6637	3.6049	0.2748
3.0000	-14.9989	-7.4136	9.8511	-1.2143	-0.4413	-126.2157	1.0404	5.1344	4.0939	0.3601

TIME



Example 2

Yaw angle = -7.13 deg      X-Path = 57.72 meters      Y-Path = 1.91 meters  
Total velocity = 48.36 KPH      Steer angle = -15.00 deg      Time = 3.00 sec  
\*\*\*\*\* TIME \*\*\*\*\*



Front Rt. Tire Locked & Saturated  
Front Lf. Tire Locked & Saturated

Scale: 1cm = 3.28 meters, Press Q to quit

This run shows the response of a rear weight biased car with brakes biased toward the front. The wheels are first steered 5 degrees to the right and then 15 degrees to the left. Heavy braking is applied at 1.5 seconds. The vehicle demonstrates directional stability. The vehicle data used for the simulation and the numerical output are presented in next pages.

VEHICLE MASS -----	1014.0000	[kg]
VEHICLE SPRUNG MASS -----	778.1000	[kg]
DISTANCE FROM SPRUNG MASS C.G. TO FRONT AXLE -----	1.3000	[m]
DISTANCE FROM SPRUNG MASS C.G. TO ROLL AXIS -----	0.6034	[m]
HEIGHT OF SPRUNG MASS C.G. -----	0.6930	[m]
YAW MOMENT OF INERTIA -----	1175.5000	[kg*m^2]
ROLL MOMENT OF INERTIA OF SPRUNG MASS -----	240.2600	[kg*m^2]
ROLL MOMENT OF INERTIA OF UNSPRUNG MASS -----	71.8300	[kg*m^2]
AUXILARY ROLL DAMPING OF FRONT AND REAR SUSPENSIONS ---	0.0000	[Nm-s/rad]
WHEELBASE -----	2.0320	[m]
FRONT TRACK WIDTH -----	1.3081	[m]
REAR TRACK WIDTH -----	1.3081	[m]
UNSPRUNG MASS OF FRONT SUSPENSION -----	117.4800	[kg]
UNSPRUNG MASS OF REAR SUSPENSION -----	117.4800	[kg]
UNSPRUNG MASS CG HEIGHT OF FRONT SUSPENSION -----	0.3302	[m]
UNSPRUNG MASS CG HEIGHT OF REAR SUSPENSION -----	0.3302	[m]
FRONT SUSPENSION AUXILARY ROLL STIFFNESS -----	3443.7300	[Nm/rad]
REAR SUSPENSION AUXILARY ROLL STIFFNESS -----	5277.3301	[Nm/rad]
FRONT PROPORTION OF TOTAL VEHICLE ROLL STIFFNESS -----	0.5600	[-]
VERTICAL STIFFNESS OF TIRES -----	113140.000	[N/m]
VERTICAL DAMPING COEFFICIENT OF TIRE -----	980.000	[N-s/m]
RATE OF CHANGE OF FRONT TIRE INCLINATION -----	-0.0400	
RATE OF CHANGE OF REAR AXLE STEER -----	0.0000	
FRACTION OF BRAKING TORQUE APPLIED TO FRONT WHEELS ----	0.8000	
HEAVY BRAKING PROPORTIONALITY FACTOR FOR FRONT WHEELS -	0.0500	
1 - FWD 2 - RWD 3 - 4WD -----	3	
FRACTION OF DRIVING TORQUE APPLIED TO FRONT (4WD) -----	0.6000	

\*\*\*\*\*TIRE DATA\*\*\*\*\*

TIRE SKID NUMBER	70.00		
A0 = -668.4600	A1 = 26.5400	A2 = 2146.6101	
A3 = 1.2740000	A4 = 2225.0701		
B1 = -6.7450E-04	B3 = 1.3070	B4 = 2.9530E-07	
P0 = 1.2073	P1 = -5.8430E-04	P2 = 3.9770E-07	
S0 = 1.17379999	S1 = -8.4580E-04	S2 = 3.9450E-07	
R0 = -0.23771000	R1 = 8.5360E-05		
K1 = -2.0610E-04	K2 = -1.7680E-04	K3 = 0.0740	
CTN = 6.000000	CA1 = 30.000000	CR1 = 0.300000	

\*\*\*\*\*SUSPENSION PARAMETERS\*\*\*\*\*

SUSPENSION SPRING TRACK WIDTH -----	0.9320	[m]
STATIC SUSPENSION SPRING LENGTH -----	0.1016	[m]
UNDEFORMED BUMP STOP LENGTH -----	0.0709	[m]
HEIGHT OF LOWER SUSPENSION SPRING MOUNT ABOVE GROUND --	0.2032	[m]
COMBINED FRONT AND REAR SUSPENSION SPRING STIFFNESSES -	84850.00	[N/m]
COMBINED FRONT AND REAR BUMP STOP STIFFNESSES -----	464030.0	[N/m]
COMBINED FRONT AND REAR SUSPENSION DAMPING COEFF. -----	3000.0000	[N-s/m]

\*\*\*\*\*AERODYNAMIC PARAMETERS\*\*\*\*\*

VEHICLE FRONTAL AREA -----	2.0000	[m^2]
CHARACTERISTIC HEIGHT OF VEHICLE -----	1.5000	[m]
AERODYNAMIC SIDEFORCE COEFFICIENT -----	0.3000000	[-]
AERODYNAMIC ALIGNING MOMENT COEFFICIENT -----	0.2000000	[-]
AERODYNAMIC YAW DAMPING COEFFICIENT -----	100.0000	[N-m-s]

COPYRIGHT (C) 1988 ANDRZEJ G. NALECZ. ALL RIGHTS RESERVED. THIS SOFTWARE  
 WAS FIRST PRODUCED IN PERFORMANCE OF CONTRACT DTRS57-88-P-82688  
 SPONSORED BY TSC/RSPA/U.S.DOT

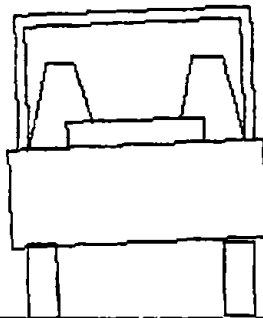
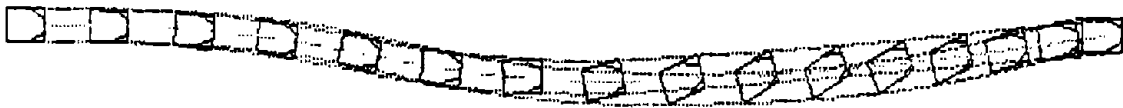
VARIABLE STEERING INPUT STEP BRAKING INPUT = 0.70 [g's] STEP SIZE = 0.0100 [Sec]

TIME	STEER	U	LATV	YAWV	ACC	HEADING	PHIU	PHISn	PHISr	AX
0.2000	3.7997	21.9900	-0.0882	0.2137	0.2855	0.9050	-0.3092	-0.8398	-0.5306	-0.0131
0.4000	4.9996	21.9171	-0.8755	0.4753	0.5221	5.0404	-1.0414	-4.3428	-3.3013	-0.0215
0.6000	1.3999	21.7266	-2.0482	0.5545	0.6086	11.1214	-1.4774	-6.7174	-5.2399	-0.0055
0.8000	-6.5995	21.4955	-2.9995	0.3023	0.4145	16.5067	-0.9967	-4.9007	-3.9039	0.0023
1.0000	-14.5989	21.4694	-2.0777	-0.5892	0.0335	15.3766	-0.2174	-1.3207	-1.1032	-0.0708
1.2000	-14.9989	21.3776	1.3235	-1.0853	-0.6170	4.6737	1.0499	3.7345	2.6845	-0.0702
1.4000	-14.9989	20.6028	4.5448	-1.0560	-0.6787	-7.6722	2.1924	8.5870	6.3944	-0.0696
1.6000	-14.9989	18.9869	7.3876	-0.8364	-0.4138	-18.9807	0.9436	5.2658	4.3221	-0.3775
1.8000	-14.9989	17.1662	8.9154	-0.5110	-0.4540	-26.6375	0.4007	0.9283	0.5276	-0.3613
2.0000	-14.9989	15.7947	9.1974	-0.2343	-0.4741	-30.8752	0.9101	3.5422	2.6321	-0.3511
2.2000	-14.9989	14.9171	8.5694	0.0202	-0.4779	-32.0909	1.1700	6.1295	4.9595	-0.3496
2.4000	-14.9989	14.4524	7.1960	0.2732	-0.4672	-30.4182	0.8536	4.1774	3.3238	-0.3566
2.6000	-14.9989	14.2380	5.1160	0.5473	-0.4422	-25.7495	0.7158	2.8109	2.0950	-0.3700
2.8000	-14.9989	14.0113	2.2767	0.8709	-0.3949	-17.6847	0.8924	3.9893	3.0969	-0.3856
3.0000	-14.9989	13.3883	-0.3605	0.8022	0.2496	-7.1344	0.1254	2.3148	2.1894	-0.3970

TIME

Example 3

Yaw angle = 0.19 deg      X-Path = 56.69 meters      Y-Path = 0.26 meters  
Total velocity = 41.91 KPH      Steer angle = -15.00 deg      Time = 3.00 sec  
\*\*\*\*\* TIME \*\*\*\*\*



Front Rt. Tire Saturated  
Front Lf. Tire Saturated  
Rear Rt. Tire Locked & Saturated  
Rear Lf. Tire Saturated

Scale: 1cm = 3.28 meters, Press Q to quit.

This run shows the response of a front weight biased car with brakes biased toward the front. The wheels are first steered 5 degrees to the right and then 15 degrees to the left. Heavy braking is applied at 1.5 seconds. The vehicle demonstrates improved directional stability when compared to the rear weight biased vehicle. The vehicle data used in the simulation and the numerical output are shown below.

VEHICLE MASS -----	1014.0000	[kg]
VEHICLE SPRUNG MASS -----	778.1000	[kg]
DISTANCE FROM SPRUNG MASS C.G. TO FRONT AXLE -----	0.7500	[m]
DISTANCE FROM SPRUNG MASS C.G. TO ROLL AXIS -----	0.6113	[m]
HEIGHT OF SPRUNG MASS C.G. -----	0.6930	[m]
YAW MOMENT OF INERTIA -----	1175.5000	[kg*m^2]
ROLL MOMENT OF INERTIA OF SPRUNG MASS -----	240.2600	[kg*m^2]
ROLL MOMENT OF INERTIA OF UNSPRUNG MASS -----	71.8300	[kg*m^2]
AUXILARY ROLL DAMPING OF FRONT AND REAR SUSPENSIONS -----	0.0000	[Nm-s/rad]
WHEELBASE -----	2.0320	[m]
FRONT TRACK WIDTH -----	1.3081	[m]
REAR TRACK WIDTH -----	1.3081	[m]
UNSPRUNG MASS OF FRONT SUSPENSION -----	117.4800	[kg]
UNSPRUNG MASS OF REAR SUSPENSION -----	117.4800	[kg]
UNSPRUNG MASS CG HEIGHT OF FRONT SUSPENSION -----	0.3302	[m]
UNSPRUNG MASS CG HEIGHT OF REAR SUSPENSION -----	0.3302	[m]
FRONT SUSPENSION AUXILARY ROLL STIFFNESS -----	3443.7300	[Nm/rad]
REAR SUSPENSION AUXILARY ROLL STIFFNESS -----	5277.3301	[Nm/rad]
FRONT PROPORTION OF TOTAL VEHICLE ROLL STIFFNESS -----	0.5600	[-]
VERTICAL STIFFNESS OF TIRES -----	113140.000	[N/m]
VERTICAL DAMPING COEFFICIENT OF TIRE -----	980.000	[N-s/m]
RATE OF CHANGE OF FRONT TIRE INCLINATION -----	-0.0400	
RATE OF CHANGE OF REAR AXLE STEER -----	0.0000	
FRACTION OF BRAKING TORQUE APPLIED TO FRONT WHEELS -----	0.8000	
HEAVY BRAKING PROPORTIONALITY FACTOR FOR FRONT WHEELS -	0.0500	
1 - FWD 2 - RWD 3 - 4WD -----	3	
FRACTION OF DRIVING TORQUE APPLIED TO FRONT (4WD) -----	0.6000	

\*\*\*\*\*TIRE DATA\*\*\*\*\*

TIRE SKID NUMBER	70.00		
A0 = -668.4600	A1 = 26.5400	A2 = 2146.6101	
A3 = 1.2740000	A4 = 2225.0701		
B1 = -6.7450E-04	B3 = 1.3070	B4 = 2.9530E-07	
P0 = 1.2073	P1 = -5.8430E-04	P2 = 3.9770E-07	
S0 = 1.17379999	S1 = -8.4580E-04	S2 = 3.9450E-07	
R0 = -0.23771000	R1 = 8.5360E-05		
K1 = -2.0610E-04	K2 = -1.7680E-04	K3 = 0.0740	
CTN = 6.000000	CA1 = 30.000000	CR1 = 0.300000	

\*\*\*\*\*SUSPENSION PARAMETERS\*\*\*\*\*

SUSPENSION SPRING TRACK WIDTH -----	0.9320	[m]
STATIC SUSPENSION SPRING LENGTH -----	0.1016	[m]
UNDEFORMED BUMP STOP LENGTH -----	0.0709	[m]
HEIGHT OF LOWER SUSPENSION SPRING MOUNT ABOVE GROUND --	0.2032	[m]
COMBINED FRONT AND REAR SUSPENSION SPRING STIFFNESSES -	84850.00	[N/m]
COMBINED FRONT AND REAR BUMP STOP STIFFNESSES -----	464030.0	[N/m]
COMBINED FRONT AND REAR SUSPENSION DAMPING COEFF. -----	3000.0000	[N-s/m]

\*\*\*\*\*AERODYNAMIC PARAMETERS\*\*\*\*\*

VEHICLE FRONTAL AREA -----	2.0000	[m^2]
CHARACTERISTIC HEIGHT OF VEHICLE -----	1.5000	[m]
AERODYNAMIC SIDEFORCE COEFFICIENT -----	0.3000000	[-]
AERODYNAMIC ALIGNING MOMENT COEFFICIENT -----	0.2000000	[-]
AERODYNAMIC YAW DAMPING COEFFICIENT -----	100.0000	[N-m-s]

COPYRIGHT (C) 1988 ANDRZEJ G. NALECZ. ALL RIGHTS RESERVED. THIS SOFTWARE  
 WAS FIRST PRODUCED IN PERFORMANCE OF CONTRACT DTRS57-88-P-82688  
 SPONSORED BY TSC/RSPA/U.S.DOT

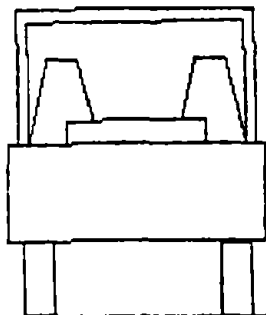
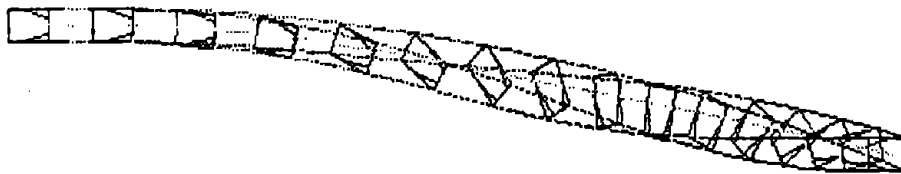
VARIABLE STEERING INPUT STEP BRAKING INPUT = 0.70 [g's] STEP SIZE = 0.0100 [Sec]

TIME	STEER	U	LATV	YAWV	ACC	HEADING	PHIU	PHISa	PHISr	AX
0.2000	3.7997	21.9863	0.0538	0.1827	0.3475	0.7701	-0.4064	-1.1687	-0.7623	-0.0198
0.4000	4.9996	21.9168	-0.4353	0.4061	0.5244	4.3156	-1.1549	-5.1519	-3.9969	-0.0331
0.6000	1.3999	21.7861	-1.2947	0.4486	0.5287	9.4367	-1.3660	-6.4825	-5.1163	-0.0078
0.8000	-6.5995	21.6906	-1.8931	0.0130	0.0223	12.7487	-0.4475	-3.0706	-2.6231	-0.0210
1.0000	-14.5989	21.6451	-0.6249	-0.7331	-0.4956	8.2058	0.9901	3.9416	2.9514	-0.1127
1.2000	-14.9989	21.3245	1.7261	-0.8413	-0.6539	-1.1760	1.9052	8.2463	6.3410	-0.1157
1.4000	-14.9989	20.6334	3.8829	-0.8027	-0.6606	-10.6038	1.2963	5.4216	4.1251	-0.1157
1.6000	-14.9989	19.2541	5.9554	-0.6276	-0.2837	-19.1707	0.6011	3.1119	2.5108	-0.5443
1.8000	-14.9989	17.5834	7.0901	-0.3384	-0.3363	-24.6897	0.4806	1.7652	1.2845	-0.5182
2.0000	-14.9989	16.2955	7.0444	-0.0634	-0.3558	-26.9804	0.7395	3.1774	2.4379	-0.5075
2.2000	-14.9989	15.3881	6.1334	0.2028	-0.3473	-26.1763	0.8933	4.4164	3.5231	-0.5132
2.4000	-14.9989	14.7157	4.4649	0.4657	-0.3104	-22.3442	0.6918	3.3826	2.6908	-0.5338
2.6000	-14.9989	14.0319	2.1969	0.7255	-0.2324	-15.5099	0.4184	1.8340	1.4155	-0.5671
2.8000	-14.9989	12.9100	0.0138	0.7047	0.0425	-6.8058	0.0132	0.4464	0.4332	-0.6877
3.0000	-14.9989	11.5048	-1.2563	0.5121	0.1207	0.1919	-0.4258	-2.0444	-1.6186	-0.6792

TIME

Example 4

Yaw angle = 179.56 deg      X-Path = 45.41 meters      Y-Path = 5.27 meters  
Total velocity = 24.68 KPH      Steer angle = 15.00 deg      Time = 3.00 sec  
\*\*\*\*\* TIME \*\*\*\*\*



Front Rt. Tire Locked & Saturated  
Front Lf. Tire Locked & Saturated  
Rear Rt. Tire Saturated  
Rear Lf. Tire Saturated

Scale: 1cm = 3.28 meters, Press Q to quit

This run shows the response of a rear weight biased car with brakes biased toward the rear. A ramp steering input of 15 degrees is applied simultaneously with a ramp braking input of 0.8g's. The vehicle is directionally unstable and spins out. The vehicle data used in the simulation together with numerical output are shown below.

VEHICLE MASS -----	1014.0000	[kg]
VEHICLE SPRUNG MASS -----	778.1000	[kg]
DISTANCE FROM SPRUNG MASS C.G. TO FRONT AXLE -----	1.3000	[m]
DISTANCE FROM SPRUNG MASS C.G. TO ROLL AXIS -----	0.6034	[m]
HEIGHT OF SPRUNG MASS C.G. -----	0.6930	[m]
YAW MOMENT OF INERTIA -----	1175.5000	[kg*m^2]
ROLL MOMENT OF INERTIA OF SPRUNG MASS -----	240.2600	[kg*m^2]
ROLL MOMENT OF INERTIA OF UNSPRUNG MASS -----	71.8300	[kg*m^2]
AUXILARY ROLL DAMPING OF FRONT AND REAR SUSPENSIONS ---	0.0000	[Nm-s/rad]
WHEELBASE -----	2.0320	[m]
FRONT TRACK WIDTH -----	1.3081	[m]
REAR TRACK WIDTH -----	1.3081	[m]
UNSPRUNG MASS OF FRONT SUSPENSION -----	117.4800	[kg]
UNSPRUNG MASS OF REAR SUSPENSION -----	117.4800	[kg]
UNSPRUNG MASS CG HEIGHT OF FRONT SUSPENSION -----	0.3302	[m]
UNSPRUNG MASS CG HEIGHT OF REAR SUSPENSION -----	0.3302	[m]
FRONT SUSPENSION AUXILARY ROLL STIFFNESS -----	3443.7300	[Nm/rad]
REAR SUSPENSION AUXILARY ROLL STIFFNESS -----	5277.3301	[Nm/rad]
FRONT PROPORTION OF TOTAL VEHICLE ROLL STIFFNESS -----	0.5600	[-]
VERTICAL STIFFNESS OF TIRES -----	113140.000	[N/m]
VERTICAL DAMPING COEFFICIENT OF TIRE -----	980.000	[N-s/m]
RATE OF CHANGE OF FRONT TIRE INCLINATION -----	-0.0400	
RATE OF CHANGE OF REAR AXLE STEER -----	0.0000	
FRACTION OF BRAKING TORQUE APPLIED TO FRONT WHEELS ----	0.2000	
HEAVY BRAKING PROPORTIONALITY FACTOR FOR FRONT WHEELS -	0.0500	
1 - FWD 2 - RWD 3 - 4WD -----	3	
FRACTION OF DRIVING TORQUE APPLIED TO FRONT (4WD) -----	0.6000	

\*\*\*\*\*TIRE DATA\*\*\*\*\*

TIRE SKID NUMBER	70.00		
A0 = -668.4600	A1 = 26.5400	A2 = 2146.6101	
A3 = 1.2740000	A4 = 2225.0701		
B1 = -6.7450E-04	B3 = 1.3070	B4 = 2.9530E-07	
P0 = 1.2073	P1 = -5.8430E-04	P2 = 3.9770E-07	
S0 = 1.17379999	S1 = -8.4580E-04	S2 = 3.9450E-07	
R0 = -0.23771000	R1 = 8.5360E-05		
K1 = -2.0610E-04	K2 = -1.7680E-04	K3 = 0.0740	
CTN = 6.000000	CA1 = 30.000000	CR1 = 0.300000	

\*\*\*\*\*SUSPENSION PARAMETERS\*\*\*\*\*

SUSPENSION SPRING TRACK WIDTH -----	0.9320	[m]
STATIC SUSPENSION SPRING LENGTH -----	0.1016	[m]
UNDEFORMED BUMP STOP LENGTH -----	0.0709	[m]
HEIGHT OF LOWER SUSPENSION SPRING MOUNT ABOVE GROUND --	0.2032	[m]
COMBINED FRONT AND REAR SUSPENSION SPRING STIFFNESSES -	84850.00	[N/m]
COMBINED FRONT AND REAR BUMP STOP STIFFNESSES -----	464030.0	[N/m]
COMBINED FRONT AND REAR SUSPENSION DAMPING COEFF. ----	3000.0000	[N-s/m]

\*\*\*\*\*AERODYNAMIC PARAMETERS\*\*\*\*\*

VEHICLE FRONTAL AREA -----	2.0000	[m^2]
CHARACTERISTIC HEIGHT OF VEHICLE -----	1.5000	[m]
AERODYNAMIC SIDEFORCE COEFFICIENT -----	0.3000000	[-]
AERODYNAMIC ALIGNING MOMENT COEFFICIENT -----	0.2000000	[-]
AERODYNAMIC YAW DAMPING COEFFICIENT -----	100.0000	[N-m-s]



COPYRIGHT (C) 1988 ANDRZEJ G. NALECZ. ALL RIGHTS RESERVED. THIS SOFTWARE  
 WAS FIRST PRODUCED IN PERFORMANCE OF CONTRACT DTRS57-88-P-82688  
 SPONSORED BY TSC/RSPA/U.S.DOT

RAMP STEERING INPUT = 15.00 [Deg] RAMP BRAKING INPUT = 0.80 [g's] STEP SIZE = 0.0100 [Sec]

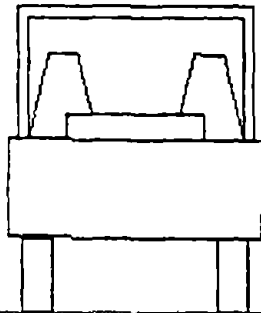
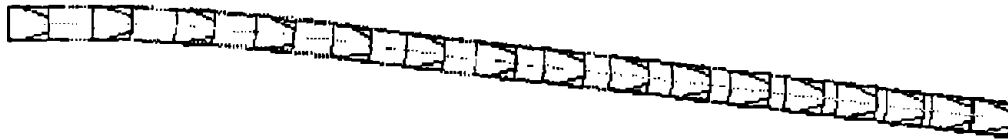
TIME	STEER	U	LATV	YAW	ACC	HEADING	PhiU	PHISa	PHISr	AX
0.2000	2.8498	21.8446	-0.0671	0.1786	0.2448	0.7338	-0.2568	-0.6815	-0.4247	-0.1606
0.4000	5.8496	21.3237	-0.8163	0.5167	0.4730	4.6440	-0.9251	-3.8492	-2.9240	-0.3131
0.6000	8.8493	20.3907	-2.5593	0.7709	0.5255	12.1817	-1.3526	-6.2103	-4.8576	-0.4116
0.8000	11.8491	18.8059	-5.0610	0.9808	0.4182	22.1763	-0.8789	-4.3400	-3.4610	-0.5212
1.0000	14.8489	16.2721	-8.2915	1.2511	0.3928	35.0733	-0.5171	-1.9523	-1.4352	-0.4871
1.2000	14.9989	12.7271	-11.3423	1.3989	0.4327	50.3680	-0.7800	-3.0528	-2.2728	-0.4216
1.4000	14.9989	8.4268	-13.4180	1.4488	0.5040	66.7236	-1.3160	-5.5235	-4.2074	-0.3219
1.6000	14.9989	3.9689	-14.1838	1.4138	0.5227	83.1254	-1.1137	-5.0882	-3.9744	-0.1690
1.8000	14.9989	-0.1695	-13.6379	1.3581	0.5144	99.1609	-0.9917	-4.3111	-3.3194	-0.0362
2.0000	14.9989	-3.3038	-12.1529	1.2778	0.5188	114.1563	-1.0535	-4.7246	-3.6710	0.2227
2.2000	14.9989	-5.5964	-10.0240	1.2553	0.4702	128.6935	-1.0443	-4.9402	-3.8959	0.3182
2.4000	14.9989	-7.0712	-7.5788	1.2157	0.4015	142.8618	-0.8578	-4.0369	-3.1791	0.4012
2.6000	14.9989	-7.7248	-5.0994	1.1643	0.3117	156.5125	-0.6184	-2.8165	-2.1980	0.5228
2.8000	14.9989	-7.5322	-2.7904	1.0134	0.1660	169.3218	-0.4554	-2.5117	-2.0562	0.5650
3.0000	14.9989	-6.6452	-1.3929	0.7910	-0.0540	179.5574	-0.0207	-0.5841	-0.5634	0.6985

TIME

Example 5

Yaw angle = 4.72 deg      X-Path = 50.73 meters      Y-Path = 3.52 meters

Total velocity = 39.49 KPH      Steer angle = 15.00 deg      Time = 3.00 sec



Front Rt. Tire Locked & Saturated  
Front Lf. Tire Locked & Saturated

Scale: 1cm = 3.28 meters, Press Q to quit

This run shows the response of a rear weight biased car with brakes biased toward the front. A ramp steering input of 15 degrees is applied simultaneously with a ramp braking input of 0.8g's. The vehicle is directionally stable. Again, the vehicle data employed in the simulation and numerical output are shown below.

VEHICLE MASS -----	1014.0000	[kg]
VEHICLE SPRUNG MASS -----	778.1000	[kg]
DISTANCE FROM SPRUNG MASS C.G. TO FRONT AXLE -----	1.3000	[m]
DISTANCE FROM SPRUNG MASS C.G. TO ROLL AXIS -----	0.6034	[m]
HEIGHT OF SPRUNG MASS C.G. -----	0.6930	[m]
YAW MOMENT OF INERTIA -----	1175.5000	[kg*m^2]
ROLL MOMENT OF INERTIA OF SPRUNG MASS -----	240.2600	[kg*m^2]
ROLL MOMENT OF INERTIA OF UNSPRUNG MASS -----	71.8300	[kg*m^2]
AUXILARY ROLL DAMPING OF FRONT AND REAR SUSPENSIONS ---	0.0000	[Nm-s/rad]
WHEELBASE -----	2.0320	[m]
FRONT TRACK WIDTH -----	1.3081	[m]
REAR TRACK WIDTH -----	1.3081	[m]
UNSPRUNG MASS OF FRONT SUSPENSION -----	117.4800	[kg]
UNSPRUNG MASS OF REAR SUSPENSION -----	117.4800	[kg]
UNSPRUNG MASS CG HEIGHT OF FRONT SUSPENSION -----	0.3302	[m]
UNSPRUNG MASS CG HEIGHT OF REAR SUSPENSION -----	0.3302	[m]
FRONT SUSPENSION AUXILARY ROLL STIFFNESS -----	3443.7300	[Nm/rad]
REAR SUSPENSION AUXILARY ROLL STIFFNESS -----	5277.3301	[Nm/rad]
FRONT PROPORTION OF TOTAL VEHICLE ROLL STIFFNESS -----	0.5600	[-]
VERTICAL STIFFNESS OF TIRES -----	113140.000	[N/m]
VERTICAL DAMPING COEFFICIENT OF TIRE -----	980.000	[N-s/m]
RATE OF CHANGE OF FRONT TIRE INCLINATION -----	-0.0400	
RATE OF CHANGE OF REAR AXLE STEER -----	0.0000	
FRACTION OF BRAKING TORQUE APPLIED TO FRONT WHEELS ----	0.8000	
HEAVY BRAKING PROPORTIONALITY FACTOR FOR FRONT WHEELS -	0.0500	
1 - FWD 2 - RWD 3 - 4WD -----	3	
FRACTION OF DRIVING TORQUE APPLIED TO FRONT (4WD) -----	0.6000	

\*\*\*\*\*TIRE DATA\*\*\*\*\*

TIRE SKID NUMBER	70.00				
A0 =	-668.4600	A1 =	26.5400	A2 =	2146.6101
A3 =	1.2740000	A4 =	2225.0701		
B1 =	-6.7450E-04	B3 =	1.3070	B4 =	2.9530E-07
P0 =	1.2073	P1 =	-5.8430E-04	P2 =	3.9770E-07
S0 =	1.17379999	S1 =	-8.4580E-04	S2 =	3.9450E-07
R0 =	-0.23771000	R1 =	8.5360E-05		
K1 =	-2.0610E-04	K2 =	-1.7680E-04	K3 =	0.0740
CTN =	6.000000	CA1 =	30.000000	CR1 =	0.300000

\*\*\*\*\*SUSPENSION PARAMETERS\*\*\*\*\*

SUSPENSION SPRING TRACK WIDTH -----	0.9320	[m]
STATIC SUSPENSION SPRING LENGTH -----	0.1016	[m]
UNDEFORMED BUMP STOP LENGTH -----	0.0709	[m]
HEIGHT OF LOWER SUSPENSION SPRING MOUNT ABOVE GROUND --	0.2032	[m]
COMBINED FRONT AND REAR SUSPENSION SPRING STIFFNESSES -	84850.00	[N/m]
COMBINED FRONT AND REAR BUMP STOP STIFFNESSES -----	464030.0	[N/m]
COMBINED FRONT AND REAR SUSPENSION DAMPING COEFF. -----	3000.0000	[N-s/m]

\*\*\*\*\*AERODYNAMIC PARAMETERS\*\*\*\*\*

VEHICLE FRONTAL AREA -----	2.0000	[m^2]
CHARACTERISTIC HEIGHT OF VEHICLE -----	1.5000	[m]
AERODYNAMIC SIDEFORCE COEFFICIENT -----	0.3000000	[-]
AERODYNAMIC ALIGNING MOMENT COEFFICIENT -----	0.2000000	[-]
AERODYNAMIC YAW DAMPING COEFFICIENT -----	100.0000	[N-m-s]

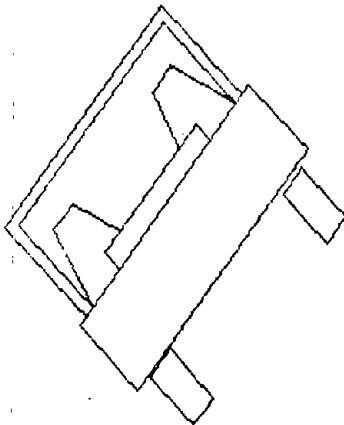
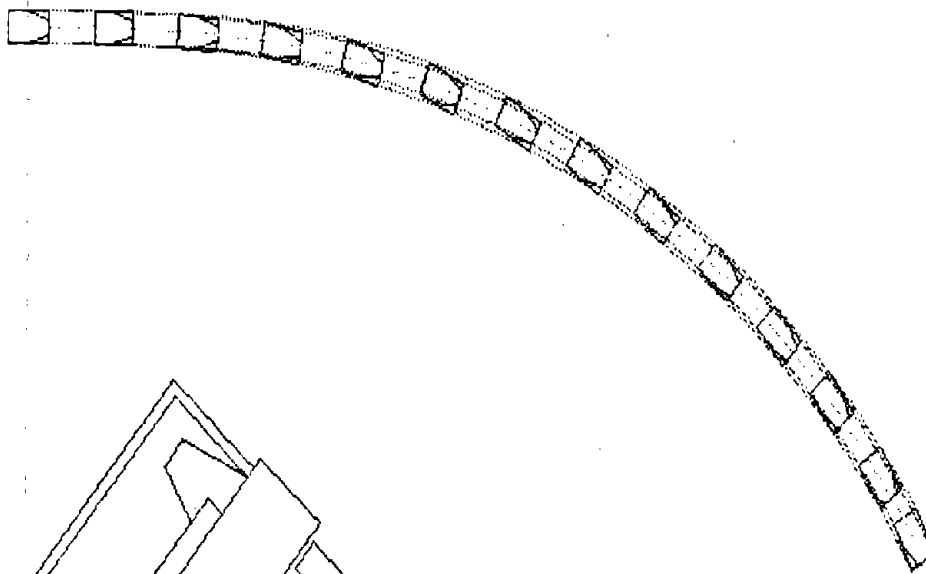
COPYRIGHT (C) 1988 ANDRZEJ G. NALECZ. ALL RIGHTS RESERVED. THIS SOFTWARE  
 WAS FIRST PRODUCED IN PERFORMANCE OF CONTRACT DTRS57-88-P-82688  
 SPONSORED BY TSC/RSPA/U.S.DOT

TIME	STEER	U	LATV	YAW	ACC	HEADING	PHIU	PHISa	PHISr	AX
0.2000	2.8498	21.8448	-0.0674	0.1737	0.2346	0.7217	-0.2500	-0.6699	-0.4199	-0.1603
0.4000	5.8496	21.3423	-0.7012	0.3471	0.3598	4.0532	-0.8015	-3.4852	-2.6836	-0.3018
0.6000	8.8493	20.5963	-1.1634	0.1605	0.3035	7.2517	-1.0131	-4.9084	-3.8952	-0.3978
0.8000	11.8491	19.8593	-0.6449	-0.1508	0.1583	7.1387	-0.3958	-2.1931	-1.7973	-0.3872
1.0000	14.8489	19.0791	0.1393	-0.1667	-0.0720	4.9910	0.2854	1.2565	0.9711	-0.4140
1.2000	14.9989	18.2606	0.2787	-0.0172	-0.0935	3.9364	0.4337	2.3959	1.9621	-0.4151
1.4000	14.9989	17.4470	0.0635	0.0549	-0.0126	4.2748	0.0403	0.4225	0.3822	-0.4153
1.6000	14.9989	16.6323	-0.0581	0.0267	0.0276	4.7907	-0.2549	-1.4236	-1.1687	-0.4153
1.8000	14.9989	15.8176	-0.0367	-0.0069	0.0135	4.8783	-0.0857	-0.6261	-0.5403	-0.4153
2.0000	14.9989	15.0029	0.0027	-0.0100	-0.0032	4.7574	0.1368	0.7774	0.2506	-0.4153
2.2000	14.9989	14.1882	0.0093	-0.0014	-0.0046	4.6924	0.0595	0.4405	0.3810	-0.4154
2.4000	14.9989	13.3736	0.0019	0.0018	-0.0008	4.7016	-0.0822	-0.4712	-0.3890	-0.4154
2.6000	14.9989	12.5589	-0.0012	0.0007	0.0007	4.7175	-0.0350	-0.2721	-0.2371	-0.4154
2.8000	14.9989	11.7442	-0.0004	-0.0001	0.0005	4.7195	0.0547	0.3151	0.2604	-0.4154
3.0000	14.9989	10.9296	0.0001	0.0001	0.0001	4.7195	0.0210	0.1694	0.1484	-0.4154

TIME

Example 6

Yaw angle = 61.50 deg      X-Path = 46.75 meters      Y-Path = 20.07 meters  
Total velocity = 68.22 KPH      Steer angle = 6.00 deg      Time = 2.57 sec



Rollover Criteria Satisfied

Do you want another run ?  Scale: 1cm = 3.28 meters, Press Q to quit

This run illustrates the rollover of a vehicle which was given a ramp steering input of 6 degrees. No braking was applied in the maneuver. The skid number of the pavement was raised, thus increasing the maximum allowable tire forces. This increased the lateral acceleration of the vehicle above that needed to initiate rollover. The vehicle data used and numerical output are shown below.

VEHICLE MASS -----	1014.0000	[kg]
VEHICLE SPRUNG MASS -----	778.1000	[kg]
DISTANCE FROM SPRUNG MASS C.G. TO FRONT AXLE -----	1.0340	[m]
DISTANCE FROM SPRUNG MASS C.G. TO ROLL AXIS -----	0.6072	[m]
HEIGHT OF SPRUNG MASS C.G. -----	0.6930	[m]
YAW MOMENT OF INERTIA -----	1175.5000	[kg*m^2]
ROLL MOMENT OF INERTIA OF SPRUNG MASS -----	240.2600	[kg*m^2]
ROLL MOMENT OF INERTIA OF UNSPRUNG MASS -----	71.8300	[kg*m^2]
AUXILARY ROLL DAMPING OF FRONT AND REAR SUSPENSIONS ---	0.0000	[Nm-s/rad]
WHEELBASE -----	2.0320	[m]
FRONT TRACK WIDTH -----	1.3081	[m]
REAR TRACK WIDTH -----	1.3081	[m]
UNSPRUNG MASS OF FRONT SUSPENSION -----	117.4800	[kg]
UNSPRUNG MASS OF REAR SUSPENSION -----	117.4800	[kg]
UNSPRUNG MASS CG HEIGHT OF FRONT SUSPENSION -----	0.3302	[m]
UNSPRUNG MASS CG HEIGHT OF REAR SUSPENSION -----	0.3302	[m]
FRONT SUSPENSION AUXILARY ROLL STIFFNESS -----	3443.7300	[Nm/rad]
REAR SUSPENSION AUXILARY ROLL STIFFNESS -----	5277.3301	[Nm/rad]
FRONT PROPORTION OF TOTAL VEHICLE ROLL STIFFNESS -----	0.5600	[-]
VERTICAL STIFFNESS OF TIRES -----	113140.000	[N/m]
VERTICAL DAMPING COEFFICIENT OF TIRE -----	980.000	[N-s/m]
RATE OF CHANGE OF FRONT TIRE INCLINATION -----	-0.0400	
RATE OF CHANGE OF REAR AXLE STEER -----	0.0000	
FRACTION OF BRAKING TORQUE APPLIED TO FRONT WHEELS ----	0.6500	
HEAVY BRAKING PROPORTIONALITY FACTOR FOR FRONT WHEELS -	0.2000	
1 - FWD 2 - RWD 3 - 4WD -----	3	
FRACTION OF DRIVING TORQUE APPLIED TO FRONT (4WD) ----	0.6000	

\*\*\*\*\*TIRE DATA\*\*\*\*\*

TIRE SKID NUMBER	100.00		
A0 = -668.4600	A1 = 26.5400	A2 = 2146.6101	
A3 = 1.2740000	A4 = 2225.0701		
B1 = -6.7450E-04	B3 = 1.3070	B4 = 2.9530E-07	
P0 = 1.2073	P1 = -5.8430E-04	P2 = 3.9770E-07	
S0 = 1.17379999	S1 = -8.4580E-04	S2 = 3.9450E-07	
R0 = -0.23771000	R1 = 8.5360E-05		
K1 = -2.0610E-04	K2 = -1.7680E-04	K3 = 0.0740	
CTN = 6.000000	CA1 = 30.000000	CR1 = 0.300000	

\*\*\*\*\*SUSPENSION PARAMETERS\*\*\*\*\*

SUSPENSION SPRING TRACK WIDTH -----	0.9320	[m]
STATIC SUSPENSION SPRING LENGTH -----	0.1016	[m]
UNDEFORMED BUMP STOP LENGTH -----	0.0709	[m]
HEIGHT OF LOWER SUSPENSION SPRING MOUNT ABOVE GROUND --	0.2032	[m]
COMBINED FRONT AND REAR SUSPENSION SPRING STIFFNESSES -	84850.00	[N/m]
COMBINED FRONT AND REAR BUMP STOP STIFFNESSES -----	464030.0	[N/m]
COMBINED FRONT AND REAR SUSPENSION DAMPING COEFF. ----	3000.0000	[N-s/m]

\*\*\*\*\*AERODYNAMIC PARAMETERS\*\*\*\*\*

VEHICLE FRONTAL AREA -----	2.0000	[m^2]
CHARACTERISTIC HEIGHT OF VEHICLE -----	1.5000	[m]
AERODYNAMIC SIDEFORCE COEFFICIENT -----	1.0000000	[-]
AERODYNAMIC ALIGNING MOMENT COEFFICIENT -----	2.5000000	[-]
AERODYNAMIC YAW DAMPING COEFFICIENT -----	1000.0000	[N-m-s]

COPYRIGHT (C) 1988 ANDRZEJ G. NALECZ. ALL RIGHTS RESERVED. THIS SOFTWARE  
 WAS FIRST PRODUCED IN PERFORMANCE OF CONTRACT DTRS57-88-P-82688  
 SPONSORED BY TSC/RSPA/U.S.DOT

RAMP STEERING INPUT = 6.00 [Deg] NO BRAKING INPUT STEP SIZE = 0.0100 [Sec]

TIME	STEER	U	LATV	YAWV	ACC	HEADING	PHIU	PHISa	PHISr	AX
0.2000	2.2798	21.9937	-0.0002	0.1724	0.3086	0.7385	-0.3376	-0.9167	-0.5790	-0.0092
0.4000	4.6797	21.9409	-0.3943	0.4257	0.6443	4.2042	-1.2142	-4.9600	-3.7457	-0.0335
0.6000	5.9996	21.7699	-1.1981	0.5853	0.8254	10.1430	-1.9203	-8.1631	-6.2427	-0.0502
0.8000	5.9996	21.4682	-2.1188	0.6068	0.9008	17.0747	-1.9315	-7.3093	-5.3777	-0.0513
1.0000	5.9996	21.0851	-2.7493	0.5337	0.9287	23.6498	-1.9184	-7.0053	-5.0868	-0.0513
1.2000	5.9996	20.7029	-2.9513	0.4443	0.9346	29.2494	-2.1043	-7.9007	-5.7962	-0.0512
1.4000	5.9996	20.3680	-2.7763	0.3701	0.9301	33.8914	-2.8348	-8.4631	-5.6280	-0.0513
1.6000	5.9996	20.0880	-2.3646	0.3310	0.9140	37.8653	-4.0619	-9.5845	-5.5223	-0.0513
1.8000	5.9996	19.8442	-1.9405	0.3503	0.8799	41.6953	-5.7317	-11.3677	-5.6356	-0.0515
2.0000	5.9996	19.6053	-1.7356	0.4113	0.8639	46.0531	-8.5071	-13.9621	-5.4564	-0.0513
2.2000	5.9996	19.3528	-1.7527	0.4647	0.8674	51.0886	-13.5147	-18.9827	-5.4670	-0.0512
2.4000	5.9996	19.0764	-1.9062	0.4964	0.8702	56.6180	-24.3857	-29.3698	-4.9823	-0.0511

ROLLOVER CRITERIA SATISFIED

TIME

## 2. DEVELOPMENT OF IMIRS SIMULATION

### 2.1 INTRODUCTION

In the past, there has been a considerable amount of debate and controversy surrounding the phenomenon of maneuver induced rollover. These are rollover accidents which typically occur on smooth pavement and are initiated by driver steering and braking inputs, rather than an excursion into a roadside feature. While maneuver induced rollover accidents occur infrequently in comparison to tripped rollover accidents, it is justifiably argued that a vehicle should not rollover as a result of steering and braking inputs which might occur in a collision avoidance situation.

The Intermediate Maneuver Induced Rollover Simulation (IMIRS) can be used to investigate vehicle maneuver induced rollover as well as limit handling maneuvers. The IMIRS represents an extension of the Lateral Weight Transfer Simulation (LWTS) described in [1] and [2]. The IMIRS utilizes a vehicle model of intermediate detail, which requires a modest amount of vehicle data and computation time. Like the LWTS the IMIRS is an interactive, menu driven PC based simulation. The menus used in the IMIRS are identical to those used in the LWTS whenever possible. The improvements made in the IMIRS include:

- The addition of a rollover model which can be used to examine the rollover propensity and behavior of vehicles subjected to severe steering and braking inputs.
- An enhanced tire model which is capable of simulating tire behavior in skidding and spinning conditions. This model includes logic for predicting wheel locking or spinning conditions caused by excessive braking or thrust torques, and automatically simulates the changes in tire behavior caused by these conditions.
- The capability of simulating step, ramp, sinusoidal, or other user specified steering inputs. The steering inputs can be stored for repeat runs.
- The capability of simulating step, ramp, or user specified braking inputs. These braking inputs can be stored for repeat runs.
- The addition of an aerodynamic model capable of estimating the aerodynamic forces and moments which act on the vehicle.
- The addition of forward motion as a degree of freedom.
- Automatic support for Hercules, CGA, EGA, and VGA graphics adapters.



## 2.2 IMIRS MODEL DESCRIPTION

The IMIRS simulation utilizes two coupled vehicle dynamic models to simulate handling and rollover behavior; an illustration of each model is given in Figures 1 and 2. The vehicle handling model has 3 degrees of freedom, while the rollover model is a 5 degree of freedom model.

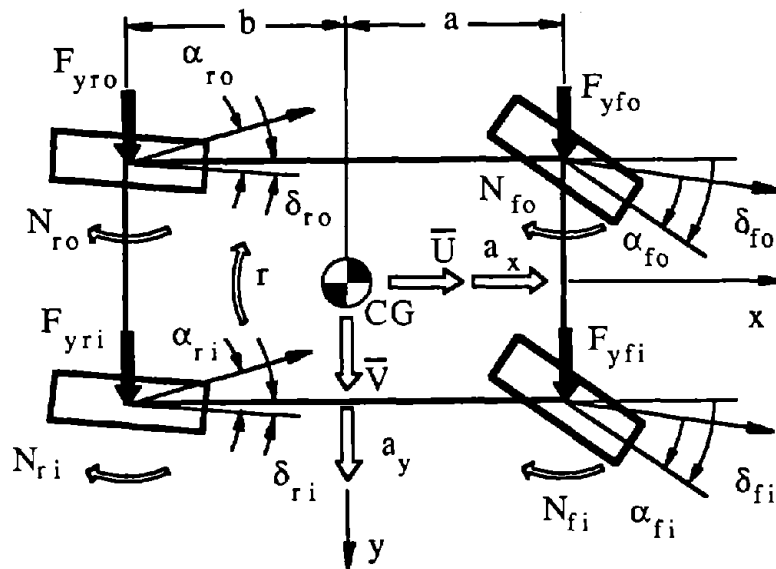


Figure 1. IMIRS Handling Model.

The generalized velocities used in the handling model are forward velocity  $U$ , lateral velocity  $V$  and yaw rate  $r$ . In this model 8 different kinematic configurations of front suspension systems can be employed in conjunction with any one of 19 different rear independent and dependent suspension systems.

The external forces and moments which act on the IMIRS handling model are those generated by pneumatic tires, gravitational and aerodynamic effects. A non-linear tire model based on the non-dimensional slip angle approach was employed in the simulation. The tire model determines the side force, braking force, and aligning moment generated by a tire in combined cornering and braking maneuvers based on the conditions of normal load, longitudinal slip, slip angle, and camber angle which are imposed on the tire.

In order to investigate untripped vehicle rollover behavior, a vehicle rollover model has been added to the IMIRS to work in conjunction with the handling model. It is a planar model and

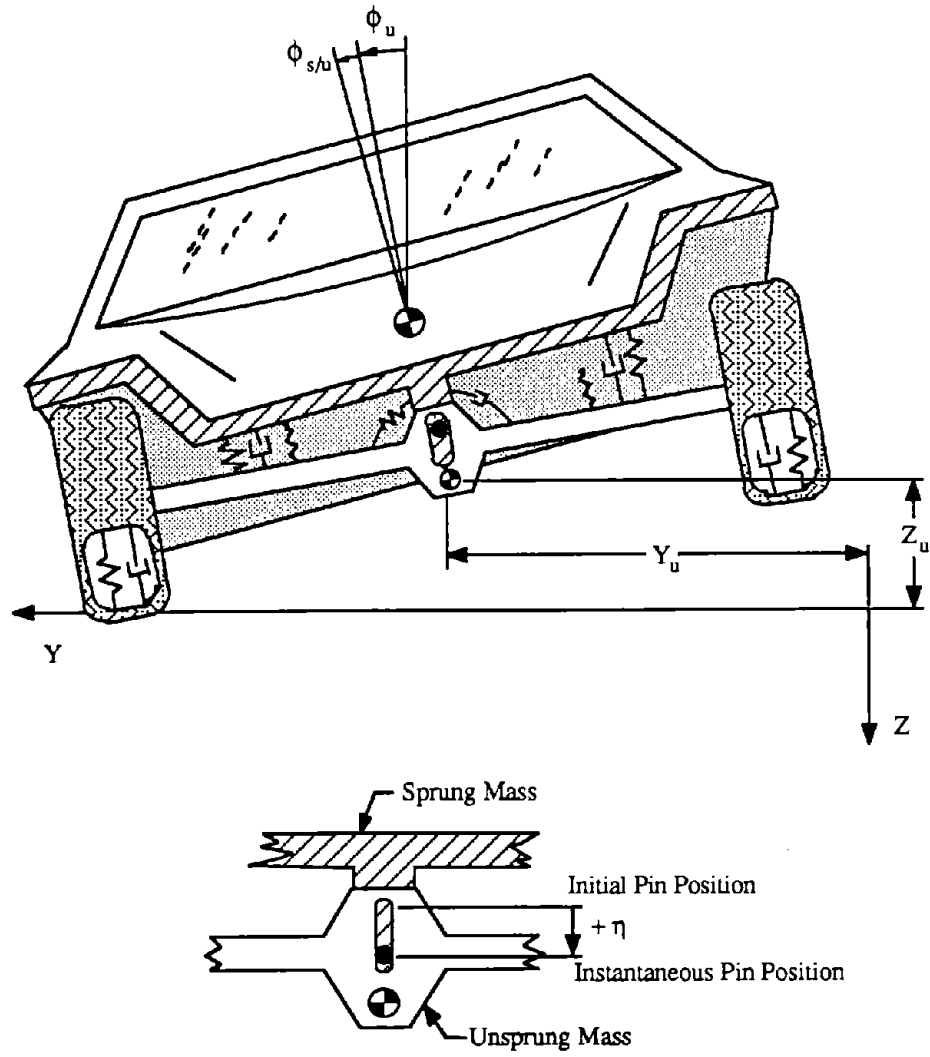


Figure 2. IMIRS Rollover Model.

consists of two masses, sprung and unsprung, which are connected through the various elements of the suspension system. The rollover model is coupled to the vehicle handling model through the external forces which are applied to the planar model. These forces include the side forces generated by the tires, the inertial forces acting on the sprung and unsprung masses, and gravity. The degrees of freedom used in the IMIRS rollover model (Figure 2) include:

- $\phi_u$  - Roll angle of the unsprung mass
- $Y_u$  - Lateral displacement of the unsprung mass center of gravity
- $Z_u$  - Vertical location of the unsprung mass center of gravity
- $\phi_{s/u}$  - Roll angle of the sprung mass relative to the unsprung mass
- $\eta$  - Heave of the sprung mass relative to the unsprung mass

The suspension system used in the rollover model is also illustrated in Figure 2. The sprung mass motion is constrained using a pin which slides in a vertical slot in the unsprung mass. Two linearly elastic springs and viscous dampers support the sprung mass. Bump stops limit the relative motion of the sprung mass in roll and heave. These bump stops are modelled using non-linear, hardening springs which become infinitely stiff if compressed to zero length. The front and rear tires are combined at the left and right sides of the vehicle and are modelled using a linearly elastic spring placed in parallel with a viscous damping element.

Because of its increased complexity IMIRS model requires more vehicle data than the LWTS. Every effort has been made to keep the vehicle and tire parameters used in both the LWTS and IMIRS models consistent. A description of the additional items of vehicle data required by the IMIRS simulation are shown below. Many of the pieces of data associated with the rollover model are illustrated in Figure 3.

Roll moment of inertia of unsprung masses $I_{xxu}$	kg m <sup>2</sup>
Auxiliary roll damping of front and rear suspension systems $C_r$	N m s / Rad
Front suspension auxiliary roll stiffness $K_{rf}$	N m / Rad
Rear suspension auxiliary roll stiffness $K_{rr}$	N m / Rad
Front portion of total vehicle roll stiffness $K_{dist}$	-
Vertical stiffness of tires $K_z$	N / m
Vertical damping of tires $B_z$	N s / m
Fraction of driving torque applied to front wheels (4WD) $Wd_4$	-
Calspan Coefficients $S_0, S_1, S_2, R_0, R_1, K_1, K_2, K_3$	-
Slope of $\mu_x$ vs. slip ratio at $S_i = 0$	-
Critical camber angle for friction reduction $\gamma_c$	Degrees
Friction factor reduction at critical camber angle $r_\gamma$	-
Suspension spring track width $t_s$	m
Static suspension spring length $L_s$	m
Undeformed bump stop length $L_b$	m
Static height of lower suspension spring mount above ground $T_{bas}$	m
Combined front and rear suspension spring stiffness $K_s$	N / m
Combined front and rear suspension bump stop stiffness $K_b$	N / m
Vehicle frontal area $S_a$	m <sup>2</sup>
Aerodynamic characteristic height of vehicle $H_a$	m
Aerodynamic sideforce coefficient $C_y$	-
Aerodynamic yawing moment coefficient $C_n$	-
Aerodynamic yaw damping coefficient $C_{nd}$	N m s / Rad

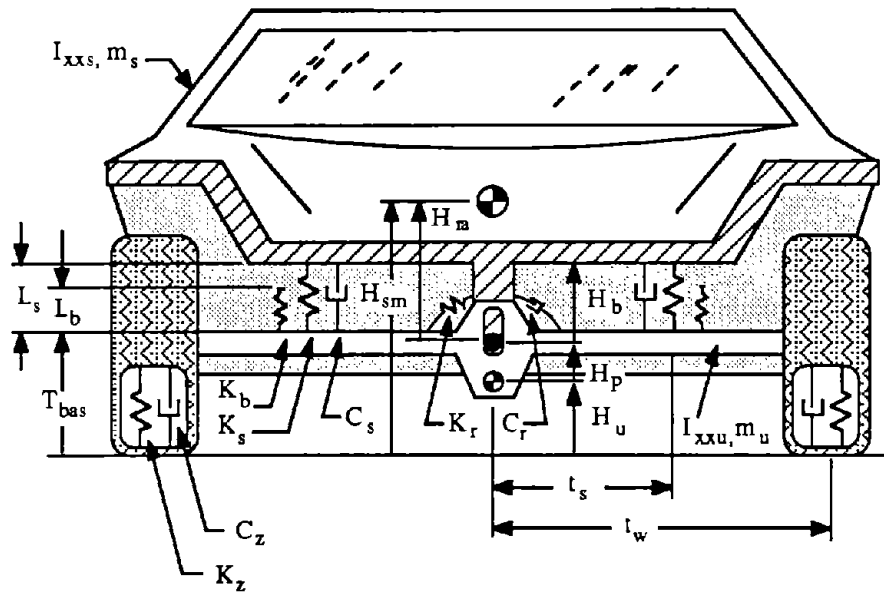


Figure 3. Notation Used in IMIRS Rollover Model.

### 2.2.1 IMIRS Handling Model

The generalized velocities used in the IMIRS handling model are forward velocity  $U$ , lateral velocity  $V$  and yaw rate  $r$ . The equations of motion of the handling model were generated using the Newton-Euler formulation and can be written in the following form:

$$\Sigma F_x = m (\dot{U} - V r) \tag{1}$$

$$\Sigma F_y = m (\dot{V} + U r) \tag{2}$$

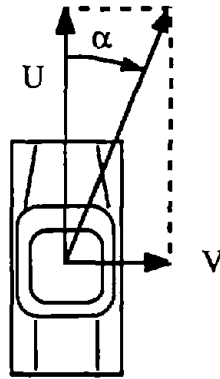
$$\Sigma M_z = I_{zz} \dot{r} \tag{3}$$

The external forces and moments which act on the vehicle include those generated by pneumatic tires, gravity and aerodynamic effects. Once these external reactions are determined then the acceleration terms  $\dot{U}$ ,  $\dot{V}$  and  $\dot{r}$  can be calculated.

## Aerodynamic Forces and Moments

The aerodynamic model computes the side force and yawing moment acting on the vehicle caused by interaction with the airflow. Both of these quantities are dependent on the sideslip angle  $\alpha$  of the vehicle which is determined as:

$$\alpha = \text{Tan}^{-1} \frac{V}{U}, \quad (4)$$



and in addition, the yawing moment depends on vehicle yaw velocity  $r$ .

Once the sideslip angle is determined then the aerodynamic yawing moment and side force can be computed:

$$M_{za} = \frac{1}{2} (V^2 + U^2) \rho_{\text{air}} S_a H_a C_n \alpha - C_{nd} r \quad (5)$$

$$F_{ya} = -\frac{1}{2} (V^2 + U^2) \rho_{\text{air}} S_a C_y \alpha \quad (6)$$

## IMIRS Tire Model

The tire model used in the IMIRS handling simulation is based on the non-dimensional slip angle approach and determines the tire side force, braking force and aligning moment based on slip angle, normal load, camber angle, and the desired braking or thrust acceleration. The slip angle of each tire depends on the velocity of the wheel center.

$$\begin{aligned}
V_{x1} &= U - \frac{T_f}{2} r & V_{y1} &= V + a r \\
V_{x2} &= U + \frac{T_f}{2} r & V_{y2} &= V + a r \\
V_{x3} &= U - \frac{T_r}{2} r & V_{y3} &= V - b r \\
V_{x4} &= U + \frac{T_r}{2} r & V_{y4} &= V - b r
\end{aligned} \tag{7}$$

The velocity vector of each tire is then normalized and the slip angle can be calculated:

$$V_{ti} = \sqrt{V_{xi}^2 + V_{yi}^2} \tag{8}$$

$$\bar{V}_{xi} = \frac{V_{xi}}{V_{ti}} \quad \bar{V}_{yi} = \frac{V_{yi}}{V_{ti}} \tag{9}$$

$$\beta_i = \text{Tan}^{-1} \left[ \frac{\bar{V}_{xi} \text{Sin } \delta_i - \bar{V}_{yi} \text{Cos } \delta_i}{\sqrt{1 - (\bar{V}_{xi} \text{Sin } \delta_i - \bar{V}_{yi} \text{Cos } \delta_i)^2}} \right] \tag{10}$$

where,  $\delta_i$  represents the steer angle of wheel i.

The camber angle of each wheel  $\gamma_i$  is determined as shown below:

$$\gamma_i = \phi_u + \phi_{s/u} \gamma_f \tag{11}$$

where,  $\phi_u$  and  $\phi_{s/u}$  denote the unsprung mass roll angle and the sprung mass relative roll angle, respectively, and factor  $\gamma_f$  represents the camber change caused by the kinematic influence of chassis roll on wheel camber.

The distribution of thrust and braking torques between the four wheels of the vehicle is dependent on the amount of braking or thrust acceleration requested by the driver through his inputs  $a_x$ , the driveline layout (i.e. front wheel drive, rear wheel drive, or four wheel drive) and the

characteristics of the vehicle's braking system (brake distribution properties  $Q_0$  and  $Q_1$ ). Positive values of  $a'_x$  denote braking while negative values denote acceleration. The torque distribution factor  $Q$  is determined in the following manner:

- If  $a'_x$  is less than zero (thrust) and the vehicle is front wheel drive then  $Q = 1$
- If  $a'_x$  is less than zero (thrust) and the vehicle is rear wheel drive then  $Q = 0$
- If  $a'_x$  is less than zero (thrust) and the vehicle is four wheel drive then  $Q = Wd_4$
- If  $0 \leq a'_x \leq 0.3$  g's (moderate braking) then  $Q = Q_0$

Under conditions of heavy braking ( $a'_x \geq 0.3g$ ) the torque distribution factor  $Q$  is modified as shown:

$$Q = Q_0 + Q_1 (a'_x - 0.3) \quad (12)$$

The torque distribution factor is then utilized to determine the desired thrust or braking force at each wheel.

$$F_{x1}' = F_{x2}' = \frac{1}{2} m a'_x g Q \quad (13)$$

$$F_{x3}' = F_{x4}' = \frac{1}{2} m a'_x g (1 - Q) \quad (14)$$

When executing a maneuver in which a vehicle is accelerating in a lateral and/or longitudinal direction the inertia forces acting on the vehicle cause the wheel normal reactions to vary from their static values. The change in wheel normal load caused by lateral accelerations is referred to as lateral weight transfer, while the change in wheel normal load caused by longitudinal accelerations (such as those caused by braking), is known as longitudinal weight transfer. The actual lateral and longitudinal acceleration of the vehicle is calculated using:

$$a_y = \dot{V} + U r \quad (15)$$

$$a_x = \dot{U} - V r \quad (16)$$

The amount and distribution of lateral weight transfer can be determined using three components, lateral weight transfer due to body roll, lateral weight transfer due to roll center height, and lateral

weight transfer due to unsprung masses. The front and rear lateral weight transfer components due to body roll are found:

$$W_{BF} = \frac{KR_{dist} a_y m_s H_{ra} \text{Cos } \phi_{s/u}}{T_f} \quad (17)$$

$$W_{BR} = \frac{(1 - KR_{dist}) a_y m_s H_{ra} \text{Cos } \phi_{s/u}}{T_r} \quad (18)$$

The front and rear lateral weight transfer components due to roll center height are computed as:

$$W_{RF} = \frac{a_y m_s b RC_f}{L T_f} \quad (19)$$

$$W_{RR} = \frac{a_y m_s a RC_r}{L T_r} \quad (20)$$

The front and rear lateral weight transfer components due to unsprung masses are determined as:

$$W_{UF} = a_y m_{uf} \frac{H_{uf}}{T_f} \quad (21)$$

$$W_{UR} = a_y m_{ur} \frac{H_{ur}}{T_r} \quad (22)$$

The weight transfer components are added together to obtain the total front and rear lateral weight transfer values:

$$W_{TF} = W_{BF} + W_{RF} + W_{UF} \quad (23)$$

$$W_{TR} = W_{BR} + W_{RR} + W_{UR} \quad (24)$$

Once the lateral weight transfer components have been determined the normal loads on each wheel are calculated:



$$\begin{aligned}
F_{z1} &= \frac{1}{2} \left[ \frac{b}{L} m g - a_x \frac{H_s m}{L} m_s \right] - W_{TF} & F_{z2} &= \frac{1}{2} \left[ \frac{b}{L} m g - a_x \frac{H_s m}{L} m_s \right] + W_{TF} \\
F_{z3} &= \frac{1}{2} \left[ \frac{a}{L} m g + a_x \frac{H_s m}{L} m_s \right] - W_{TR} & F_{z4} &= \frac{1}{2} \left[ \frac{a}{L} m g + a_x \frac{H_s m}{L} m_s \right] + W_{TR}
\end{aligned} \tag{25}$$

If  $F_{z1}$  is less than zero then  $F_{z1}$  is reset equal to zero and  $F_{z2}$  is set equal to:

$$F_{z2} = \left[ \frac{b}{L} m g - a_x \frac{H_s m}{L} m_s \right] \tag{26}$$

If  $F_{z2}$  is less than zero then  $F_{z2}$  is reset equal to zero and  $F_{z1}$  is set equal to:

$$F_{z1} = \left[ \frac{b}{L} m g - a_x \frac{H_s m}{L} m_s \right] \tag{27}$$

If  $F_{z3}$  is less than zero then  $F_{z3}$  is reset equal to zero and  $F_{z4}$  is set equal to:

$$F_{z4} = \left[ \frac{a}{L} m g + a_x \frac{H_s m}{L} m_s \right] \tag{28}$$

If  $F_{z4}$  is less than zero then  $F_{z4}$  is reset equal to zero and  $F_{z3}$  is set equal to:

$$F_{z3} = \left[ \frac{a}{L} m g + a_x \frac{H_s m}{L} m_s \right] \tag{29}$$

If any of the normal loads are equal to zero and a braking or driving torque is being applied to the wheel then the slip ratio is determined using:

$$S_i = \text{Sgn}(a_x) = \begin{cases} + 1.0 & \text{if } a_x > 0 \\ 0.0 & \text{if } a_x = 0 \\ - 1.0 & \text{if } a_x < 0 \end{cases} \quad (30)$$

After the normal loads have been determined based on longitudinal and lateral weight transfer the tire frictional properties can be computed using Calspan tire measurement. The peak braking friction is determined as:

$$\mu_{xp_i} = \text{SN} (P_0 + P_1 F_{z_i} + P_2 F_{z_i}^2) \quad (31)$$

The tire sliding coefficient of friction:

$$\mu_{xs_i} = \text{SN} (S_0 + S_1 F_{z_i} + S_2 F_{z_i}^2) \quad (32)$$

The longitudinal slip ratio at peak braking:

$$Sp_i = -R_0 - R_1 F_{z_i} \quad (33)$$

The peak lateral friction coefficient:

$$\mu_{y_i} = \text{SN} (B_3 + B_1 F_{z_i} + B_4 F_{z_i}^2) \quad (34)$$

Tire frictional properties  $\mu_{xp_i}$ ,  $\mu_{xs_i}$  and  $\mu_{y_i}$  are reduced due to camber using the following relations:

If  $|\gamma_i|$  is greater than the critical value of camber  $\gamma_c$  then

$$\mu_{xp_i} = \mu_{xp_i} (1 - r_\gamma) \quad (35)$$

$$\mu_{xs_i} = \mu_{xs_i} (1 - r_\gamma) \quad (36)$$

$$\mu_{y_i} = \mu_{y_i} (1 - r_\gamma) \quad (37)$$

where,  $r_\gamma$  represents the percentage reduction at camber angle  $\gamma_c$ , otherwise

$$\mu_{xp_i} = \mu_{xp_i} \left( 1 - \frac{r_\gamma |\gamma_i|}{\gamma_c} \right) \quad (38)$$

$$\mu_{xs_i} = \mu_{xp_i} \left( 1 - \frac{r_\gamma |\gamma_i|}{\gamma_c} \right) \quad (39)$$

$$\mu_{y_i} = \mu_{xp_i} \left( 1 - \frac{r_\gamma |\gamma_i|}{\gamma_c} \right) \quad (40)$$

Once the tire frictional properties have been determined then the maximum allowable cornering and braking forces can be computed. These forces represent the maximum forces which the tire can generate in pure cornering and braking conditions. In the absence of braking forces  $F_{y_{max}}$  represents the maximum allowable side force which the tire can generate, while in the absence of cornering force  $F_{x_{max}}$  represents the maximum allowable braking force.

$$F_{y_{max}} = \mu_{y_i} F_{z_i} \quad (41)$$

$$F_{x_{max}} = \mu_{xp_i} F_{z_i} \quad (42)$$

The maximum allowable braking force under conditions of combined cornering and braking is determined using the polar form for the equation of an ellipse:

If  $|F_{y_{max}}|$  is less than  $|F_{x_{max}}|$  then the eccentricity of the ellipse can be determined using the following relation:

$$\zeta = \frac{\sqrt{F_{x_{\max}}^2 - F_{y_{\max}}^2}}{F_{x_{\max}}} \quad (43)$$

When the eccentricity has been determined then maximum allowable braking force can be found:

$$F'_{x_{\max}} = \frac{\cos \beta_i F_{x_{\max}} (1 - \zeta^2)}{1 - \zeta \cos \beta_i} \quad (44)$$

If  $|F_{y_{\max}}|$  is greater than  $|F_{x_{\max}}|$  then the major axis of the ellipse is along the tire's longitudinal axis and the eccentricity and maximum allowable braking force must be calculated using the following relations:

$$\zeta = \frac{\sqrt{F_{y_{\max}}^2 - F_{x_{\max}}^2}}{F_{y_{\max}}} \quad (45)$$

$$F'_{x_{\max}} = \frac{\cos \beta_i F_{y_{\max}} (1 - \zeta^2)}{1 - \zeta \cos \left( \frac{\pi}{2} - \beta_i \right)} \quad (46)$$

If the requested braking force ( $F'_{x_i}$ ) is greater than the maximum braking force which the tire can generate ( $F'_{x_{\max}}$ ) then it is assumed that the tire stops rotating and becomes locked up ( $S_i = 1$ ). If the desired thrust force is greater than that which the tire can generate then it is assumed that wheel spin occurs ( $S_i = -1$ ). The tire friction coefficients in both of these conditions are determined by:

$$\mu_{x_i} = \mu_{xs_i} \text{Sgn}(F'_{x_i}) \quad (47)$$

$$S_i = \text{Sgn}(F'_{x_i}) = \begin{cases} + & 1.0 & \text{if } ax > 0 \\ & 0.0 & \text{if } ax = 0 \\ - & 1.0 & \text{if } ax < 0 \end{cases}$$

If  $|F_{x_i}'|$  is less than  $F_{x_{max}}'$  then the braking coefficient of friction can be determined by dividing the desired braking force by the normal load in the tire:

$$\mu_{x_i} = \frac{F_{x_i}'}{F_{z_i}} \quad (48)$$

If the tire can generate the desired braking or thrust force then the tire model uses a golden section search to find the slip ratio which corresponds to the braking friction coefficient  $\mu_{x_i}$ . The golden section search is an optimization method which finds the slip ratio  $S_i$  in the region  $-S_{p_i} \leq S_i \leq S_{p_i}$  which minimizes the function  $F_{gold}$  where:

$$F_{gold} = |Sgn(S_i) (F_1 |S_i^3| + F_2 S_i^2 + C_\eta |S_i|) - \mu_{x_i}| \quad (49)$$

In this relation the braking coefficient of friction  $\mu_{x_i}$  is assumed to be related to slip ratio using the following cubic function:

$$\mu_{x_i} = Sgn(S_i) (F_1 |S_i^3| + F_2 S_i^2 + C_\eta |S_i|) \quad (50)$$

Terms  $F_1$  and  $F_2$  are shown below:

$$F_1 = \frac{C_\eta S_{p_i} - 2 \mu_{x_{p_i}}}{S_{p_i}^3} \quad (51)$$

$$F_2 = \frac{3 \mu_{x_{p_i}} - 2 C_\eta S_{p_i}}{S_{p_i}^2} \quad (52)$$

Once  $\mu_{x_i}$  is determined then the tire's circumferential force can be calculated using the following steps.

If  $a'_x$  is less than or equal to zero then:

$$F_{c_i} = \mu_{x_i} F_{z_i} \quad (53)$$

If  $a'_x$  is greater than zero and  $\rho_s$  is not equal to zero then:

$$F_{c_i} = \frac{\mu_{y_i} F_{z_i} \text{Sgn}(\rho_s)}{\sqrt{\text{Tan}^2 \beta_i + \frac{1}{\rho_s^2}}} \quad (54)$$

where,

$$\rho_s = \frac{\mu_{x_i}}{\mu_{y_i}} \quad (55)$$

After the tire's circumferential force has been determined the tire side force can be calculated. Let:

$$\rho_{s_{\max}} = \frac{\mu_{x_{p_i}}}{\mu_{y_i}} \quad (56)$$

If  $|S_i|$  is less than or equal to  $S_{p_i}$  then

$$\varepsilon = \frac{1}{\rho_{s_{\max}}^2} \quad (57)$$

otherwise:

$$\varepsilon = \frac{1}{\rho_s^2} \quad (58)$$

If the quantity  $\epsilon F_{c_i}^2$  is greater than or equal to the quantity  $(\mu_{y_i}^2 F_{z_i}^2 - 1)$  then the tire is completely saturated due to braking or thrust forces and the side force  $F_{s_i} = 0$ .

The effect of camber thrust is included in the tire model by modifying the slip angle by a value denoted by  $\beta_i'$  which is determined using the following relation:

$$\beta_i' = -\frac{AT3 (A4 - F_{z_i}) F_{z_i}}{A4 [A1 F_{z_i} (F_{z_i} - A2) - AT2]} \left( \gamma_i - \frac{2}{\pi} \gamma_i |\gamma_i| \right) \quad (59)$$

where, A1, A2, A3 and A4 are Calspan coefficients and

$$AT3 = A2 A3$$

$$AT2 = A0 A2$$

This relation represents a parabolic function of camber angle  $\gamma_i$  and results in a maximum value of  $\beta_i'$  at a camber angle of 45 degrees. At camber angles greater than 45 degrees the value of  $\beta_i'$  begins to decrease.

The non-dimensional slip angle can be determined using the following relation:

$$\bar{\beta}_i = \frac{-SN [A1 F_{z_i} (F_{z_i} - A2) - AT2] (\beta_i + \beta_i')}{A2 \sqrt{|\mu_{y_i}^2 F_{z_i}^2 - \epsilon F_{c_i}^2|}} \quad (60)$$

If the tire is in a free rolling condition ( $-1 < S_i < 1$ ) then the tire's lateral force is determined using the non-dimensional slip angle approach. When the absolute value of  $\bar{\beta}_i$  is greater than or equal to 3 then the tire is assumed to be saturated and the tire side force is determined from:

$$F_{s_i} = \text{Sgn}(\bar{\beta}_i) \sqrt{\mu_{y_i}^2 F_{z_i}^2 - \epsilon F_{c_i}^2} \quad (61)$$

If  $-3 \leq \bar{\beta}_i \leq 3$  then the tire is not saturated and the tire side force is calculated as:

$$F_{S_i} = \sqrt{\mu_{y_i}^2 F_{Z_i}^2 - \epsilon F_{C_i}^2} \left( \bar{\beta}_i - \frac{\bar{\beta}_i |\bar{\beta}_i|}{3} + \frac{\bar{\beta}_i^3}{27} \right) \quad (62)$$

If the tire is locked due to excessive braking torque ( $S_i = 1$ ) then the tire's lateral and longitudinal forces are determined using coulomb friction which acts in a direction which opposes the tire's direction of motion:

$$F_{S_i} = \mu_{xS_i} F_{Z_i} \text{Sin } \beta_i \quad (63)$$

$$F_{C_i} = \mu_{xS_i} F_{Z_i} \text{Cos } \beta_i \quad (64)$$

If the wheelspin occurs ( $S_i = -1$ ) then the tire's lateral force is assumed to be zero and the thrust force is equal to sliding frictional force:

$$F_{S_i} = 0 \quad (65)$$

$$F_{C_i} = \mu_{xS_i} F_{Z_i} \quad (66)$$

Once the tire's lateral and longitudinal forces  $F_{S_i}$  and  $F_{C_i}$  are known these forces can be transformed from the tire's coordinate system to the vehicle coordinate system as shown below:

$$F_{x_i} = \text{Sgn}(V_{x_i}) (-F_{C_i} \text{Cos } \delta_i - F_{S_i} \text{Sin } \delta_i) \quad (67)$$

$$F_{y_i} = -F_{C_i} \text{Sin } \delta_i + F_{S_i} \text{Cos } \delta_i \quad (68)$$

The aligning moment generated by each tire is determined using relations developed by Calspan Corporation and utilizes Calspan tire measurement data to compute aligning moment based on normal force  $F_{Z_i}$ , side force  $F_{y_i}$  and camber angle  $\gamma_i$ :



$$M_{z_i} = K_1 F_{z_i} F_{y_i} - K_2 F_{y_i} |F_{y_i}| + \frac{K_3 F_{z_i} \gamma_i}{\sqrt{|\gamma_i|}} \quad (69)$$

If the tire is either locked or spinning due to excessive braking or driving torques ( $S_i = -1$  or  $S_i = 1$ ) then the aligning moment is set to zero.

### Equations of Motion

Once the aerodynamic and pneumatic forces and moments have been determined then these forces can be supplied to the equations of motion. Solving for the acceleration terms and substituting in the aerodynamic and pneumatic forces and moments yields:

$$\dot{U} = \frac{F_{x_1} + F_{x_2} + F_{x_3} + F_{x_4}}{m} + V_r \quad (70)$$

$$\dot{V} = \frac{F_{y_1} + F_{y_2} + F_{y_3} + F_{y_4} + F_{y_a}}{m} - U_r \quad (71)$$

$$\dot{r} = \frac{a(F_{y_1} + F_{y_2}) - b(F_{y_3} + F_{y_4}) + \frac{T_f}{2}(F_{x_2} - F_{x_1}) + \frac{T_f}{2}(F_{x_4} - F_{x_3}) + \sum_{i=1}^4 M_{z_i} + M_{z_a}}{I_z} \quad (72)$$

These accelerations can be integrated to obtain the following values,

Forward velocity U:

$$U = \int \dot{U} dt \quad (73)$$

Lateral velocity V:

$$V = \int \dot{V} dt \quad (74)$$

Yaw rate  $r$ :

$$r = \dot{\psi} \quad (75)$$

Heading angle  $\psi$ :

$$\psi = \int r \, dt \quad (76)$$

The vehicle's X-Y path:

$$X = \int (U \cos \psi - V \sin \psi) \, dt \quad (77)$$

$$Y = \int (U \sin \psi + V \cos \psi) \, dt$$

The initial conditions for  $V$ ,  $r$ ,  $\Psi$ ,  $X$  and  $Y$  can be assumed to be equal to zero.

### 2.2.2 IMIRS Rollover Model

The IMIRS rollover model (Figure 2) uses 5 generalized coordinates as degrees of freedom. These coordinates are listed below:

- $\phi_u$  - Roll angle of the unsprung mass
- $Y_u$  - Lateral displacement of the unsprung mass center of gravity
- $Z_u$  - Vertical position of the unsprung mass center of gravity
- $\phi_{s/u}$  - Roll angle of the sprung mass relative to the unsprung mass
- $\eta$  - Heave of the sprung mass relative to the unsprung mass

The equations of motion of the IMIRS rollover model have been derived using the Lagrangian formulation. The system's Equations of Motion can be written in the general form:

$$\frac{d}{dt} \left( \frac{\partial T}{\partial \dot{Y}_u} \right) = Q_{y_u} + \frac{\partial T}{\partial Y_u} - \frac{\partial V}{\partial Y_u} - \frac{\partial F}{\partial \dot{Y}_u} \quad (78)$$

$$\frac{d}{dt} \left( \frac{\partial T}{\partial \dot{Z}_u} \right) = Q_{z_u} + \frac{\partial T}{\partial Z_u} - \frac{\partial V}{\partial Z_u} - \frac{\partial F}{\partial \dot{Z}_u} \quad (79)$$

$$\frac{d}{dt} \left( \frac{\partial T}{\partial \dot{\phi}_u} \right) = Q_{\phi_u} + \frac{\partial T}{\partial \phi_u} - \frac{\partial V}{\partial \phi_u} - \frac{\partial F}{\partial \dot{\phi}_u} \quad (80)$$

$$\frac{d}{dt} \left( \frac{\partial T}{\partial \dot{\phi}_{s/u}} \right) = Q_{\phi_{s/u}} + \frac{\partial T}{\partial \phi_{s/u}} - \frac{\partial V}{\partial \phi_{s/u}} - \frac{\partial F}{\partial \dot{\phi}_{s/u}} \quad (81)$$

$$\frac{d}{dt} \left( \frac{\partial T}{\partial \dot{\eta}} \right) = Q_{\eta} + \frac{\partial T}{\partial \eta} - \frac{\partial V}{\partial \eta} - \frac{\partial F}{\partial \dot{\eta}} \quad (82)$$

### Kinetic Energy

The system's total kinetic energy  $T$  can be expressed as functions of the generalized coordinates and generalized velocities and is equal to the kinetic energy of the sprung mass  $T_s$  plus the kinetic energy of the unsprung mass  $T_u$ :

$$T = T_u + T_s \quad (83)$$

where,

$$T_u = \frac{1}{2} m_u (\dot{Y}_u^2 + \dot{Z}_u^2) + \frac{1}{2} I_{xu} \dot{\phi}_u^2 \quad (84)$$

$$\begin{aligned} T_s = \frac{1}{2} m_s \left\{ \left[ \dot{Y}_u + H_p \dot{\phi}_u \cos \phi_u - \eta \dot{\phi}_u \cos \phi_u - \dot{\eta} \sin \phi_u + H_{raz} (\dot{\phi}_u + \dot{\phi}_{s/u}) \right]^2 \right. \\ \left. + \left[ \dot{Z}_u + H_p \dot{\phi}_u \sin \phi_u - \eta \dot{\phi}_u \sin \phi_u + \dot{\eta} \cos \phi_u + H_{ray} (\dot{\phi}_u + \dot{\phi}_{s/u}) \right]^2 \right\} \\ + \frac{1}{2} I_{xs} (\dot{\phi}_u + \dot{\phi}_{s/u})^2 \end{aligned} \quad (85)$$

and

$$H_{ray} = H_{ra} \text{Sin} (\phi_{s/u} + \phi_u) \quad (86)$$

$$H_{raz} = H_{ra} \text{Cos} (\phi_{s/u} + \phi_u) \quad (87)$$

The resulting kinetic energy expression can be differentiated with respect to the generalized velocities,

$$\frac{\partial T}{\partial \dot{Y}_u} = m_u \dot{Y}_u + m_s V_y \quad (88)$$

$$\frac{\partial T}{\partial \dot{Z}_u} = m_u \dot{Z}_u + m_s V_z \quad (89)$$

$$\frac{\partial T}{\partial \dot{\phi}_u} = I_{xu} \dot{\phi}_u + m_s [V_y (h_d \text{Cos} \phi_u + H_{raz}) + V_z (h_d \text{Sin} \phi_u + H_{ray})] + I_{xs} (\dot{\phi}_u + \dot{\phi}_{s/u}) \quad (90)$$

$$\frac{\partial T}{\partial \dot{\phi}_{s/u}} = m_s (V_y H_{raz} + V_z H_{ray}) + I_{xs} (\dot{\phi}_u + \dot{\phi}_{s/u}) \quad (91)$$

$$\frac{\partial T}{\partial \dot{\eta}} = m_s (-V_y \text{Sin} \phi_u + V_z \text{Cos} \phi_u) \quad (92)$$

where,

$$V_y = \dot{Y}_u + H_d \dot{\phi}_u \text{Cos} \phi_u - \dot{\eta} \text{Sin} \phi_u + H_{raz} (\dot{\phi}_u + \dot{\phi}_{s/u}) \quad (93)$$

$$V_z = \dot{Z}_u + H_d \dot{\phi}_u \text{Sin} \phi_u + \dot{\eta} \text{Cos} \phi_u + H_{ray} (\dot{\phi}_u + \dot{\phi}_{s/u}) \quad (94)$$

$$H_d = H_p - \eta \quad (95)$$

The time derivatives of the above expressions are given:

$$\begin{aligned} \frac{d}{dt} \left( \frac{\partial T}{\partial \dot{Y}_u} \right) &= (m_s + m_u) \ddot{Y}_u + m_s (h_d \text{Cos} \phi_u + H_{raz}) \ddot{\phi}_u + m_s H_{raz} \ddot{\phi}_{s/u} - m_s \text{Sin} \phi_u \ddot{\eta} \\ &\quad - m_s \left[ H_d \dot{\phi}_u^2 \text{Sin} \phi_u + 2\dot{\eta} \dot{\phi}_u \text{Cos} \phi_u + H_{ray} (\dot{\phi}_u + \dot{\phi}_{s/u})^2 \right] \end{aligned} \quad (96)$$

$$\begin{aligned} \frac{d}{dt} \left( \frac{\partial T}{\partial \dot{Z}_u} \right) &= (m_s + m_u) \ddot{Z}_u + m_s (h_d \sin \phi_u + H_{ray}) \ddot{\phi}_u + m_s H_{ray} \ddot{\phi}_{s/u} + m_s \cos \phi_u \ddot{\eta} \\ &\quad - m_s \left[ -H_d \dot{\phi}_u^2 \cos \phi_u + 2 \dot{\eta} \dot{\phi}_u \sin \phi_u - H_{raz} (\dot{\phi}_u + \dot{\phi}_{s/u})^2 \right] \end{aligned} \quad (97)$$

$$\begin{aligned} \frac{d}{dt} \left( \frac{\partial T}{\partial \dot{\phi}_u} \right) &= m_s T_1 \ddot{Y}_u + m_s T_3 \ddot{Z}_u \\ &\quad + \ddot{\phi}_u \left\{ (I_{xu} + I_{xs}) + m_s [(H_d \cos \phi_u + H_{raz}) T_1 + (H_d \sin \phi_u + H_{ray}) T_3] \right\} \\ &\quad + \ddot{\phi}_{s/u} [I_{xs} + m_s (T_1 H_{raz} + T_3 H_{ray})] + \ddot{\eta} [m_s (-T_1 \sin \phi_u + T_3 \cos \phi_u)] \\ &\quad + m_s \left\{ T_1 \left[ -H_d \dot{\phi}_u^2 \sin \phi_u - 2 \dot{\eta} \dot{\phi}_u \cos \phi_u - H_{ray} (\dot{\phi}_u + \dot{\phi}_{s/u})^2 \right] \right. \\ &\quad \left. + V_y T_2 + T_3 \left[ H_d \dot{\phi}_u^2 \cos \phi_u - 2 \dot{\eta} \dot{\phi}_u \sin \phi_u + H_{raz} (\dot{\phi}_u + \dot{\phi}_{s/u})^2 \right] + T_4 V_z \right\} \end{aligned} \quad (98)$$

$$\begin{aligned} \frac{d}{dt} \left( \frac{\partial T}{\partial \dot{\phi}_{s/u}} \right) &= m_s H_{raz} \ddot{Y}_u + m_s H_{ray} \ddot{Z}_u + [I_{xs} + m_s (T_1 H_{raz} + T_3 H_{ray})] \ddot{\phi}_u \\ &\quad + [I_{xs} + m_s H_{ra}^2] \ddot{\phi}_{s/u} - [m_s (-H_{raz} \sin \phi_u + H_{ray} \cos \phi_u)] \ddot{\eta} \\ &\quad + m_s \left\{ \left[ -H_d \dot{\phi}_u^2 \sin \phi_u - 2 \dot{\eta} \dot{\phi}_u \cos \phi_u - H_{ray} (\dot{\phi}_u + \dot{\phi}_{s/u})^2 \right] H_{raz} \right. \\ &\quad \left. - V_y (\dot{\phi}_u + \dot{\phi}_{s/u}) H_{ray} + \left[ H_d \dot{\phi}_u^2 \cos \phi_u - 2 \dot{\eta} \dot{\phi}_u \sin \phi_u + H_{raz} (\dot{\phi}_u + \dot{\phi}_{s/u})^2 \right] H_{ray} \right. \\ &\quad \left. + V_z H_{raz} (\dot{\phi}_u + \dot{\phi}_{s/u}) \right\} \end{aligned} \quad (99)$$

$$\begin{aligned} \frac{d}{dt} \left( \frac{\partial T}{\partial \dot{\eta}} \right) &= -m_s \sin \phi_u \ddot{Y}_u + m_s \cos \phi_u \ddot{Z}_u + m_s (-H_{raz} \sin \phi_u + H_{ray} \cos \phi_u) (\ddot{\phi}_u + \ddot{\phi}_{s/u}) \\ &\quad + [m_s \ddot{\eta} + m_s (\dot{\phi}_u + \dot{\phi}_{s/u})^2 (H_{ray} \sin \phi_{s/u} + H_{raz} \cos \phi_{s/u}) + H_d \dot{\phi}_u^2 \\ &\quad - V_y \dot{\phi}_u \cos \phi_u - V_z \dot{\phi}_u \sin \phi_u] \end{aligned} \quad (100)$$

where,

$$\begin{aligned}
T_1 &= H_d \text{Cos } \phi_u + H_{raz} \\
T_2 &= -H_d \dot{\phi}_u \text{Sin } \phi_u - \dot{\eta} \text{Cos } \phi_u - (\dot{\phi}_u + \dot{\phi}_{s/u}) H_{ray} \\
T_3 &= H_d \text{Sin } \phi_u + H_{ray} \\
T_4 &= H_d \dot{\phi}_u \text{Cos } \phi_u + \dot{\eta} \text{Sin } \phi_u + (\dot{\phi}_u + \dot{\phi}_{s/u}) H_{raz}
\end{aligned} \tag{101}$$

Next, the partial derivatives of the kinetic energy with respect to the generalized coordinates are found:

$$\begin{aligned}
\frac{\partial T}{\partial Y_u} &= 0 \\
\frac{\partial T}{\partial Z_u} &= 0 \\
\frac{\partial T}{\partial \phi_u} &= m_s V_y T_2 + m_s V_z T_4 \\
\frac{\partial T}{\partial \phi_{s/u}} &= m_s (\dot{\phi}_u + \dot{\phi}_{s/u}) (V_z H_{raz} - V_y H_{ray}) \\
\frac{\partial T}{\partial \eta} &= -m_s \dot{\phi}_u (V_y \text{Cos } \phi_u + V_z \text{Sin } \phi_u)
\end{aligned} \tag{102}$$

### Potential Energy

The potential energy of the system can be subdivided into 9 components. The vehicle components which store potential energy are illustrated in Figure 4. These potential energy terms can be expressed using the relations shown below:

The gravitational potential energies of the sprung and unsprung masses:

$$V_{Gs} = -m_s g [-Z_u + (H_p - \eta) \text{Cos } \phi_u + H_{ra} \text{Cos } (\phi_u + \phi_{s/u})] \tag{103}$$

$$V_{Gu} = -m_u g Z_u \tag{104}$$

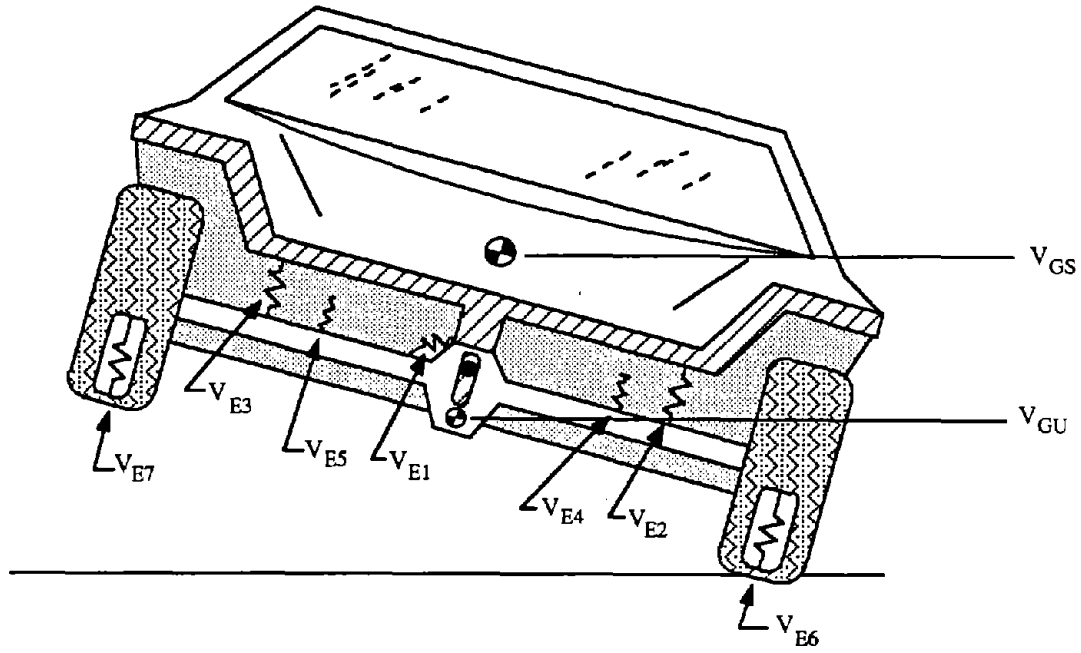


Figure 4. Vehicle Components Which Store Potential Energies.

The elastic potential energy of the left and right suspension springs and the suspension anti-roll bar are:

$$V_{E1} = \frac{1}{2} K_r \phi_{s/u}^2 \quad (105)$$

$$V_{E2} = \frac{1}{2} K_s X_l^2 \quad (106)$$

$$V_{E3} = \frac{1}{2} K_s X_r^2 \quad (107)$$

where, the deformations in the left and right springs  $X_l$  and  $X_r$  are calculated using the following formulas:

$$X_l = L_u - \sqrt{(t_s + H_b \sin \phi_{s/u} - t_s \cos \phi_{s/u})^2 + (L_s - H_b - \eta + H_b \cos \phi_{s/u} + t_s \sin \phi_{s/u})^2}$$

$$X_r = L_u - \sqrt{(t_s - H_b \sin \phi_{s/u} - t_s \cos \phi_{s/u})^2 + (L_s - H_b - \eta + H_b \cos \phi_{s/u} - t_s \sin \phi_{s/u})^2}$$

(108)

and the undeformed suspension spring length  $L_u$  is calculated as:

$$L_u = L_s + \frac{1}{2} \frac{m_s g}{K_s} \quad (109)$$

The potential energy stored in the suspension bump stops is determined using the following expressions:

$$\begin{aligned} V_{E4} &= -\delta_4 K_b L_b \left[ \Delta_{lb} + L_b \log_e |L_b - \Delta_{lb}| - L_b \log_e (L_b) \right] \\ V_{E5} &= -\delta_5 K_b L_b \left[ \Delta_{rb} + L_b \log_e |L_b - \Delta_{rb}| - L_b \log_e (L_b) \right] \end{aligned} \quad (110)$$

where, the bump stop deflections  $\Delta_{lb}$  and  $\Delta_{rb}$  are calculated using:

$$\begin{aligned} \Delta_{lb} &= L_b - \left[ H_u + H_p - \eta - T_{bas} + H_b \cos \phi_{s/u} + (t_s + H_b \sin \phi_{s/u}) \tan \phi_{s/u} \right] \\ \Delta_{rb} &= L_b - \left[ H_u + H_p - \eta - T_{bas} + H_b \cos \phi_{s/u} - (t_s - H_b \sin \phi_{s/u}) \tan \phi_{s/u} \right] \end{aligned} \quad (111)$$

and

$\delta_4$  equals one if  $\Delta_{lb}$  is less than 0, otherwise  $\delta_4$  is equal to zero

$\delta_5$  equals one if  $\Delta_{rb}$  is less than 0, otherwise  $\delta_5$  is equal to zero.

The expressions used to determine the potential energies  $V_{E4}$  and  $V_{E5}$  represent non-linear rising rate springs which become infinitely stiff when the amount of compression ( $\Delta_{lb}$  or  $\Delta_{rb}$ ) equals the undeformed bump stop length  $L_b$ .

The potential energy stored in tires is determined:

$$V_{E6} = \frac{1}{2} K_t \delta_6 \Delta_{lt}^2 \quad (112)$$

$$V_{E7} = \frac{1}{2} K_t \delta_7 \Delta_{rt}^2 \quad (113)$$



where the radial deformations in the left and right tires are calculated:

$$\Delta_{lt} = H_u + \frac{g (m_s + m_u)}{2 K_t} - \left( \frac{-Z_u}{\cos \phi_u} + t_w \tan \phi_u \right) \quad (114)$$

$$\Delta_{rt} = H_u + \frac{g (m_s + m_u)}{2 K_t} - \left( \frac{-Z_u}{\cos \phi_u} - t_w \tan \phi_u \right) \quad (115)$$

and

$\delta_6$  equals one if  $\Delta_{lt}$  is less than zero, otherwise  $\delta_6$  equals zero

$\delta_7$  equals one if  $\Delta_{rt}$  is less than zero, otherwise  $\delta_7$  equals zero

The partial derivatives of potential energy with respect to the generalized coordinates can now be found:

$$\frac{\partial V}{\partial Y_u} = 0 \quad (116)$$

$$\left. \frac{\partial V}{\partial Z_u} \right|_{G_u} = -m_u g \quad (117)$$

$$\left. \frac{\partial V}{\partial Z_u} \right|_{G_s} = -m_s g \quad (118)$$

$$\left. \frac{\partial V}{\partial Z_u} \right|_{E6} = \frac{K_t \delta_6 \Delta_{lt}}{\cos \phi_u} \quad (119)$$

$$\left. \frac{\partial V}{\partial Z_u} \right|_{E7} = \frac{K_t \delta_7 \Delta_{rt}}{\cos \phi_u} \quad (120)$$

$$\frac{\partial V}{\partial Z_u} = \left. \frac{\partial V}{\partial Z_u} \right|_{G_u} + \left. \frac{\partial V}{\partial Z_u} \right|_{G_s} + \left. \frac{\partial V}{\partial Z_u} \right|_{E6} + \left. \frac{\partial V}{\partial Z_u} \right|_{E7} \quad (121)$$

$$\left. \frac{\partial V}{\partial \phi_u} \right|_{G_s} = -m_s g (H_d \sin \phi_u + H_{ray}) \quad (122)$$

$$\left. \frac{\partial V}{\partial \phi_u} \right|_{E6} = -\delta_6 K_t \Delta l_t \left[ \frac{-Z_u \tan \phi_u}{\cos \phi_u} + t_w (1 + \tan^2 \phi_u) \right] \quad (123)$$

$$\left. \frac{\partial V}{\partial \phi_u} \right|_{E7} = -\delta_7 K_t \Delta r_t \left[ \frac{-Z_u \tan \phi_u}{\cos \phi_u} - t_w (1 + \tan^2 \phi_u) \right] \quad (124)$$

$$\frac{\partial V}{\partial \phi_u} = \left. \frac{\partial V}{\partial \phi_u} \right|_{G_s} + \left. \frac{\partial V}{\partial \phi_u} \right|_{E6} + \left. \frac{\partial V}{\partial \phi_u} \right|_{E7} \quad (125)$$

$$\left. \frac{\partial V}{\partial \phi_{s/u}} \right|_{G_s} = -m_s g H_{ray} \quad (126)$$

$$\left. \frac{\partial V}{\partial \phi_{s/u}} \right|_{E1} = K_r \phi_{s/u} \quad (127)$$

$$\left. \frac{\partial V}{\partial \phi_{s/u}} \right|_{E2} = \frac{-K_s (L_u - X_l)}{X_l} (T_5 T_6 + T_7 T_8) \quad (128)$$

$$\left. \frac{\partial V}{\partial \phi_{s/u}} \right|_{E3} = \frac{-K_s (L_u - X_r)}{X_r} (T_9 T_{10} + T_{11} T_{12}) \quad (129)$$

$$\left. \frac{\partial V}{\partial \phi_{s/u}} \right|_{E4} = \frac{-\delta_4 K_b L_b (L_b - X_{lb})}{X_{lb}} \times \left( -H_b \sin \phi_{s/u} + \frac{t_s + H_b \sin \phi_{s/u}}{\cos^2 \phi_{s/u}} + (t_s + H_b \cos \phi_{s/u}) \tan \phi_{s/u} \right) \quad (130)$$

$$\frac{\partial V}{\partial \phi_{s/u}} \Big|_{E5} = \frac{-\delta_5 K_b L_b (L_b - X_{rb})}{X_{rb}} \times \left( -H_b \sin \phi_{s/u} - \frac{t_s - H_b \sin \phi_{s/u}}{\cos^2 \phi_{s/u}} - (t_s - H_b \cos \phi_{s/u}) \tan \phi_{s/u} \right) \quad (131)$$

$$\frac{\partial V}{\partial \phi_{s/u}} = \frac{\partial V}{\partial \phi_{s/u}} \Big|_{G_s} + \frac{\partial V}{\partial \phi_{s/u}} \Big|_{E1} + \frac{\partial V}{\partial \phi_{s/u}} \Big|_{E2} + \frac{\partial V}{\partial \phi_{s/u}} \Big|_{E3} + \frac{\partial V}{\partial \phi_{s/u}} \Big|_{E4} + \frac{\partial V}{\partial \phi_{s/u}} \Big|_{E5} \quad (132)$$

$$\frac{\partial V}{\partial \eta} \Big|_{G_s} = -m_s g \cos \phi_u \quad (133)$$

$$\frac{\partial V}{\partial \eta} \Big|_{E2} = \frac{K_s (L_u - X_l)}{X_l} T_7 \quad (134)$$

$$\frac{\partial V}{\partial \eta} \Big|_{E3} = \frac{K_s (L_u - X_r)}{X_r} T_{11} \quad (135)$$

$$\frac{\partial V}{\partial \eta} \Big|_{E4} = \frac{\delta_4 K_b L_b (L_b - X_{lb})}{X_{lb}} \quad (136)$$

$$\frac{\partial V}{\partial \eta} \Big|_{E5} = \frac{\delta_5 K_b L_b (L_b - X_{rb})}{X_{rb}} \quad (137)$$

$$\frac{\partial V}{\partial \eta} = \frac{\partial V}{\partial \eta} \Big|_{G_s} + \frac{\partial V}{\partial \eta} \Big|_{E2} + \frac{\partial V}{\partial \eta} \Big|_{E3} + \frac{\partial V}{\partial \eta} \Big|_{E4} + \frac{\partial V}{\partial \eta} \Big|_{E5} \quad (138)$$

### Energy Dissipation Terms

The IMIRS rollover model contains 5 viscous damping elements. Two elements represent the suspension shock absorbers, two other represent the damping which is inherent in the tire, and the fifth represents an anti-roll damping element in the suspension system. These dampers are shown in Figure 3. The Rayleigh Dissipation Function of the system can be written as shown:

$$F = \frac{1}{2} \left[ C_t \left( \delta_6 \dot{\Delta}_{lt}^2 + \delta_7 \dot{\Delta}_{rt}^2 \right) + C_s \left( \dot{X}_l^2 + \dot{X}_r^2 \right) + C_r \dot{\phi}_{s/u}^2 \right] \quad (139)$$

where,

$$\dot{\Delta}_{lt} = \frac{\dot{Z}_u}{\cos \phi_u} + \frac{\dot{\phi}_u (Z_u \sin \phi_u - t_w)}{\cos^2 \phi_u} \quad (140)$$

$$\dot{\Delta}_{rt} = \frac{\dot{Z}_u}{\cos \phi_u} + \frac{\dot{\phi}_u (Z_u \sin \phi_u + t_w)}{\cos^2 \phi_u} \quad (141)$$

$$\dot{X}_l = \frac{T_5 \dot{\phi}_{s/u} T_6 + T_7 (-\dot{\eta} + T_8 \dot{\phi}_{s/u})}{X_l} \quad (142)$$

$$\dot{X}_r = \frac{T_9 \dot{\phi}_{s/u} T_{10} + T_{11} (-\dot{\eta} + T_{12} \dot{\phi}_{s/u})}{X_r} \quad (143)$$

and

$$T_5 = t_s + H_b \sin \phi_{s/u} - t_s \cos \phi_{s/u} \quad (144)$$

$$T_6 = H_b \cos \phi_{s/u} + t_s \sin \phi_{s/u} \quad (145)$$

$$T_7 = H_u - T_{bas} + H_d + H_b \cos \phi_{s/u} + t_s \sin \phi_{s/u} \quad (146)$$

$$T_8 = -H_b \sin \phi_{s/u} + t_s \cos \phi_{s/u} \quad (147)$$

$$T_9 = t_s - H_b \sin \phi_{s/u} - t_s \cos \phi_{s/u} \quad (148)$$

$$T_{10} = -H_b \cos \phi_{s/u} + t_s \sin \phi_{s/u} \quad (149)$$

$$T_{11} = H_u - T_{bas} + H_d + H_b \cos \phi_{s/u} - t_s \sin \phi_{s/u} \quad (150)$$

$$T_{12} = -H_b \sin \phi_{s/u} - t_s \cos \phi_{s/u} \quad (151)$$

The partial derivatives of the Rayleigh dissipation function with respect to generalized velocities are found:

$$\frac{\partial F}{\partial \dot{Y}_u} = 0 \quad (152)$$

$$\frac{\partial F}{\partial \dot{Z}_u} = \frac{C_t (\delta_6 \dot{\Delta}_{lt} + \delta_7 \dot{\Delta}_{rt})}{\cos \phi_u} \quad (153)$$

$$\frac{\partial F}{\partial \dot{\phi}_u} = \frac{C_t [\delta_6 \dot{\Delta}_{lt} (Z_u \sin \phi_u - t_w) + \delta_7 \dot{\Delta}_{rt} (Z_u \sin \phi_u + t_w)]}{\cos^2 \phi_u} \quad (154)$$

$$\frac{\partial F}{\partial \dot{\phi}_{s/u}} = C_s \left( \dot{X}_l \frac{T_5 T_6 + T_7 T_8}{X_l} + \dot{X}_r \frac{T_9 T_{10} + T_{11} T_{12}}{X_r} \right) + C_r \dot{\phi}_{s/u} \quad (155)$$

$$\frac{\partial F}{\partial \dot{\eta}} = -C_s \left( \frac{\dot{X}_l T_7}{X_l} + \frac{\dot{X}_r T_{11}}{X_r} \right) \quad (156)$$

### External Generalized Forces

The rollover model is coupled to the vehicle handling model through the external forces which are applied to the planar model. These forces include the lateral reaction forces generated by the tires and the inertial forces acting on the vehicle masses and are illustrated in Figure 5.

$$Q_y = F_s + F_u + F_r + F_l \quad (157)$$

$$F_r = F_{y1} + F_{y3} \quad (158)$$

$$F_l = F_{y2} + F_{y4} \quad (159)$$

$$F_s = -m_s a_y \quad (160)$$

$$F_u = -m_u a_y \quad (162)$$

$$Q_{\phi_u} = F_s (H_{raz} + H_d \cos \phi_u) + F_l (t_w \sin \phi_u - H_u \cos \phi_u) - F_r (t_w \sin \phi_u + H_u \cos \phi_u) \quad (163)$$

$$Q_{\phi_{s/u}} = F_s H_{raz} \quad (164)$$

$$Q_{\eta} = -F_s \sin \phi_u \quad (165)$$

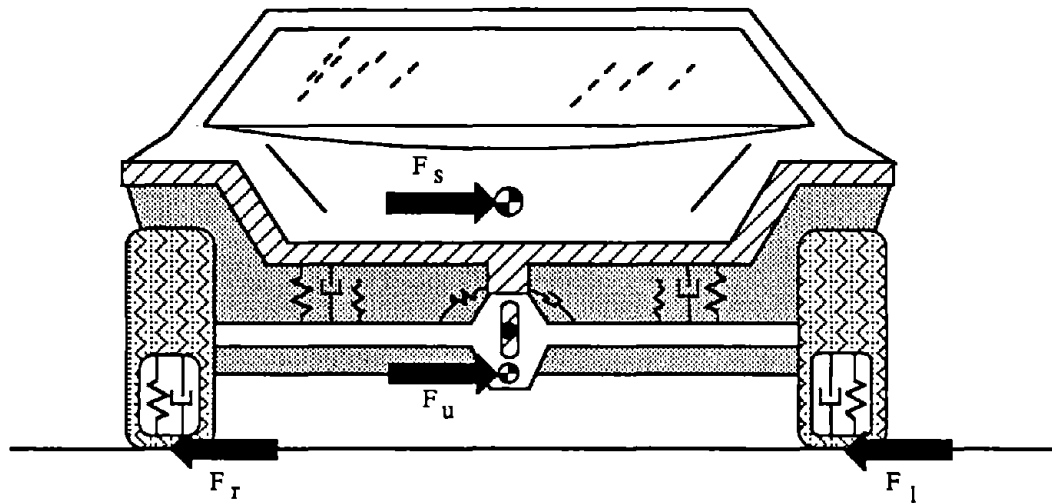


Figure 5. External Forces to Planar Rollover Model.

Equations of Motion for the IMIRS Rollover Model

After each of the terms shown in equations (78) - (82) have been found the equations of motion can be written in the following matrix form:

$$\begin{bmatrix} A_{11} & A_{12} & A_{13} & A_{14} & A_{15} \\ A_{21} & A_{22} & A_{23} & A_{24} & A_{25} \\ A_{31} & A_{32} & A_{33} & A_{34} & A_{35} \\ A_{41} & A_{42} & A_{43} & A_{44} & A_{45} \\ A_{51} & A_{52} & A_{53} & A_{54} & A_{55} \end{bmatrix} \begin{bmatrix} \ddot{Y}_u \\ \ddot{Z}_u \\ \ddot{\phi}_u \\ \ddot{\phi}_{s/u} \\ \ddot{\eta} \end{bmatrix} = \begin{bmatrix} B_1 \\ B_2 \\ B_3 \\ B_4 \\ B_5 \end{bmatrix} \quad (166)$$

where,

$$A_{11} = m_s + m_u \quad (167)$$

$$A_{12} = 0 \quad (168)$$

$$A_{13} = m_s (h_d \cos \phi_u + H_{raz}) \quad (169)$$

$$A_{14} = m_s H_{raz} \quad (170)$$

$$A_{15} = -m_s \sin \phi_u \quad (171)$$

$$A_{21} = 0 \quad (172)$$

$$A_{22} = A_{11} \quad (173)$$

$$A_{23} = m_s (h_d \sin \phi_u + H_{ray}) \quad (174)$$

$$A_{24} = m_s H_{ray} \quad (175)$$

$$A_{25} = m_s \cos \phi_u \quad (176)$$

$$A_{31} = m_s T_1 \quad (177)$$

$$A_{32} = m_s T_3 \quad (178)$$

$$A_{33} = (I_{xu} + I_{xs}) + m_s [(H_d \cos \phi_u + H_{raz}) T_1 + (H_d \sin \phi_u + H_{ray}) T_3] \quad (179)$$

$$A_{34} = I_{xs} + m_s (T_1 H_{raz} + T_3 H_{ray}) \quad (180)$$

$$A_{35} = m_s (-T_1 \sin \phi_u + T_3 \cos \phi_u) \quad (181)$$

$$A_{41} = m_s H_{raz} \quad (182)$$

$$A_{42} = m_s H_{ray} \quad (183)$$

$$A_{43} = A_{34} \quad (184)$$

$$A_{44} = I_{xs} + m_s H_{ra}^2 \quad (185)$$

$$A_{45} = m_s (-H_{raz} \sin \phi_u + H_{ray} \cos \phi_u) \quad (186)$$

$$A_{51} = -m_s \sin \phi_u \quad (187)$$

$$A_{52} = m_s \cos \phi_u \quad (188)$$

$$A_{53} = A_{45} \quad (189)$$

$$A_{54} = A_{53} \quad (190)$$

$$A_{55} = m_s \quad (191)$$

$$B_1 = Q_y + m_s [H_d \dot{\phi}_u^2 \sin \phi_u + 2\dot{\eta} \dot{\phi}_u \cos \phi_u + H_{ray} (\dot{\phi}_u + \dot{\phi}_{s/u})^2] \quad (192)$$

$$B_2 = -\frac{\partial V}{\partial Z_u} - \frac{\partial F}{\partial \dot{Z}_u} + m_s [-H_d \dot{\phi}_u^2 \cos \phi_u + 2\dot{\eta} \dot{\phi}_u \sin \phi_u - H_{raz} (\dot{\phi}_u + \dot{\phi}_{s/u})^2] \quad (193)$$



$$\begin{aligned}
B_3 = & Q_{\dot{\phi}_u} + \frac{\partial T}{\partial \dot{\phi}_u} - \frac{\partial V}{\partial \dot{\phi}_u} - \frac{\partial F}{\partial \dot{\phi}_u} - m_s \left\{ T_1 \left[ -H_d \dot{\phi}_u^2 \sin \phi_u - 2\dot{\eta} \dot{\phi}_u \cos \phi_u - H_{ray} (\dot{\phi}_u + \dot{\phi}_{s/u})^2 \right] \right. \\
& \left. + V_y T_2 + T_3 \left[ H_d \dot{\phi}_u^2 \cos \phi_u - 2\dot{\eta} \dot{\phi}_u \sin \phi_u + H_{raz} (\dot{\phi}_u + \dot{\phi}_{s/u})^2 \right] + T_4 V_z \right\}
\end{aligned} \tag{194}$$

$$\begin{aligned}
B_4 = & Q_{\dot{\phi}_{s/u}} + \frac{\partial T}{\partial \dot{\phi}_{s/u}} - \frac{\partial V}{\partial \dot{\phi}_{s/u}} - \frac{\partial F}{\partial \dot{\phi}_{s/u}} \\
& - m_s \left\{ \left[ -H_d \dot{\phi}_u^2 \sin \phi_u - 2\dot{\eta} \dot{\phi}_u \cos \phi_u - H_{ray} (\dot{\phi}_u + \dot{\phi}_{s/u})^2 \right] H_{raz} \right. \\
& - V_y (\dot{\phi}_u + \dot{\phi}_{s/u}) H_{ray} + \left[ H_d \dot{\phi}_u^2 \cos \phi_u - 2\dot{\eta} \dot{\phi}_u \sin \phi_u + H_{raz} (\dot{\phi}_u + \dot{\phi}_{s/u})^2 \right] H_{ray} \\
& \left. + V_z H_{raz} (\dot{\phi}_u + \dot{\phi}_{s/u}) \right\}
\end{aligned} \tag{195}$$

$$\begin{aligned}
B_5 = & Q_{\dot{\eta}} + \frac{\partial T}{\partial \dot{\eta}} - \frac{\partial V}{\partial \dot{\eta}} - \frac{\partial F}{\partial \dot{\eta}} \\
& - m_s \left[ (\dot{\phi}_u + \dot{\phi}_s)^2 (H_{ray} \sin \phi_{s/u} + H_{raz} \cos \phi_{s/u}) + H_d \dot{\phi}_u^2 - V_y \dot{\phi}_u \cos \phi_u - V_z \dot{\phi}_u \sin \phi_u \right]
\end{aligned} \tag{196}$$

Matrix [A] can be inverted allowing us to solve for acceleration terms as shown below:

$$\begin{bmatrix} \ddot{Y}_u \\ \ddot{Z}_u \\ \ddot{\phi}_u \\ \ddot{\phi}_{s/u} \\ \ddot{\eta} \end{bmatrix} = \begin{bmatrix} A_{11} & A_{12} & A_{13} & A_{14} & A_{15} \\ A_{21} & A_{22} & A_{23} & A_{24} & A_{25} \\ A_{31} & A_{32} & A_{33} & A_{34} & A_{35} \\ A_{41} & A_{42} & A_{43} & A_{44} & A_{45} \\ A_{51} & A_{52} & A_{53} & A_{54} & A_{55} \end{bmatrix}^{-1} \begin{bmatrix} B_1 \\ B_2 \\ B_3 \\ B_4 \\ B_5 \end{bmatrix} \tag{197}$$

The generalized accelerations can be integrated to obtain the generalized velocities.

$$\begin{aligned}
 \dot{Y}_u &= \int_0^t \ddot{Y}_u dt & \dot{Z}_u &= \int_0^t \ddot{Z}_u dt \\
 \dot{\phi}_u &= \int_0^t \ddot{\phi}_u dt & \dot{\phi}_{s/u} &= \int_0^t \ddot{\phi}_{s/u} dt \\
 \dot{\eta} &= \int_0^t \ddot{\eta} dt
 \end{aligned} \tag{198}$$

At  $t=0$   $\dot{Y}_u$ ,  $\dot{Z}_u$ ,  $\dot{\phi}_u$ ,  $\dot{\phi}_{s/u}$ , and  $\dot{\eta}$  all equal zero.

The generalized velocities  $\dot{Y}_u$ ,  $\dot{Z}_u$ ,  $\dot{\phi}_u$ ,  $\dot{\phi}_{s/u}$ , and  $\dot{\eta}$  can be integrated in order to determine the generalized coordinates  $Y_u$ ,  $Z_u$ ,  $\phi_u$ ,  $\phi_{s/u}$ , and  $\eta$ .

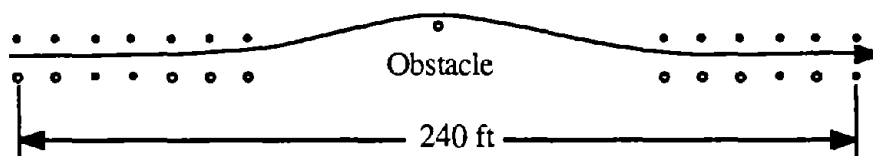
$$\begin{aligned}
 Y_u &= \int_0^t \dot{Y}_u dt & Z_u &= \int_0^t \dot{Z}_u dt + Z_{u0} \\
 \phi_u &= \int_0^t \dot{\phi}_u dt & \phi_{s/u} &= \int_0^t \dot{\phi}_{s/u} dt \\
 \eta &= \int_0^t \dot{\eta} dt
 \end{aligned} \tag{199}$$

At  $t=0$   $Y_u$ ,  $\phi_u$ ,  $\phi_{s/u}$ , and  $\eta$  all equal zero,  $Z_u$  equals  $Z_{u0}$ .

### 2.3 VALIDATION OF IMIRS SIMULATION

A preliminary version of the IMIRS model was tested using experimental results obtained for a Suzuki Samurai from the Vehicle Transportation Research Center in Ohio. A comparison of experimental and simulation results obtained using a 50 mile per hour J-turn are shown in Figure 6. Apart from the oscillation in the yaw rate the simulation results are quite close to those obtained from the experiment.

A later version of the IMIRS vehicle model was validated using experimental results obtained from Failure Analysis Associates tests of the Suzuki Samurai and Isuzu Trooper II. The test simulated an emergency lane change maneuver performed under conditions identical to those used by Consumers Union in their much publicized test of the Suzuki Samurai. The vehicles were equipped with outriggers and driven through a pylon course with an initial forward speed of approximately 40 miles per hour. The vehicle data employed in the simulation assumed that the vehicle had a single occupant (the driver). The influence of outriggers on vehicle center of gravity height, sprung mass, sprung mass roll moment of inertia and vehicle yaw inertia was taken into account while running the IMIRS simulation. An illustration of the pylon course is shown below.



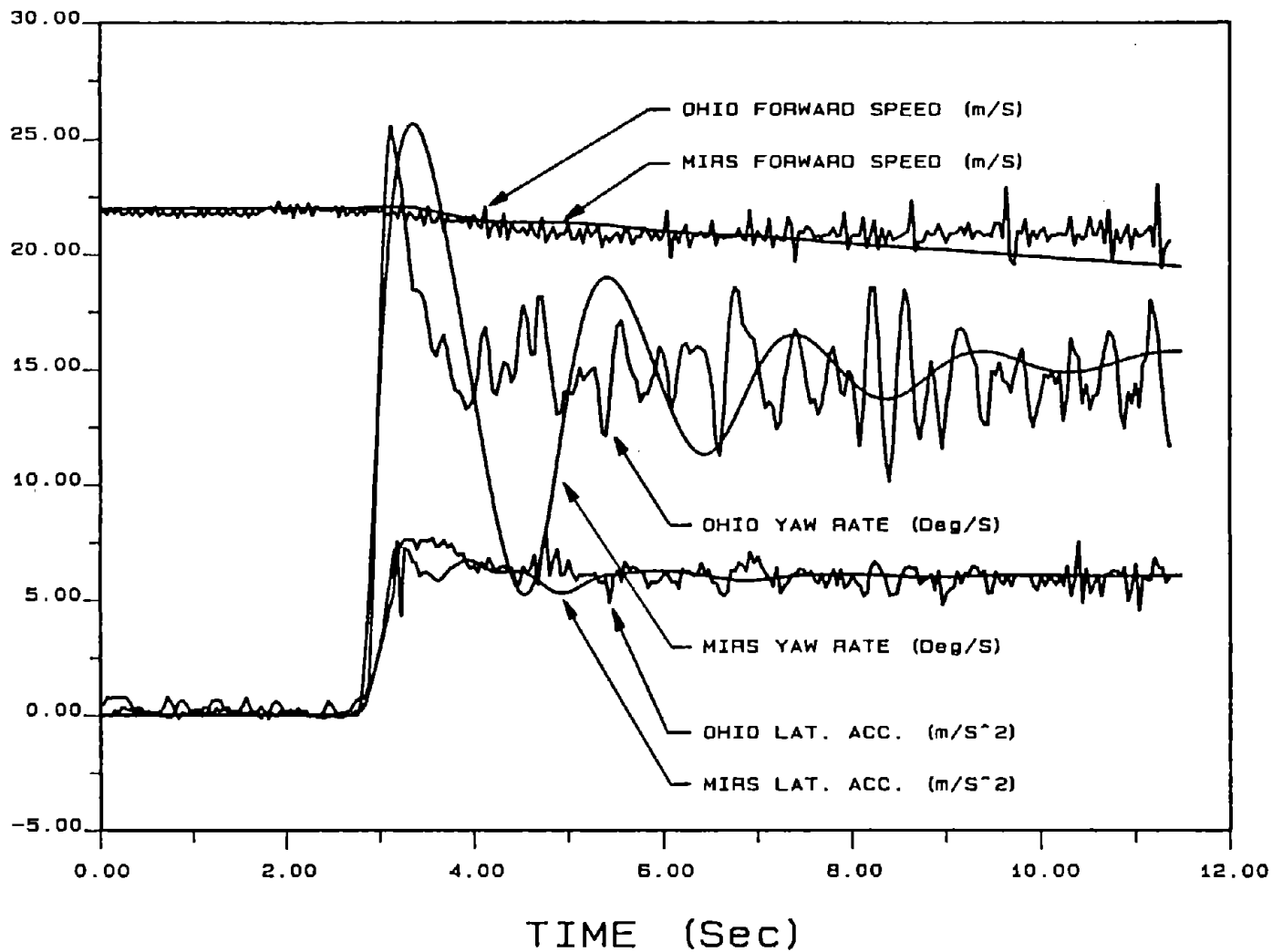
Consumers Union Collision Avoidance Course

Failure Analysis Associates repeated CU's tests of Suzuki Samurai using steering inputs which differed in their level of severity (in both magnitude and rate of application) and concluded that rollover could occur if unrealistically large or rapid steering inputs were applied in the maneuver. These results of the Failure Analysis Associates tests were presented in the form of graphs which showed the steering input vs. distance, lateral acceleration vs. distance, roll angle vs. distance, and yaw rate vs. distance. The graphs were digitized and converted from a distance base to a time base using an assumed value for the average test speed. Two cases which involved the Suzuki Samurai were selected for validation, one which resulted in a rollover and one which did not result in rollover.

A comparison of the steering inputs used in the experiment with those used in the simulation are shown in Figure 7. The time histories of lateral acceleration measured in the test and computed using the simulation are plotted in Figure 8. It was assumed that the accelerometer used to measure the lateral acceleration was attached to the sprung mass. The change in accelerometer

output caused by its rotation in the presence of a gravitational field was accounted for in Figure 8. The figure shows excellent correlation between simulation and experiment in the non-rollover case and good correlation in the rollover case. The time histories of the sprung mass roll angles are shown in Figure 9. This plot demonstrates the simulation's ability to reliably predict the occurrence of rollover. The correlation of roll angle between simulation and experiment in both cases is very good. The final validation plot (Figure 10) shows the yaw rate obtained through measurement and simulation in both cases. The correlation in the non-rollover case is very good as is the correlation in the rollover case. The simulation and experimental yaw velocities tend to diverge in the later phase of the rollover case. This could be due to the influence of vehicle roll on the yaw velocity transducer or some other unforeseen experimental measurement phenomenon, or it could also be caused by inaccuracies in the tire model since very little is known on tire behavior at large camber angles.

# COMPARISION MIRS WITH OHIO TEST



75

0.6G J-TURN AT 50 MPH

Figure 6.

# STEERING INPUT VS. TIME

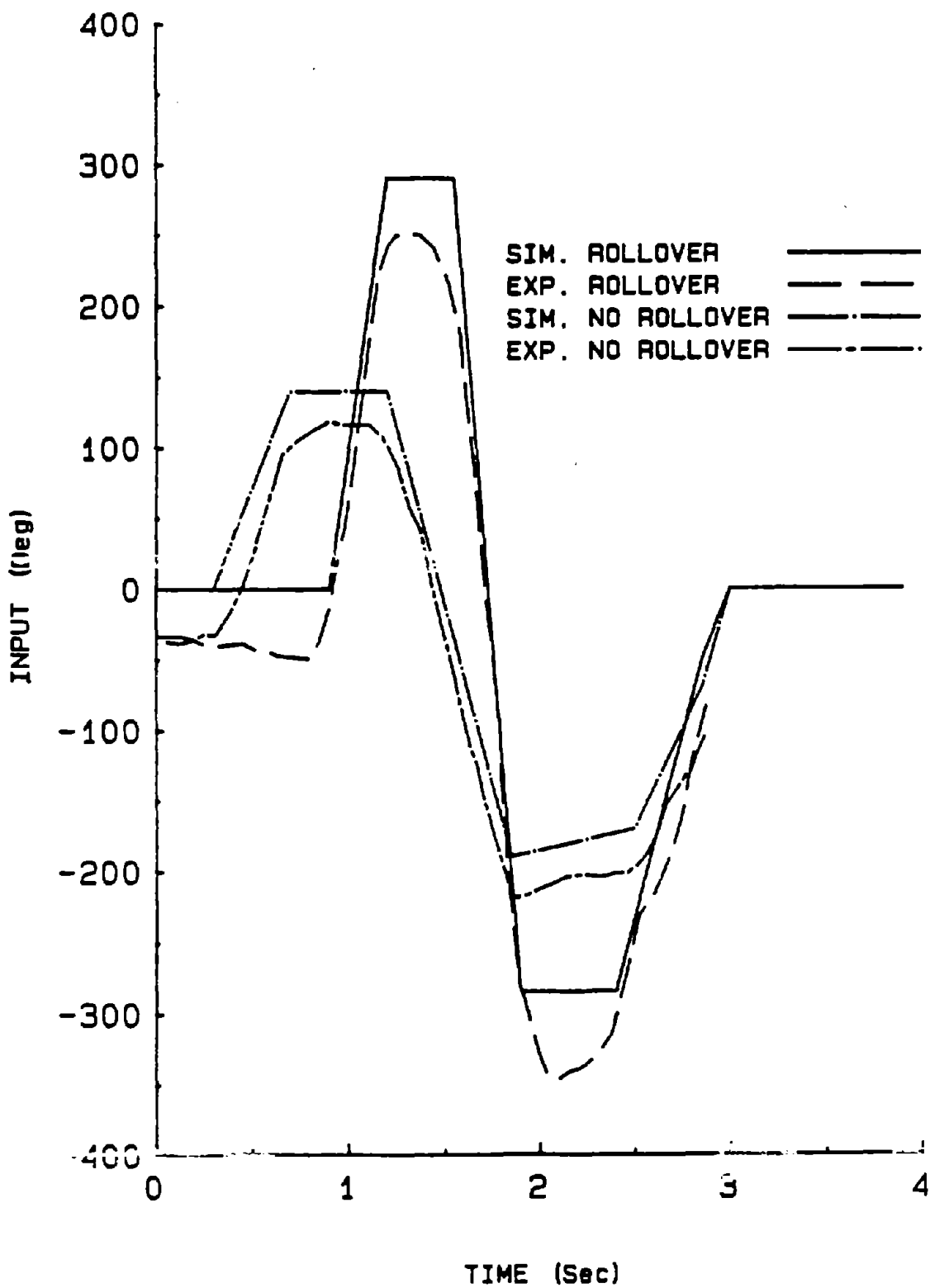


Figure 7.

# LATERAL ACCELERATION VS. TIME

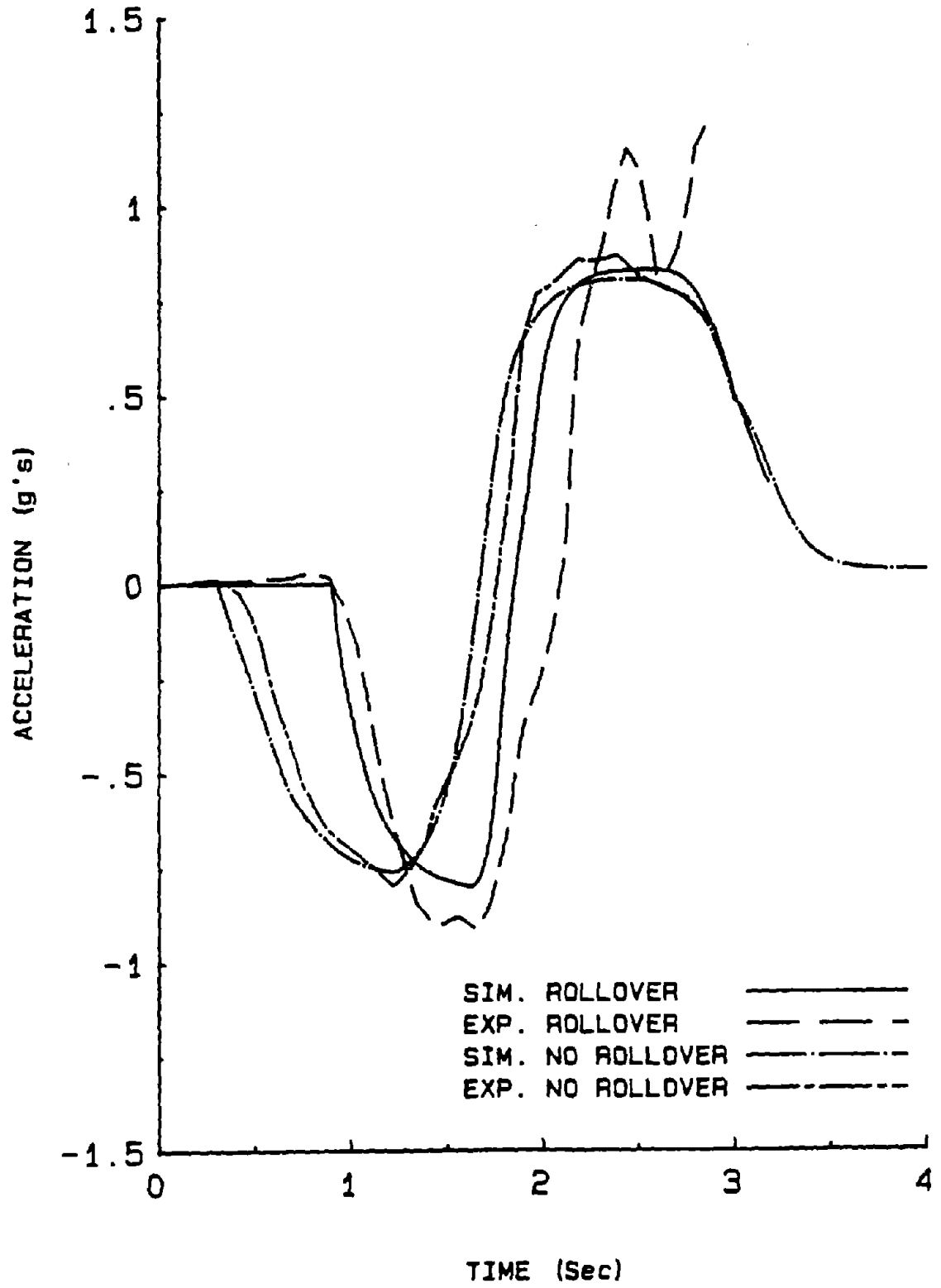


Figure 8.

# ROLL ANGLE VS. TIME

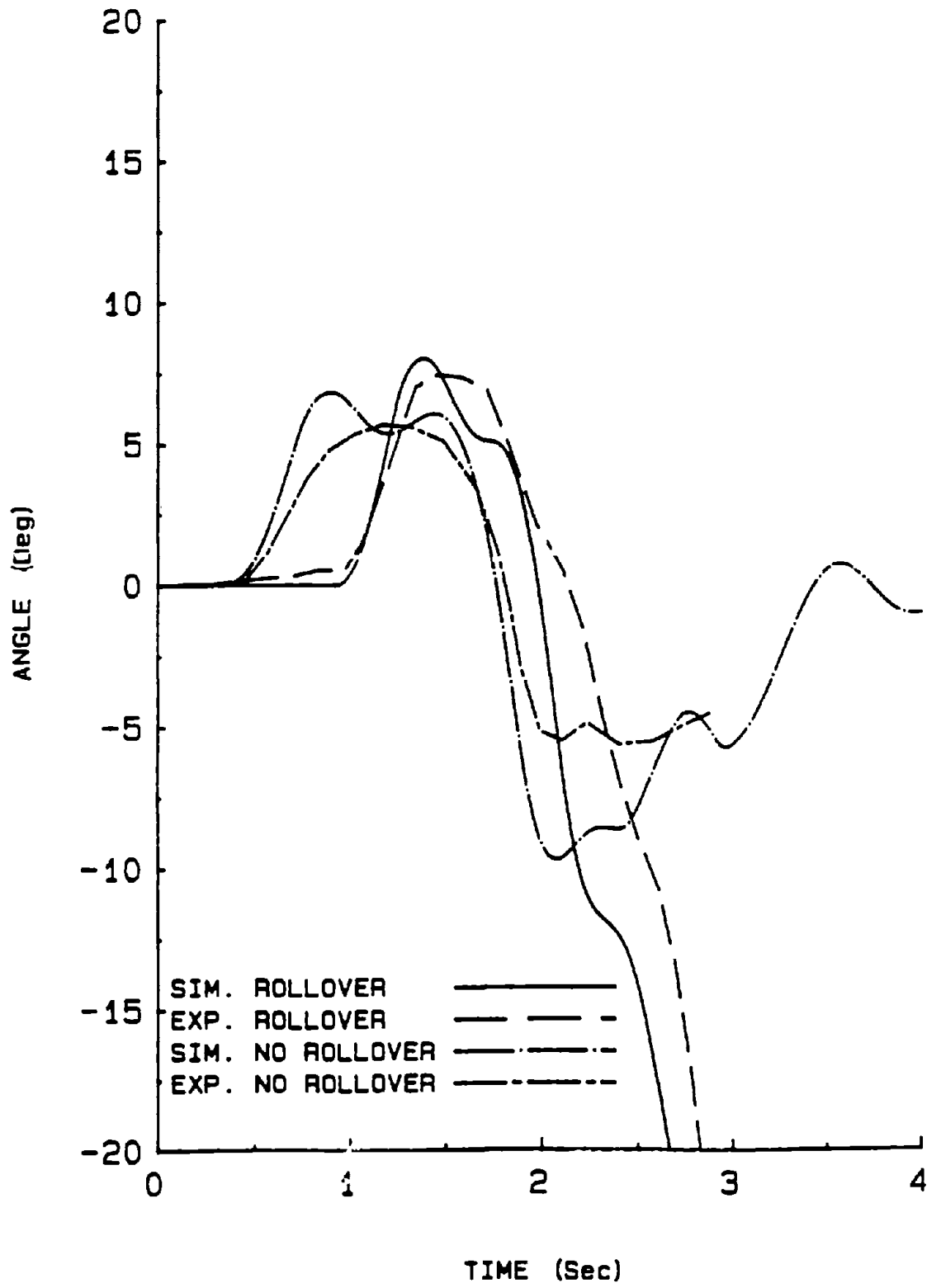


Figure 9.



# YAW RATE VS. TIME

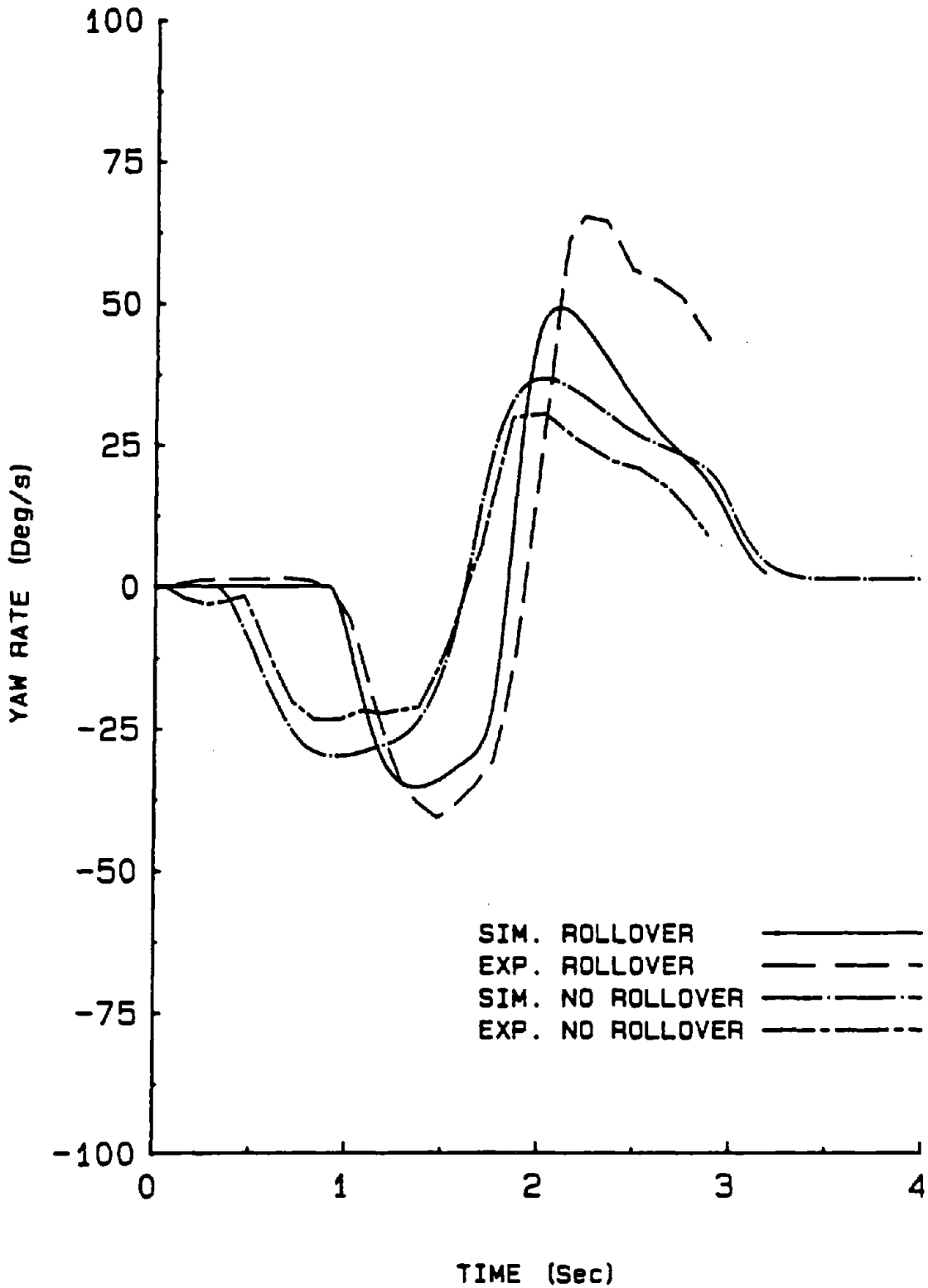


Figure 10.

### 3. APPLICATION OF IMIRS SIMULATION

#### 3.1 DEVELOPMENT OF FORTRAN VERSION OF IMIRS MODEL

In order to perform a sensitivity analysis of the IMIRS model it was necessary to create a model subroutine written in Fortran which would work in conjunction with the general purpose Sensitivity Algorithms developed by the University of Missouri-Columbia [4], [5], [9]. The Fortran version of the IMIRS model was employed in two programs. The first program utilized a fourth order Runge Kutta integration algorithm to determine the time history of the vehicle's response to various steering and braking inputs. Results obtained using the Fortran version of the IMIRS model were compared to those obtained using the PC based Basic version and were found to be identical in all tested instances. The second program, a time domain sensitivity algorithm, utilized to examine the IMIRS model was similar to those used in previous sensitivity studies [4], [5]. However, the sensitivity algorithm employed to study the IMIRS model contained a fourth order Runge Kutta integration method whereas previous studies employed the more complex Gears method.

#### 3.2 DYNAMIC CRITERIA TO ASSESS STABILITY OF VEHICLES IN MANEUVER INDUCED ROLLOVER SITUATIONS

Before performing a sensitivity analysis to investigate the influence of vehicle design parameters on vehicle stability it was necessary to develop a measure which could be used as a basis for comparison. Previous studies performed by the University of Missouri-Columbia utilize the concept of Rollover Prevention Energy Reserve as basis for assessment of vehicle rollover stability [10], [11], [15]. A vehicle's Rollover Prevention Energy Reserve represents the energy required to bring vehicle to an unstable rollover position and in its simplest form can be computed by subtracting the kinetic energy associated with the vehicle's rolling motion from the change in gravitational potential energy required to raise the vehicle's center of gravity height from its static position to the static tipover angle.

The measure of RPER used in the sensitivity analysis of the IMIRS model was computed using the following relation:

$$RPER_a = V_{crit} - (V_g - V_{g0}) - T$$

where,

- $V_{crit}$  - the change of gravitational potential energy of the vehicle from static to tipover position
- $V_g$  - the instantaneous gravitational potential energy of the vehicle
- $V_{g0}$  - the gravitational potential energy of the vehicle in static position
- $T$  - the rolling kinetic energy of the vehicle

This form of RPER will become negative, indicating that the vehicle will rollover, if the vehicle achieves enough rolling kinetic energy  $T$  to raise its center of gravity position from the instantaneous position to the static rollover position. In cases in which vehicle rollover will not occur, the RPER will remain positive.

Previous investigations into the influence of vehicle parameters on vehicle rollover propensity which utilized the concept of Rollover Prevention Energy Reserve examined the behavior of vehicles in tripped rollover accidents. There are several fundamental differences between the behavior of a vehicle in tripped rollover accident and that of a vehicle involved in a maneuver induced rollover. One of these differences is the manner in which the vehicles gain the rotational kinetic energy associated with a vehicle's rolling motion. In a tripped rollover a portion of the vehicle's translational kinetic energy is converted to rotational kinetic energy during impact. In the case of a maneuver induced rollover the vehicle's rolling kinetic energy is generated by inertial forces which act on the mass centers of the vehicle. The time history of vehicle energy in a tripped rollover behavior is largely dissipative in nature, while in a maneuver induced rollover the external forces acting on the vehicle tend to excite it from a position of equilibrium.

Four different maneuvers were selected for sensitivity analysis. These cases were vehicle rollover in a J-turn maneuver, non-rollover in a J-turn, rollover in a S-turn maneuver and non-rollover in a S-turn. The time histories of the steering inputs used in the J and S turn maneuvers are shown in Figure 11, while the resulting vehicle roll angles can be seen in Figures 12 - 15. The pavement skid number was adjusted to control the occurrence of rollover. At high skid numbers a vehicle's tires can produce higher forces and hence the vehicle can generate larger values of lateral acceleration and will be more prone to rollover. At low skid numbers the vehicle's tires will saturate earlier and the vehicle will tend to skid or spin rather than rollover. The table below shows the conditions used in each test.

Table 1: Test Conditions for Sensitivity Analysis

<u>Test Number</u>	<u>Description</u>	<u>Skid Number</u>
1	J-Turn with Rollover	110
2	J-Turn without Rollover	90
3	S-Turn with Rollover	110
4	S-Turn without Rollover	90

The initial conditions in each test represented straight line motion with an initial forward speed of 40 miles per hour

The time histories of RPER in each case are shown in Figures 16 and 17. In the non-rollover cases the values of RPER are nearly constant, however, in the rollover cases the RPER curves tend to drop rapidly as vehicle roll angle and rolling velocity increase. The shape of the RPER curves in maneuver induced rollover is different, however, than the shape of RPER curves generated under tripped rollover conditions. In tripped rollover (see reference [10]) the RPER curves reach a minimum value (usually a negative value) as the vehicle generates its maximum value of rolling kinetic energy and then increases as the rolling kinetic energy is exchanged for gravitational potential energy. In the maneuver induced rollover the RPER tends to decrease steadily. This is because in a maneuver induced rollover the rolling moment arm (vertical distance from the ground to the vehicle center of gravity), and hence the roll moment, increases with roll angle and this can cause rapid and, in most cases, irreversible rollover.

### 3.3 SENSITIVITY ANALYSIS OF IMIRS MODEL

The influence of all significant vehicle parameters on vehicle rollover stability was determined in each of the four maneuvers for the vehicle data shown in Appendix B. Percentage sensitivity functions were utilized to determine the change in vehicle RPER caused by a one percent change in parameter values. The vehicle parameters were divided into seven groups. These groups are listed below and are described in the Appendix C.

Geometrical Parameter Set #1	: a, b, $TRW_f$ , $TRW_r$ , $H_{sm}$ , $H_{uf}$ , $H_{ur}$
Geometrical Parameter Set #2	: BSLNG, $RC_f$ , $RC_r$ , s, SPRLNG, $T_{bas}$
Mass Inertia Parameter Set	: $I_{xxs}$ , $I_{xxu}$ , $I_{zz}$ , $M_s$ , $M_{uf}$ , $M_{ur}$ , $W_{DIST}$
Stiffness Parameter Set	: $K_1$ , $K_2$ , $KR_{DIST}$ , $K_{rf}$ , $K_{rr}$ , $K_z$
Damping Parameter Set	: $B_1$ , $B_z$
Tire Frictional Parameter Set	: $C_{a1}$ , $C_{r1}$ , SN
Aerodynamic Parameter Set	: $C_n$ , $C_{nd}$ , $C_y$ , $H_{aero}$ , S

A detailed description of general purpose sensitivity algorithms can be found in references [4], [5], and [9].

#### 3.3.1 Parameter Sensitivity in J-Turn Maneuver Rollover Case

The influence of various parameters groups on RPER in a 40 mile per hour J-turn rollover are shown in Figures 18 - 24. Figure 18 indicates that an increase of the sprung mass center of gravity height  $H_{sm}$  decreases vehicle  $RPER_a$ , while an increase in the front  $TRW_f$  and rear  $TRW_r$  track widths increases  $RPER_a$ . The influence of geometrical parameter set #2 is shown in Figure 19 from which it is seen that  $RPER_a$  can be raised by increasing spring track width s. Changes in front and rear roll center heights  $RC_f$  and  $RC_r$ , static suspension spring length SPRLNG, and undeformed bump stop length BSLNG appear to have very little effect on  $RPER_a$  in the J-turn rollover. The most influential geometrical parameters appear to be, in order of importance, sprung mass center of gravity height, front and rear track width, suspension spring track width, the distance from the front axle to the vehicle CG a, and the unsprung mass center of gravity heights  $H_{uf}$  and  $H_{ur}$ .

The influence of vehicle mass/inertia parameters on  $RPER_a$  in J-turn rollover case is presented in Figure 20. The results show that the sprung mass initially has a beneficial effect, however, when the vehicle begins to roll an increase in the sprung mass reduces  $RPER_a$ . Increases in the unsprung masses  $M_{uf}$  and  $M_{ur}$ , and yaw moment of inertia  $I_{zz}$  seem to have a positive influence on  $RPER_a$ , however, an increase of the sprung mass roll moment of inertia  $I_{xxs}$

tends to reduce  $RPER_a$ . This seems to contradict the results obtained from previous sensitivity analyses of tripped rollover maneuvers [10], [11], [12] where increases in roll moments of inertia raised vehicle  $RPER$ . In order to investigate these results further a test was carried out using the model integration program which determines the time history of vehicle response to steering and braking inputs. Two runs were performed using different values for roll moment of inertia. The run carried out using the higher roll moment of inertia rolled over sooner than the simulation using the lower value for roll moment of inertia, validating the results obtained from the sensitivity program. One reason for this difference in results obtained from tripped and maneuver induced rollover sensitivity studies is that in the J-turn maneuver the sprung mass roll acceleration changes signs as the sprung mass rolls to the outside and is stopped by the suspension elements which oppose this motion. Since inertia tends to oppose acceleration it may exert a negative influence in a maneuver induced rollover. Figure 20 also shows that shifting the vehicle weight distribution toward the rear of the vehicle increases  $RPER_a$ , which is in agreement with the sensitivity of parameter  $a$  shown in Figure 18.

The sensitivity of  $RPER_a$  to changes in the stiffness parameters is illustrated in Figure 21. This figure shows that  $RPER_a$  can be increased by increasing the stiffness of the suspension springs  $K_1$  and tires  $K_z$  and by shifting the vehicle roll stiffness distribution  $KR_{DIST}$  toward the front of the vehicle. The stiffness of the bump stops  $K_2$  as well as the auxiliary roll stiffness contribution from anti-roll bars  $K_{rf}$  and  $K_{rr}$  had little influence on vehicle  $RPER_a$  in the J-turn rollover.

Figure 22 illustrates the influence of changes in the damping parameters on  $RPER_a$  in a J-turn maneuver resulting in rollover. The figure shows that the damping coefficients of the shock absorbers  $B_1$  and the tires  $B_z$  have little influence on vehicle  $RPER_a$  in the J-turn maneuver.

The influence of vehicle parameters associated with aerodynamics on vehicle  $RPER_a$  in the J-turn rollover are shown in Figure 23. The yaw damping parameter  $C_{nd}$  is the only influential parameter in this group. The figure shows that  $RPER_a$  can be raised by increasing the yaw damping. This is logical since increasing  $C_{nd}$  will reduce the vehicle's steady state yaw rate and reduce the steady state value of lateral acceleration which acts on the vehicle. By reducing the lateral acceleration of the vehicle the inertia forces which act on the vehicle's mass centers are also reduced.

The sensitivity of  $RPER_a$  to changes in tire frictional parameters  $CA1$ ,  $CR1$ , and skid number  $SN$  in a J-turn rollover are illustrated in Figure 24. The figure shows that skid number has a substantial influence on  $RPER_a$ . Increasing the skid number increases the maximum allowable forces which the tires can generate and hence raises the maximum lateral acceleration the vehicle can attain. With a lower skid number the vehicle is more prone to skid or spin rather than rollover. Parameter  $CR1$  which represents the percentage reduction in peak friction caused by a critical camber angle  $CA1$  is shown to have positive sensitivity. Reducing the peak friction will make the vehicle less prone to rollover and more prone to skid or spin. The relative importance of

parameters CA1 and CR1 illustrate the need for more experimental data describing the behavior of light truck tires at large camber angles for the purpose of rollover research.

Similar sensitivity results of J-turn vehicle rollover were presented in [14], but different data for the reduction of tire frictional properties due to camber was utilized to obtain those results.

### 3.3.2 Parameter Sensitivity in J-Turn Maneuver Non-rollover Case

To examine the influence of the vehicle parameters in a 40 mile per hour J-turn maneuver without rollover the skid number was reduced from 110 to 90 and the sensitivity runs were repeated. The time history of  $RPER_a$  in this case is shown in Figure 16 and the percentage sensitivity of  $RPER_a$  to parameter changes are illustrated in Figures 25 - 31. Since rotational kinetic energy associated with the non-rollover case is considerably smaller than that associated with the rollover case, and because the change in gravitational potential energy is small at small roll angles the vehicle's  $RPER_a$  is nearly constant. As a result the percentage sensitivity functions are also nearly constant.

The influence of geometrical parameter set #1 on  $RPER_a$  in the J-turn without rollover is presented in Figure 25. The figure indicates that  $RPER_a$  in a J-turn without rollover can be raised by increasing front and rear vehicle track width, and by decreasing the static height of the sprung mass center of gravity. Changes in the static heights of the front and rear unsprung masses and longitudinal distances from vehicle center of gravity to front and rear axles,  $a$  and  $b$ , had very little influence on vehicle  $RPER_a$ .

Figure 26 shows that none of the elements of geometrical parameter set #2 had a significant effect on  $RPER_a$  in the non-rollover case. The influence of mass-inertia parameters are shown in Figure 27. The figure indicates that  $RPER_a$  can be increased in the non-rollover J-turn case by raising the sprung mass of the vehicle. The other elements of the mass-inertia parameter set had relatively smaller influence on  $RPER_a$ . The influence of the stiffness, damping, aerodynamic, and tire frictional parameters sets on  $RPER_a$  are shown in Figures 28 - 31 and they illustrate that all of the parameters associated with these groups have little influence on vehicle  $RPER_a$ .

### 3.3.3 Parameter Sensitivity in S-Turn Maneuver Rollover Case

Figures 32 - 38 show the percentage sensitivity results obtained in the 40 miles per hour S-Turn which resulted in rollover. In general, the results shown in these figures correspond closely with those obtained in the J-turn rollover case. However, the results obtained in the S-turn are more erratic than those obtained in the J-turn due to the increased complexity of the maneuver.

The sensitivity of  $RPER_a$  to changes in the elements of geometrical parameter set #1 is presented in Figure 32. This figure shows that  $RPER_a$  can be increased by increasing front and rear track widths  $TRW_f$  and  $TRW_r$  and by decreasing the static sprung mass center of gravity height  $H_{sm}$ . The influence of geometrical parameter set #2 on  $RPER_a$  is illustrated in Figure 33 which shows that  $RPER_a$  can be increased in the S-turn maneuver by increasing the suspension spring track width, static suspension spring length and height of front roll center.

The percentage sensitivity functions of  $RPER_a$  taken with respect to the vehicle's mass parameters are presented in Figure 34. The results obtained in the S-turn rollover are similar to those generated in the J-turn rollover with the exception of yaw moment of inertia  $I_{zz}$  which appears to be less influential in S-turn than in J-turn type rollover.

The effect of changes in vehicle stiffness parameters on  $RPER_a$  in the S-turn maneuver are shown in Figure 35. Comparison of these results with those obtained in the J-turn rollover shows that the results are similar. An increase in  $KR_{DIST}$  and  $K_1$  results in an increase of  $RPER_a$  and an increase of  $K_z$  decreases  $RPER_a$ . The vertical tire stiffness  $K_z$ , however, appears to be less influential in the S-turn rollover case. The influence of damping parameters on  $RPER_a$  in the S-turn rollover maneuver is presented in Figure 36, which shows that tire and shock absorber damping parameters  $B_z$  and  $B_1$  have little influence on vehicle  $RPER_a$  when compared to other parameter groups such as geometrical parameter groups 1 and 2.

The percentage sensitivity functions of  $RPER_a$  associated with the aerodynamic and tire frictional parameters groups in the S-turn rollover are quite similar to those obtained in the J-turn rollover. Aerodynamic parameter  $C_{nd}$  (Figure 37) exhibited strongly positive sensitivity, while tire frictional parameters  $SN$  and  $C_{a1}$  exhibited negative sensitivity functions (Figure 38). Tire frictional parameter  $C_{r1}$  exhibited positive sensitivity.

#### 3.3.4 Parameter Sensitivity in S-Turn Maneuver Non-Rollover Case

The S-turn sensitivity analysis was repeated using a skid number of 90 to examine the influence of vehicle parameters on  $RPER_a$  in an S-turn which did not result in rollover. The percentage sensitivity functions for each parameter group are plotted in Figures 39 - 45. While the results obtained in the S-turn non-rollover case are more erratic than those obtained in the J-turn non-rollover case the interpretation of the results for each parameter group are identical. The transient oscillation which occurs at approximately 1.8 seconds is caused by the rapid dynamic change which accompanies the steering reversal in the S-turn. The sensitivity functions in the non-rollover S-turn maneuver tend to oscillate about their initial ( $t=0$ ) values.



## 4. CONCLUSIONS AND RECOMMENDATIONS

The results presented in this report demonstrate that the IMIRS is very useful simulation which is capable of predicting maneuver induced rollover in addition to vehicle response in a variety of sub-limit and limit handling maneuvers of light vehicles. This simulation was successfully validated using experimental results in "J" and "S" maneuvers including those which resulted in rollover. The IMIRS utilizes a vehicle model of intermediate level of complexity and requires a modest amount of vehicle data and computation time.

The Rollover Prevention Energy Reserve (RPER) is dependable dynamic function which can be used to determine whether or not vehicle rollover will occur. The RPER represents the energy required to bring vehicle to an unstable rollover position and when used in conjunction with the IMIRS simulation can be used to assess vehicle rollover propensity. The results showed that the occurrence of maneuver induced rollover depends upon whether the minimum value of the vehicle's RPER is negative or positive. Identical criteria were used previously to assess the stability of vehicles in tripped rollover situations in studies [10], [12] and [14] done by the University of Missouri-Columbia. It becomes evident, therefore, that the concept of RPER can successfully be used as an indicator of dynamic rollover stability for both maneuver induced and tripped rollover situations.

The RPER is a dynamic function which not only determines but governs the vehicle rollover behavior. For this reason RPER is best suited (and not the vehicle's roll angle, roll velocity or acceleration) for detailed investigation whenever the effects of parameter changes on vehicle rollover behavior are of interest to us. The utilization of the sensitivity methods in finding the influence of vehicle and environmental parameters on RPER represents an effective and practical approach to dynamic analysis of vehicle rollover.

The reader should be aware that sensitivity results described in this report were obtained under assumption that tire frictional properties are linearly reduced by 30 percent when wheel camber becomes 30 degrees. Although this assumption seems to be reasonable it is fair to say that it was not yet confirmed by tire experimental data. The sensitivity analysis demonstrated that reduction of tire peak friction coefficient makes the vehicle less prone to rollover and more prone to skid or spin. However, until tire experimental data at large camber and slip angles is available no firm conclusions should be drawn with regard to the amount of increase of vehicle RPER caused by decrease in values of tire frictional properties.

In this project the influence of vehicle and roadway factors on rollover was investigated using the same forward speed in J-turn and S-turn maneuvers and by changing the skid number to control the rollover occurrence. It is not expected that changing the vehicle's forward speed would qualitatively change the results described in this report, however, for the sake of completeness of analysis it is recommended that future research be continued at different forward speeds and different skid numbers. Obviously, change of the vehicle speed and skid number would require

modification of the steering inputs for J and S maneuvers to secure the appropriate basis for comparison of the two rollovers caused by different maneuvers.

It is also felt that an investigation should be initiated using the IMIRS simulation to determine the influence of steering input frequency and amplitude on vehicle rollover behavior. It has been author's experience that some steering frequencies can bring the vehicle to unstable rollover position which otherwise would not be achieved if the exciting frequency was different. The frequency response analysis should determine the unfavorable range of steering frequencies which are capable of exciting the vehicle roll mode to the extent that rollover would occur.

The study described in this report is limited to steering maneuvers only. Future investigation of maneuver induced vehicle rollover should also include combined braking and steering maneuvers as a cause of rollover initiation. It is author's opinion that braking in a turn, when appropriately applied, can generate couplings between yaw and pitch which can bring a vehicle to an unstable rollover position. Investigation into the effects of dynamic couplings between vehicle yaw, pitch and roll on rollover behavior would be most appropriate when done using a vehicle model such as the AVRMS simulation model [15]. Utilization of stability methods [3] which are capable of determining and analyzing unstable vibrational modes and aperiodical motions of a vehicle would enhance analysis. Such study would help to understand how couplings of vehicle motions, including those created as a result of braking in a turn, might contribute to vehicle rollover. Use of sensitivity methods in conjunction with stability methods would allow examination of the influence of vehicle and environmental parameters on the creation of dangerous couplings of vehicle motions which could result in rollover.

Finally, it would be beneficial to examine the sprung mass roll angles at which dynamic criteria for vehicle rollover are satisfied (RPER becomes negative). Knowledge of these critical roll angles at different motion conditions leading to vehicle rollover (different maneuvers, speeds, skid numbers, frequency of steering input, braking deceleration, ect.) would be very useful when designing an experimental test to determine vehicle rollover propensity.

## REFERENCES

1. Nalecz, A.G., "Investigation into the Effects of Suspension Design on Stability of Light Vehicles", SAE Transactions, Vol. 96, No. 1, Paper No. 870497, 1987.
2. Nalecz, A.G., "Lateral Weight Transfer Simulation", Final Report - User's Manual, NHTSA ✓  
- U.S. DOT Contract No. DTNH22-86-P-07326, June 1986.
3. Nalecz, A.G., "The Nonholonomic Constraints of a Vehicle on Pneumatic Tires", International Journal of Vehicle Mechanics and Mobility (Vehicle System Dynamics), Vol. 12, No. 1-3, 1983, pp. 390 - 406.
4. Nalecz, A.G., Bindemann, A.C., "Sensitivity Analysis of Vehicle Design Attributes that Affect Vehicle Response in Critical Accident Situations - Part I: User's Manual", NHTSA - U.S. DOT Final Report No. DOT HS 807 229, December 1987.
5. Nalecz, A.G., Bindemann, A.C., "Sensitivity Analysis of Vehicle Design Attributes that Affect Vehicle Response in Critical Accident Situations - Part II: Technical Report", NHTSA - U.S. DOT Final Report No. DOT HS 807 230, December 1987.
6. Nalecz, A.G., Wicher, J., "Design Sensitivity Analysis of Mechanical Systems in Frequency Domain", Journal of Sound and Vibration., Vol. 120, No. 3, 1988, pp. 517 - 526.
7. Wicher, J., Nalecz, A.G., "Second Order Sensitivity Analysis of Lumped Mechanical Systems in the Frequency Domain", International Journal for Numerical Methods in Engineering, Vol. 24, No. 12, 1987, pp. 2357 - 2366.
8. Nalecz, A.G., "Sensitivity Analysis of Vehicle Design Attributes in Frequency Domain", International Journal of Vehicle Mechanics and Mobility (Vehicle System Dynamics), Vol. 17, No. 3, 1988, pp. 141 - 163.
9. Nalecz, A.G., "Application of Sensitivity Methods to Analysis and Synthesis of Vehicle Dynamic Systems", State of the Art Paper at 11th IAVSD-IUTAM Symposium, International Journal of Vehicle Mechanics and Mobility (Vehicle System Dynamics), Vol. 18, No. 1-3, 1989, pp. 1 - 45.
10. Nalecz, A.G., "Influence of Vehicle and Roadway Factors on the Dynamics of Tripped Rollover", International Journal of Vehicle Design, Vol. 10, No. 3, 1989, pp. 321 - 347.
11. Nalecz, A.G., Bindemann, A.C., Bare, C., "Sensitivity Analysis of Vehicle Tripped Rollover Model", NHTSA - U.S. DOT Final Report No. DOT HS 807 300, July 1988.

12. Nalecz, A.G., Bare, C. I., "Development and Application of ITRS", NHTSA - U.S. DOT Contract No. DTNH22-87-D-27174, Final Report 1989.
13. Nalecz, A.G., Bindemann, A.C., "Handling Properties of Four Wheel Steering Vehicles", The 4th Autotechnologies Conference, Monte Carlo, Monaco, SAE Transactions, Vol. 98, No. 1, Paper No. 890080, January 1989.
14. Nalecz, A.G., Bindemann, A.C., Brewer, H.K., "Dynamic Analysis of Vehicle Rollover", Proceedings of the 12th International ESV Conference, Goteborg, Sweden, May 1989.
15. Nalecz, A.G., et al., "Advanced Dynamic Rollover Model", NHTSA - U.S. DOT Contract No. DTNH-87-D-27174, Final Report , 1989.

# IMIRS STEERING INPUT

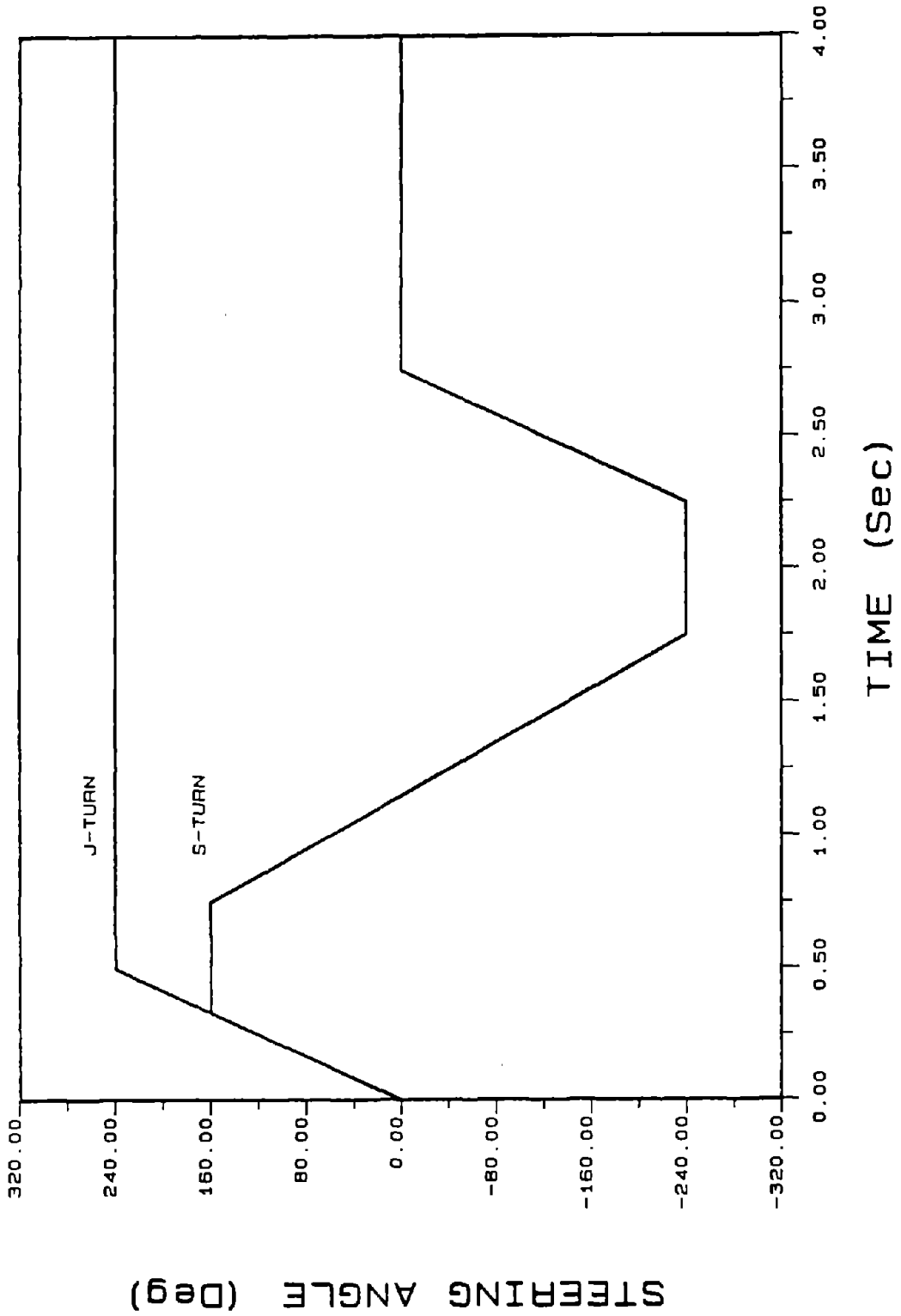


Figure 11.

IMIRS ROLL ANGLES  
ROLLOVER IN J-TURN

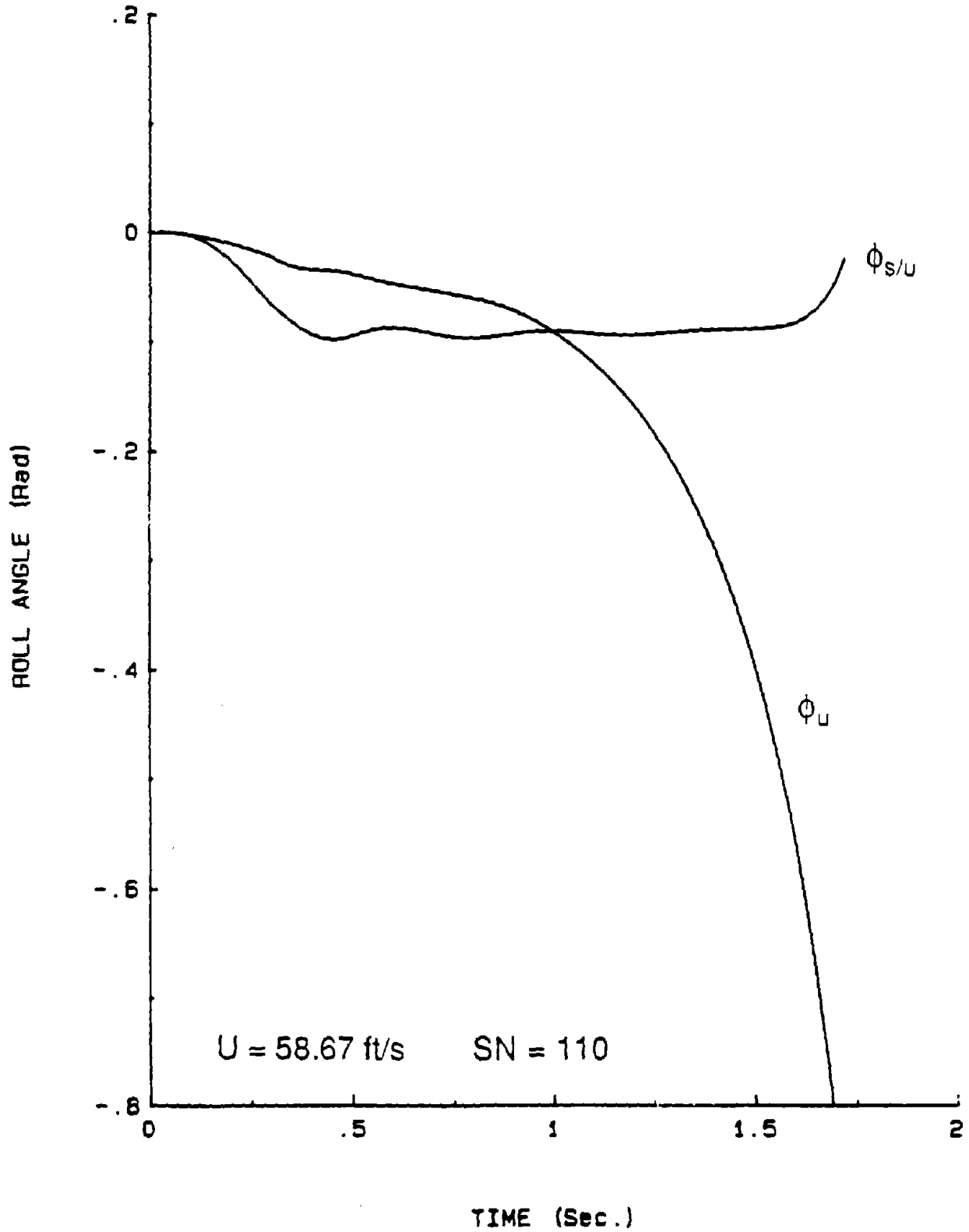


Figure 12.

IMIRS ROLL ANGLES  
NON-ROLLOVER IN J-TURN

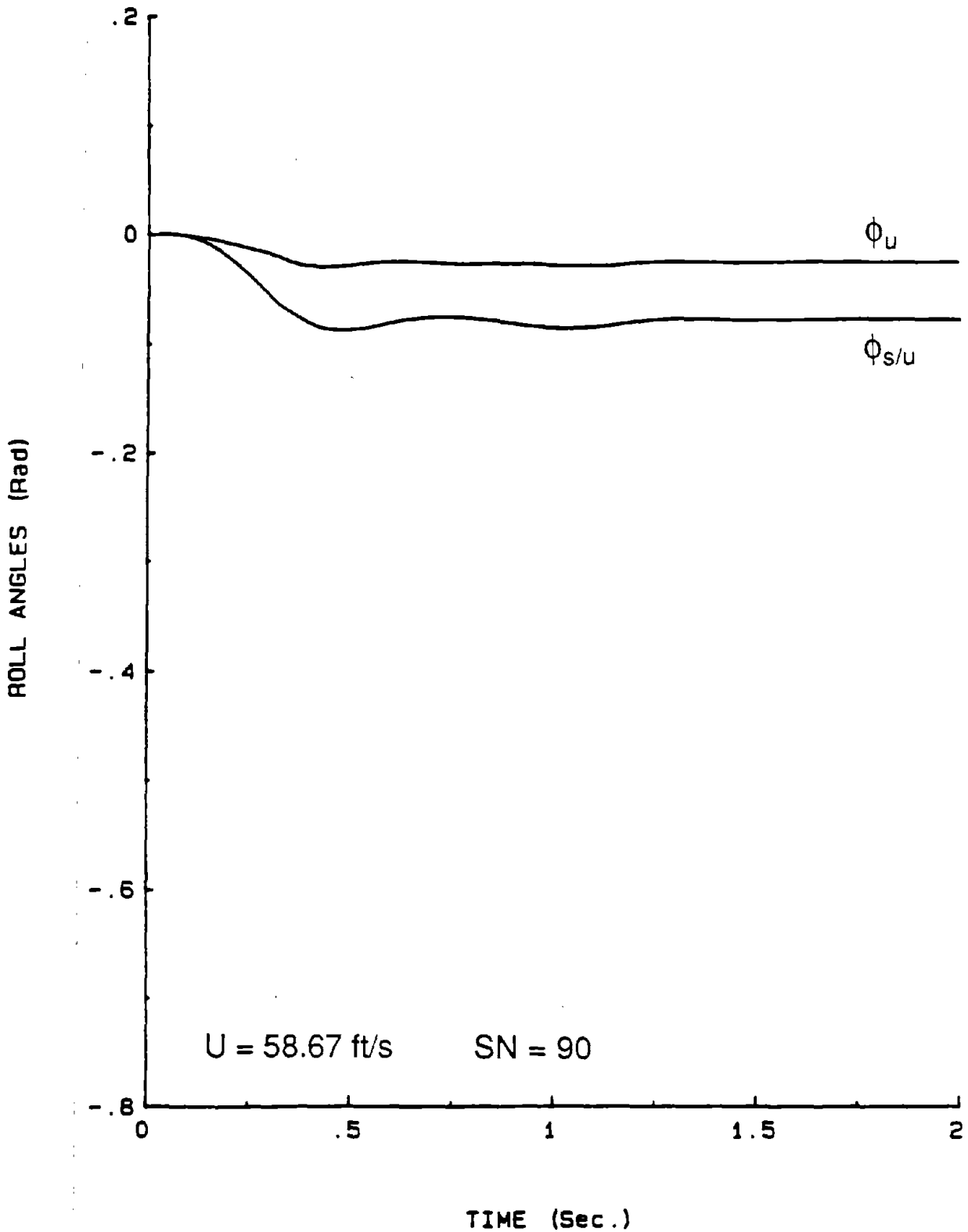


Figure 13.

IMIRS ROLL ANGLES  
ROLLOVER IN S-TURN

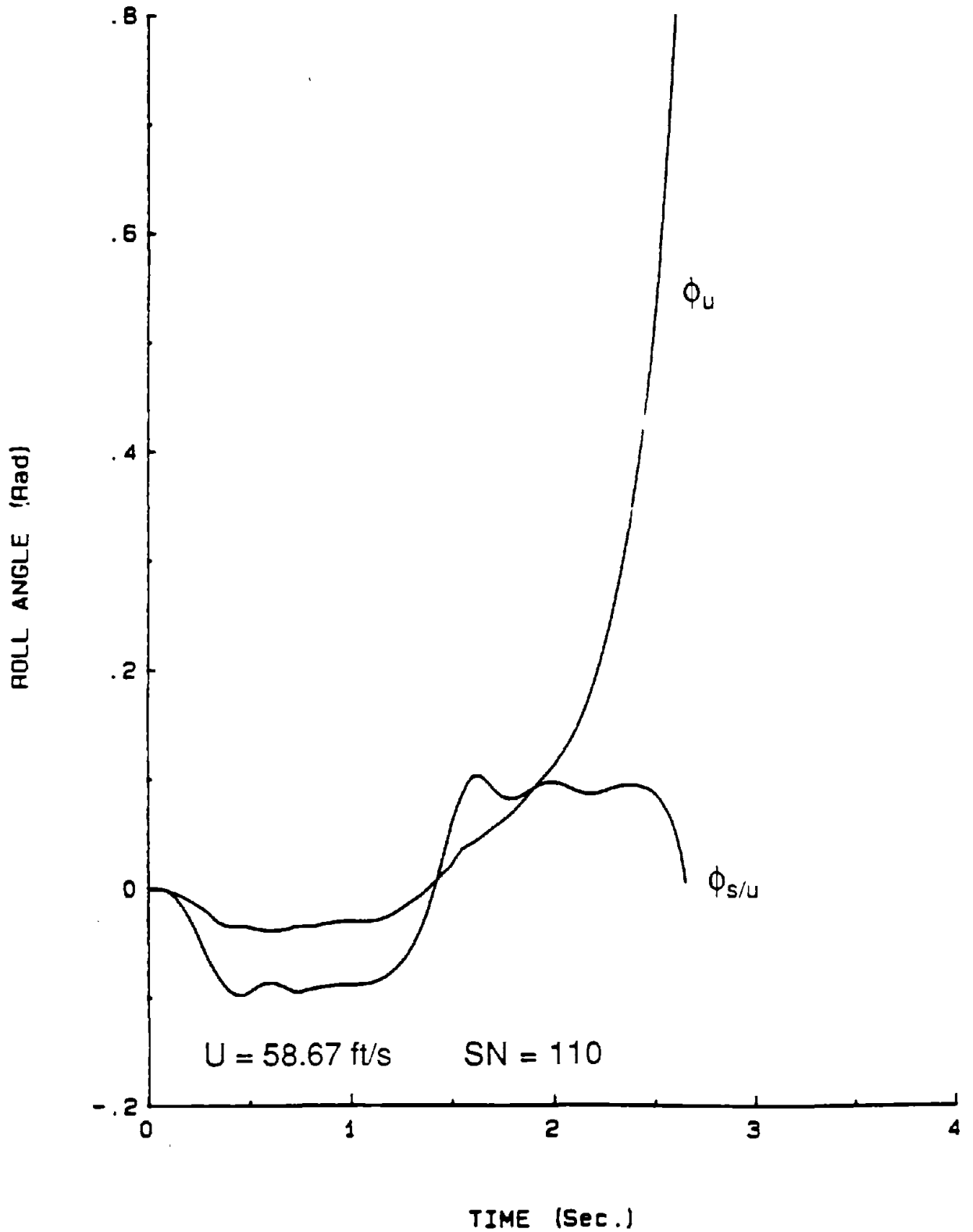


Figure 14.



IMIRS ROLL ANGLES  
NON-ROLLOVER IN S-TURN

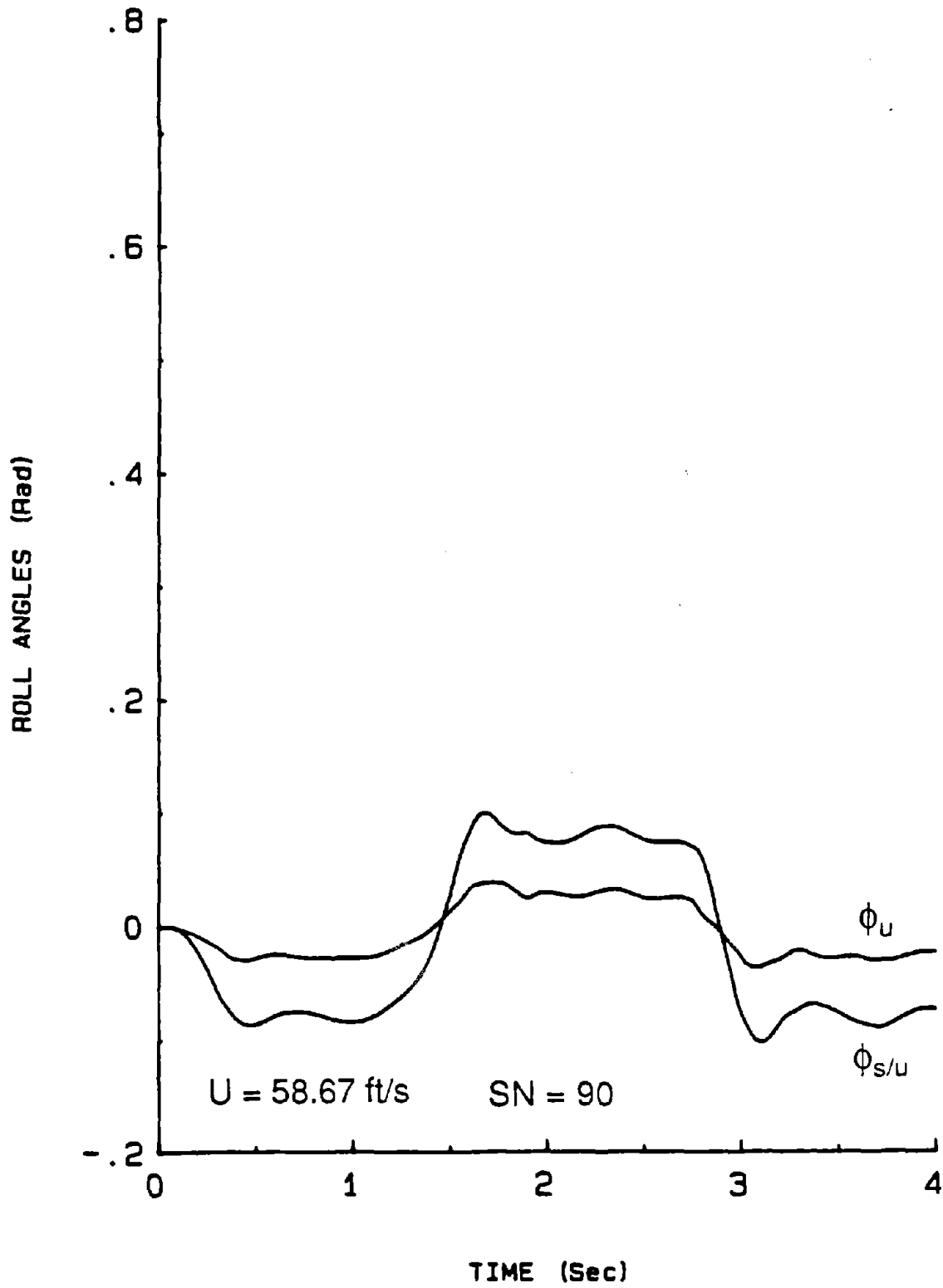


Figure 15.

ROLLOVER PREVENTION ENERGY RESERVE  
ROLLOVER AND NON-ROLLOVER IN J-TURN

RPER<sub>a</sub>

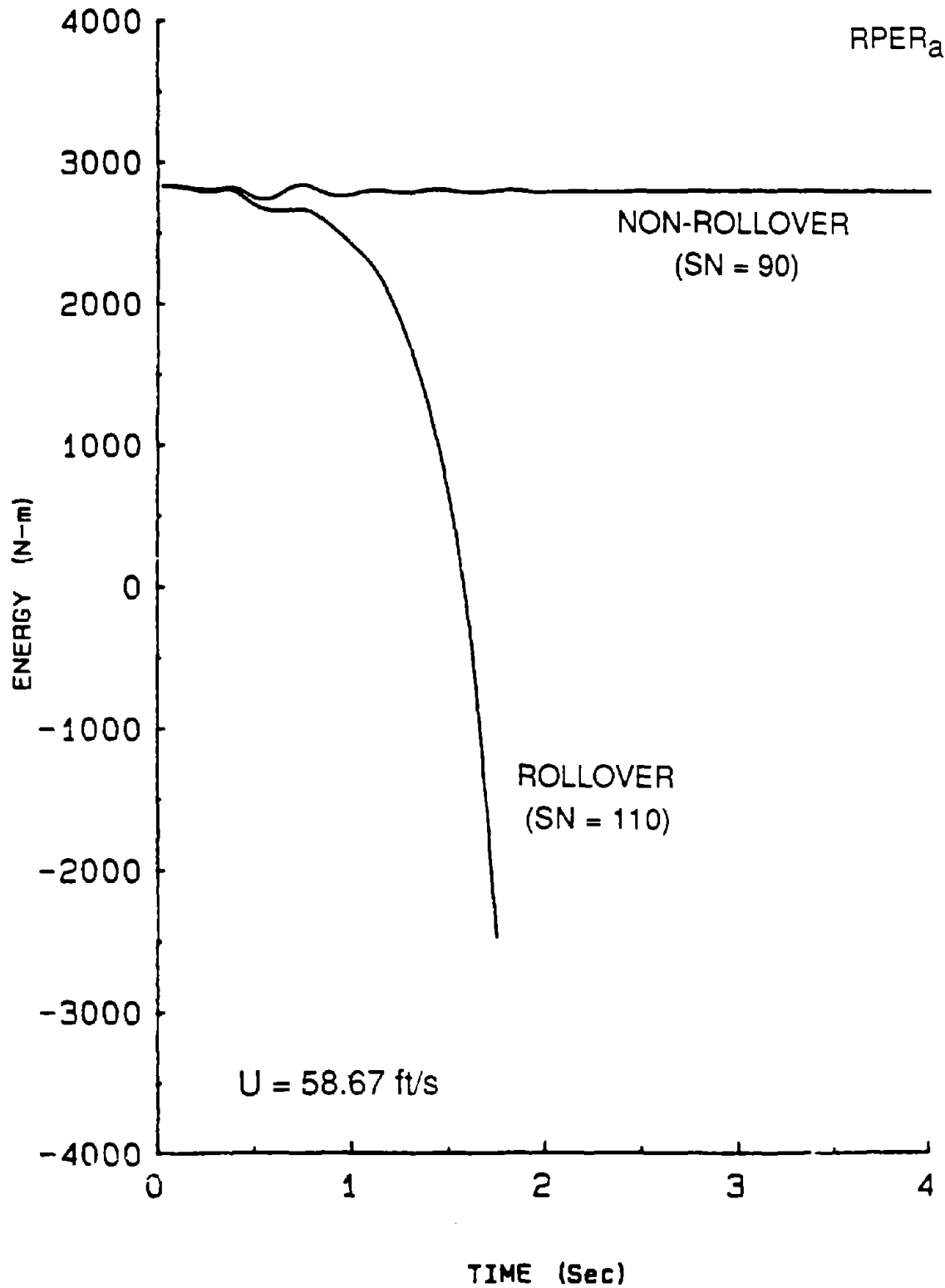


Figure 16.

ROLLOVER PREVENTION ENERGY RESERVE  
ROLLOVER AND NON-ROLLOVER IN S-TURN

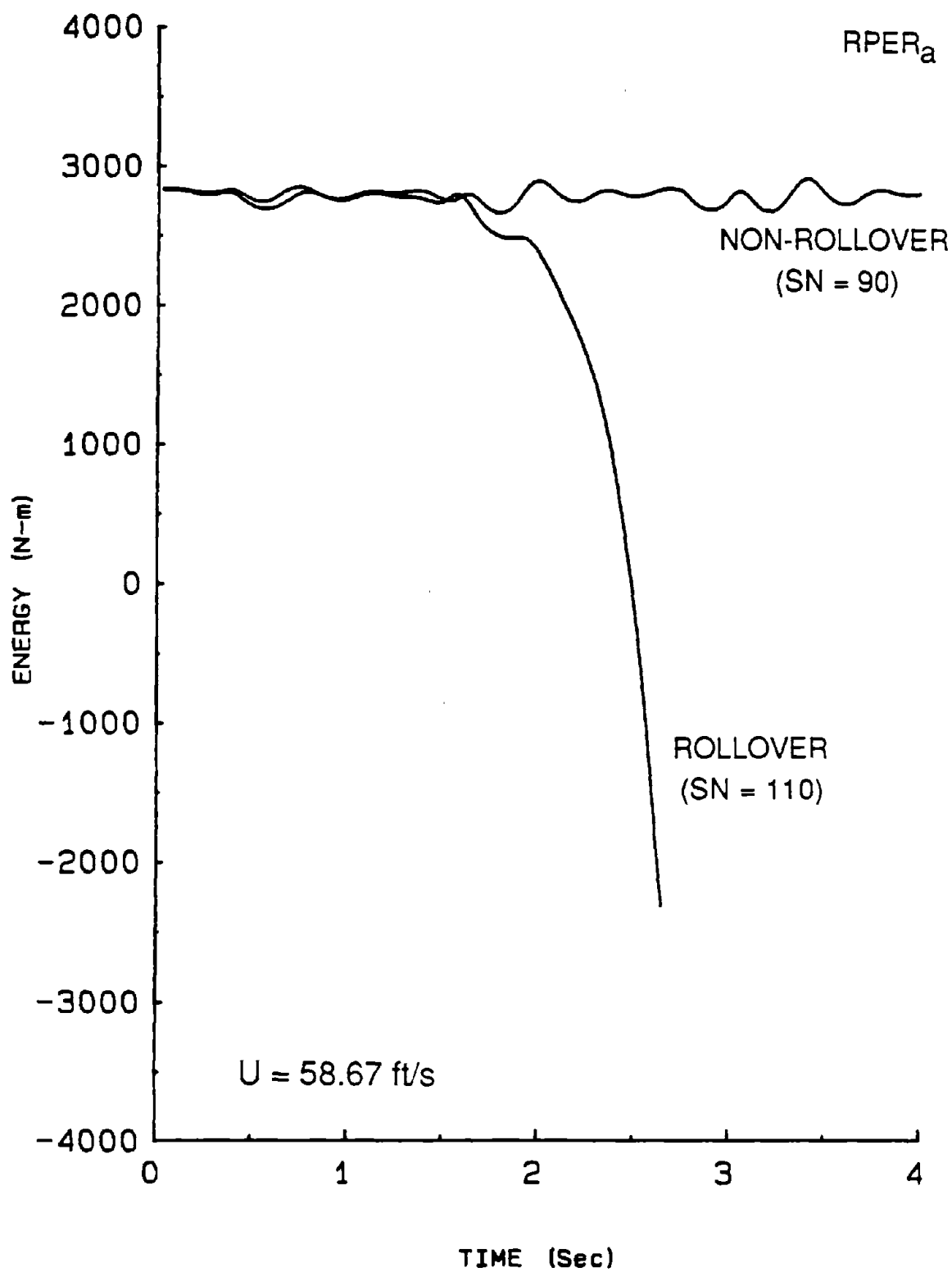


Figure 17.

SENSITIVITY OF RPER IN IMIRS  
 ROLLOVER IN J-TURN  
 GEOMETRIC PARAMETER SET #1

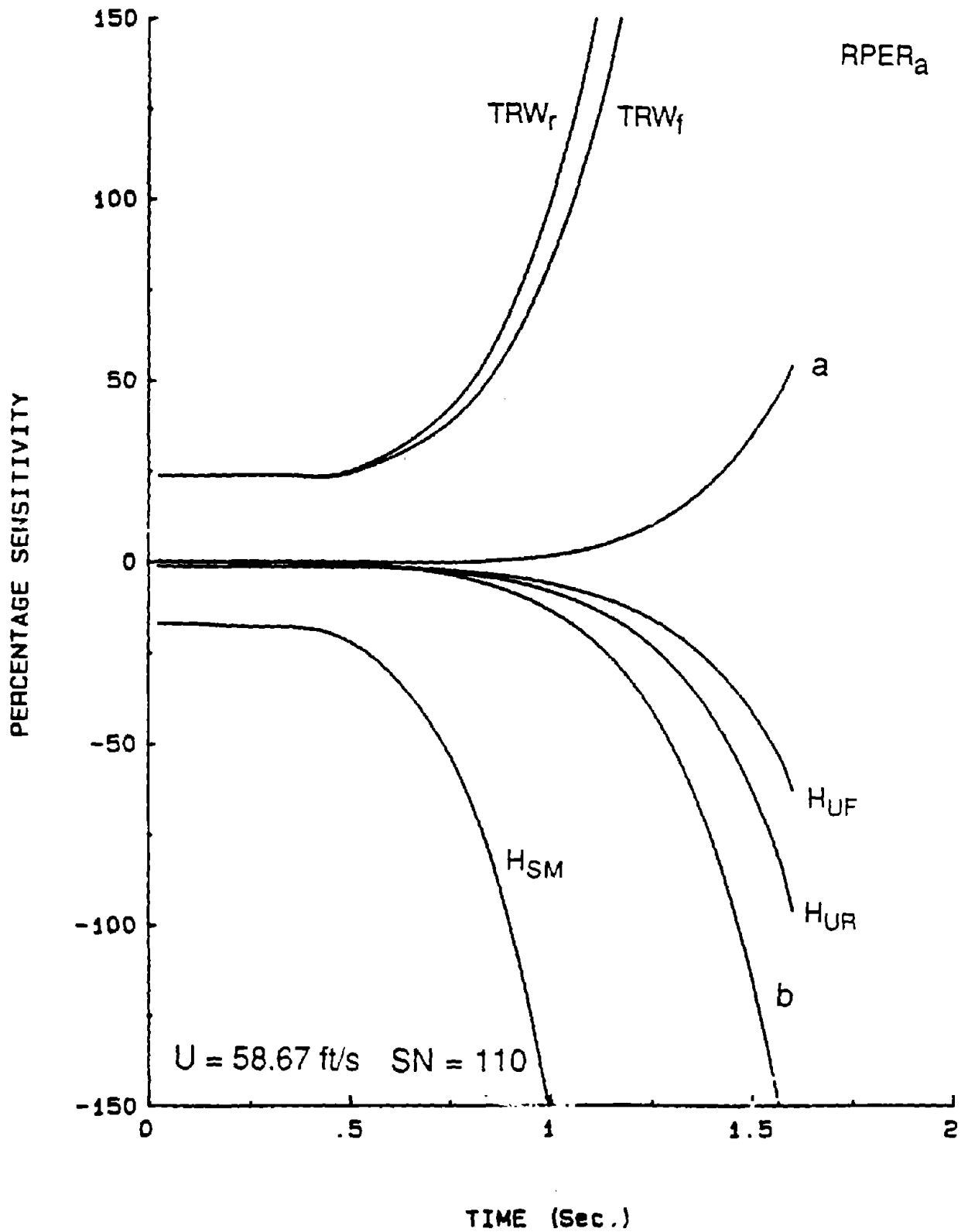


Figure 18.

SENSITIVITY OF RPER IN IMIRS  
 ROLLOVER IN J-TURN  
 GEOMETRIC PARAMETER SET #2

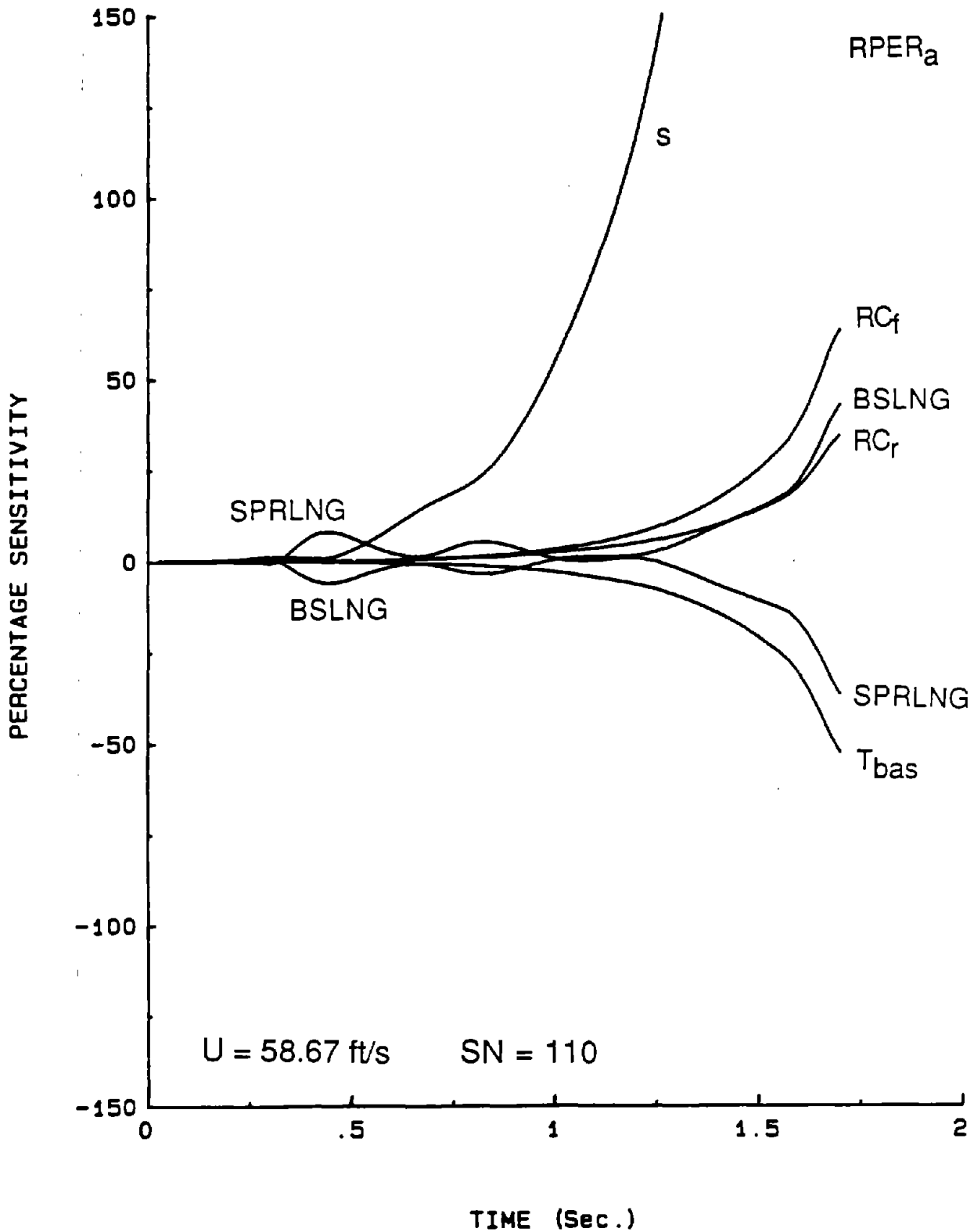


Figure 19.

SENSITIVITY OF RPER IN IMIRS  
 ROLLOVER IN J-TURN  
 MASS-INERTIA PARAMETER SET

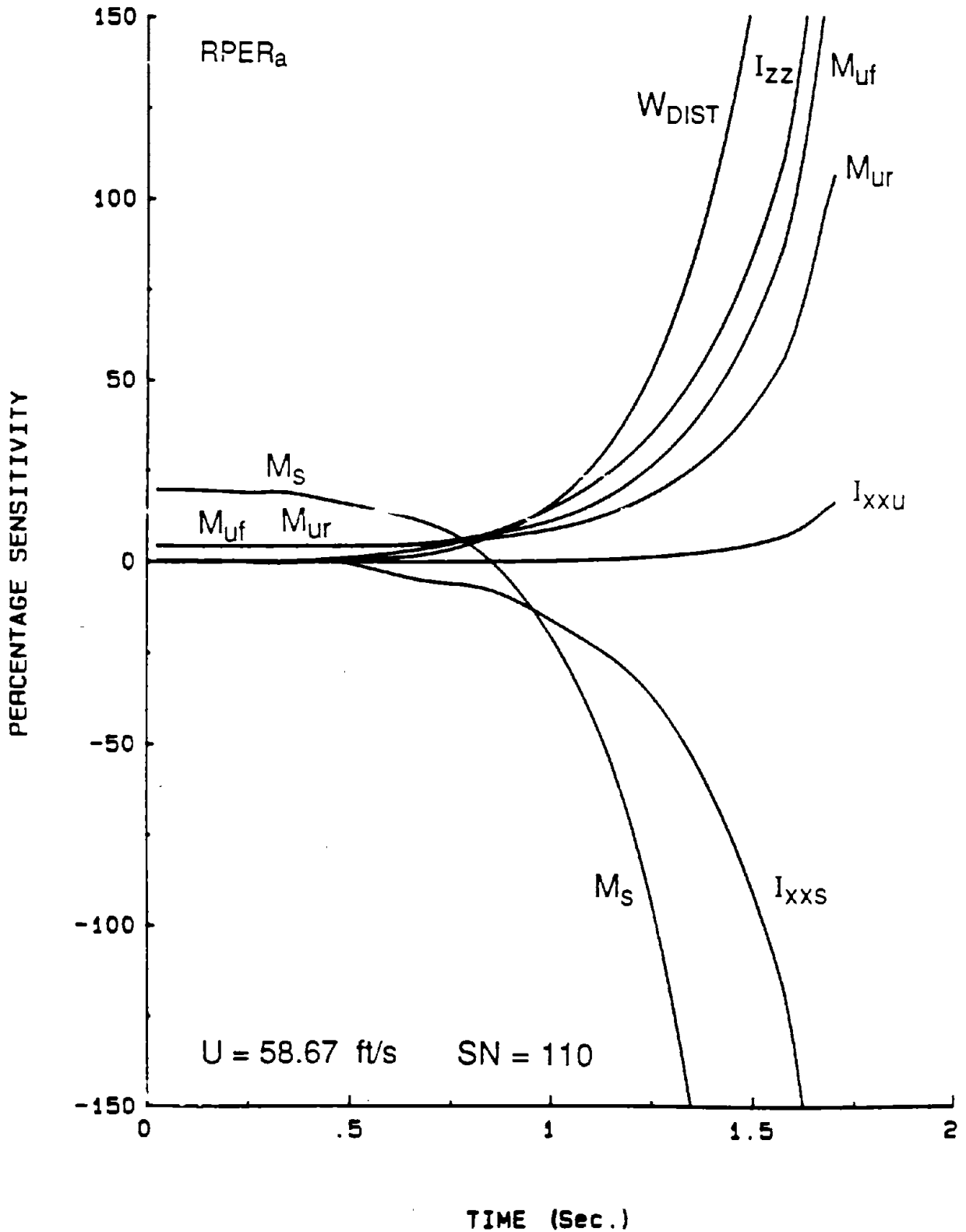


Figure 20.

SENSITIVITY OF RPER IN IMIRS  
ROLLOVER IN J-TURN  
STIFFNESS PARAMETER SET

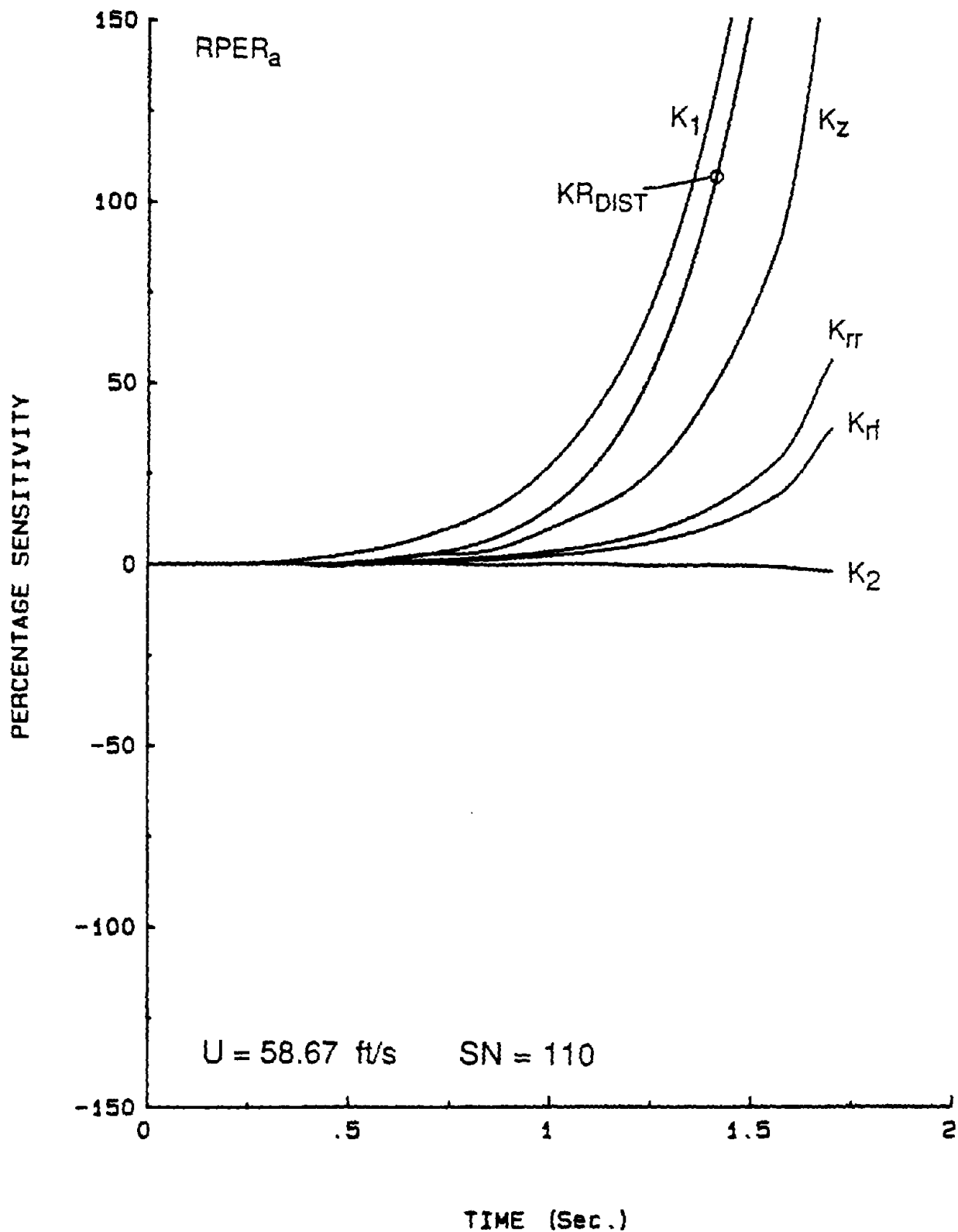


Figure 21.

SENSITIVITY OF RPER IN IMIRS  
ROLLOVER IN J-TURN  
DAMPING PARAMETER SET

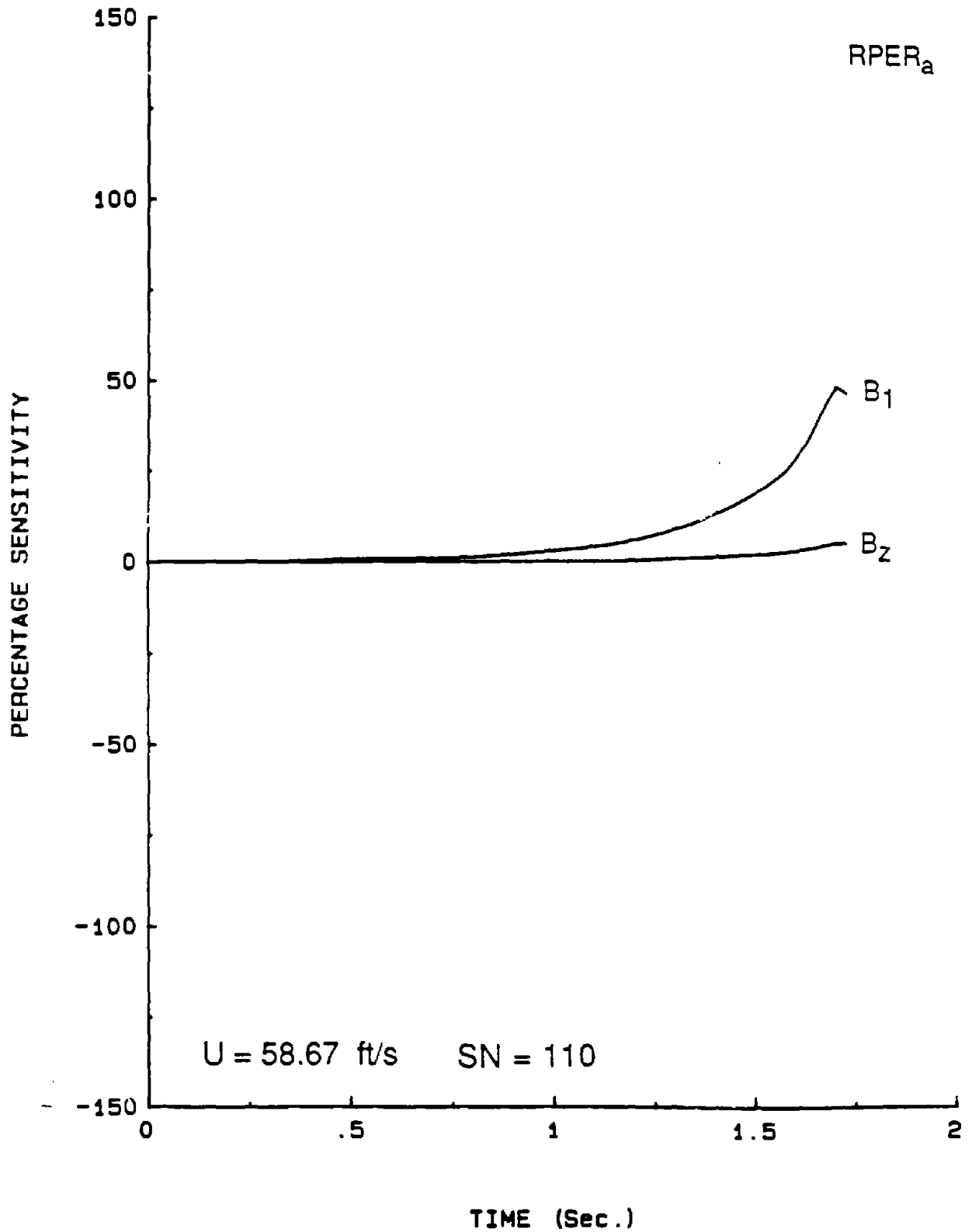


Figure 22.



SENSITIVITY OF RPER IN IMIRS  
ROLLOVER IN J-TURN  
AERODYNAMIC PARAMETER SET

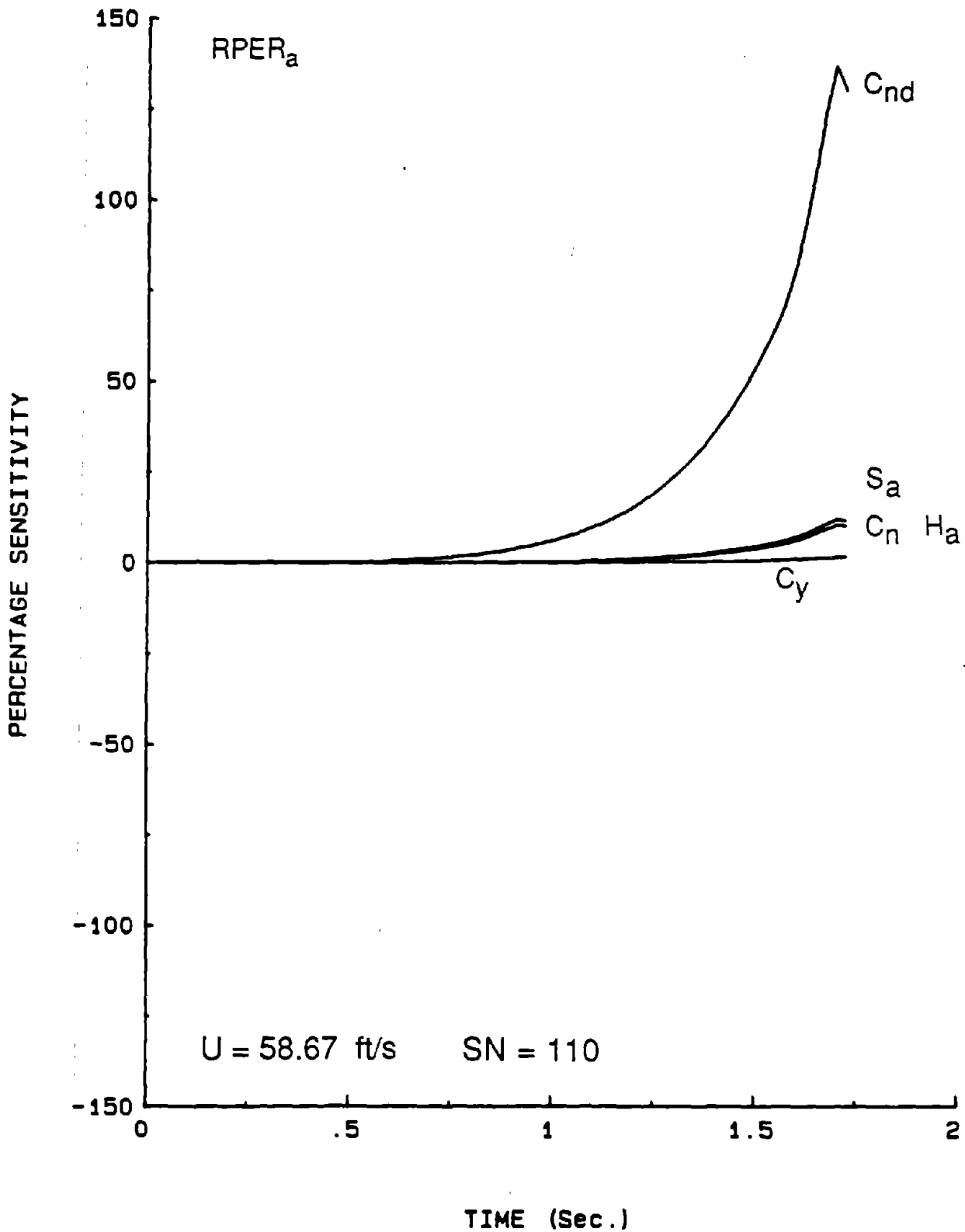


Figure 23.

SENSITIVITY OF RPER IN IMIRS  
ROLLOVER IN J-TURN  
TIRE FRICTIONAL PARAMETER SET

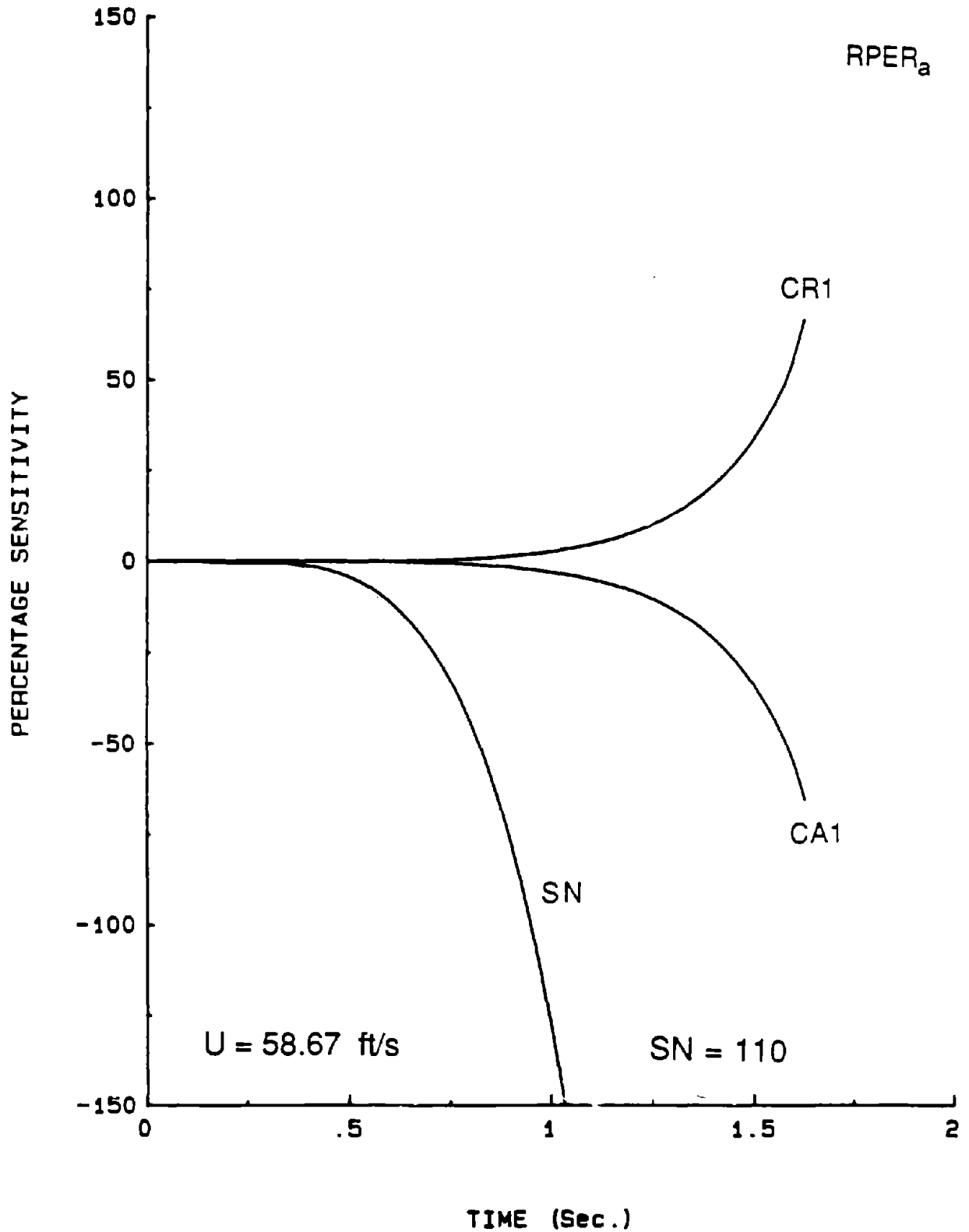


Figure 24.

SENSITIVITY OF RPER IN IMIRS  
NON-ROLLOVER IN J-TURN  
GEOMETRIC PARAMETER SET #1

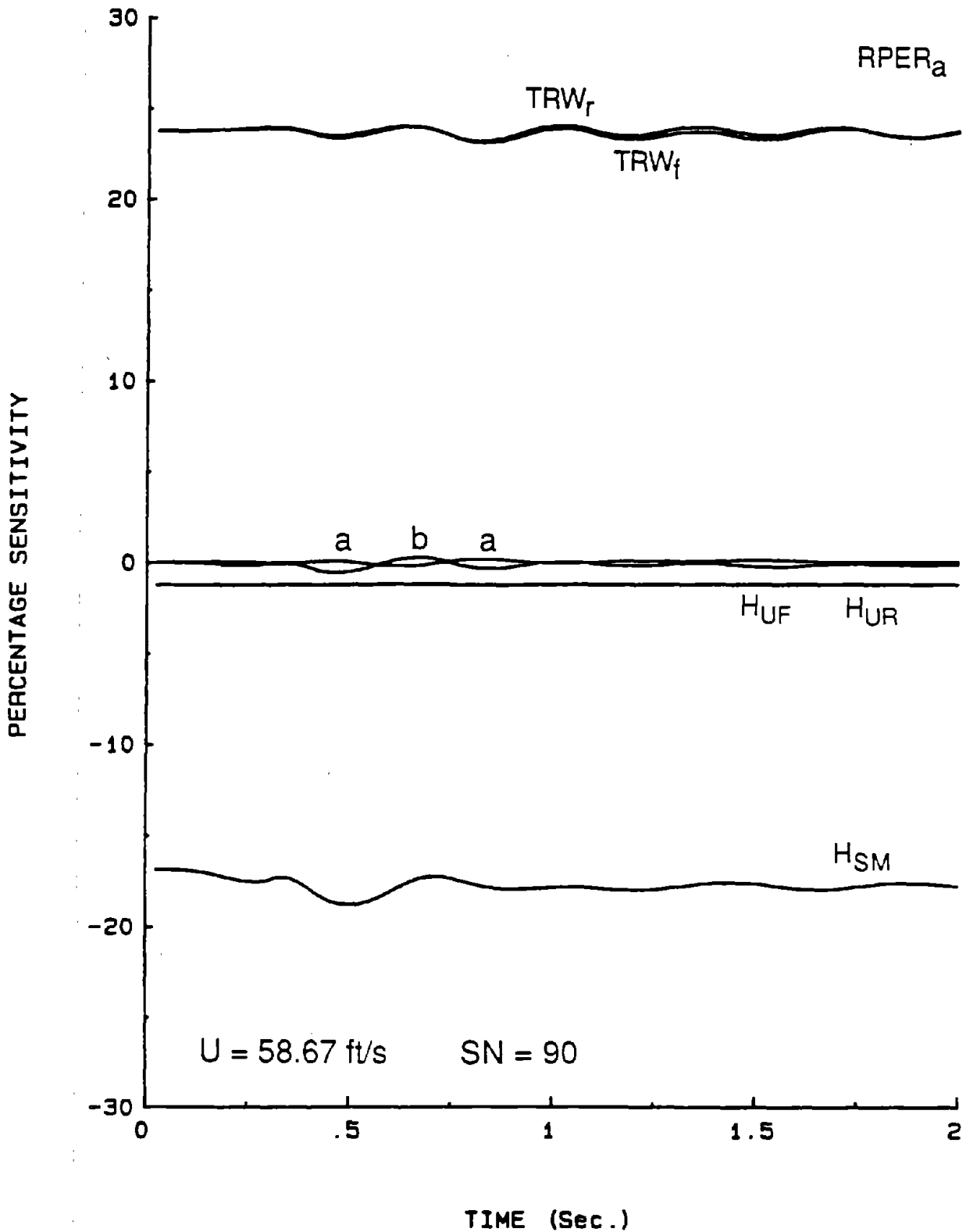


Figure 25.

SENSITIVITY OF RPER IN IMIRS  
NON-ROLLOVER IN J-TURN  
GEOMETRIC PARAMETER SET #2

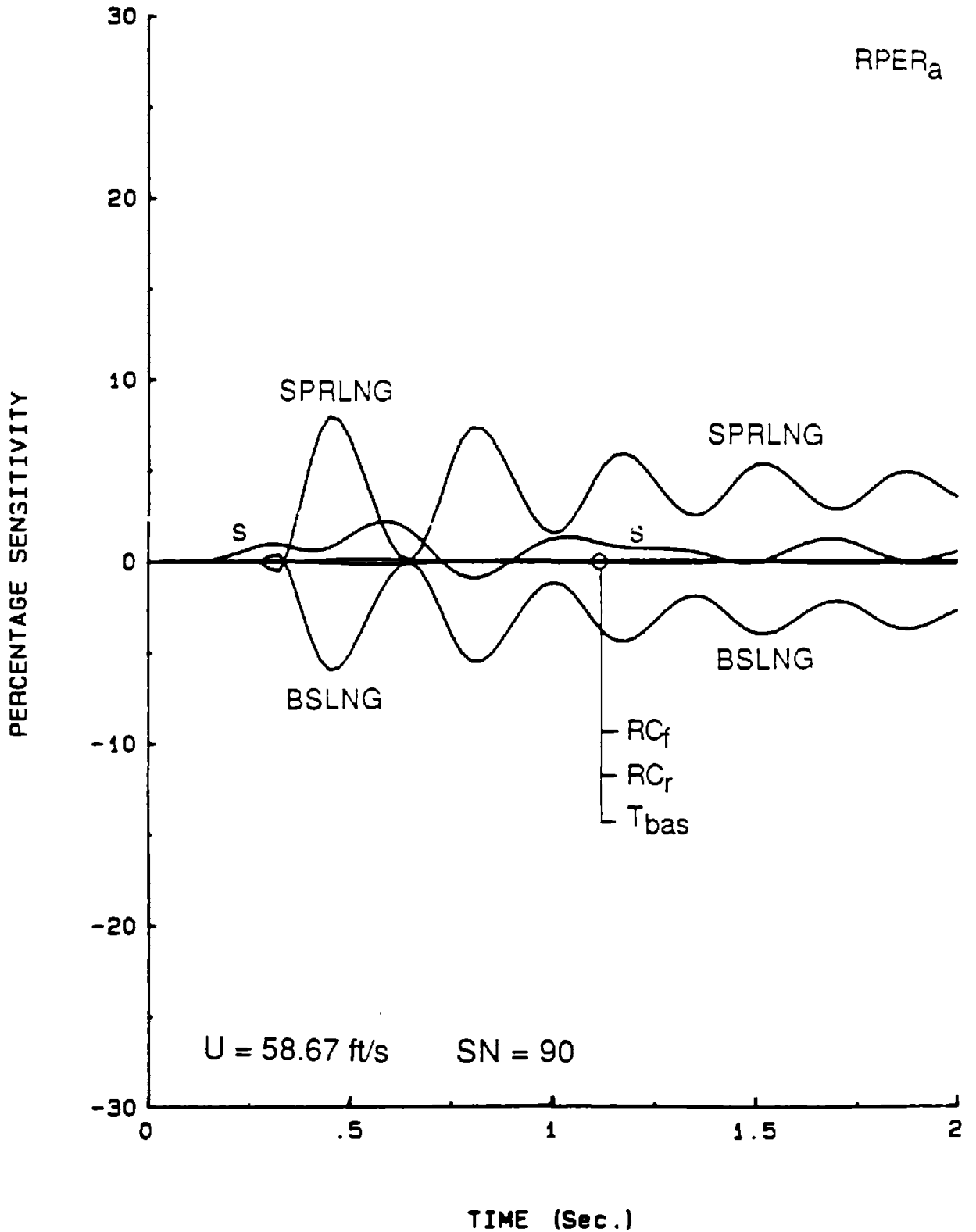


Figure 26.

SENSITIVITY OF RPER IN IMIRS  
NON-ROLLOVER IN J-TURN  
MASS-INERTIA PARAMETER SET

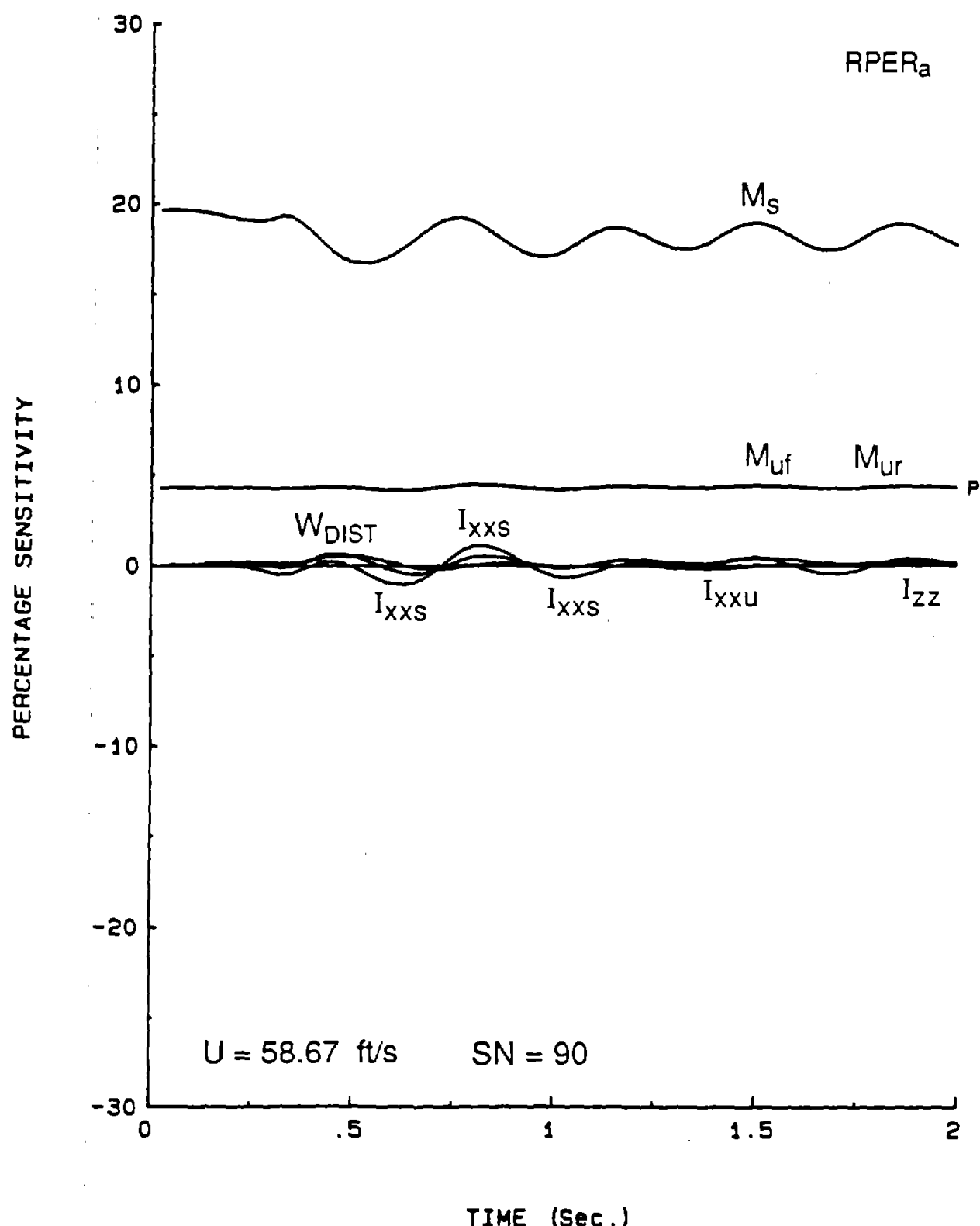


Figure 27.

SENSITIVITY OF RPER IN IMIRS  
NON-ROLLOVER IN J-TURN  
STIFFNESS PARAMETER SET

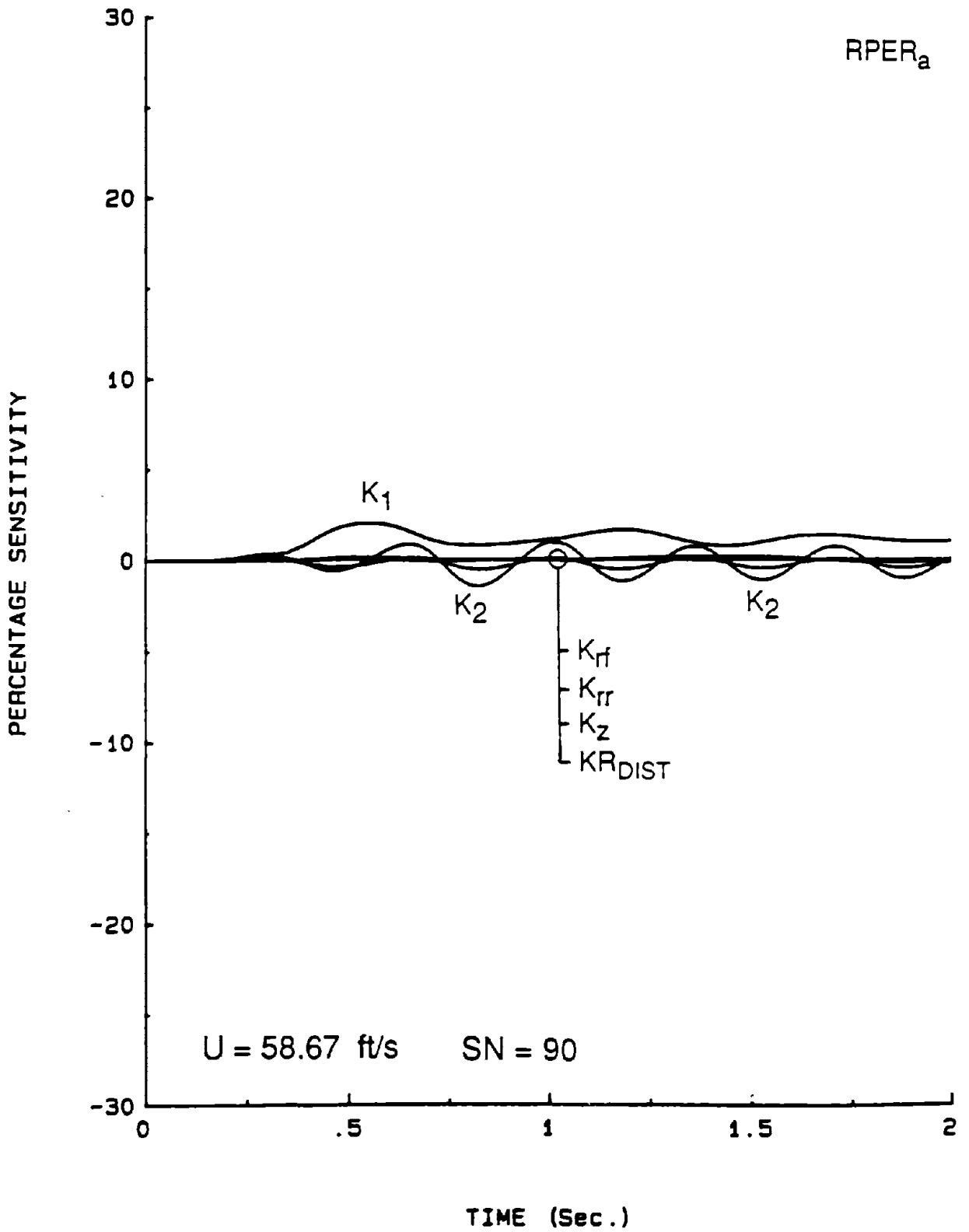


Figure 28.

SENSITIVITY OF RPER IN IMIRS  
NON-ROLLOVER IN J-TURN  
DAMPING PARAMETER SET

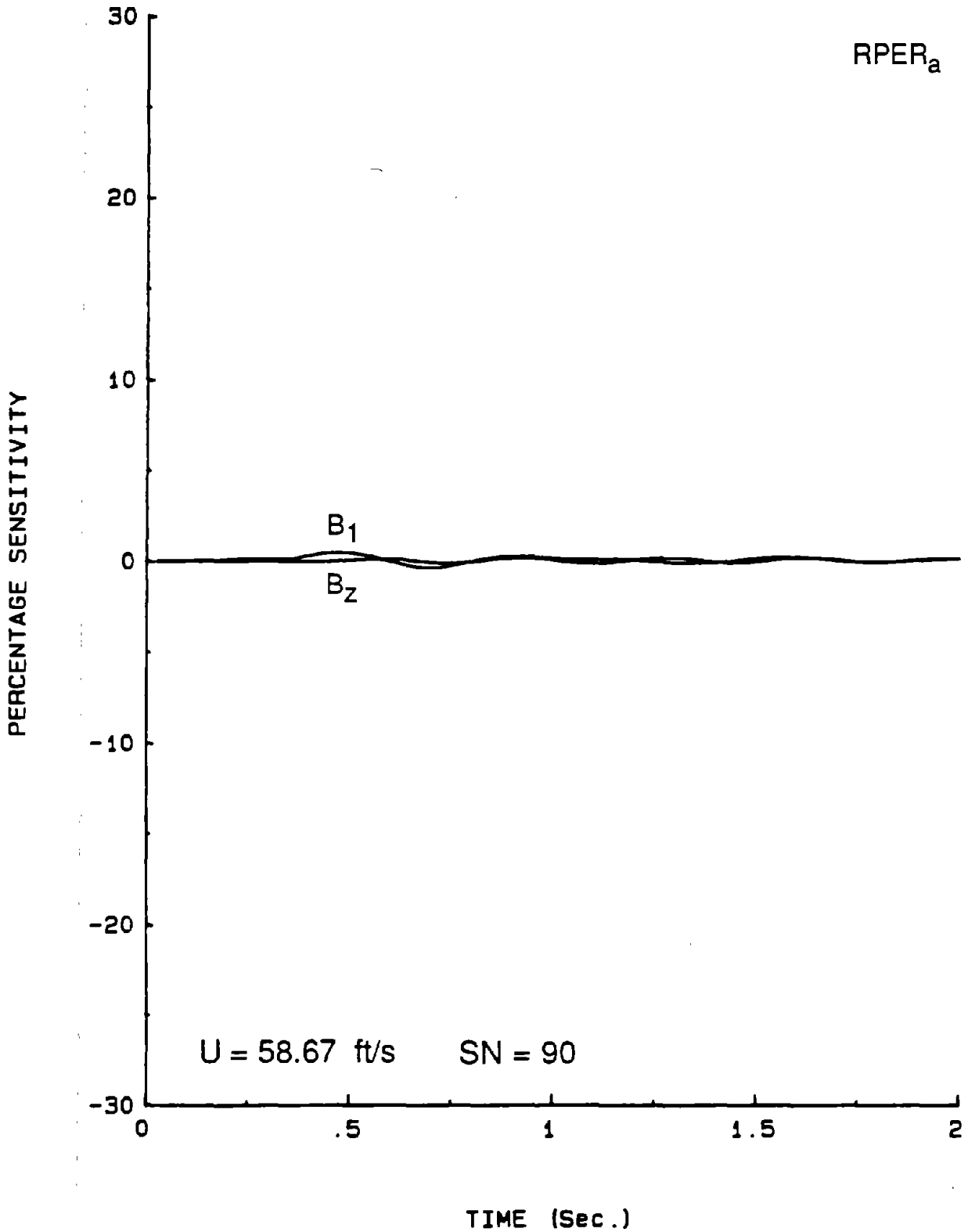


Figure 29.

SENSITIVITY OF RPER IN IMIRS  
NON-ROLLOVER IN J-TURN  
AERODYNAMIC PARAMETER SET

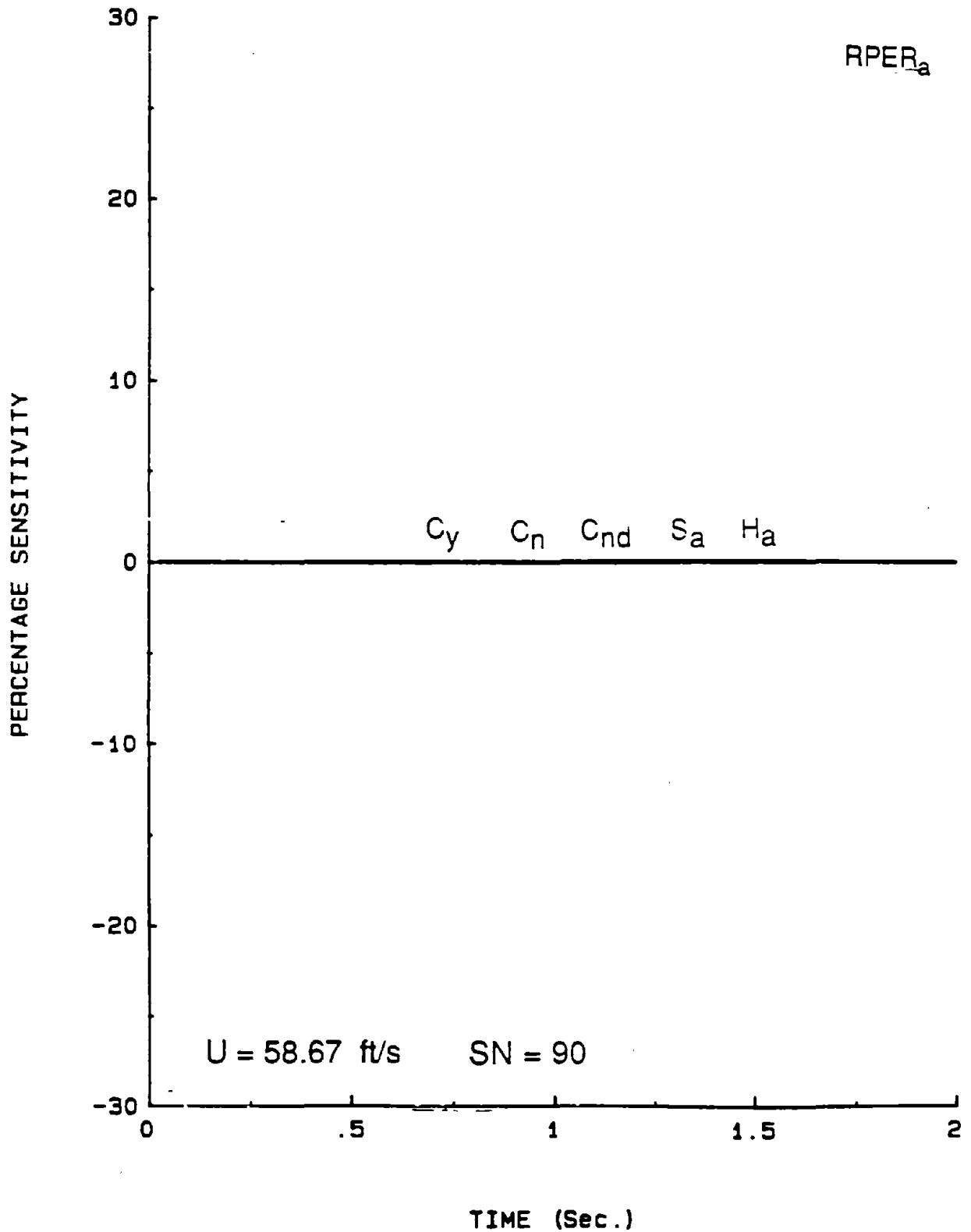


Figure 30.



SENSITIVITY OF RPER IN IMIRS  
NON-ROLLOVER IN J-TURN  
TIRE FRICTIONAL PARAMETER SET

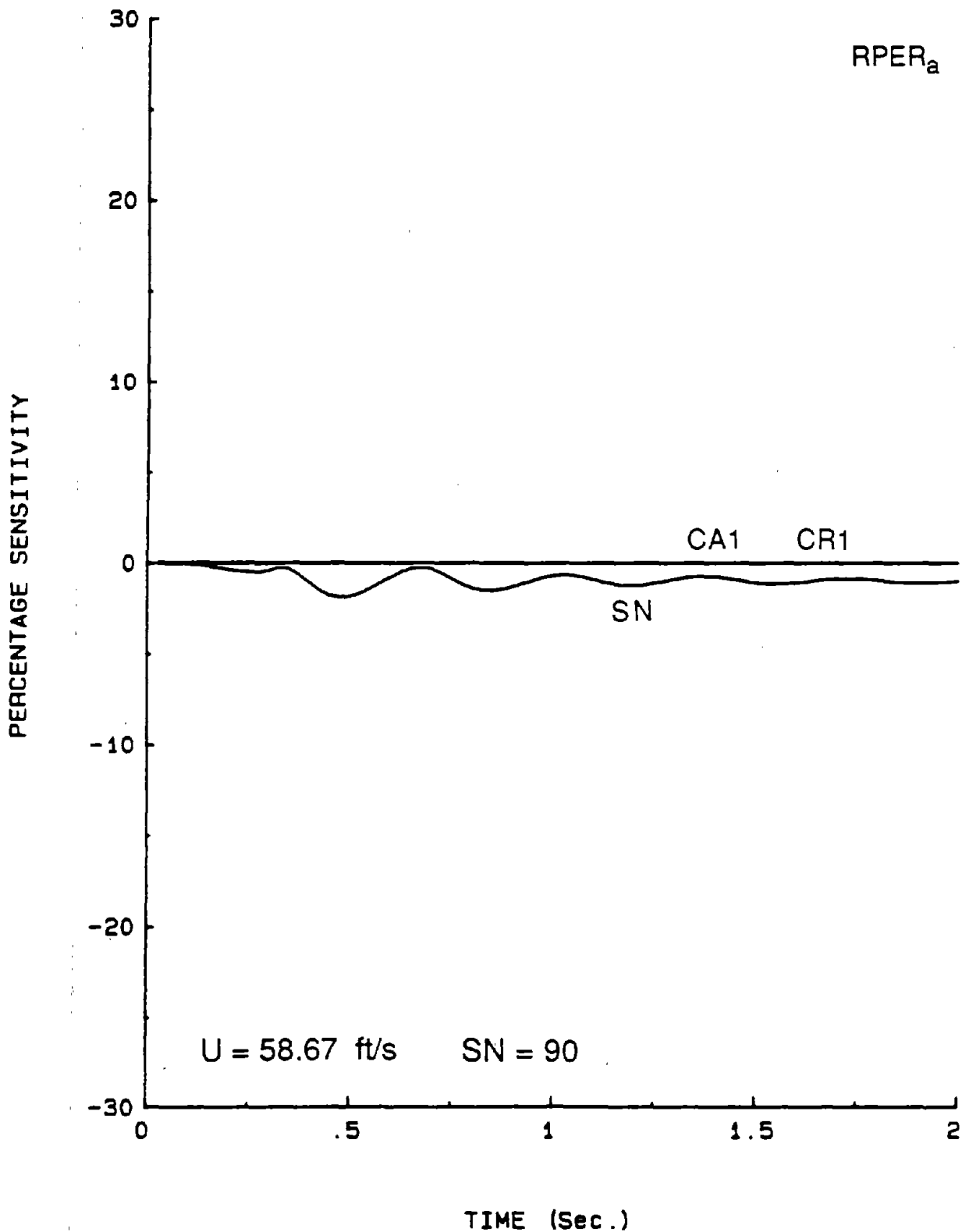


Figure 31.

SENSITIVITY OF RPER IN IMIRS  
 ROLLOVER IN S-TURN  
 GEOMETRIC PARAMETER SET #1

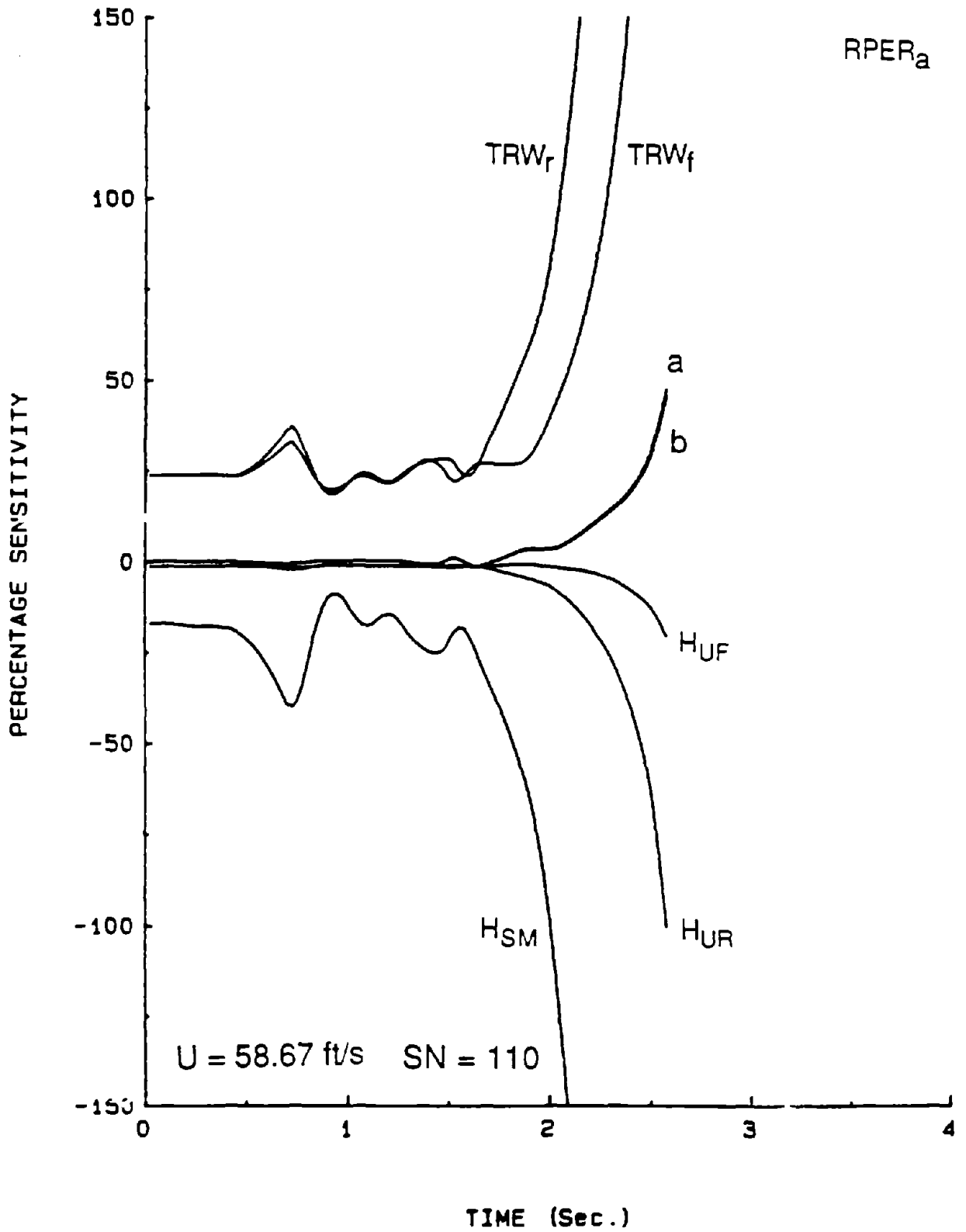


Figure 32.

SENSITIVITY OF RPER IN IMIRS  
 ROLLOVER IN S-TURN  
 GEOMETRIC PARAMETER SET #2

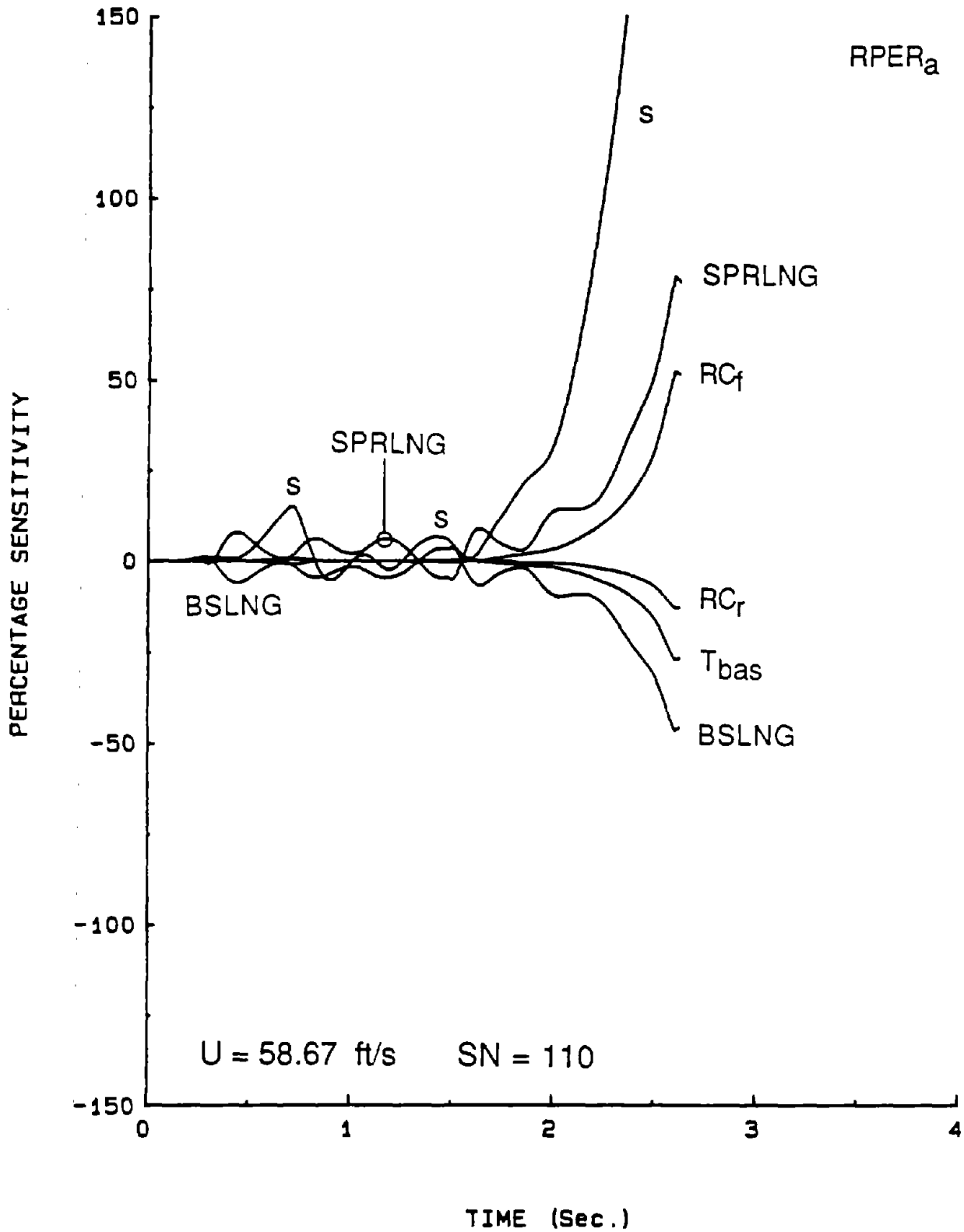


Figure 33.

SENSITIVITY OF RPER IN IMIRS  
 ROLLOVER IN S-TURN  
 MASS-INERTIA PARAMETER SET

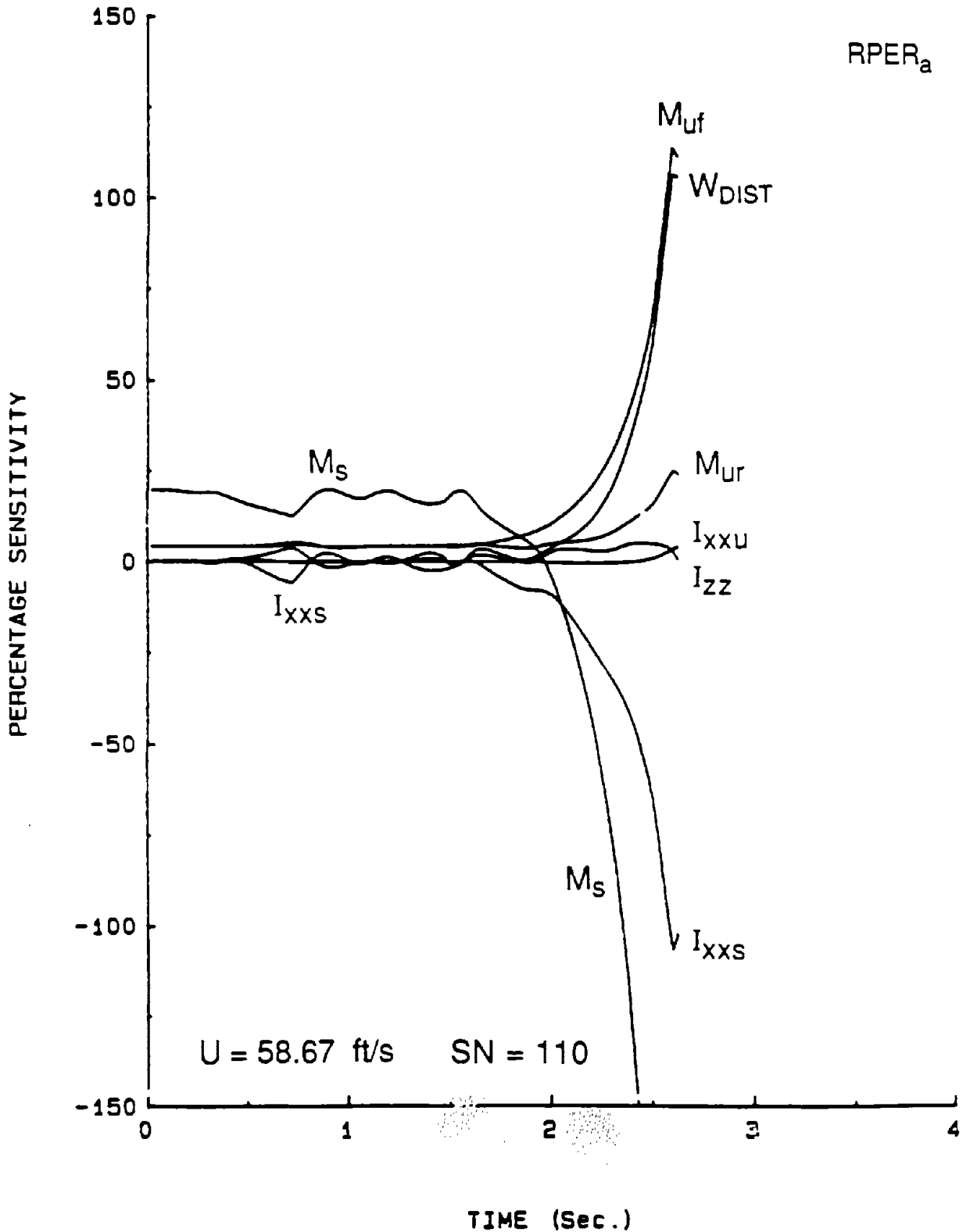


Figure 34.

SENSITIVITY OF RPER IN IMIRS  
ROLLOVER IN S-TURN  
STIFFNESS PARAMETER SET

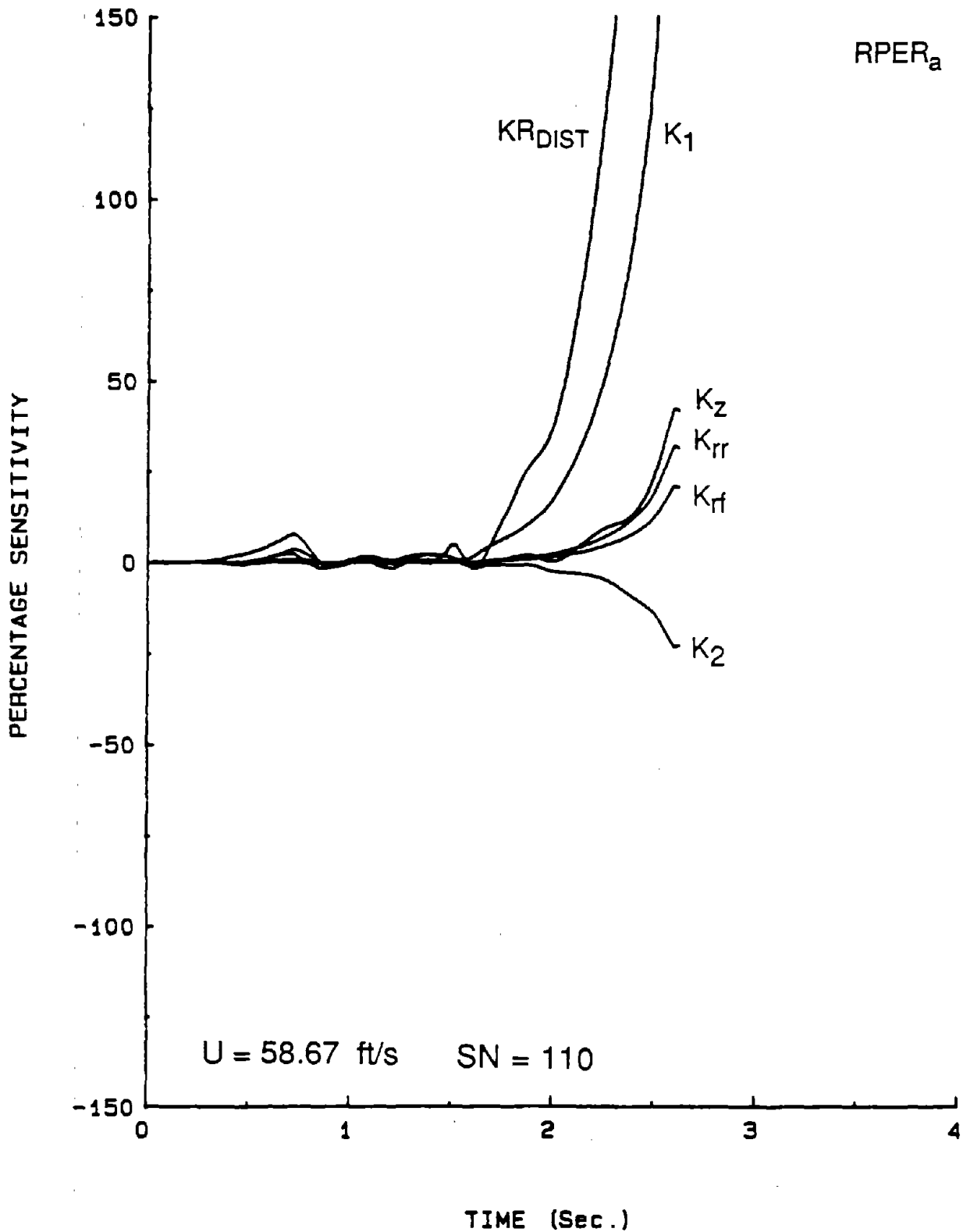


Figure 35.

SENSITIVITY OF RPER IN IMIRS  
ROLLOVER IN S-TURN  
DAMPING PARAMETER SET

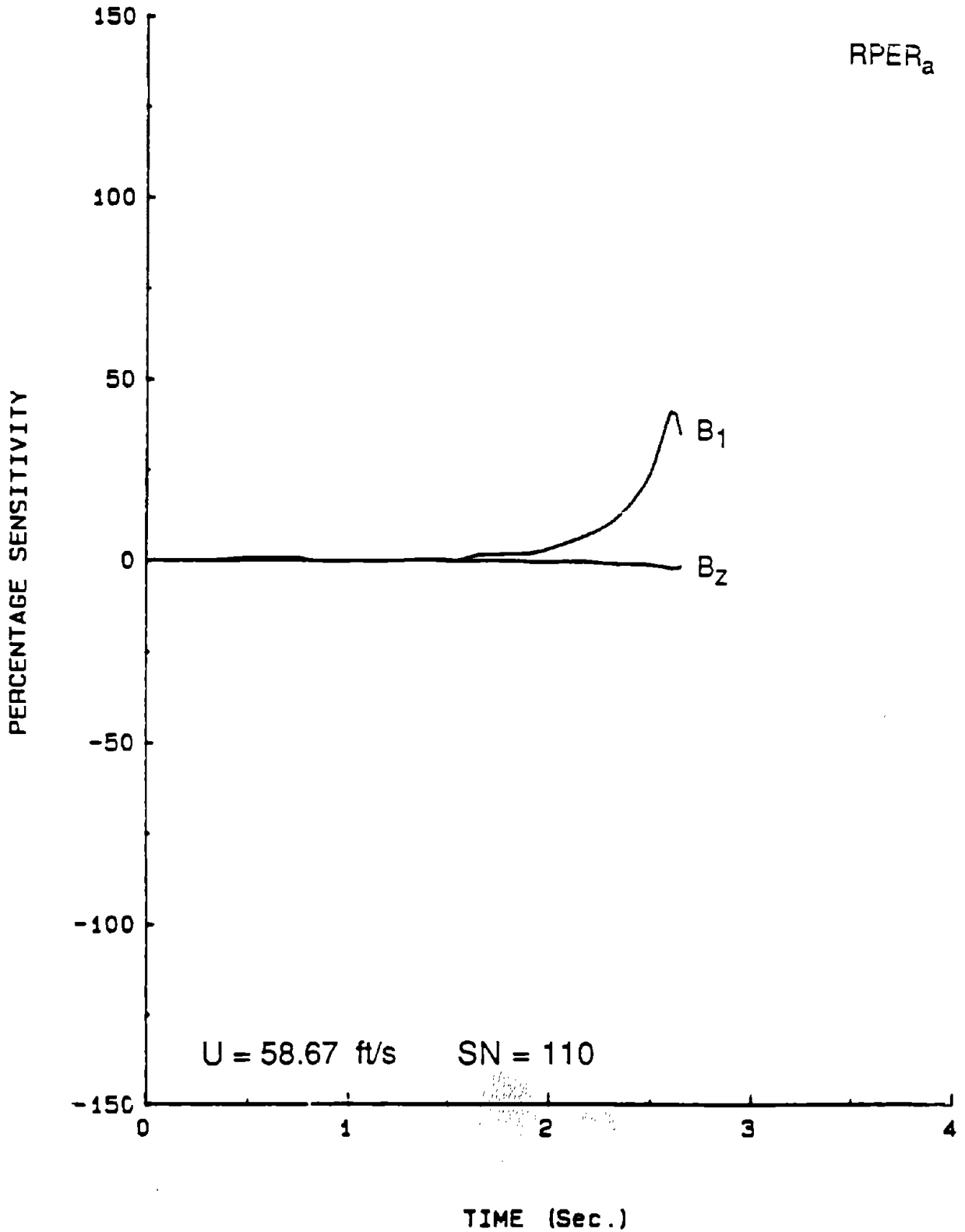


Figure 36.

SENSITIVITY OF RPER IN IMIRS  
ROLLOVER IN S-TURN  
AERODYNAMIC PARAMETER SET

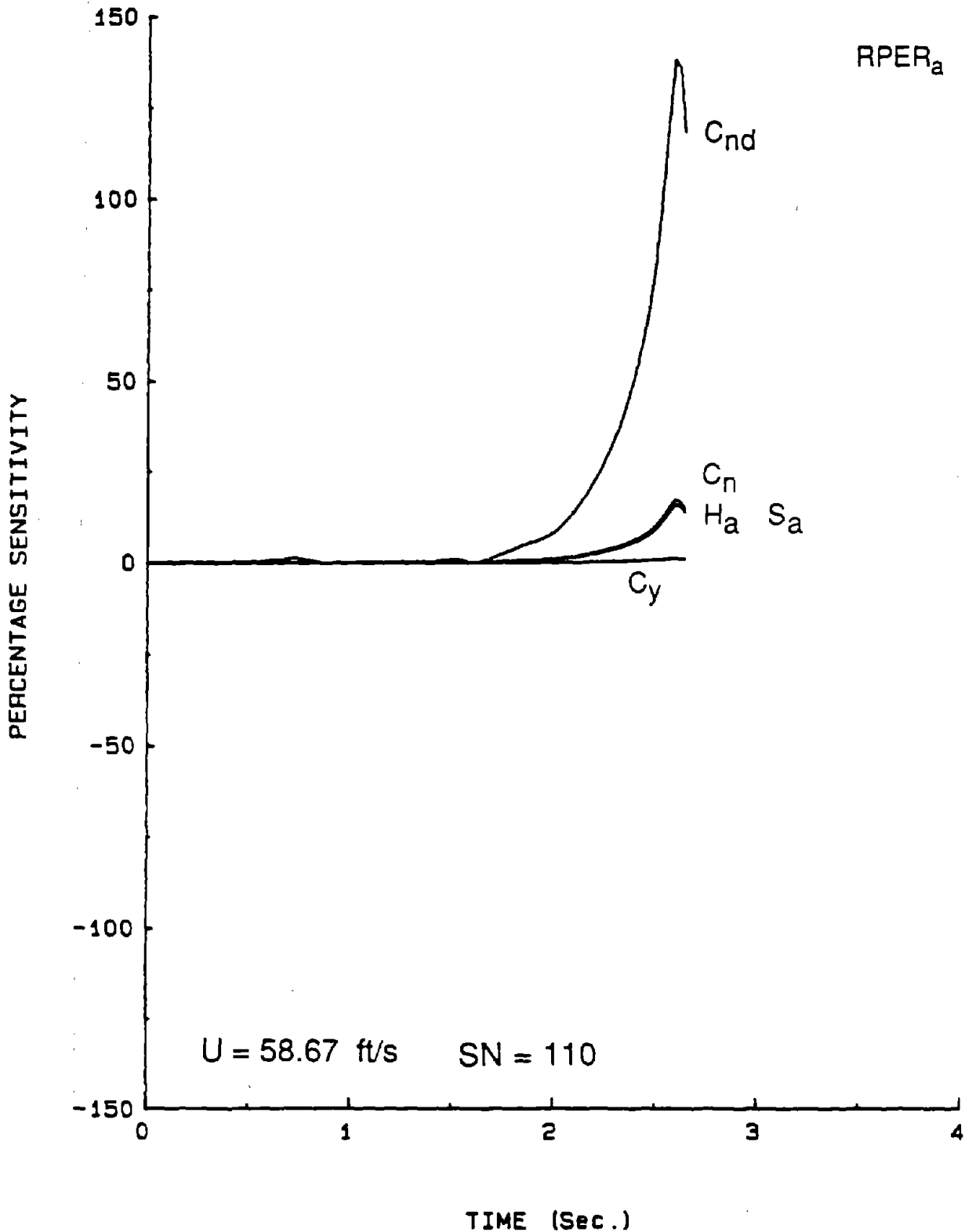


Figure 37.

SENSITIVITY OF RPER IN IMIRS  
ROLLOVER IN S-TURN  
TIRE FRICTIONAL PARAMETER SET

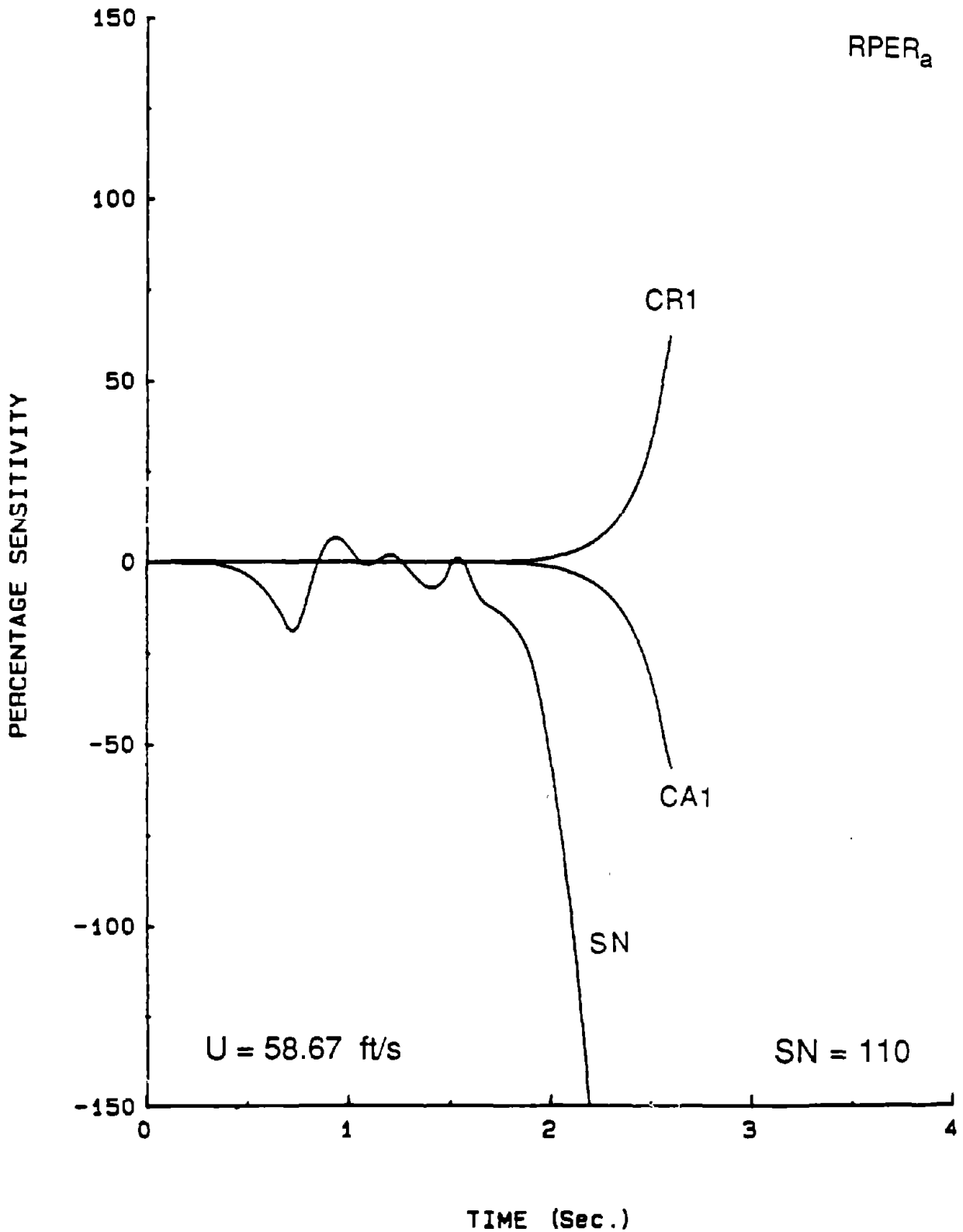


Figure 38.



SENSITIVITY OF RPER IN IMIRS  
 NON-ROLLOVER IN S-TURN  
 GEOMETRIC PARAMETER SET #1

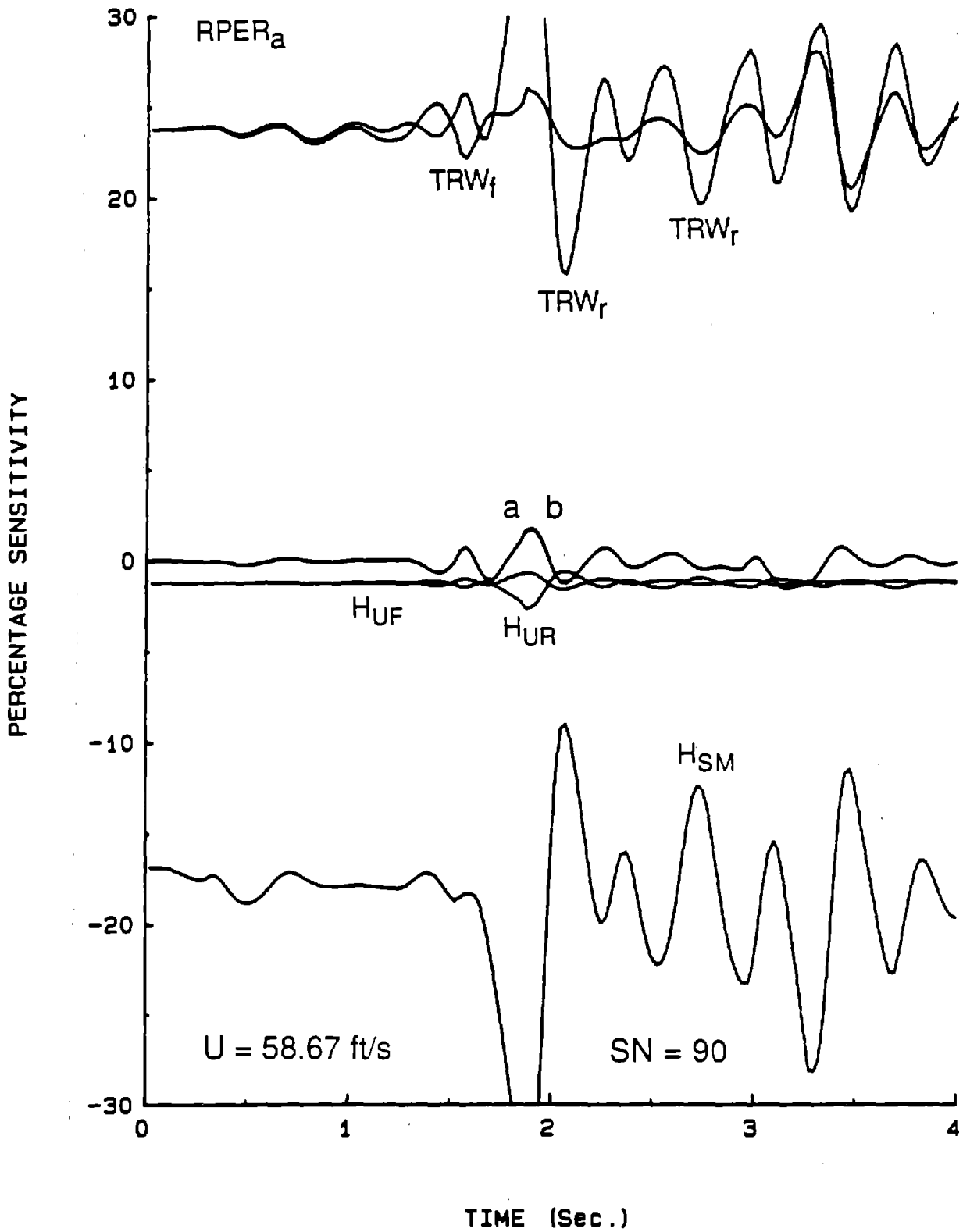


Figure 39.

SENSITIVITY OF RPER IN IMIRS  
NON-ROLLOVER IN S-TURN  
GEOMETRIC PARAMETER SET #2

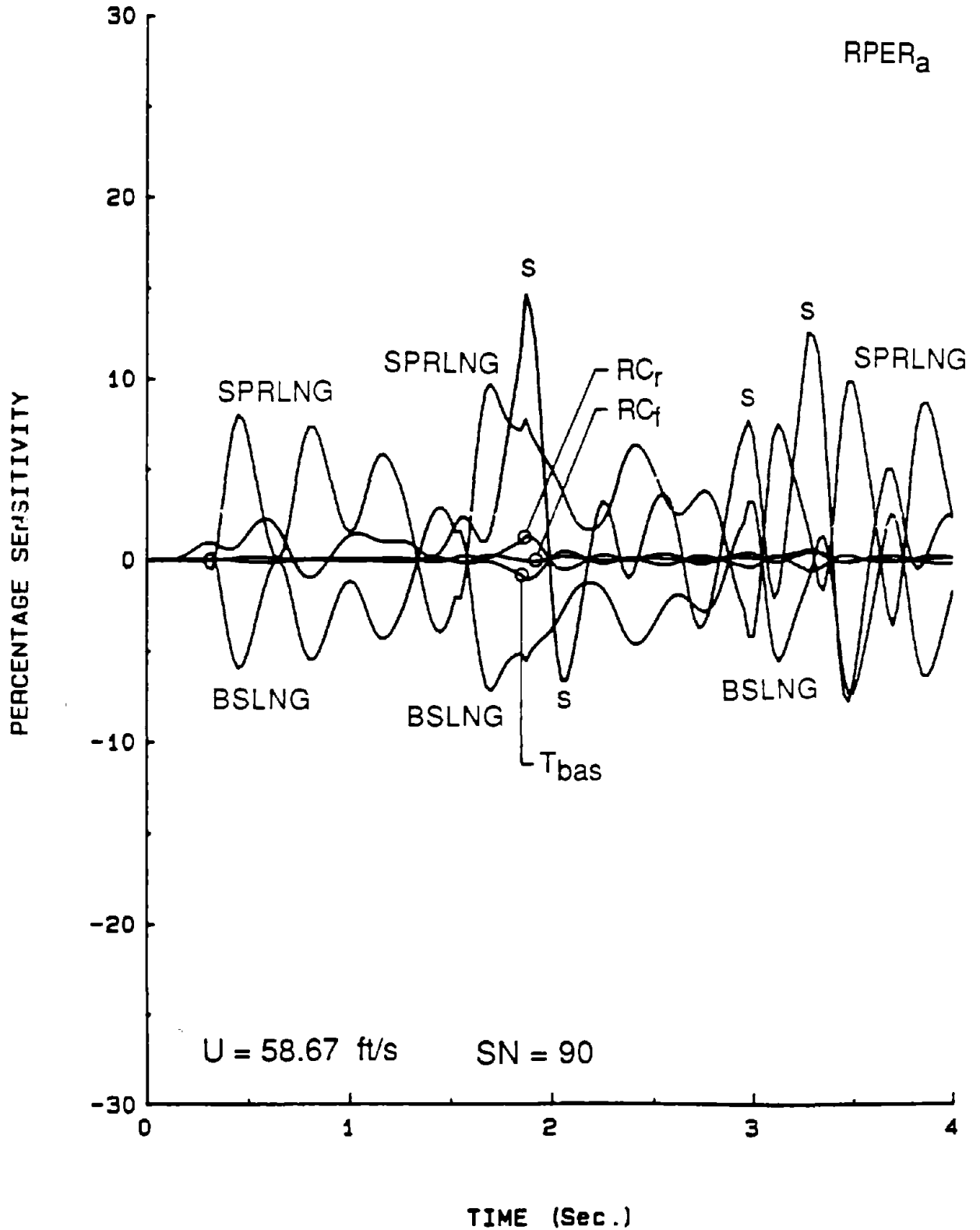


Figure 40.

SENSITIVITY OF RPER IN IMIRS  
 NON-ROLLOVER IN S-TURN  
 MASS-INERTIA PARAMETER SET

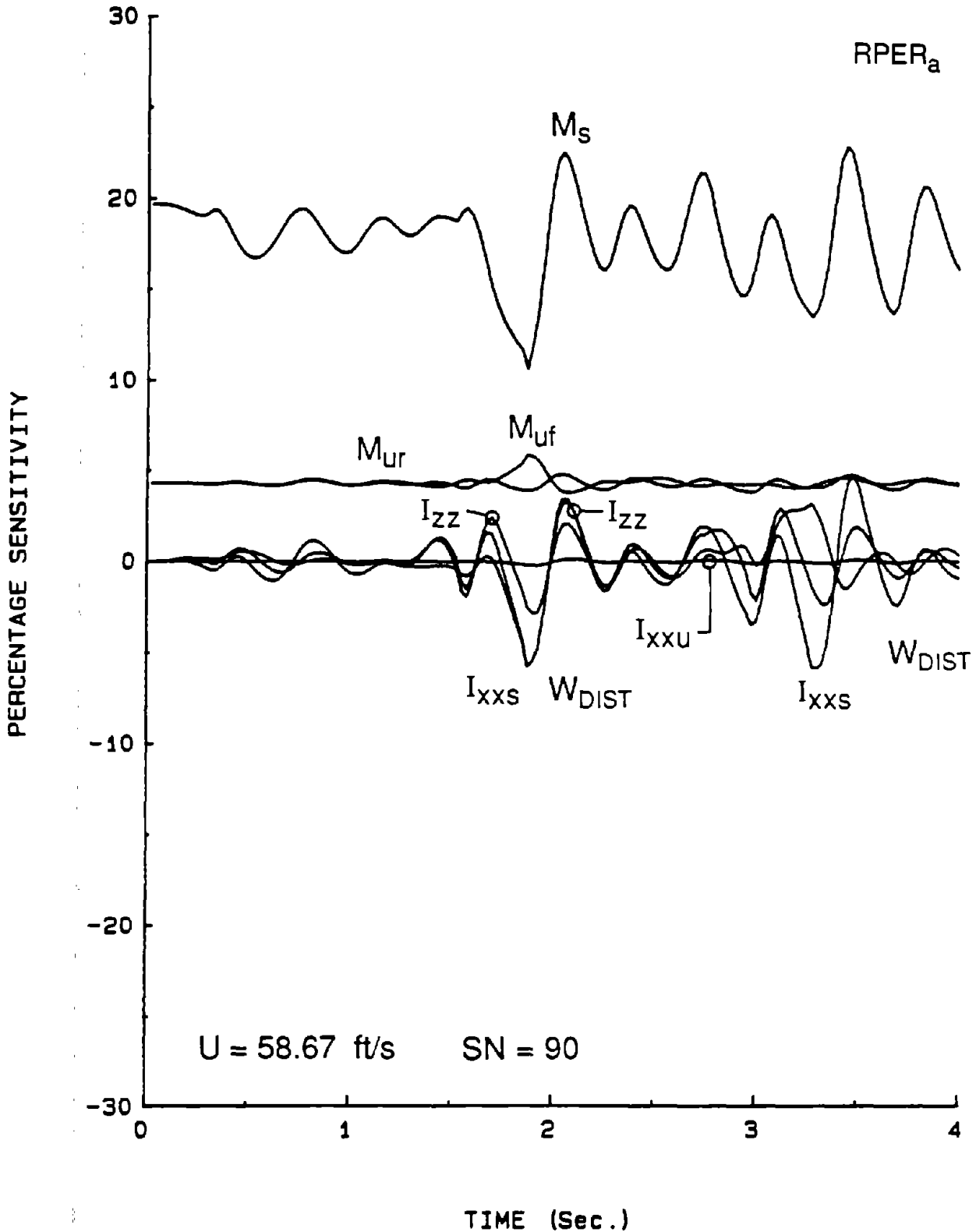


Figure 41.

SENSITIVITY OF RPER IN IMIRS  
NON-ROLLOVER IN S-TURN  
STIFFNESS PARAMETER SET

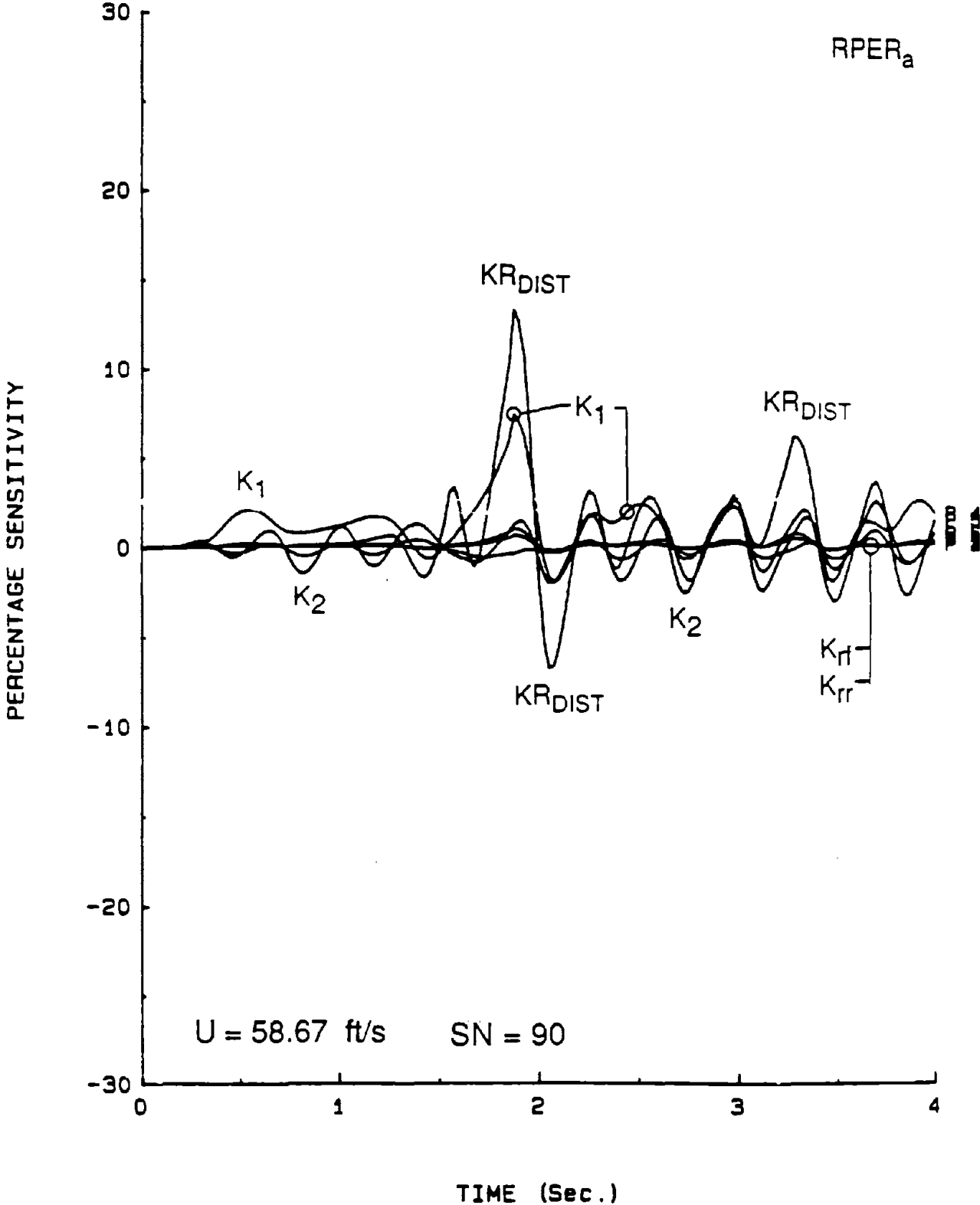


Figure 42.

SENSITIVITY OF RPER IN IMIRS  
NON-ROLLOVER IN S-TURN  
DAMPING PARAMETER SET

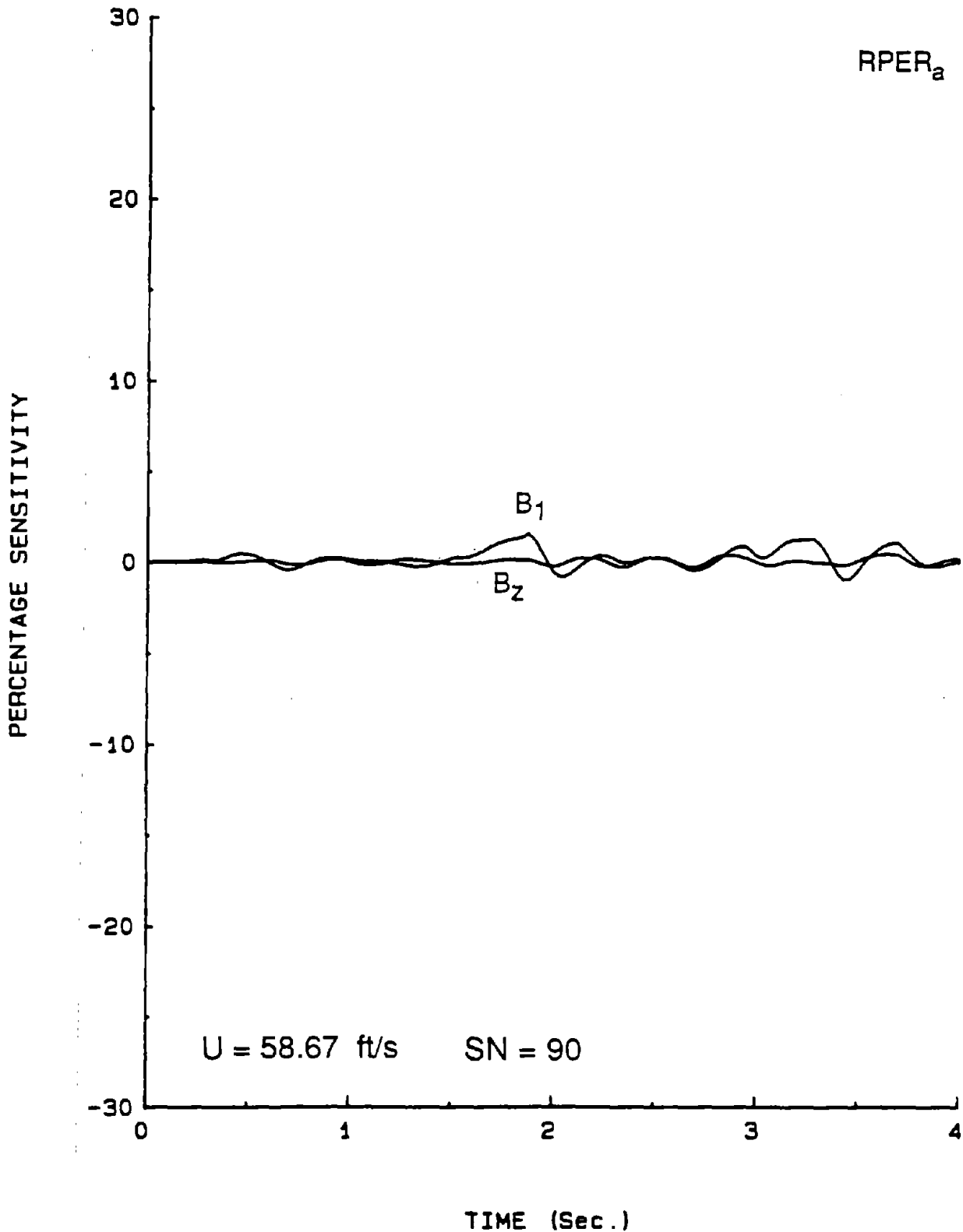


Figure 43.

SENSITIVITY OF RPER IN S-TURN  
NON-ROLLOVER IN S-TURN  
AERODYNAMIC PARAMETER SET

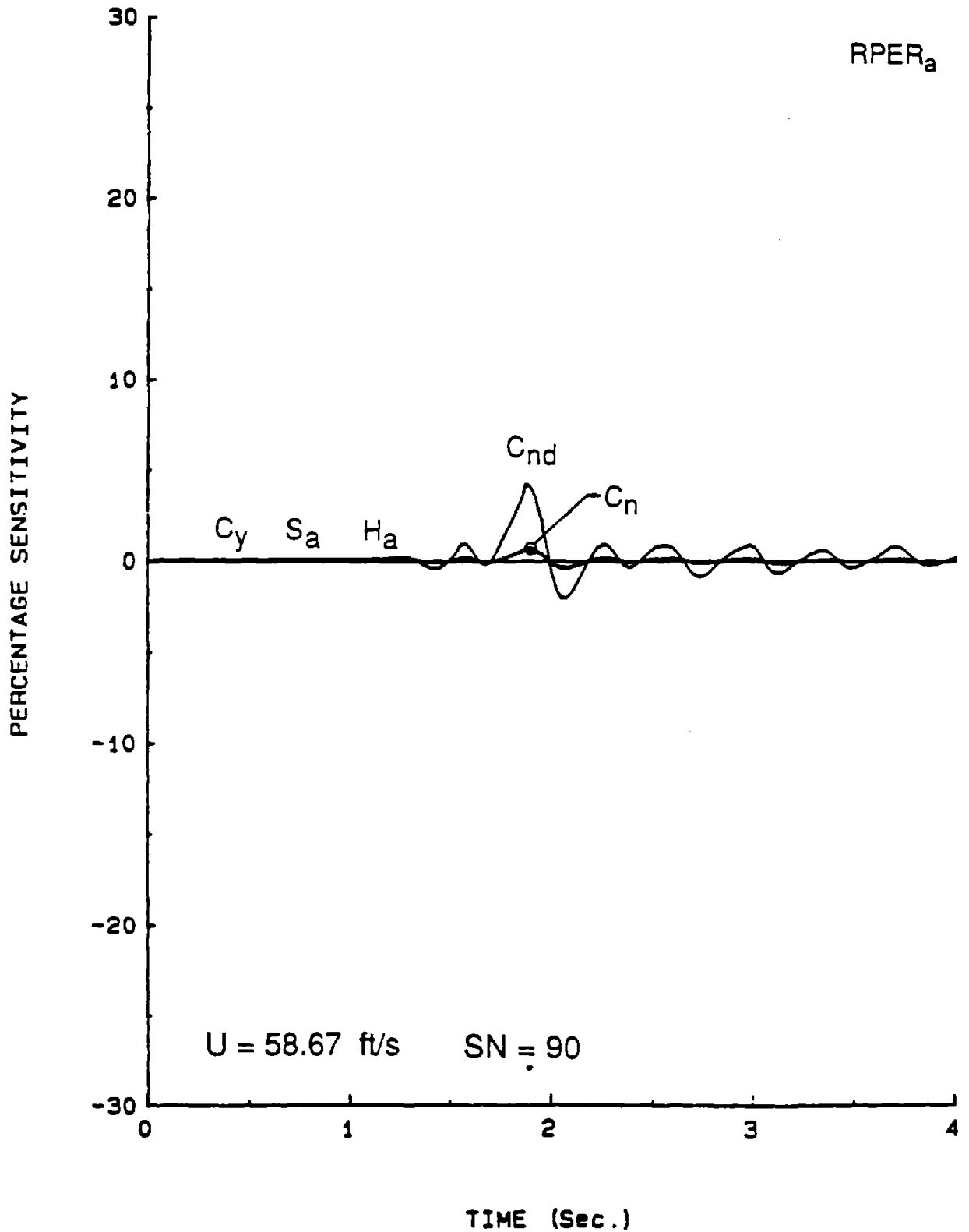


Figure 44.

SENSITIVITY OF RPER IN IMIRS  
NON-ROLLOVER IN S-TURN  
TIRE FRICTIONAL PARAMETER SET

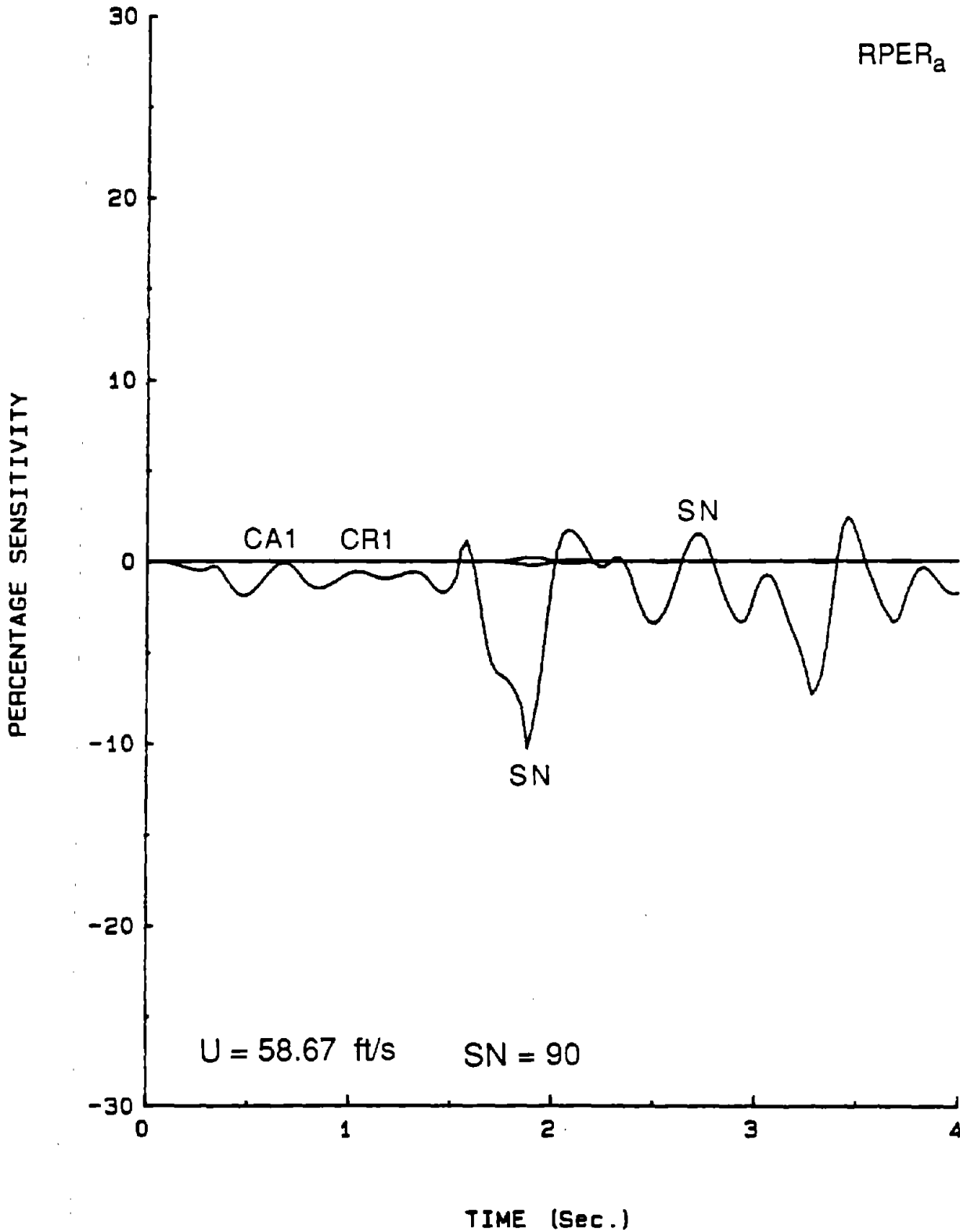
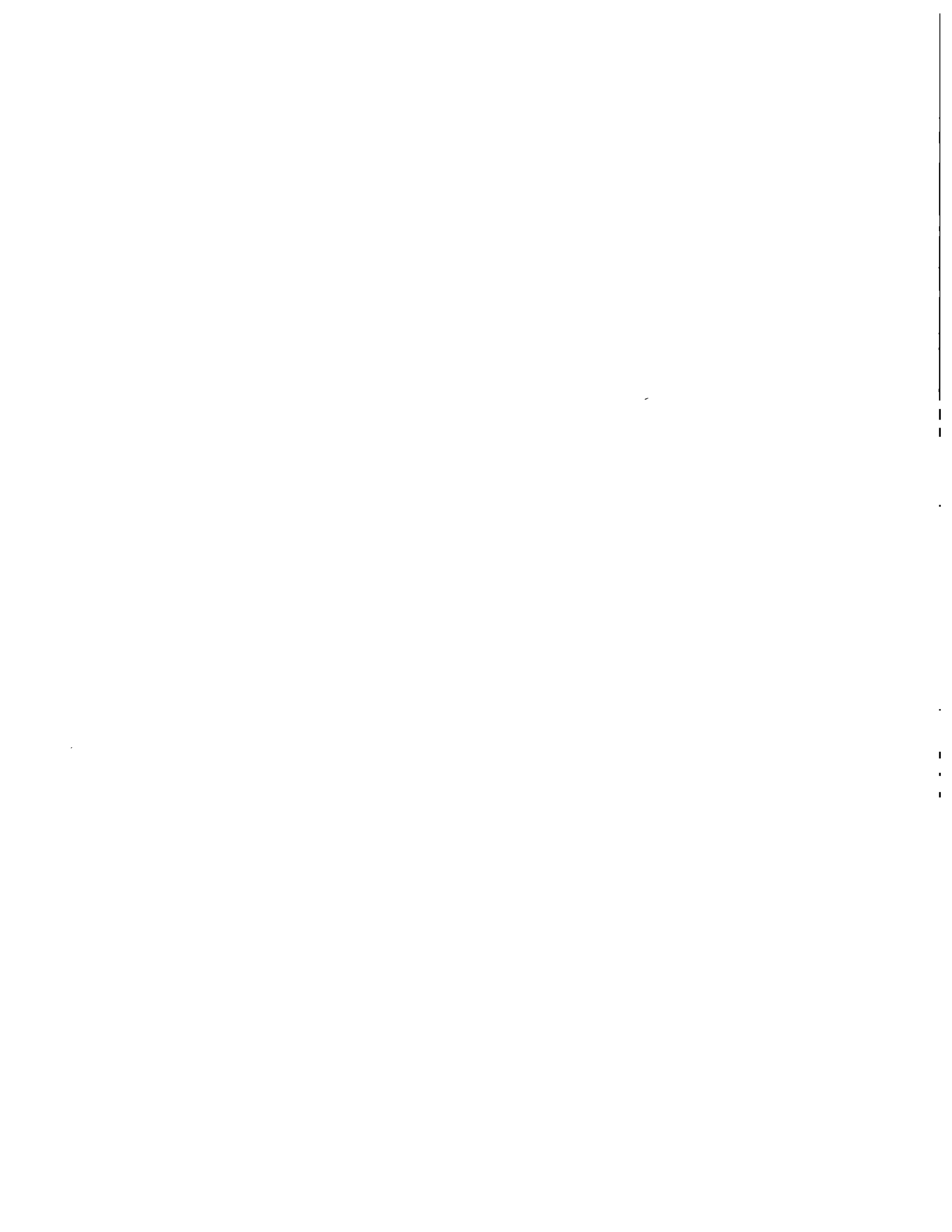


Figure 45.





## APPENDIX A

### ILLUSTRATIONS OF SUSPENSION SYSTEMS

#### Front

Upper and lower control arms (Converging towards car center).....	A-2
Upper and lower control arms (Converging away from car center).....	A-3
Parallel upper and lower control arms .....	A-4
Macpherson strut.....	A-5
Trailing link.....	A-6
Twin I-beam .....	A-7
Sliding pillar .....	A-8
Live Hotchkiss drive .....	A-9

#### Rear Independent

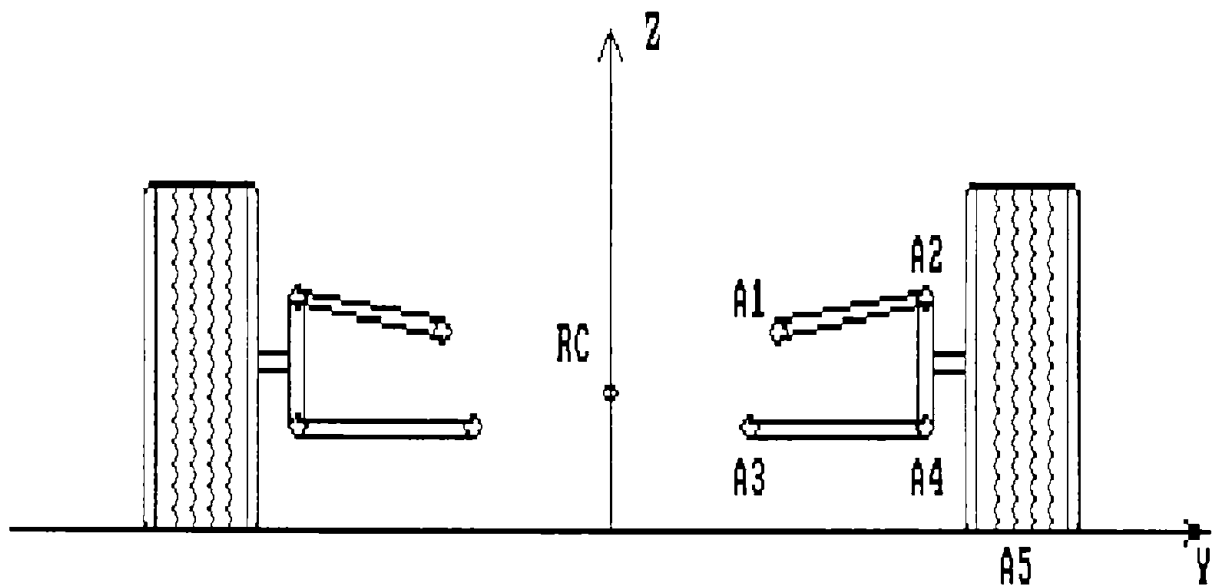
Swing axle .....	A-10
Low pivot swing axle.....	A-11
Single transverse a-arms for FWD .....	A-12
Single trailing arm.....	A-13
Semi-trailing arm .....	A-14
Chapman strut.....	A-15
Semi-independent for FWD .....	A-16
Weissach axle.....	A-17
Upper and lower control arms (Converging towards car center) .....	A-18
Upper and lower control arms (Converging away from car center) .....	A-19

#### Rear Dependent

Hotchkiss drive .....	A-20
Torque tube with panhard rod .....	A-21
Three link with panhard rod.....	A-22
Four link with parallel lower links.....	A-23
Four link with non-parallel lower links.....	A-24
Beam twist axle with panhard rod FWD.....	A-25
Rear wheel drive with sideways location on the center of axle .....	A-26
De Dion Axle.....	A-27
Beam Axle with leaf springs and lateral locating device.....	A-28

UNEQUAL-LENGTH UPPER AND LOWER CONTROL ARMS  
 (CONVERGING TOWARDS CAR CENTER)

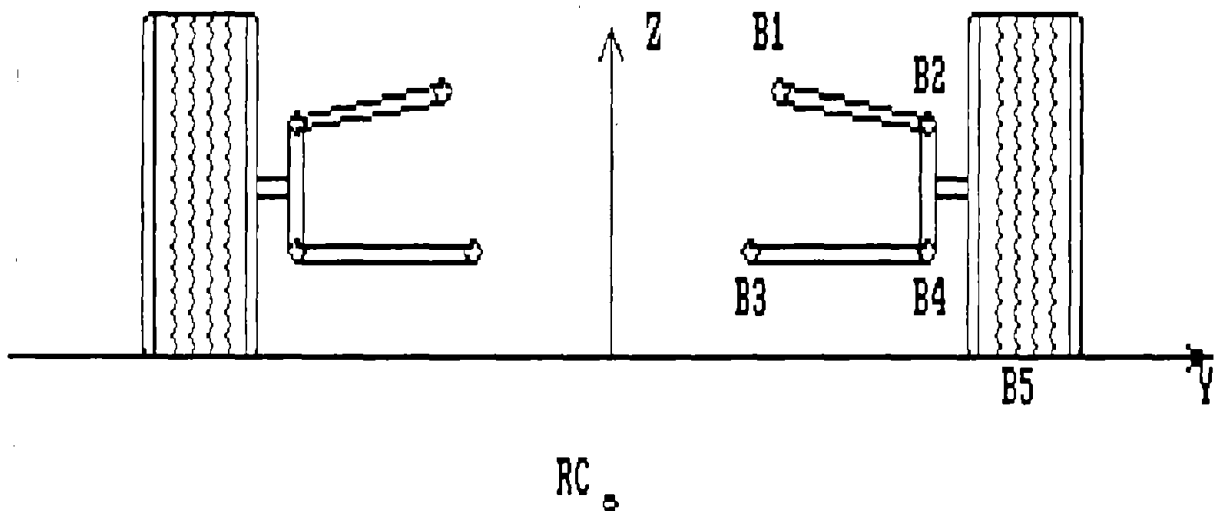
ENTER FOR A1: A1X,A1Y,A1Z 2.50, 0.20, 0.45  
 ENTER FOR A2: A2X,A2Y,A2Z 2.50, 0.40, 0.55  
 ENTER FOR A3: A3X,A3Y,A3Z 2.50, 0.15, 0.25  
 ENTER FOR A4: A4X,A4Y,A4Z 2.50, 0.45, 0.20  
 ENTER FOR A5: A5X,A5Y 2.50, 0.65



ROLL CENTER RC [ 2.5000, 0.0000, 0.2504]

UPPER AND LOWER CONTROL ARMS  
 (CONVERGING AWAY FROM CAR CENTER)

ENTER FOR B1: B1X, B1Y, B1Z 2.50, 0.20, 0.60  
 ENTER FOR B2: B2X, B2Y, B2Z 2.50, 0.40, 0.55  
 ENTER FOR B3: B3X, B3Y, B3Z 2.50, 0.15, 0.17  
 ENTER FOR B4: B4X, B4Y, B4Z 2.50, 0.45, 0.20  
 ENTER FOR B5: B5X, B5Y 2.50, 0.65

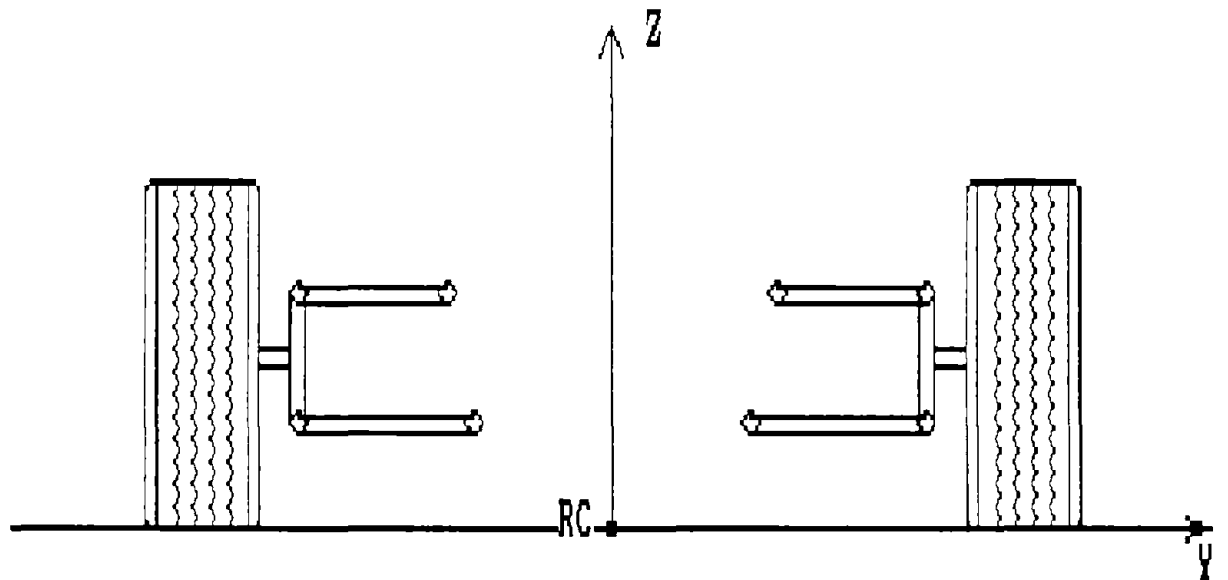


ROLL CENTER RC [ 2.5000, 0.0000, -0.25211

PARALLEL UPPER AND LOWER CONTROL ARMS

ENTER WHEELBASE 2.5

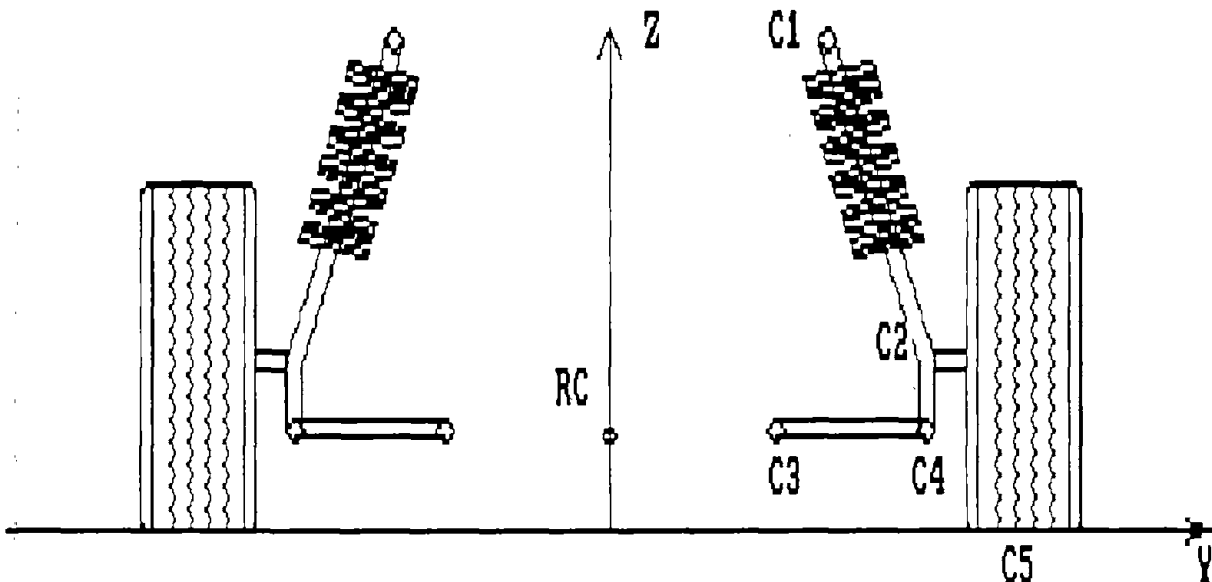
ENTER FRONT TRACK WIDTH 1.3



ROLL CENTER RC [ 2.5000, 0.0000, 0.0000]

MACPHERSON STRUT

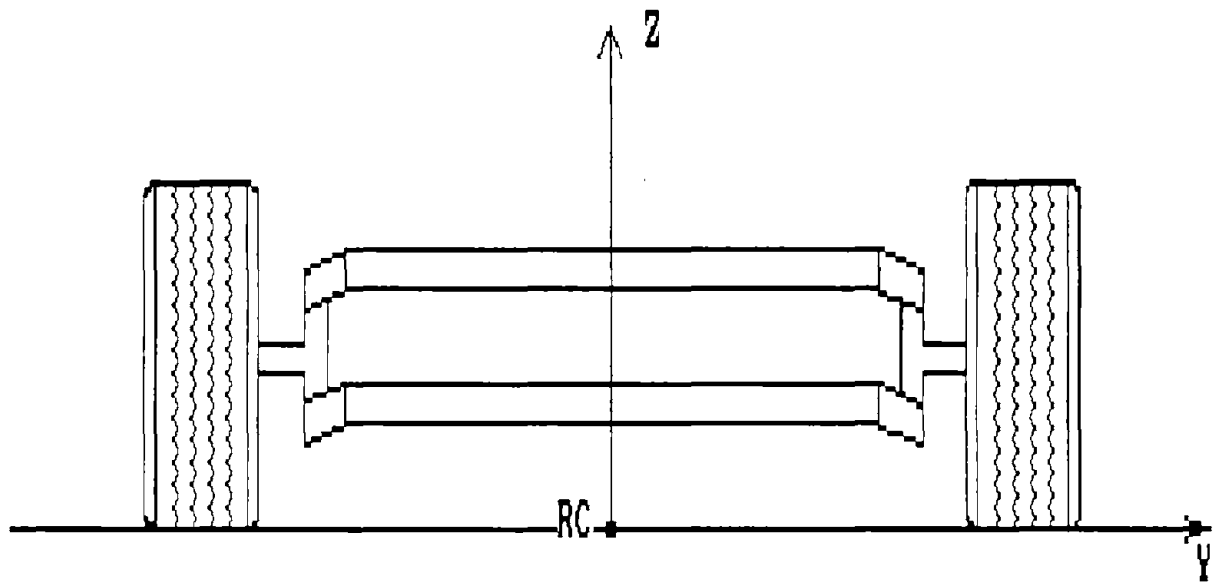
ENTER FOR C1: C1X, C1Y, C1Z 2.50, 0.40, 0.75  
 ENTER FOR C2: C2X, C2Y, C2Z 2.50, 0.47, 0.40  
 ENTER FOR C3: C3X, C3Y, C3Z 2.50, 0.15, 0.25  
 ENTER FOR C4: C4X, C4Y, C4Z 2.50, 0.45, 0.20  
 ENTER FOR C5: C5X, C5Y 2.50, 0.65



ROLL CENTER RC [ 2.5000, 0.0000, 0.17111

TRAILING LINK

ENTER WHEELBASE 2.50  
ENTER FRONT TRACK WIDTH 1.30

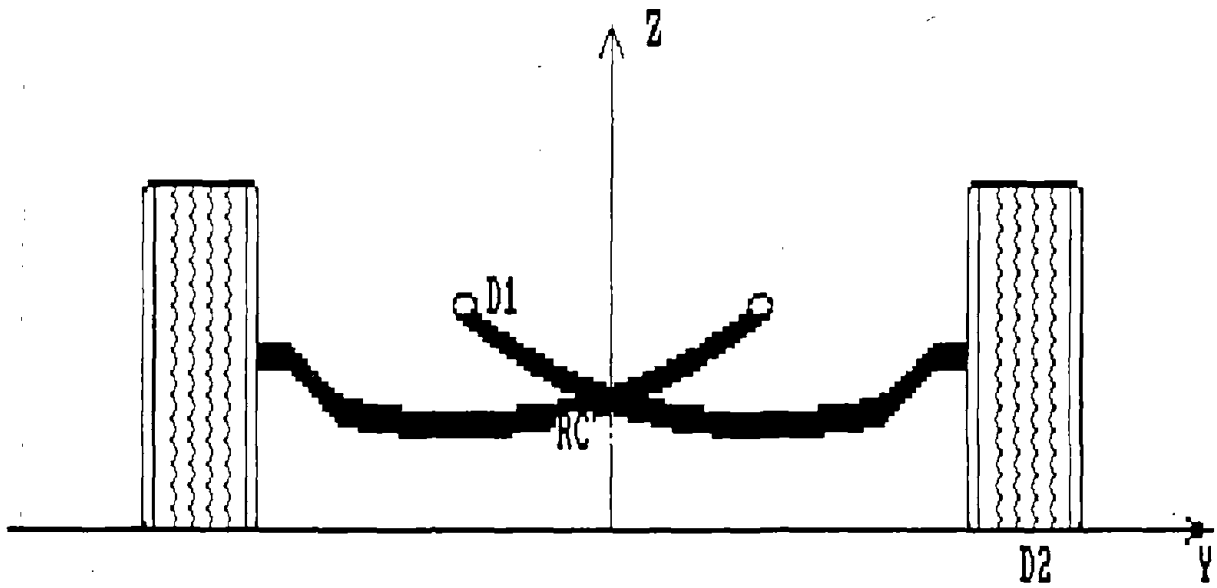


ROLL CENTER RC [ 2.5000, 0.0000, 0.0000]

TWIN I BEAM

ENTER FOR D1: D1X,D1Y,D1Z 2.50, -0.35, 0.25

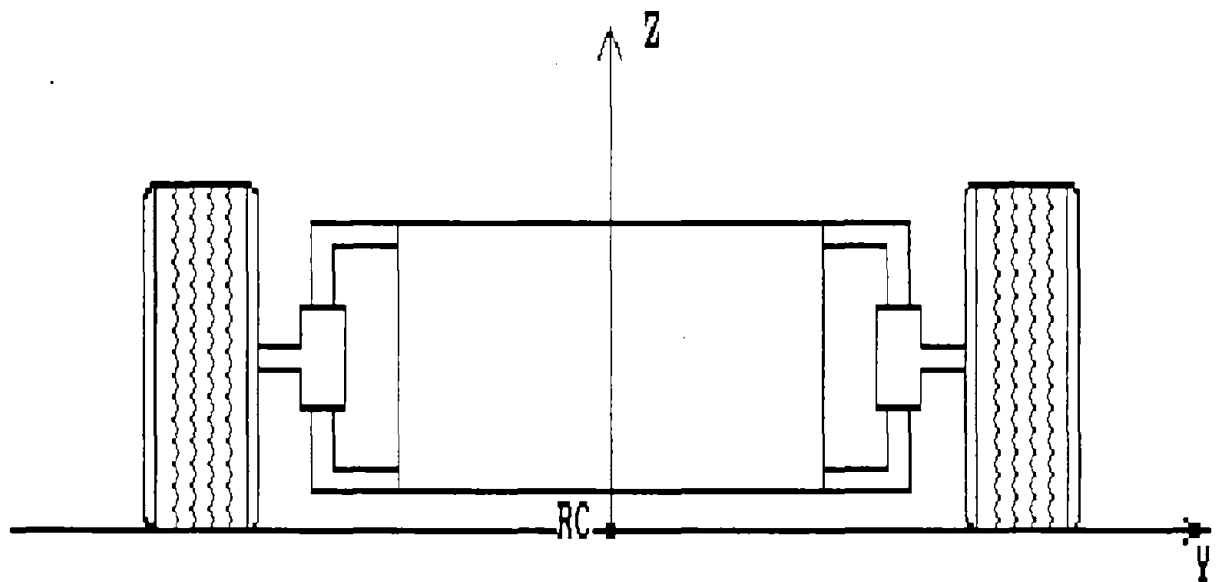
ENTER FOR D2: D2X,D2Y 2.50, 0.65



ROLL CENTER RC [ 2.5000, 0.0000, 0.1625]

SLIDING PILLAR

ENTER WHEELBASE 2.50  
ENTER FRONT TRACK WIDTH 1.30

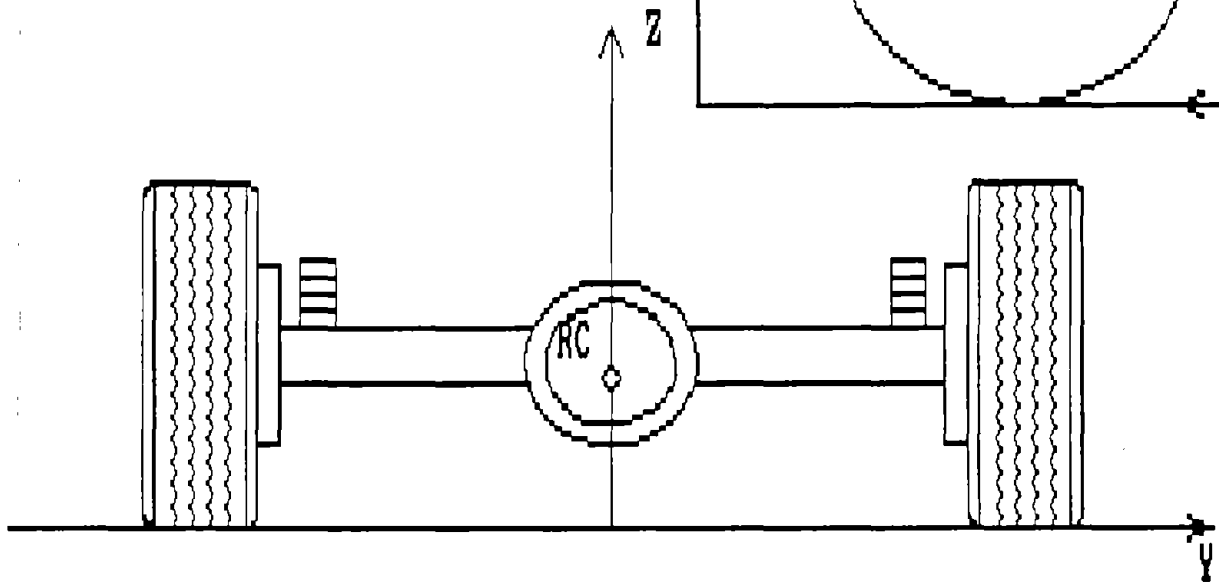
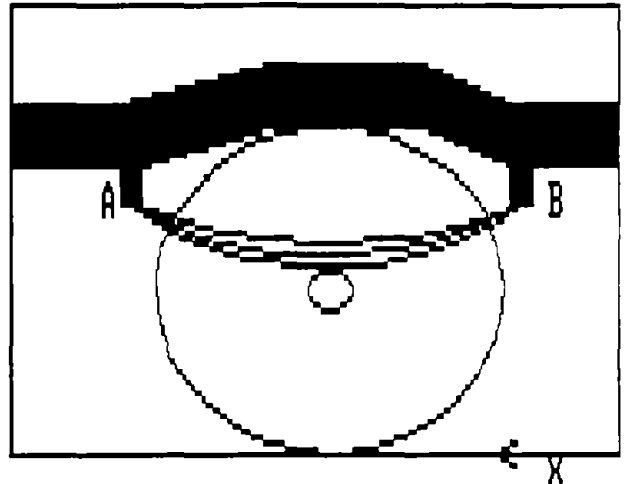


ROLL CENTER RC [ 2.5000, 0.0000, 0.0000]



LIVE HOTCHKISS DRIVE

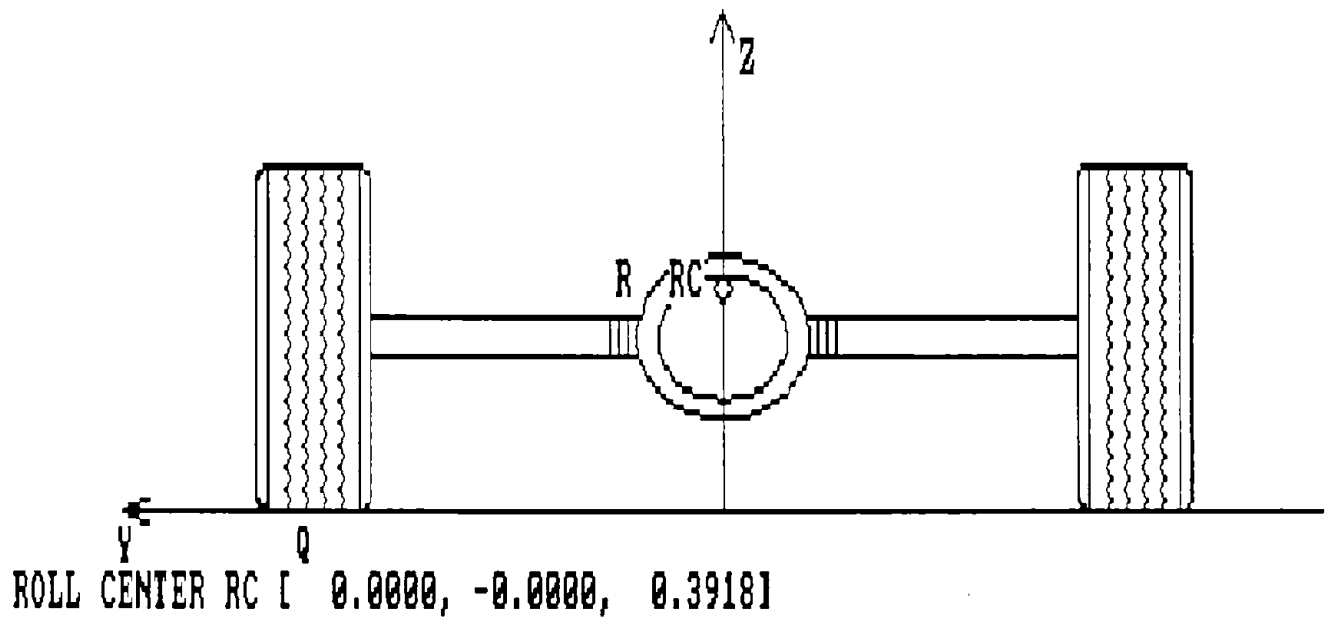
ENTER WHEELBASE 2.50  
ENTER FRONT TRACK WIDTH 1.30  
ENTER FOR A: AX,AY,AZ 0.00, 0.44, 0.27  
ENTER FOR B: BX,BY,BZ 0.00, 0.44, 0.43



ROLL CENTER RC [ 0.0000, 0.0000, 0.2700]

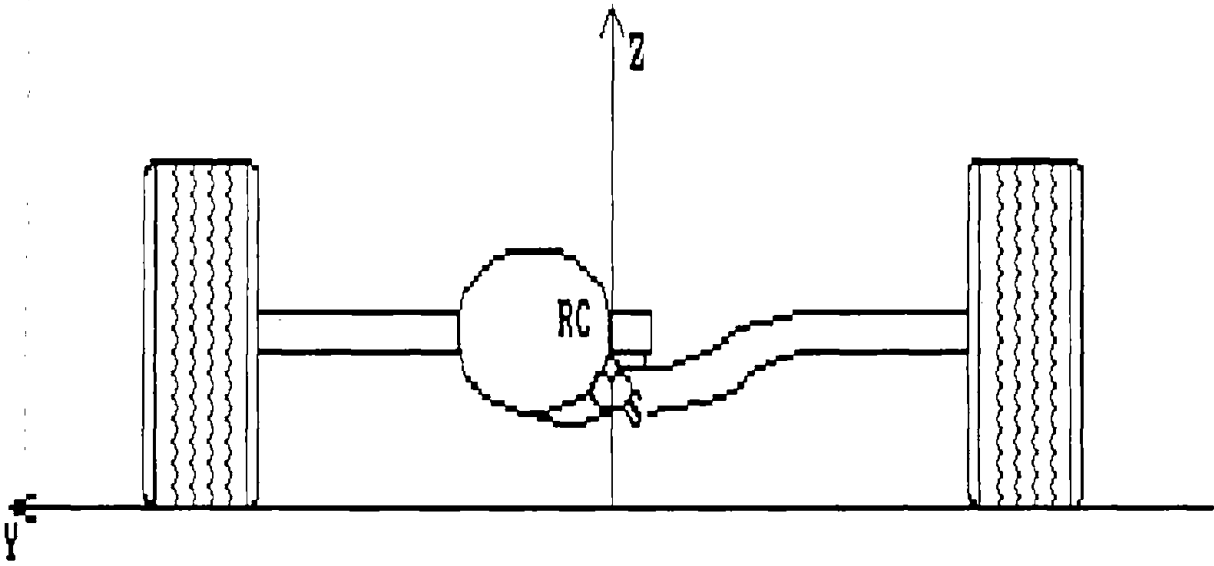
SWING AXLE

ENTER FOR R:  $R_X, R_Y, R_Z$  0.00, 0.15, 0.30  
ENTER FOR Q:  $Q_X, Q_Y$  0.00, 0.64



LOW PIVOT SWING AXLE

ENTER REAR TRACK WIDTH 1.30  
ENTER FOR S: SX, SZ 0.00, 0.25

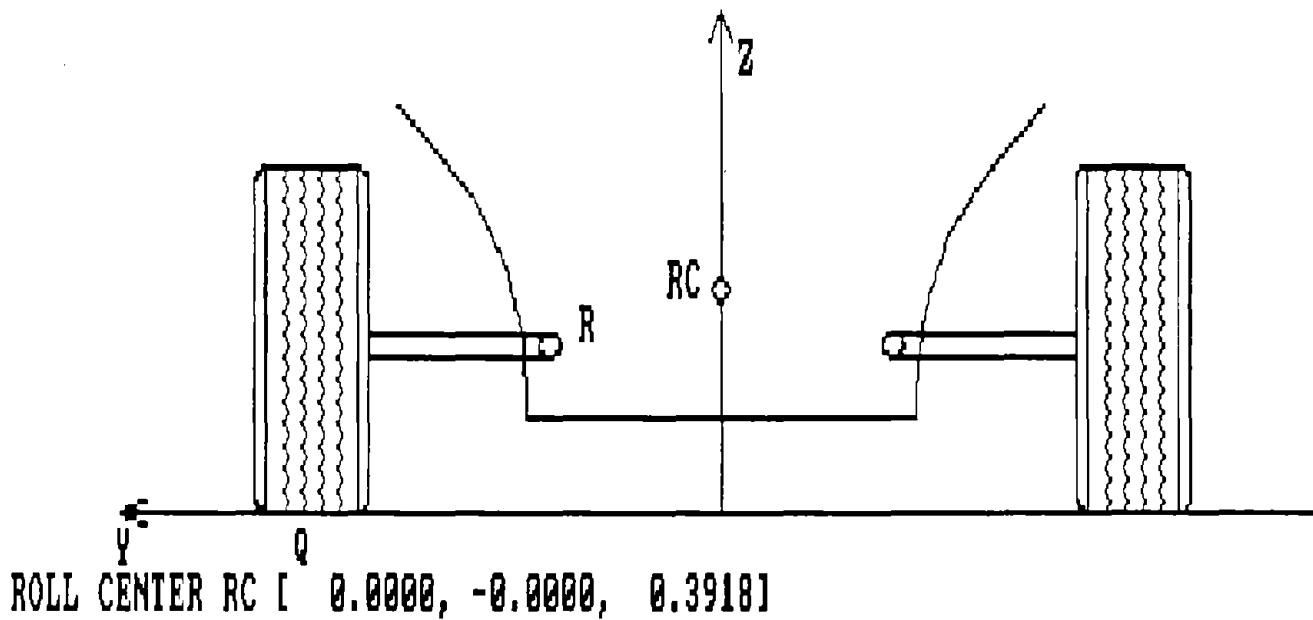


ROLL CENTER RC I 0.0000, 0.0000, 0.25001

SINGLE TRANSVERSE A-ARMS USED ON FWD

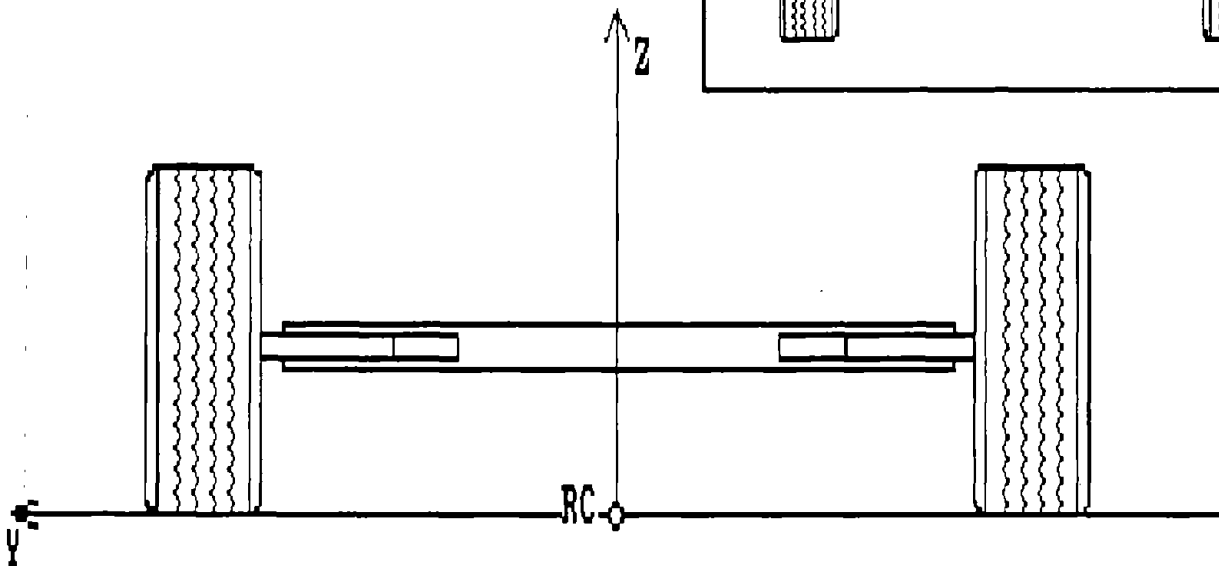
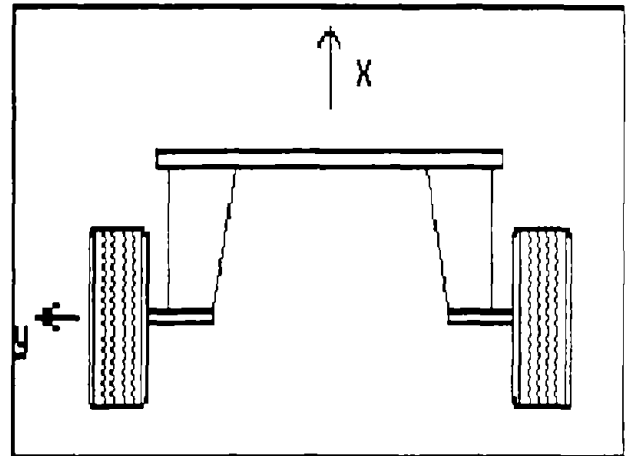
ENTER FOR R: RX,RY,RZ 0.00, 0.15, 0.30

ENTER FOR Q: QX,QY 0.00, 0.64



SINGLE TRAILING ARM

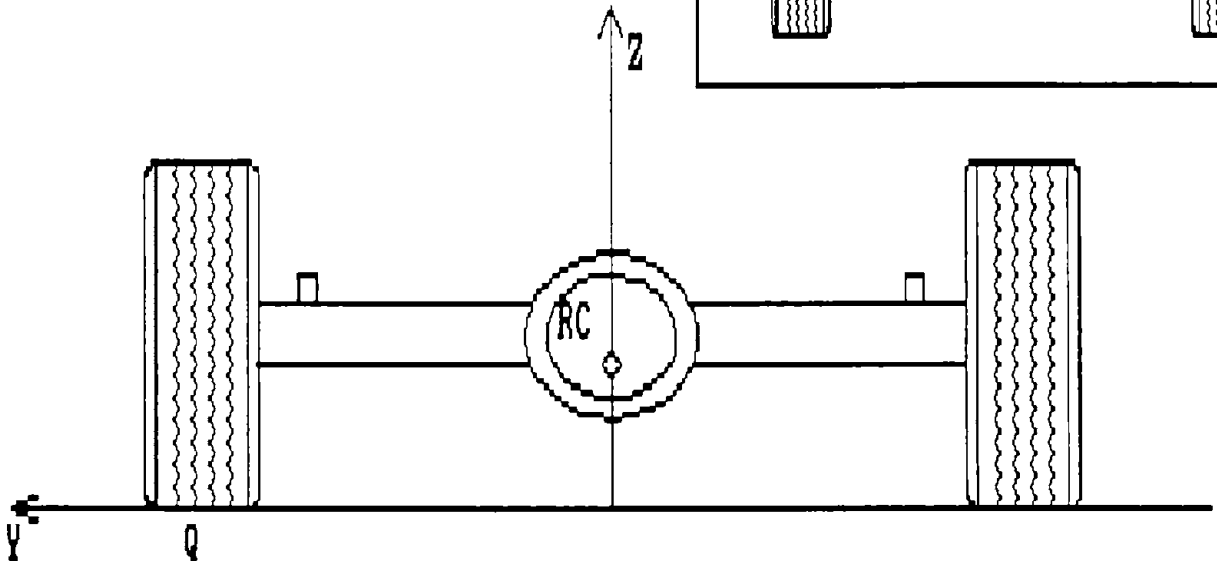
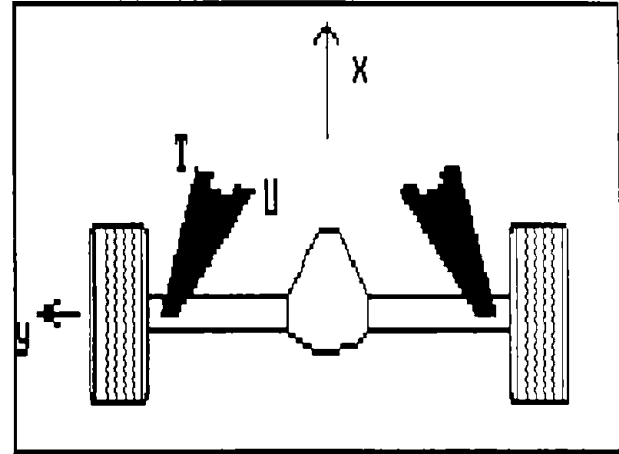
ENTER REAR TRACK WIDTH 1.30



ROLL CENTER RC I 0.0000, 0.0000, 0.00001

SEMI-TRAILING

ENTER FOR T: TX, TY, TZ 0.40, 0.44, 0.30  
 ENTER FOR U: UX, UY, UZ 0.30, 0.30, 0.30  
 ENTER FOR Q: QX, QY 0.00, 0.64

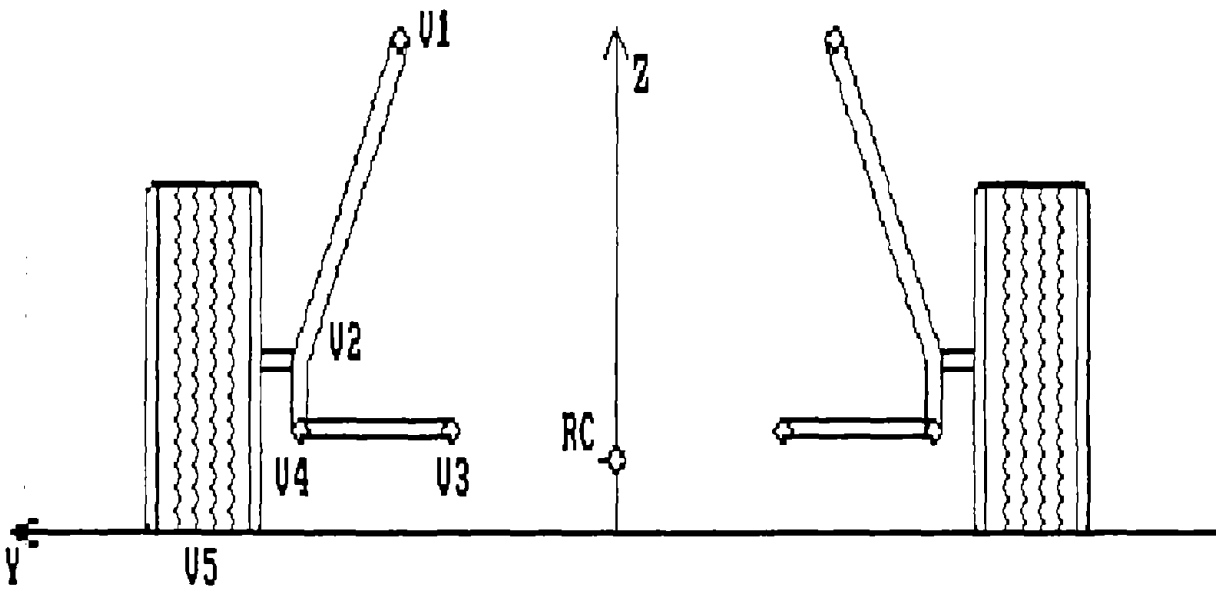


ROLL CENTER RC [ 0.0000, -0.0000, 0.2526 ]

# CHAPMAN STRUT

```

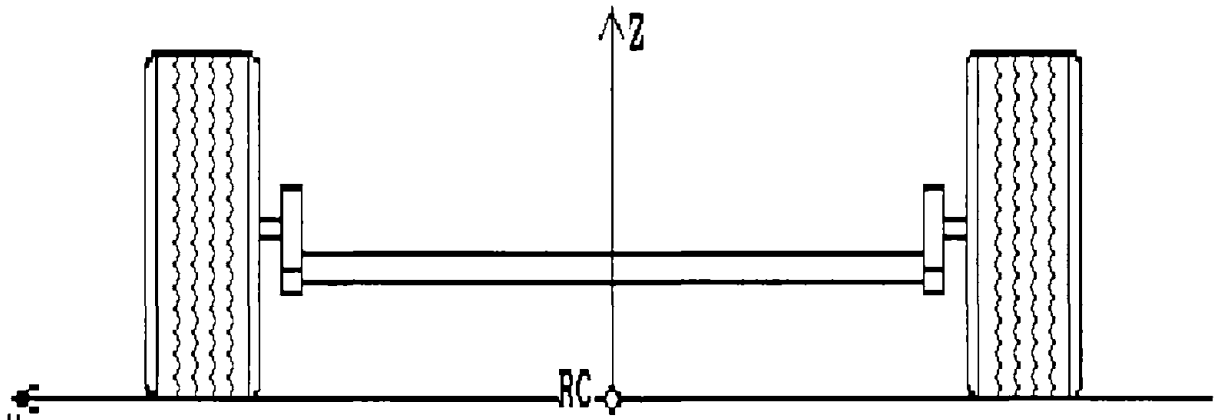
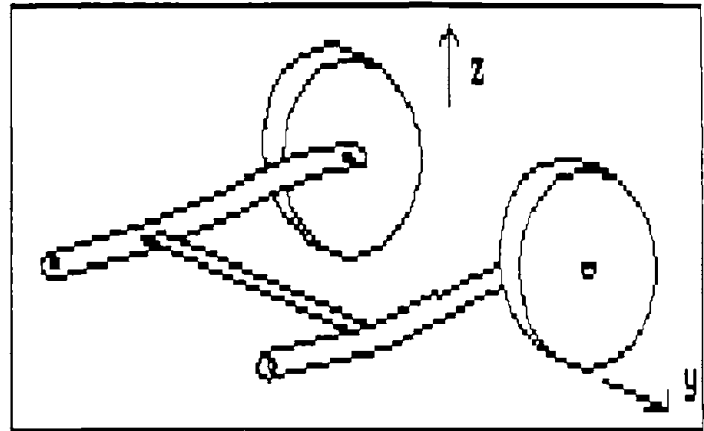
ENTER FOR U1: U1X,U1Y,U1Z  0.00, 0.40, 0.75
ENTER FOR U2: U2X,U2Y,U2Z  0.00, 0.50, 0.25
ENTER FOR U3: U3X,U3Y,U3Z  0.00, 0.15, 0.26
ENTER FOR U4: U4X,U4Y,U4Z  0.00, 0.50, 0.23
ENTER FOR U5: U5X,U5Y      0.00, 0.64
    
```



ROLL CENTER RC [ 0.0000, -0.0000, 0.1236 ]

SEMI-INDEPENDENT FOR FWD

ENTER REAR TRACK WIDTH 1.30

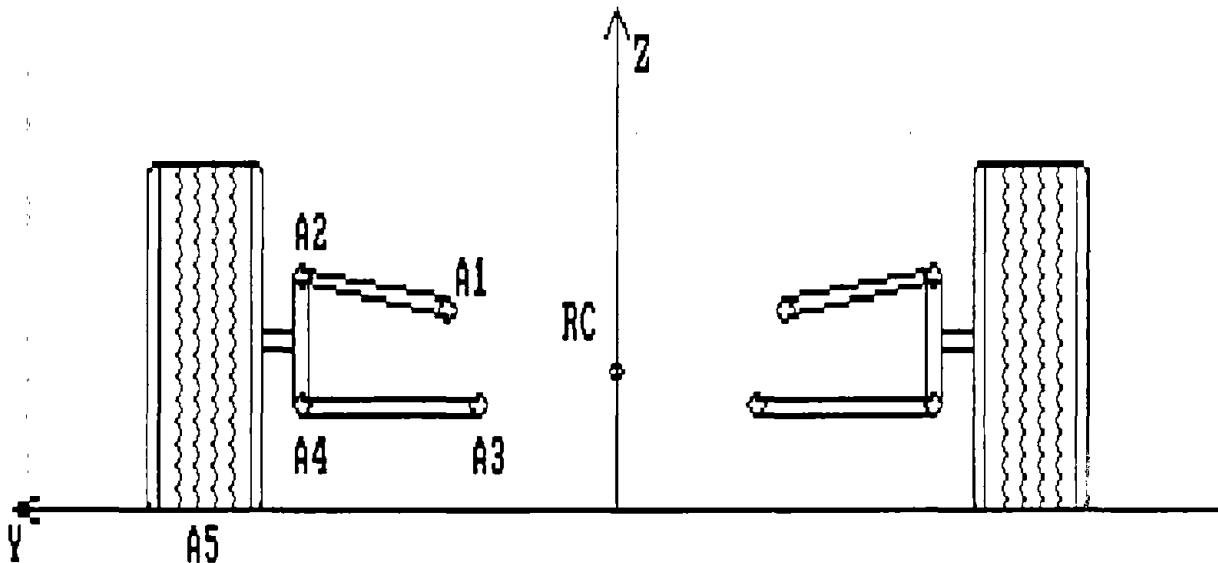


ROLL CENTER RC [ 0.0000, 0.0000, 0.0000]



WEISSACH AXLE

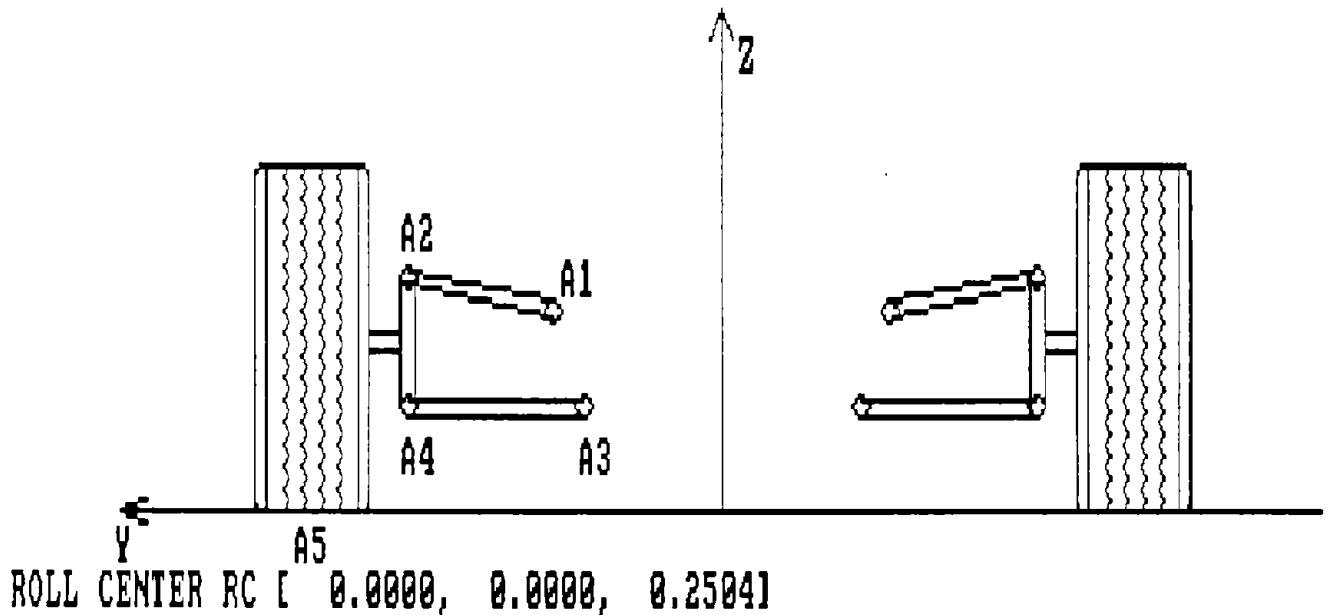
ENTER FOR A1: A1X,A1Y,A1Z 0.00, 0.20, 0.45  
ENTER FOR A2: A2X,A2Y,A2Z 0.00, 0.40, 0.55  
ENTER FOR A3: A3X,A3Y,A3Z 0.00, 0.15, 0.25  
ENTER FOR A4: A4X,A4Y,A4Z 0.00, 0.45, 0.20  
ENTER FOR A5: A5X,A5Y 0.00, 0.64



ROLL CENTER RC [ 0.0000, 0.0000, 0.2498]

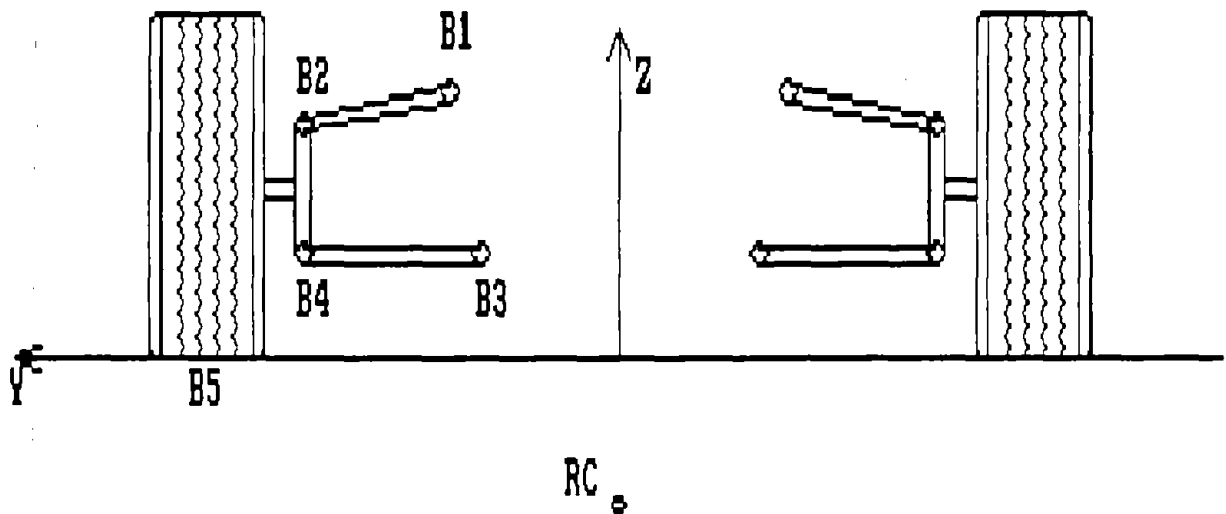
UNEQUAL-LENGTH UPPER AND LOWER CONTROL ARMS  
 (CONVERGING TOWARDS CAR CENTER)

ENTER FOR A1: A1X, A1Y, A1Z 0.00, 0.20, 0.45  
 ENTER FOR A2: A2X, A2Y, A2Z 0.00, 0.40, 0.55  
 ENTER FOR A3: A3X, A3Y, A3Z 0.00, 0.15, 0.25  
 ENTER FOR A4: A4X, A4Y, A4Z 0.00, 0.45, 0.20  
 ENTER FOR A5: A5X, A5Y 0.00, 0.65



UPPER AND LOWER CONTROL ARMS  
 (CONVERGING AWAY FROM CAR CENTER)

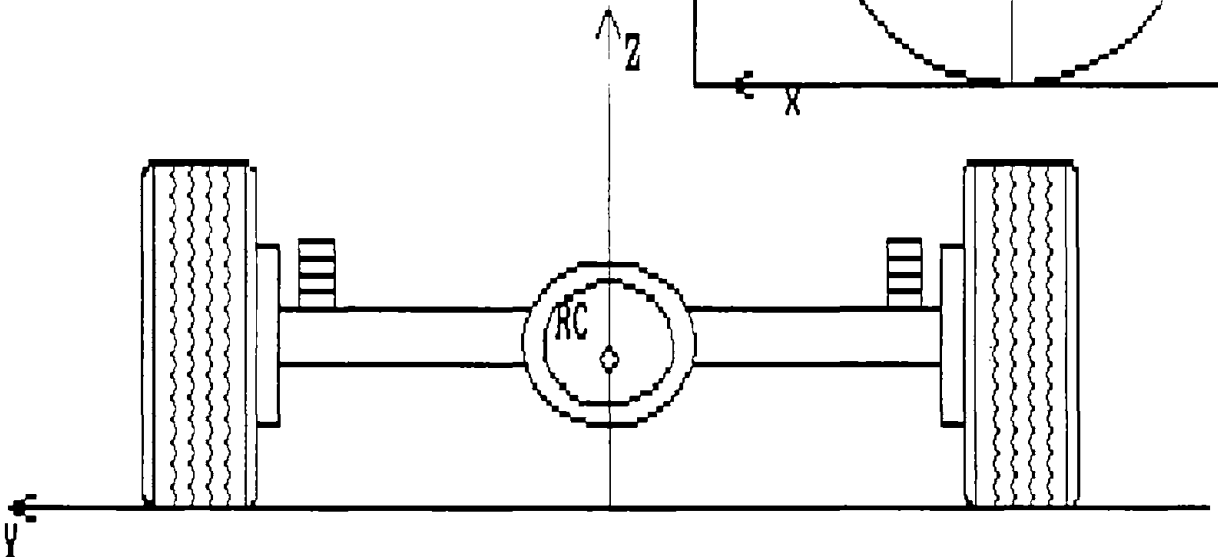
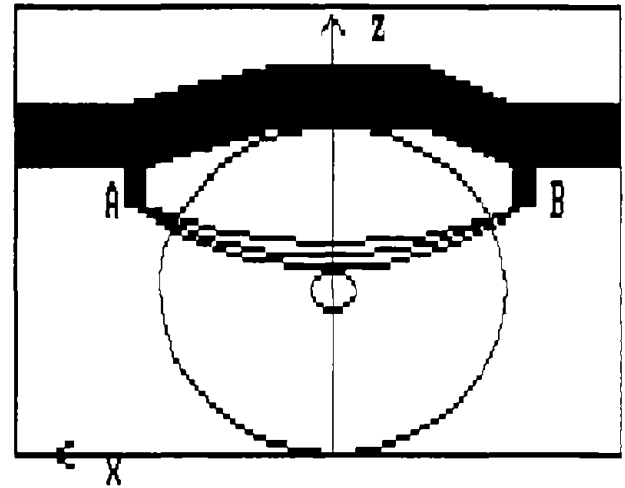
ENTER FOR B1: B1X, B1Y, B1Z 0.00, 0.20, 0.60  
 ENTER FOR B2: B2X, B2Y, B2Z 0.00, 0.40, 0.55  
 ENTER FOR B3: B3X, B3Y, B3Z 0.00, 0.15, 0.17  
 ENTER FOR B4: B4X, B4Y, B4Z 0.00, 0.45, 0.20  
 ENTER FOR B5: B5X, B5Y 0.00, 0.65



ROLL CENTER RC [ 0.0000, 0.0000, -0.2521]

# HOTCHKISS DRIVE

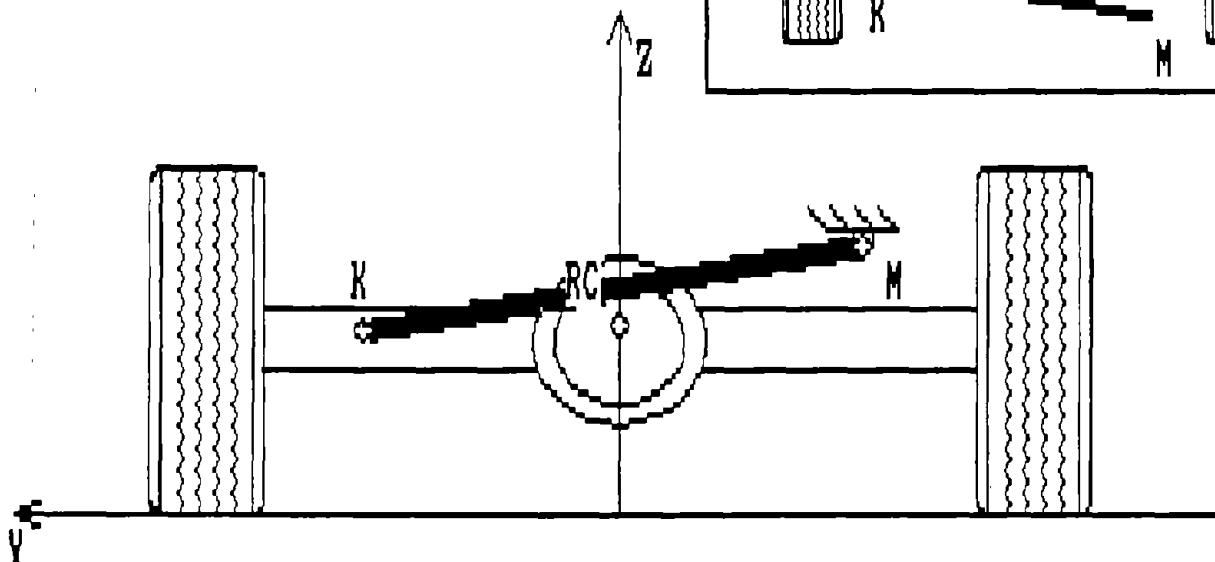
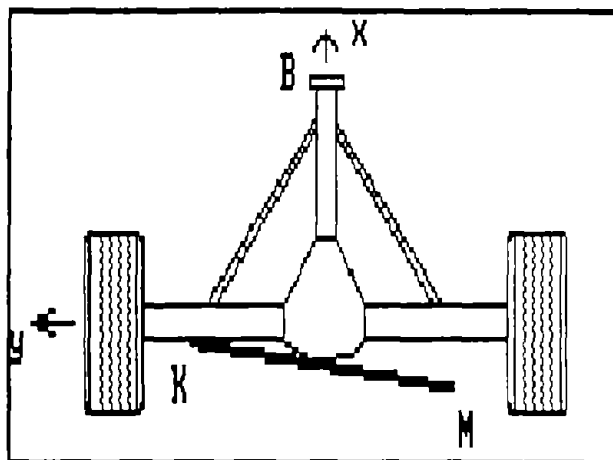
ENTER REAR TRACK WIDTH 1.30  
ENTER FOR A: AX,AY,AZ 0.00, 0.44, 0.27  
ENTER FOR B: BX,BY,BZ 0.00, 0.44, 0.43



ROLL CENTER RC I 0.0000, 0.0000, 0.27001

TORQUE TUBE WITH PANHARD ROD

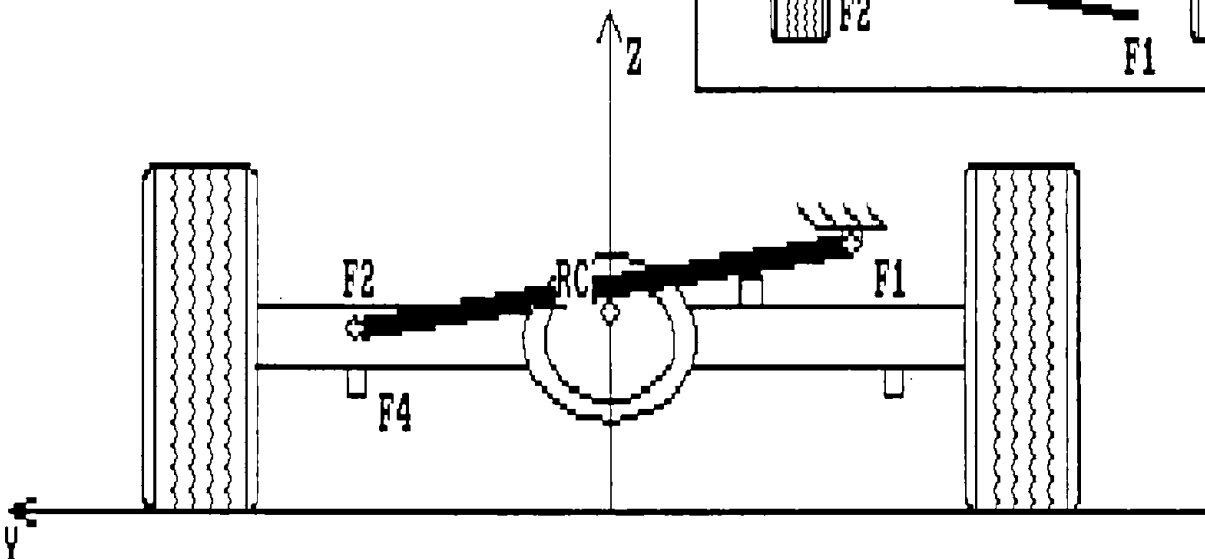
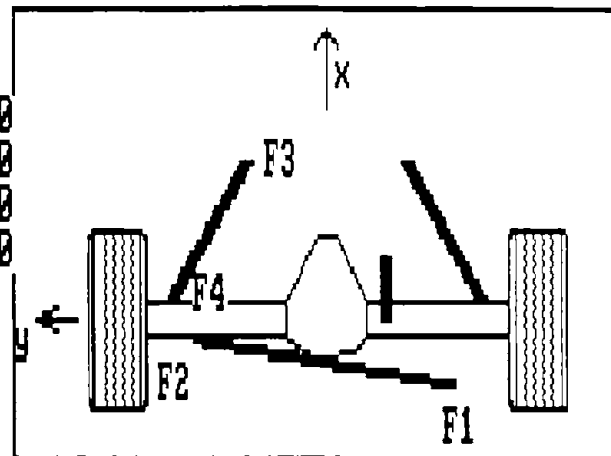
ENTER REAR TRACK WIDTH 1.30  
 ENTER FOR K: KX, KY, KZ -0.10, 0.35, 0.30  
 ENTER FOR M: MX, MY, MZ -0.15, -0.38, 0.40  
 ENTER FOR B: BX, BZ 0.60, 0.25



ROLL CENTER RC [ -0.0000, -0.0000, 0.33121

THREE LINK WITH PANHARD ROD

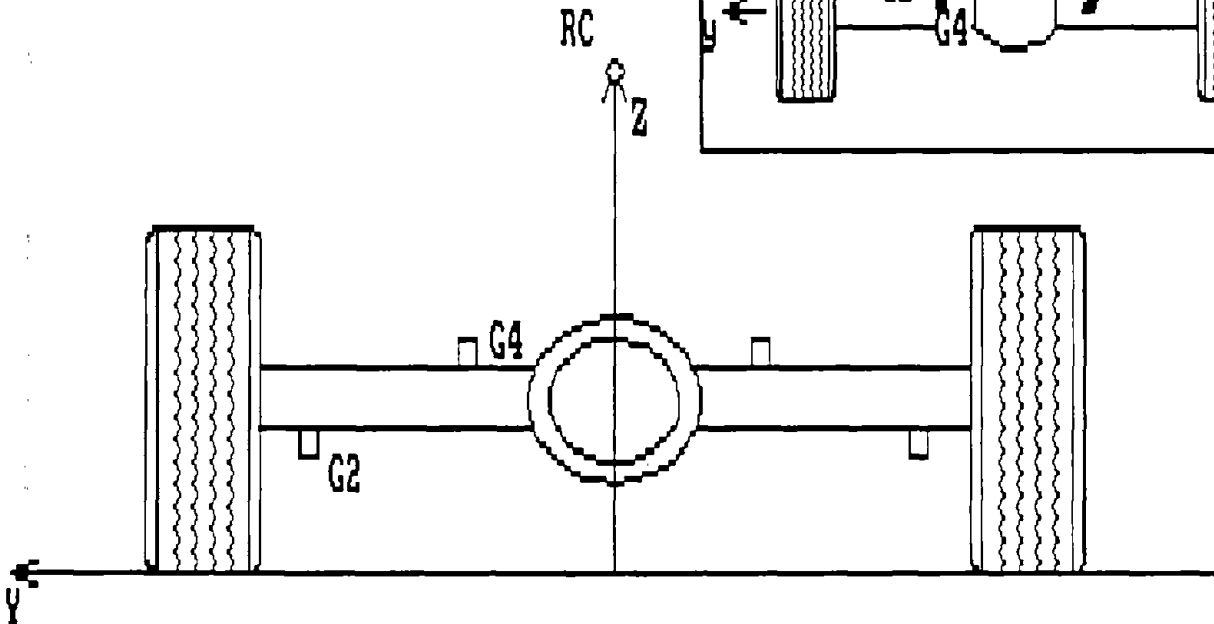
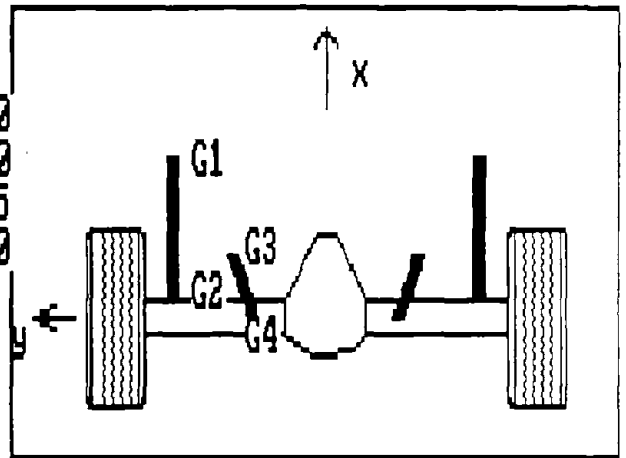
ENTER REAR TRACK WIDTH 1.30  
 ENTER FOR F1: F1X, F1Y, F1Z -0.15, -0.38, 0.40  
 ENTER FOR F2: F2X, F2Y, F2Z -0.10, 0.35, 0.30  
 ENTER FOR F3: F3X, F3Y, F3Z 0.40, -0.20, 0.30  
 ENTER FOR F4: F4X, F4Y, F4Z 0.10, -0.44, 0.20



ROLL CENTER RC [ 0.0000, 0.0000, 0.35361

FOUR LINK WITH PARALLEL LOWER LINKS

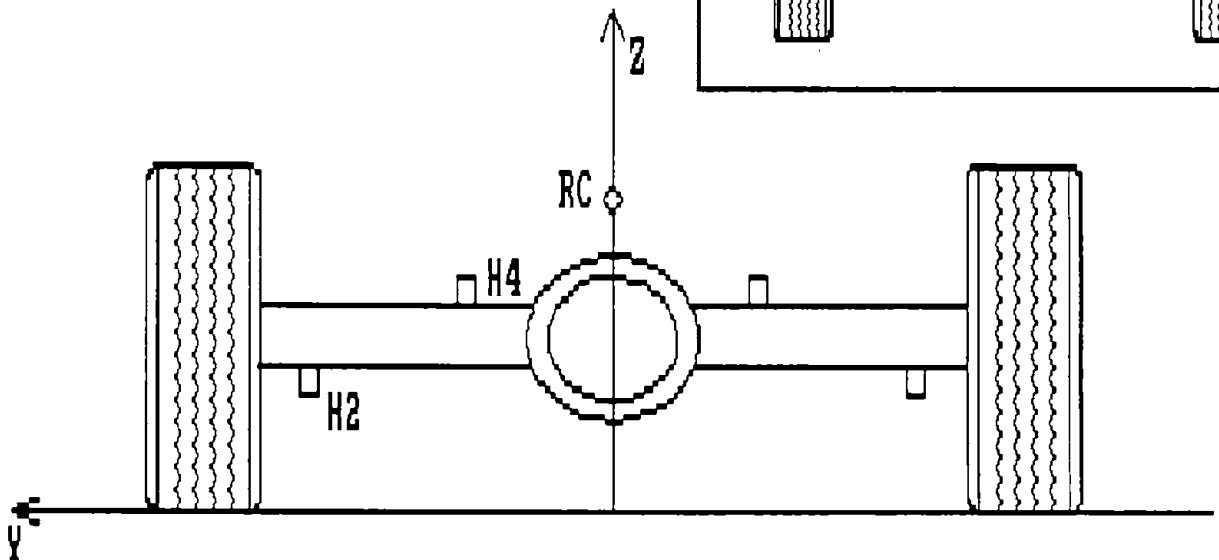
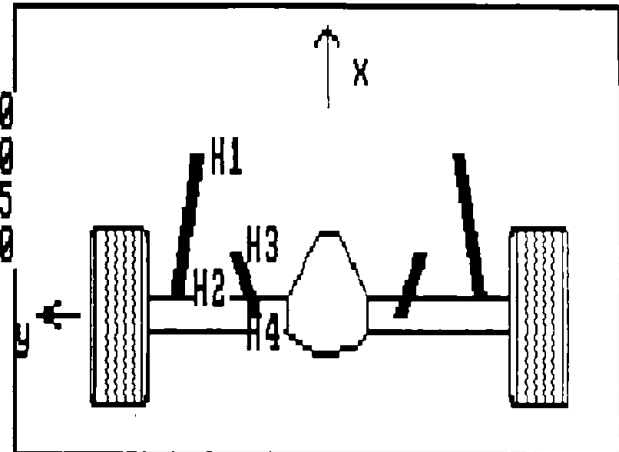
ENTER REAR TRACK WIDTH 1.30  
 ENTER FOR G1: G1X, G1Y, G1Z 0.40, -0.44, 0.30  
 ENTER FOR G2: G2X, G2Y, G2Z 0.10, -0.44, 0.20  
 ENTER FOR G3: G3X, G3Y, G3Z 0.20, -0.25, 0.45  
 ENTER FOR G4: G4X, G4Y, G4Z 0.05, -0.20, 0.50



ROLL CENTER RC [ 0.0000, 0.0000, 0.88331

# FOUR LINK WITH NON-PARALLEL LINKS

ENTER REAR TRACK WIDTH 1.30  
 ENTER FOR H1: H1X, H1Y, H1Z 0.40, -0.20, 0.30  
 ENTER FOR H2: H2X, H2Y, H2Z 0.10, -0.44, 0.20  
 ENTER FOR H3: H3X, H3Y, H3Z 0.20, -0.25, 0.45  
 ENTER FOR H4: H4X, H4Y, H4Z 0.05, -0.20, 0.50

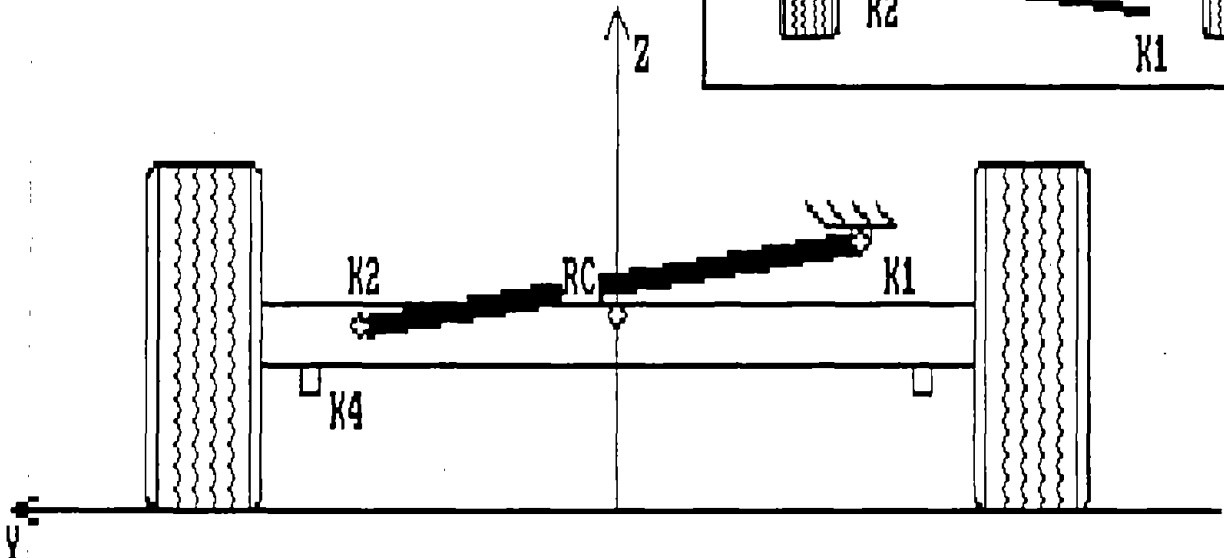
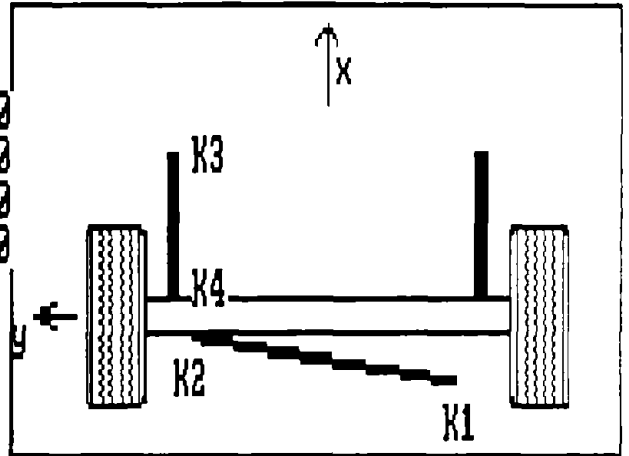


ROLL CENTER RC [ 0.0000, 0.0000, 0.5549]



BEAM TWIST AXLE WITH PANHARD ROD FWD

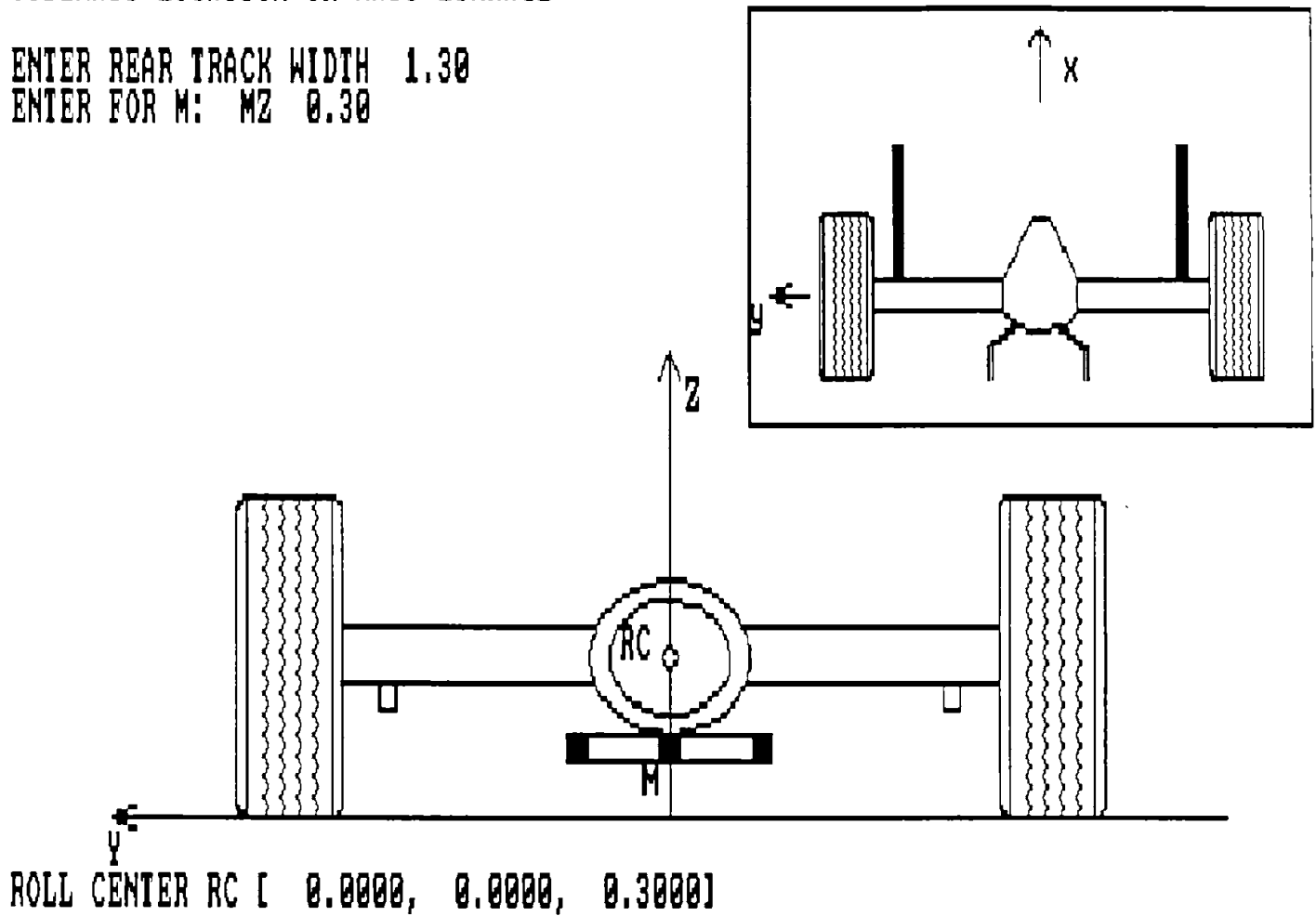
ENTER REAR TRACK WIDTH 1.30  
 ENTER FOR K1: K1X, K1Y, K1Z -0.15, -0.38, 0.40  
 ENTER FOR K2: K2X, K2Y, K2Z -0.10, 0.35, 0.30  
 ENTER FOR K3: K3X, K3Y, K3Z 0.40, -0.44, 0.20  
 ENTER FOR K4: K4X, K4Y, K4Z 0.10, -0.44, 0.20



ROLL CENTER RC [ 0.0000, 0.0000, 0.34791

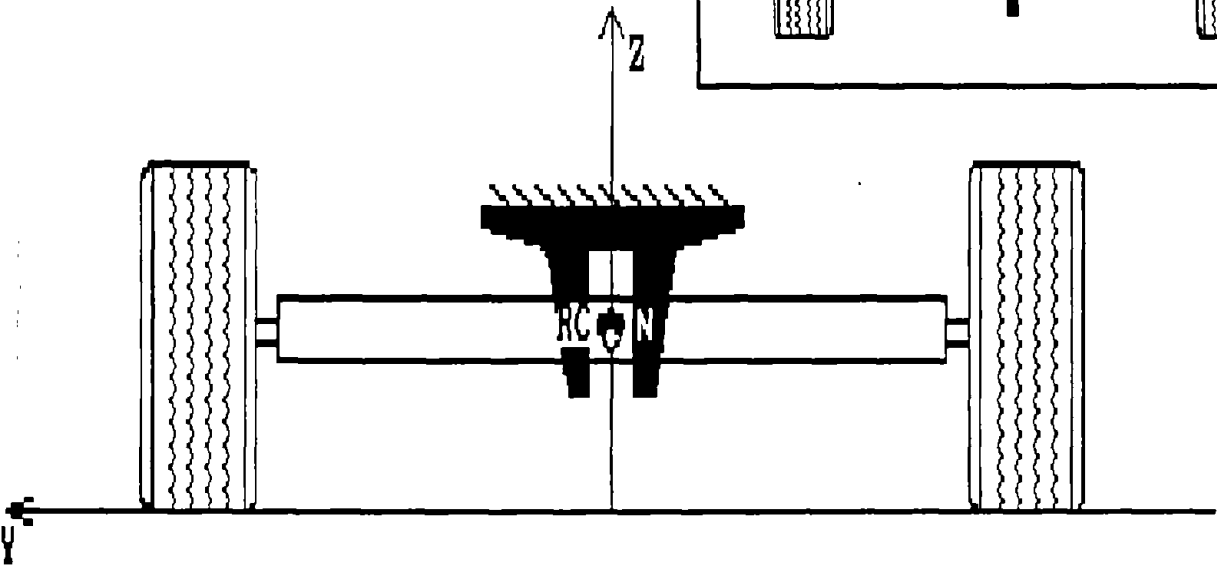
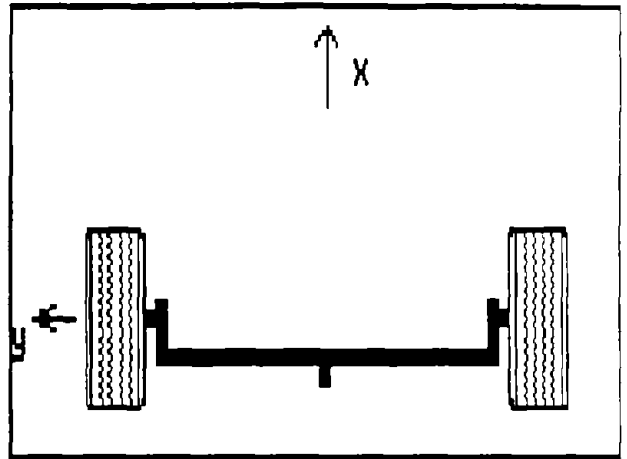
SIDEWAYS LOCATION OR WATT LINKAGE

ENTER REAR TRACK WIDTH 1.30  
ENTER FOR M: MZ 0.30



DE DIOM AXLE

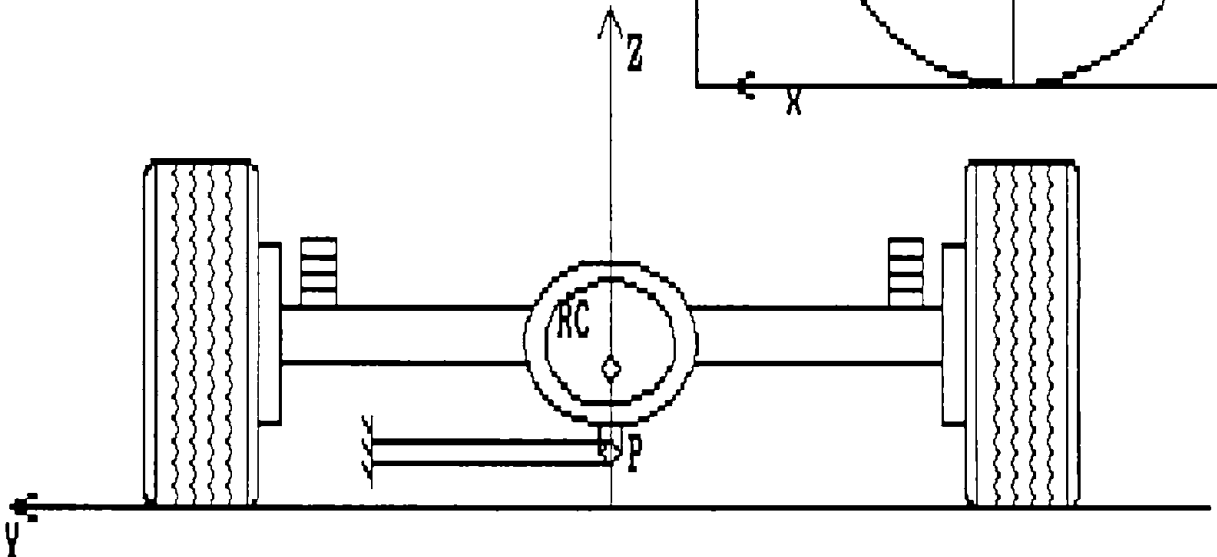
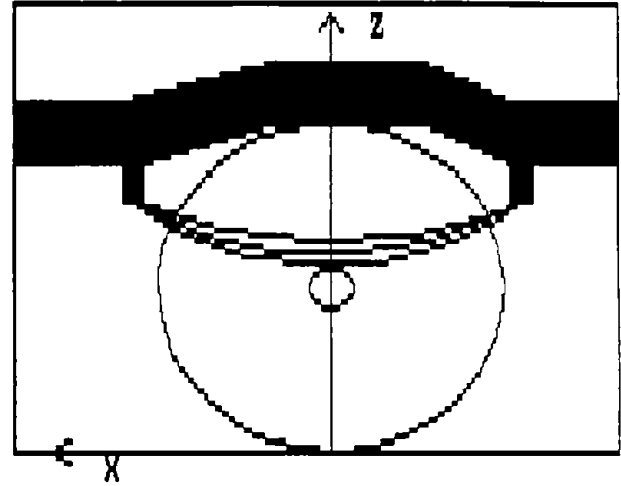
ENTER REAR TRACK WIDTH 1.30  
ENTER FOR N: NZ 0.30



ROLL CENTER RC [ 0.0000, 0.0000, 0.3000]

BEAM AXLE WITH LONGITUDINAL LEAF SPRINGS AND LATERAL LOCATING DEVICE

ENTER REAR TRACK WIDTH 1.30  
ENTER FOR P: PZ 0.25



ROLL CENTER RC [ 0.0000, 0.0000, 0.2500]

## APPENDIX B

### VEHICLE DATA USED IN SENSITIVITY ANALYSIS

```

9, ' =====', 0.000D0
9, ' ===== Analyzed Parameters =====', 0.000D0
9, ' =====', 0.000D0
9, ' ===== Primary Geometrical =====', 0.000D0
0, 'A - Dist. From Front Axle to C.G. ', 1.034D0
0, 'Anom - Non-Parameter Constant A ', 1.034D0
0, 'B - Dist. From Rear Axls to C.G. ', 0.998D0
0, 'Bnom - Non-Parameter Constant B ', 0.998D0
0, 'Hs - Static Height Sprung Mass G.G.', 0.693D0
0, 'HUF - Height of Unsprung Mass C.G. ', 0.3302D0
0, 'HUR - Height of Unsprung Mass C.G. ', 0.3302D0
0, 'L - Wheelbase ', 2.032D0
0, 'Lnom - Non-Parameter Constant L ', 2.032D0
0, 'Tf - Front Track Width ', 1.3081D0
0, 'Tr - Rear Track Width ', 1.3081D0
9, '===== Mass/Inertia Parameters =====', 0.000D0
0, 'Ixs - Roll Inertia of Sprung Mass ', 240.26D0
0, 'Ixu - Roll Inertia of Unsprung Mass', 71.83D0
0, 'Iz - Vehicle Yaw Inertia ', 1175.5D0
0, 'Ms - Vehicle Sprung Mass ', 778.1D0
0, 'Muf - Front Unsprung Mass ', 117.48D0
0, 'Mur - Rear Unsprung Mass ', 117.48D0
0, 'wgtdis - Wgt distribution ', 0.50885827D0
0, 'WDnom - Nominal Wt. Distribution ', 0.50885827D0
9, '===== Aerodynamic Parameters =====', 0.000D0
0, 'Caerod - Aero. Yaw Damping Coeff. ', 1000.0D0
0, 'Cnaero - Aero. Aligning Mom. Coeff.', 2.50D0
0, 'Cyaero - Aero. Side Force Coeff. ', 1.0D0
0, 'Hchar - Aero. Characteristic Height', 1.5D0
0, 'Sfrontal - Vehicle Frontal Area ', 2.0D0
9, '==== Tire Frictional Parameters ====', 0.000D0
0, 'CAL - Cam. Crit. Ang. Frict. Reduc.', .523598770D0
0, 'CR1 - %Fric. Reduc. at Crit. Camber', 0.30D0
0, 'SN - Skid Number / 100 ', 1.00D0
9, '===== Damping Parameters =====', 0.000D0
0, 'Cr - Aux. Suspension Roll Damping ', 0.0D0
0, 'Cs - Damp. Coeff. of Shock Absorb. ', 3000.0D0
0, 'Ctire - Damp. Coeff. of Tire ', 980.0D0
9, '===== Stiffness Parameters =====', 0.000D0
0, 'Kb - Bump Stop Spring Stiffness ', 464030.0D0
0, 'Krf - Aux. Roll Stiff. of Frt. Sus.', 3443.73D0
0, 'Krr - Aux. Roll Stiff. of Rear Sus.', 5277.33D0
0, 'Ks - Suspension Spring Stiffness ', 84850.0D0
0, 'Ktire - Tire Spring Stiffness ', 113140.0D0
0, 'RSDstb - Front Roll Stiff. Distrib.', 0.56D0
9, '==== Suspension Geom. Parameters ====', 0.000D0
0, 'FRCZ - Front Roll Center Height ', 0.0709D0
0, 'Lb - Undeformed Bump Stop Length ', 0.0762D0
0, 'Ls - Static Spring Length ', 0.1016D0
0, 'RRCZ - Rear Roll Center Height ', 0.10D0
0, 'Tbas - Height of Lower Spring Mount', 0.2032D0
0, 'Ts - Half Suspension Spring Track ', 0.466D0

```

```

9, '=====', 0.000D0
9, '==== Parameters not Analyzed =====', 0.000D0
9, '=====', 0.000D0
9, '==== Calspan Coefficients =====', 0.000D0
0, 'A0 - Calspan Coeff.', -668.46D0
0, 'A1 - Calspan Coeff.', 26.54D0
0, 'A2 - Calspan Coeff.', 2146.6101D0
0, 'A3 - Calspan Coeff.', 1.274D0
0, 'A4 - Calspan Coeff.', 2225.0701D0
0, 'B1 - Calspan Coeff.', -6.745D-04
0, 'B3 - Calspan Coeff.', 1.307D0
0, 'B4 - Calspan Coeff.', 2.953D-07
0, 'K1 - Calspan Coeff.', -2.061D-04
0, 'K2 - Calspan Coeff.', -1.768D-04
0, 'K3 - Calspan Coeff.', 0.074D0
0, 'P0 - Calspan Coeff.', 1.2073
0, 'P1 - Calspan Coeff.', -5.843D-04
0, 'P2 - Calspan Coeff.', 3.977D-07
0, 'R0 - Calspan Coeff.', -0.23771D0
0, 'R1 - Calspan Coeff.', 8.5360D-05
0, 'S0 - Calspan Coeff.', 1.1738D0
0, 'S1 - Calspan Coeff.', -8.458D-04
0, 'S2 - Calspan Coeff.', 3.9450D-07
9, '==== Braking Parameters =====', 0.000D0
0, 'Ctn - Slope of Mux vs. Slip Ratio', 6.0D0
0, 'Q0 - Brake Proportion Coeff.', 0.65D0
0, 'Q1 - Heavy Braking Coeff.', 0.10D0
0, 'WD - Drive (1-FWD,2-RWD,3-4WD)', 3.0D0
0, 'WD4 - 4WD Front/Rear Torque Split', 0.6D0
9, '==== Steering Input Parameters =====', 0.000D0
0, 'DF - Rate of Tire Incl. w/ Roll', -0.04D0
0, 'Hy - Steering Wheel Hysteresis', 0.0D0
0, 'StRatio - Steering Ratio', 22.0D0
9, '==== Environmental Parameters =====', 0.000D0
0, 'G - Gravitational Acceleration', 9.807D0
0, 'RHOair - Air Density', 1.2260D0
0, 'ENDPP', 0.0D0
0, 'ENDSP', 0.0D0
0, 'Y(1) - Time', 0.0D0
0, 'Y(2) - Forward Speed U', 0.0D0
0, 'Y(3) - Lateral Speed V', 0.0D0
0, 'Y(4) - Yaw Velocity r', 0.0D0
0, 'Y(5) - Yaw Angle Psi', 0.0D0
0, 'Y(6) - X-Coordinate', 0.0D0
0, 'Y(7) - Y-Coordinate', 0.0D0
0, 'Y(8) - Y-Vel. of Unsprung Mass', 0.0D0
0, 'Y(9) - Z-Vel. of Unsprung Mass', 0.0D0
0, 'Y(10) - Roll Vel. of Unsprung Mass', 0.0D0
0, 'Y(11) - Roll Vel. of Sprung Mass', 0.0D0
0, 'Y(12) - Heave Vel. of Sprung Mass', 0.0D0
0, 'Y(13) - Lat. Disp. of Unsprung Mass', 0.0D0
0, 'Y(14) - Vrt. Disp. of Unsprung Mass', 0.0D0
0, 'Y(15) - Roll Angle of Unsprung Mass', 0.0D0
0, 'Y(16) - Rel. Roll of Sprung Mass', 0.0D0
0, 'Y(17) - Rel. Heave of Sprung Mass', 0.0D0
0, 'V(18) - EPE Anti-Roll Bar', 0.0D0
0, 'V(19) - EPE Left Suspension Spring', 0.0D0
0, 'V(20) - EPE Right Suspension Spring', 0.0D0

```

```

0,'V(21) - EPE Left Bump Stop           ',0.0D0
0,'V(22) - EPE Right Bump Stop          ',0.0D0
0,'V(23) - EPE Left Tire                ',0.0D0
0,'V(24) - EPE Right Tire               ',0.0D0
0,'V(25) - Total Elastic Pot. Energy    ',0.0D0
0,'V(26) - GPE of Unsprung Mass         ',0.0D0
0,'V(27) - GPE of Sprung Mass           ',0.0D0
0,'V(28) - Total Grav. Pot. Energy      ',0.0D0
0,'V(29) - Total Potential Energy       ',0.0D0
0,'V(30) - KE of Unsprung Mass          ',0.0D0
0,'V(31) - KE of Sprung Mass            ',0.0D0
0,'V(32) - Total Kinetic Energy         ',0.0D0
0,'V(33) - Total System Energy          ',0.0D0
1,'V(34) - RPER                         ',0.0D0
0,'V(35) - RPERA                        ',0.0D0
0,'V(36) - Power Dissap. in Left Tire  ',0.0D0
0,'V(37) - Power Dissap. in Right Tire ',0.0D0
0,'V(38) - Power Dissap. in Lt. Shock  ',0.0D0
0,'V(39) - Power Dissap. in Rt. Shock  ',0.0D0
0,'V(40) - Power Dissap. in Aux. Shock ',0.0D0
0,'V(41) - Tot. Power Dissap. in Damp. ',0.0D0
0,'ENDOV                                ',0.0D0

```





## APPENDIX C

### NOMENCLATURE USED IN SENSITIVITY PLOTS

#### Geometrical Parameter Set #1

a	- Longitudinal distance from the front axle to the vehicle center of gravity
b	- Longitudinal distance from the rear axle to the vehicle center of gravity
H <sub>SM</sub>	- Center of gravity height of the sprung mass in static conditions
H <sub>UF</sub>	- Center of gravity height of the front unsprung mass in static conditions
H <sub>UR</sub>	- Center of gravity height of the rear unsprung mass in static conditions
TRW <sub>f</sub>	- Front track width
TRW <sub>r</sub>	- Rear track width

#### Geometrical Parameter Set #2

BSLNG	- Undeformed bump stop length
RC <sub>f</sub>	- Front suspension roll center height
RC <sub>r</sub>	- Rear suspension roll center height
s	- Half suspension spring track width
SPRLNG	- Suspension spring length in static conditions
T <sub>bas</sub>	- Height of lower suspension spring mount above ground

#### Mass Inertia Parameter Set

I <sub>xxs</sub>	- Roll moment of inertia of sprung mass
I <sub>xxu</sub>	- Roll moment of inertia of unsprung masses
I <sub>zz</sub>	- Vehicle yaw moment of inertia
M <sub>s</sub>	- Sprung mass
M <sub>uf</sub>	- Front unsprung mass
M <sub>ur</sub>	- Rear unsprung mass
WDIST	- % Weight on the rear axle

#### Stiffness Parameter Set

K <sub>1</sub>	- Combined stiffness of the front and rear suspension springs
K <sub>2</sub>	- Combined stiffness of the front and rear bump stops
K <sub>RDIST</sub>	- % of total suspension roll stiffness at front suspension

- $K_{rf}$  - Front auxiliary roll stiffness
- $K_{rr}$  - Rear auxiliary roll stiffness
- $K_z$  - Combined stiffness of the front and rear tires

#### Damping Parameter Set

- $B_1$  - Combined damping coefficient of the front and rear suspension dampers
- $B_z$  - Combined damping coefficients of the front and rear tires

#### Tire Frictional Parameter Set

- CA1 - Critical camber angle  $\gamma_c$
- CR1 - Friction reduction factor  $r_\gamma$  at critical camber angle  $\gamma_c$
- SN - Skid number

#### Aerodynamic Parameter Set

- $C_n$  - Aerodynamic yawing moment coefficient
- $C_{nd}$  - Aerodynamic yaw damping coefficient
- $C_y$  - Aerodynamic side force coefficient
- $H_a$  - Characteristic height of the vehicle
- $S_a$  - Projected frontal area of the vehicle